



RĪGAS TEHNISKĀ
UNIVERSITĀTE

Elīna Līdumniece

MALĀRIJAS ENZĪMU INHIBITORU IZVEIDE

Promocijas darbs

DEVELOPMENT OF MALARIAL ENZYME INHIBITORS

Doctoral Thesis



RIGA TECHNICAL UNIVERSITY

Faculty of Material Science and Applied Chemistry

Institute of Technology of Organic Chemistry

Department of Chemical Technology of Biologically Active Compounds

Elīna Līdumniece

Doctoral student of the Doctoral Programme “Chemistry”

**DEVELOPMENT OF MALARIAL ENZYME
INHIBITORS**

Doctoral Thesis

Scientific supervisor

Professor *Dr. chem.* Aigars JIRGENSONS

Riga 2023

Abstract

Development of malarial enzyme inhibitors. Lidumniece E., scientific supervisor Prof., *Dr. Chem.* Jirgensons A. Doctoral thesis, 126 pages, 29 figures, 14 schemes, 7 tables, 51 reference, 2 appendices. In English.

MALARIA, PEPTIDIC BORONIC ACIDS, α -KETOAMIDES, SUB1 INHIBITORS.

The research presented in the thesis describes the development of synthesis methods to obtain peptidic boronic acid SUB1 inhibitors. The synthetic routes established enabled an access of various peptidic boronic acids with modified P1, P3 and P5 positions. The newly synthesized inhibitors were evaluated for their ability to inhibit SUB1 as well as for their antimalarial potency in cell based assays and *in vitro* selectivity counter screen tests (in collaboration with prof. Michael Blackman's group at the Francis Crick institute). The research has resulted in a series of compounds with low nanomolar inhibitory potency in SUB1 enzymatic assays several of which displayed sub-micromolar inhibitory potency in *P. falciparum* parasite growth tests.

Abbreviations

Ac – acetyl	IR – infrared
ACT – artemisinin-based combination therapy	Leu –leucine
Ala – alanine	LDA –lithium diisopropylamide
A.U. – arbitrary unit	MD – Molecular dynamics
Boc – <i>tert</i> -butoxycarbonyl	Me – methyl
BOP-Cl – bis(2-oxo-3-oxazolidinyl)phosphinic chloride	MeCN – acetonitrile
CDI – 1,1'-carbonyldiimidazole	MSP – merozoite surface protein
<i>c</i>-Butyl – cyclobutyl	<i>n</i>-Bu – <i>n</i> -butyl
Cbz – carboxybenzyl	NMM – <i>N</i> -methylmorpholine
<i>c</i>-Hex – cyclohexyl	NMR – nuclear magnetic resonance
<i>c</i>-Pent – cyclopentyl	Ph – phenyl
<i>c</i>-Propyl – cyclopropyl	Pin – pinacole
DCM – dichloromethane	PMB – <i>p</i> -methoxybenzyl
DIPEA – <i>N,N</i> -diisopropylethylamine	P.T. – proton transfer
DMAP – 4-(dimethylamino)pyridine	PV – parasitophorous vacuole
DMF – <i>N,N</i> -Dimethylformamide	RBC – red blood cell
DMP – Dess–Martin periodinane	r. t. – room temperature
DMSO – dimethyl sulfoxide	SAR – structure-activity relationship
DPEPhos – bis[(2-diphenylphosphino)phenyl] ether	SERA – serine-rich antigen family
EDC·HCl – 1-Ethyl-3-(3-dimethylaminopropyl)carbodiimide hydrochloride	SUB1 – subtilisin-like serine protease 1
EDTA – ethylenediaminetetraacetic acid	T3P – propanephosphonic acid anhydride
ESI – electrospray ionization	<i>t</i>-Bu – <i>tert</i> -butyl
Et – ethyl	TFA – Trifluoroacetic acid
Fmoc – fluorenylmethoxycarbonyl	TFE – 2,2,2-trifluoroethanol
GC-MS – gas chromatography–mass spectrometry	THF – tetrahydrofuran
Gly – glycine	Thr – threonine
HATU – <i>O</i> -(7-Azabenzotriazol-1-yl)- <i>N,N,N',N'</i> -tetramethyluronium hexafluorophosphate	TLC – thin-layer chromatography
Hex – hexyl	TMS – trimethylsilyl
HMDS – hexamethyldisilazane	TOF – time-of-flight
HOBT – hydroxybenzotriazole	UPLC – ultra-performance liquid chromatography–mass spectrometry
HRMS – high resolution mass spectrometry	UV – ultraviolet
<i>i</i>-Bu – isobutyl	Val – valine
Ile – isoleucine	

Table of content

Introduction	5
Literature review.....	10
1. Structure and a substrate specificity of SUB1	10
2. Rationally designed SUB1 inhibitors	12
3. Inhibitors identified by a screening of compound libraries	17
Results and discussion.....	23
1. Synthesis and inhibitory potency of peptidic α -ketoamide inhibitors	23
2. Synthesis and inhibitory activity of peptidic boronic acid inhibitors.....	27
2.1 Synthesis of peptidic boronic acids with a modified P1 position	27
2.2 PfSUB1 inhibitory potency and selectivity of peptidic boronic acids with a modified P1 position.....	32
2.3 Synthesis of peptidic boronic acids with a modified P3 position	34
2.4 PfSUB1 inhibitory potency and selectivity of peptidic boronic acids with a modified P3 position.....	37
2.5 Synthesis of peptidic boronic acids with a modified P5 position	38
2.6 PfSUB1 inhibitory potency and selectivity of peptidic boronic acids with a modified P5 position.....	40
2.7 Synthesis of peptidic boronic acids with a modified P5 and P1 positions.....	41
2.8 PfSUB1 inhibitory potency and selectivity of peptidic boronic acids with a modified P5 and P1 positions	44
Experimental part	46
1. General information.....	46
2. Synthesis of α -ketoamides 5a–j and intermediates.....	46
3. Synthesis of peptidic boronic acids and intermediates.....	68
3.1 Synthesis of peptidic boronic acids with a modified P1 position	68
3.2 Synthesis of peptidic boronic acids with a modified P3 position	68
3.3 Synthesis of peptidic boronic acids with a modified P5 position	86
3.4 Synthesis of peptidic boronic acids with a modified P5 and P1 position	104
Conclusions	119
References	121
Appendix	126

Introduction

Malaria is an acute febrile disease caused by *Plasmodium* parasites and spread to people through the bites of infected *Anopheles* mosquitoes. According to the latest malaria report¹ in 2020 there were estimated 241 million cases of malaria and 627 000 of deaths caused by this infectious disease.

Enzymes of microbial pathogens are well-established drug targets, from the bacterial transpeptidase targets of beta-lactam antibiotics to the protease and reverse transcriptase targets of several anti-viral drugs. Pathogenic protozoa such as the *Plasmodium* species that cause malaria are no exception, and two of the historically most successful antimalarial drugs (pyrimethamine and proguanil) target the parasite dihydrofolate reductase.² However, resistance to these antifolate drugs is now widespread and reports of the emergence of parasite resistance to other front-line antimalarial therapeutics, including artemisinin-based combinations (ACTs), are of great concern.³ There is a widely accepted need to strengthen the antimalarial drug pipeline by the identification of new classes of antimalarial drugs with new modes of action.

All the clinical manifestations of malaria are caused by cycles of parasite proliferation within red blood cells (Fig. 1). Specialised developmental forms called merozoites invade the red cell and rapidly transform within a parasitophorous vacuole (PV) into feeding forms called trophozoites. Over a period of around 48 hours in the case of the most virulent *Plasmodium* species, *Plasmodium falciparum*, the intracellular parasite enlarges, undergoes nuclear division, and finally segments to form 16 or more daughter merozoites. These are released from the host cell in a lytic process called egress to allow the merozoites to invade fresh red cells and repeat the cycle. Research over the past 3 decades has revealed that egress is regulated by a parasite enzyme pathway, with a central role for a calcium-dependent serine protease called SUB1. A single orthologue of SUB1 is found in the genomes of all known *Plasmodium* species, and gene disruption studies have shown that SUB1 is essential for parasite survival. SUB1 is synthesized as an enzymatically inactive zymogen, which undergoes at least two proteolytic processing events⁴. First, autocatalytic cleavage forms p54 (a 54-kDa form), then a second processing step produces the mature p47 (47-kDa form) from p54. The second processing event is mediated by plasmepsin X, a parasite aspartic protease.⁵

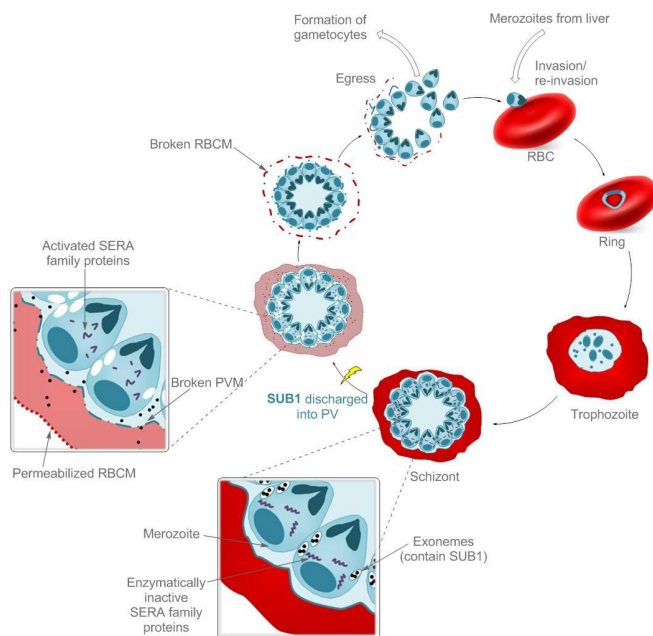
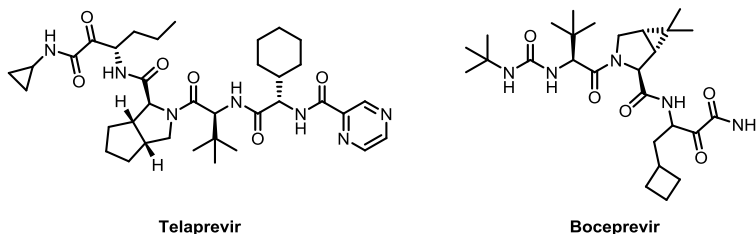


Fig. 1. The asexual blood stage life cycle of *P. falciparum* and the role of SUB1 in egress.

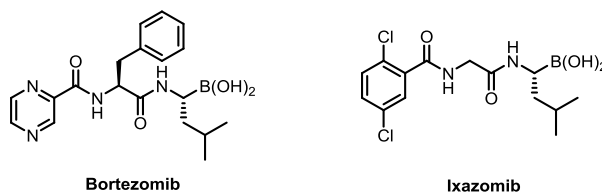
SUB1 is initially stored in a set of merozoite secretory organelles called exonemes and then discharged into the PV lumen just prior to egress in order to encounter and precisely cleave its substrates, leading ultimately to rupture of the PV and red blood cell (RBC) membranes (Fig. 1). A cGMP-dependent parasite protein kinase G (PKG) is required for discharge of SUB1 from exonemes⁶. Multiple substrates of SUB1 have been identified, including merozoite surface proteins and a set of soluble PV proteins called the serine-rich antigen (SERA) family⁷. In genetically SUB1-null parasites, rupture of neither the PV nor RBC membrane occurs, leading eventually to death of the trapped parasites, so small-molecule inhibitors of SUB1 are anticipated to similarly block egress and prevent parasite replication.

Over recent decades, target-based and structure-guided approaches have been applied in drug discovery. Rather than identifying active compounds in cell-based assays first and establishing their target and mechanism of action afterwards, target-based discovery focuses on a specific protein and mechanism of action⁸. Applying reversible covalent warheads in drug design has led to covalent enzyme inhibitors that serve as powerful therapeutics, as well as molecular probes with striking target selectivity⁹. One of the known electrophilic warheads that targets hydroxyl groups in proteins/enzymes is α -ketoamide. And α -ketoamide-based inhibitors form hemiketals when attacked by serine

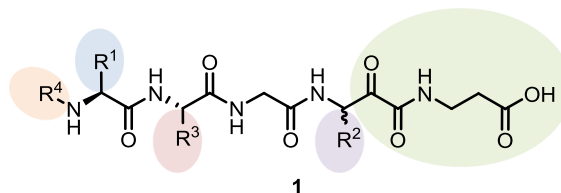
proteases. This approach gave two FDA approved drugs, Telaprevir and Boceprevir; both for treatment of hepatitis C. Unfortunately, both have been recently suspended due to toxicity and less optimal efficacy, highlighting the challenges for reversible covalent inhibitors⁹. Rationally designed α -ketoamide inhibitors derived from SUB1 natural substrate have showed proof-of-concept to inhibit the proteolytic activity of SUB1 (see section 2 in literature review), yet, overall these inhibitors showed no anti-parasite activity in cell based assays, presumably due to the polar nature of these compounds.



Hydroxyl groups in proteins and enzymes, such as the side chains of serine and threonine, can be bound also to boronic acid warhead by forming ate complex, which mimics the tetrahedral transition state⁹. This has made an impact in medicinal chemistry, yielding FDA approved peptidic boronic acid inhibitors, Bortezomib and Ixazomib; both are proteasome inhibitors used for treatment of multiple myeloma. Besides these, there are also other boron-based enzyme inhibitors¹⁰.



The **aim of the Thesis** is to optimize structure **1** in order to improve the inhibitory potency against SUB1 and achieve the inhibition of parasite replication in cell based models.



To achieve the aim of the Doctoral Thesis, **the following tasks were set:**

- ✓ to summarize all the published SUB1 inhibitor discovery efforts;
- ✓ to develop the methods for the synthesis of peptidic derivatives containing boronic acids as warheads for reversible covalent binding to serine residue in the catalytic center of SUB1;
- ✓ to develop the methods for the synthesis of the peptidic ketoamide and boronic acid based inhibitors enabling the installation of different R¹⁻⁴ groups;
- ✓ to determine SUB1 inhibitory potency and parasite growth inhibition in cell based assays of synthesized compounds as well as to evaluate the selectivity *versus* inhibition of mammalian serine and threonine proteases;
- ✓ to analyze structure-activity relationships (SAR) of the synthesized compounds and to use these observations for the design of new SUB1 inhibitors.

Approbation of the thesis

Scientific publications:

1. **Lidumniece, E.**; Withers-Martinez, C.; Hackett, F.; Collins, C. R.; Perrin, A. J.; Koussis, K.; Bisson, C.; Blackman, M. J.; Jirgensons, A. Peptidic boronic acids are potent cell-permeable inhibitors of the malaria parasite egress serine protease SUB1. *Proc. Natl. Acad. Sci. U. S. A.*, **2021**, *118*, e2022696118 (IF(2021): 12.779)
2. **Lidumniece, E.**; Withers-Martinez, C.; Hackett, F.; Blackman, M. J.; Jirgensons, A. Subtilisin-like Serine Protease 1 (SUB1) as an Emerging Antimalarial Drug Target: Current Achievements in Inhibitor Discovery. *J. Med. Chem.* **2022**, *65*, 12535–12545 (IF(2021): 8.039)

Patent application:

Jirgensons, A.; **Lidumniece, E.**; Withers-Martinez, C.; Blackman, M. J.; Finn, P. W. Novel boronic acid containing peptidomimetics as malarial serine protease inhibitors. WO2021/001697, **2021**.

Results of the thesis were presented at the following conferences:

1. **Petrova, E.**; Jirgensons, A. Synthesis of Peptidic α -Ketoamide Analogues of Known PfSUB1 Inhibitor. 10th Paul Walden Symposium on Organic Chemistry, June 15 – 16, **2017**, Riga, Latvia.
2. **Lidumniece, E.**; Jirgensons, A. Peptidic α -ketoamides as PfSUB1 Inhibitors. Balticum Organicum Syntheticum (BOS 2018), July 1 – 4, **2018**, Tallinn, Estonia.

3. **Lidumniece, E.**; Jirgensons, A. Peptidic α -ketoamides as an inhibitors of PfSUB1. VIII EFMC International Symposium on Advances in Synthetic and Medicinal Chemistry, September 1 – 5, **2019**, Athens, Greece.
4. **Lidumniece, E.**; Jirgensons, A. Peptidic boronic acids as inhibitors of PfSUB1. 12th Paul Walden Symposium on Organic Chemistry, October 28 – 29, **2021**, Riga, Latvia.
5. **Lidumniece, E.**; Withers-Martinez, C.; Blackman, M. J.; Jirgensons, A. New peptidic boronic acid containing inhibitors of malarial subtilisin-like serine protease (SUB1). Balticum Organicum Syntheticum (BOS 2022), July 3 – 6, **2022**, Vilnius, Lithuania.
6. **Lidumniece, E.**; Withers-Martinez, C.; Blackman, M. J.; Jirgensons, A. Substrate based inhibitors of malarial subtilisin-like serine protease containing boronic acid warhead. 2nd Drug Discovery Conference, September 22 – 24, **2022**, Riga, Latvia.
7. **Lidumniece, E.**; Withers-Martinez, C.; Blackman, M. J.; Jirgensons, A. Rationally designed inhibitors of malarial subtilisin-like serine protease containing boronic acid warhead. ACS Publications Symposium: Biological and Medicinal Chemistry, March 6–8, **2023**, Bonn, Germany.

Literature review

Several review articles have been published summarizing the function of SUB1 in the life cycle of parasite.^{11,12} To complement these, we here have prepared a comprehensive mini-review covering inhibitor discovery effort for SUB1 inhibitors.

1. Structure and a substrate specificity of SUB1

X-ray crystal structures of SUB1 have shown that it is closely related to several bacterial subtilisins¹³ and have provided detailed insights into the architecture of the SUB1 active site cleft which interacts with protein and peptide substrates. This was aided by the fact that both structures comprise a complex between the SUB1 catalytic domain and its inhibitory prodomain, the C-terminal segment of which lies in the active site groove in a substrate-like manner.¹⁴

A detailed understanding of protease specificity is useful to design potent, selective inhibitors. Towards this, substrate scanning methods were performed to identify protease preferences for certain amino acids.¹⁵ In initial work to evaluate specific substrates of PfSUB1, peptides were synthesised based on the known autocatalytic cleavage site between Asp²¹⁹ and Asn²²⁰ within the decapeptide motif ²¹⁵LVSAD↓NIDI²²³ (Fig. 2).⁴ The specificity of subtilases mainly relies on interactions between P4–P1 residue side chains with enzyme S4–S1 binding sites.¹⁶ Therefore, a range of modifications of the original motif at the P1, P2 or P4 positions were made and tested for efficiency of cleavage by recombinant *P. falciparum* SUB1 (rPfSUB1).

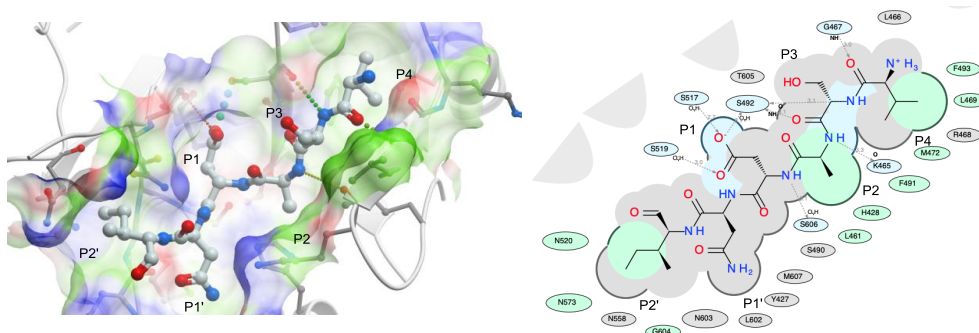


Fig. 2. SUB1 P4-P2' endogenous substrate peptide (SUB1 prodomain) within the SUB1 active site (PDB 4VLO). Figure generated in ICM-Pro (Molsoft).

The results indicated that the enzyme prefers polar or small amino acid residues at the P1 position and is unable to cleave the peptide bond if leucine is at this position. Replacing the P4 valine with either lysine or alanine resulted in a remarkable decrease in

cleavage efficiency, revealing that the P4 position has a significant role in substrate recognition by PfSUB1 and consistent with the hydrophobic nature of the S4 pocket.^{13,17} Substrate scanning of the P2 position clearly showed that only alanine or glycine could be accommodated at this position, with a slight preference for glycine.¹⁷ A comparison of merozoite surface protein (MSP) processing sites with the internal PfSUB1 processing site, the known SERA5 processing sites and the predicted processing sites in SERA4 and SERA6, identified a consensus PfSUB1 recognition motif of Ile/Leu/Val/Thr-Xaa-Gly/Ala-Paa(not Leu)↓Xaa (where Xaa is any amino acid residue and Paa tends to be a polar residue), and an intriguing preference for acidic residues and/or serine and threonine on the prime side of the scissile bond.^{7,17} A structural model of the enzyme and the identification that the most efficiently cleaved peptide corresponded to the SERA4 cleavage site 1 (KITAQ↓DDEES)¹⁷ showed that the P1-P4 segment is held relatively tightly in the enzyme active site groove. Molecular modelling demonstrated that the enzyme S4 pocket is characterised by a lining of hydrophobic residues well suited to the aliphatic residues preferred at the P4 position. The PfSUB1 S3 pocket is not well defined, whilst the substrate P3 residue side chain extends out towards the solvent, explaining the relative lack of specificity at this position. The most obvious characteristic of the S2 pocket is that it is small due to the side chain of lysine 465 (for most of the S8A subtilisins this residue is glycine), explaining the strict limitation for accommodating only small residues at the P2 position. The S1 pocket of PfSUB1 is characterised by a cluster of five polar serine residues. Molecular modelling showed that the S' surface has a highly basic character, supporting the evidence from cleavage site alignments that prime side interactions are important for substrate binding. Experimental investigation of a modified SERA4 site1 substrate confirmed the preference for acidic or hydroxyl-containing prime side substrate residues.¹⁸

Molecular dynamics simulations together with free energy calculations were used to further understand which residues are essential for binding and what are the key interactions. These results¹⁹ suggested that strong canonical hydrogen bonds are formed between peptide residues P4-P2' and the PfSUB1 binding site cleft, but the P3'-P5' residues undergo pronounced conformational changes and bind only occasionally for a short period of time to different regions of the PfSUB1 structure. It was concluded that peptide residues P4 and P2-P1' have the largest impact on the effective free energy with the most favourable interactions formed by residues P4 and P1. The results further suggested that the P5 residue might not be needed to achieve strong binding.¹⁹

2. Rationally designed SUB1 inhibitors

Since peptide α -ketoamides are known to act as covalent inhibitors of serine proteases,²⁰ a potential inhibitor **2** (Fig. 3) was synthesised based on the sequence of the best known natural substrate SERA4 site1 (KITAQ↓DDEES).¹⁸ Ketoamide **2** contained the KITA segment of the peptide sequence, an ethyl group in the P1 position and a cyclopropyl group placed towards the P' side. Dose-response experiments confirmed this proof-of-concept inhibitor, determining an IC_{50} for inhibition of rPfSUB1 of $\sim 6 \mu\text{M}$. Compound **2** was also able to inhibit SUB1 of the other important *Plasmodium* species *P. vivax* (PvSUB1) and *P. knowlesi* (PkSUB1) with similar IC_{50} values of $\sim 12 \mu\text{M}$ and $\sim 6 \mu\text{M}$, respectively. Based on further modelling and experimental data, a modified compound **3** (called KS-466) was synthesised which possessed a carboxylic group on the prime side of the α -ketoamide functionality, designed to mimic the prime side preference for acid groups. Dose-response experiments showed improved IC_{50} values against PfSUB1 and PkSUB1 of $\sim 1 \mu\text{M}$, and an IC_{50} against PvSUB1 of $\sim 2 \mu\text{M}$.

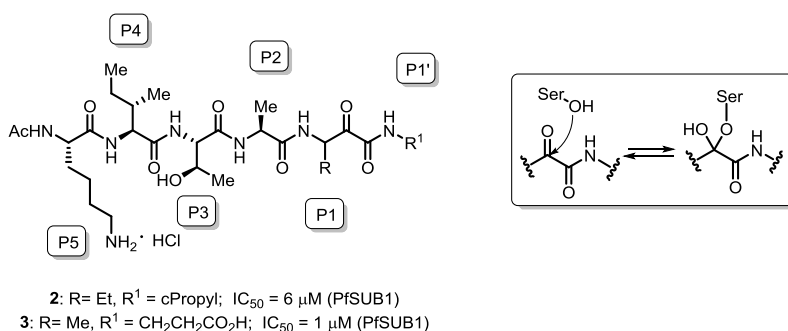


Fig. 3. PoC substrate derived SUB1 inhibitor with α -ketoamide functionality as a serine trap.

Systematic structure-activity relationship investigation of peptidic α -ketoamides based on the structure of **3** (Fig. 4) was performed to explore crucial enzyme-inhibitor interactions²¹. When the P5 lysine residue was omitted (based on the outcome of the MD simulation studies), this resulted in 2-fold lower inhibitory activity compared to compound **3**; however, the structure was considerably simpler so subsequent analogues for SAR were synthesised without this lysine residue. Analysis of the prime side residue (P1') revealed that the best linker resembles an aspartic acid residue. Longer or shorter chains or an amide analogue resulted in decreased activity. Previous data suggested that only small amino acids can be accommodated at the P2 position, so the original methyl- substituent was replaced with di-methyl- and cyclopropyl- substituents; again, both compounds showed

decreased activity. As a result, only glycine at the P2 position showed increased activity with respect to the starting compound. The relevance of the substituent at the P4 position was investigated by substitution with alanine. This produced a dramatic loss of inhibitory activity, in agreement with previous results showing that the hydrophobic S4 pocket accommodates an isoleucine residue very well and that this is important for binding. Substitution of this residue with a less hydrophobic methyl group resulted in loss of crucial Van der Waals interactions. Replacement of the threonine at the P3 position with alanine led to decreased inhibitory potency which was interpreted as likely resulting from an increased solvation penalty as the side chain of P3 points away from the binding site towards the solvent. Exploration of the P1 position revealed that a glutamine side chain (preferred in the original substrate sequence KITAQ↓DDEES) was not compatible with the ketoamide functional group. A series of different P1 substituents were investigated, showing that only small substituents can be placed at this position.

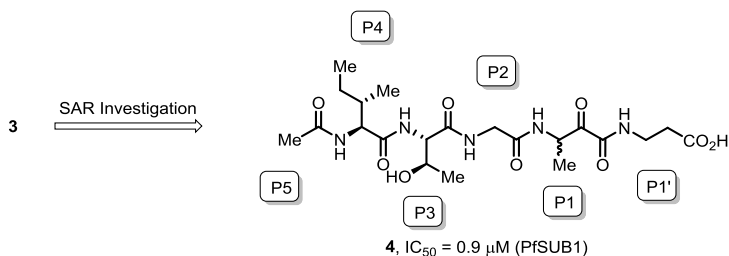


Fig. 4. Optimized ketoamide containing inhibitor **4** and SAR of P5-P1' substitution (see text).

Based on the importance of the P4 position for binding and recognition, a peptidic ketoamide series **5** was synthesised by the incorporation of a range of unnatural amino acids to explore this side chain (Fig. 5).²² Investigations of potency relative to the parent isoleucine analogue **4** revealed an improved inhibitor **5** containing a hydrophobic P4 cyclopentyl- substituent ($IC_{50} \sim 370$ nM). Unfortunately, none of the ketoamide inhibitors **5a-j** showed measurable activity against the parasite in vitro at concentrations up to 100 μM , probably due to poor membrane-permeability properties and their charged nature.

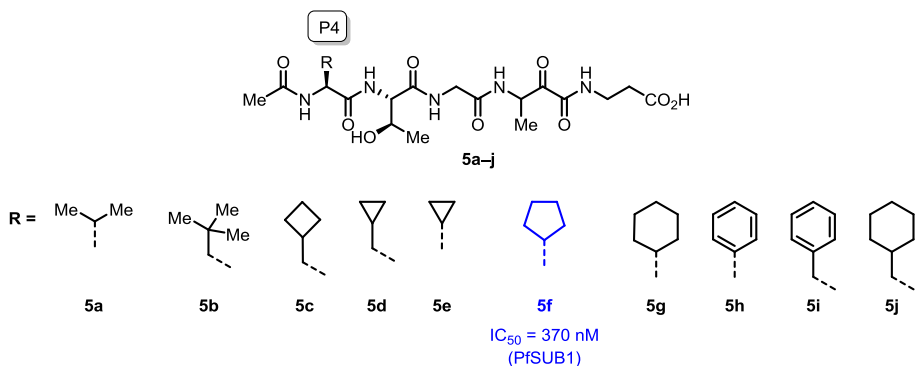


Fig. 5. Peptidic ketoamide series **4** with a modified P4 position.

The SERA4 site1 cleavage sequence was used as the basis for another ketoamide-based inhibitor,²³ the nonapeptide isocaproyl-KITAQ(CO)DDEE-NH₂ **6** (called JMV5126). Reported IC₅₀ values for this compound were 17.8 ± 2.9 μM against PfSUB1 and 10.5 ± 1.6 μM against PvSUB1 (Fig. 6).

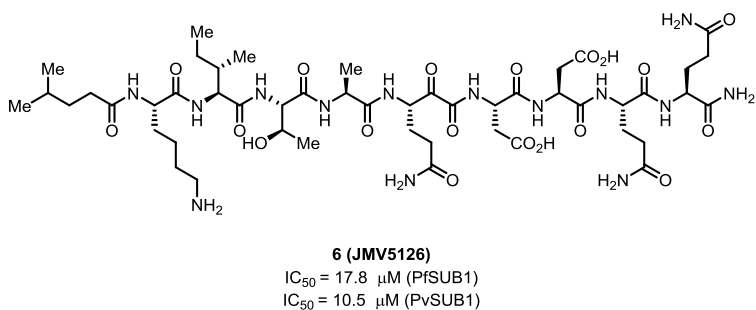


Fig. 6. Ketoamide containing inhibitor **JMV5126** with substituents extended to the prime part of the SUB1 active site.

A difluorostatone moiety (a substructure of statine derived 3,3-difluoro-6,6-dimethyl-2-heptanoic acid²⁴) was another serine trap which was exploited for rationally designed inhibitors of PfSUB1. These compounds were also based on the PfSUB1 substrate SERA4 site 1 (Fig. 2). A carboxylic acid with one or two carbon linkers (compounds **7–10**) was added to mimic the P1' element of the substrate (Fig. 7).²⁵ Molecular dynamics simulations were confirmed by potency assays which indicated that the best length of the linker is one carbon, as in compound **7**. Molecular docking results showed that compound **7** can form several important hydrogen bonds with key residues in the SUB1 binding cleft, as well as strong interactions between the terminal carboxylic group and amino acid residues in the S' pocket, while inhibitor **10** did not show this pattern of interactions. Removal of the terminal lysine generated compound **8** with the same IC₅₀

value as the parent compound ($IC_{50} = 0.6 \mu\text{M}$). This was in line with modelling experiments indicating that the P5 side-chain is not involved in important binding interactions with the enzyme. However, further truncation of the P4 amino acid (**9**) resulted in almost no inhibition of recombinant enzyme suggesting that it is necessary to have at least a tripeptide at the non-prime side of difluorostatones for binding to the enzyme. Both inhibitors **7** and **8** were tested against other *Plasmodium* species SUB1 enzymes and found to possess low micromolar activity against PkSUB1 ($IC_{50} = 1.12 \mu\text{M}$ for **7** and $IC_{50} = 0.68 \mu\text{M}$ for **8**) and PvSUB1 ($IC_{50} = 2.5 \mu\text{M}$ and $IC_{50} = 2.2 \mu\text{M}$, respectively).²⁶

SAR investigation of P2-P4 substituents of the difluorostatone-based inhibitor **8** involved modification of the original structure by replacing amino acids in the parent inhibitor with different natural and non-natural amino acid analogues.²⁷ Overall, from these SAR studies it was concluded that the P4 and P3 side chains form hydrophobic interactions with SUB1, since isoleucine was preferred in the P4 position and valine as well as benzyl-protected threonine at P3 helped to improve the inhibitory potency. The most potent inhibitor **11** from these series of compounds, with an $IC_{50} = 0.25 \mu\text{M}$ possessed valine in P3 together with glycine in the P2 position (Fig. 7).

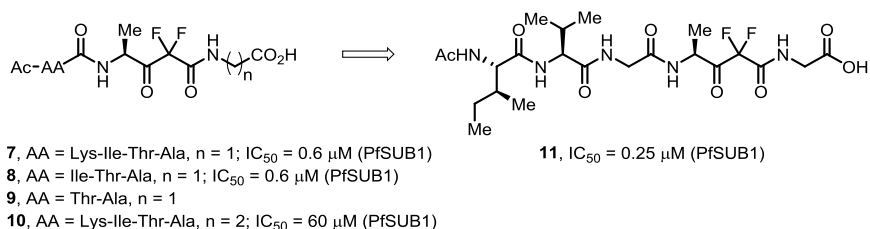


Fig. 7. SUB1 inhibitors containing a difluorostatone moiety.

An attempt to reduce the peptidic nature of the inhibitors was made by introducing different end-capping groups at the P3/P4 position. Decent inhibitory activity against PfSUB1 ($IC_{50} = 1 \mu\text{M}$) was achieved for compound **12** (Fig. 8) from all of the synthesised analogues with a reduced peptidic nature.

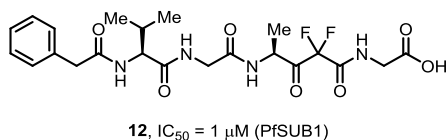


Fig. 8. Difluorostatone based SUB1 inhibitor with reduced peptidic nature.

Examination of the structurally related serine traps trifluoromethylketone and carboxydifluoromethylketone (Fig. 9) was performed. However, compounds **13** and **14** were not able to inhibit SUB1 at concentrations as high as $50 \mu\text{M}$.

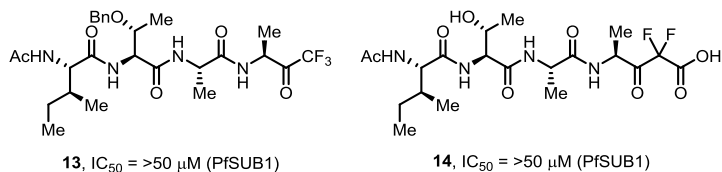


Fig. 9. Trifluoromethylketone and carboxydifluoromethylketone containing inhibitors.

Boronic acids are well-established warheads in inhibitors of serine proteases^{10,28,29} and have been clinically validated as drug compatible substructures in marketed drugs such as Bortezomib, Ixazomib, Vaborbactam and Tavorole.³⁰ Replacement of the α -ketoamide functionality in compound **4** with boronic acid resulted in inhibitor **15** with substantially increased PfSUB1 inhibitory potency ($IC_{50} = 69 \text{ nM}$, Fig. 10).²² A 10-fold lower IC_{50} value was achieved when both the cyclopentyl group at P4 and the boronic acid serine trap moiety were combined, resulting in compound **16a** with low nanomolar potency ($IC_{50} = 9.3 \text{ nM}$). Expanding the study to analyse the stereochemistry of the boronic acid moiety indicated that the chiral center has to resemble L-amino acid stereochemistry. SAR investigations of substituents at the P1 position of the boronic acid compounds revealed a compound bearing a hydroxyethyl substituent **16d** that displayed increased SUB1-inhibitory potency ($IC_{50} = 4.6 \text{ nM}$). Unfortunately, compound **16d** did not show high anti-parasite potency in vitro compared to the parental compound **16a** ($EC_{50} = 15.0 \mu\text{M}$ vs $2.3 \mu\text{M}$).

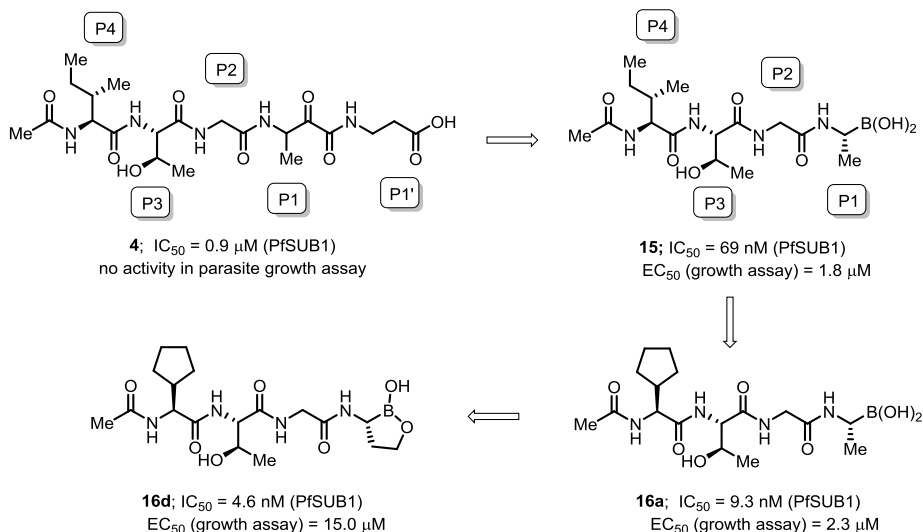


Fig. 10. Development of boronic acid-containing peptidic SUB1 inhibitors.

Interestingly, significantly improved potency in the parasite growth assay was achieved for boronic acid based peptidic inhibitors **17a** and **17b** which possessed a modified P3 position, i.e. replacement of threonine with alanine and valine, respectively (Fig. 11). This was explained by the increased lipophilicity of these compounds which likely resulted in better membrane permeability. Compound **17b** is the best inhibitor of PfSUB1 known to date in the literature, with low nanomolar enzymatic inhibitory activity and submicromolar potency in parasite growth assays ($IC_{50} = 5.7$ nM and $EC_{50} = 0.26$ μ M). Importantly the compounds showed considerable potency in inhibiting merozoite egress from infected RBCs.²²

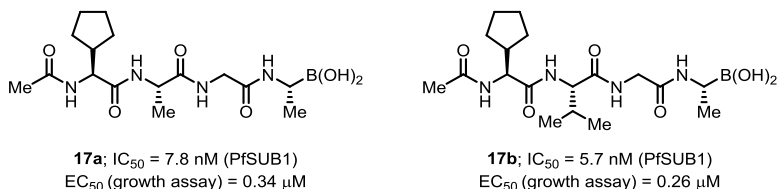


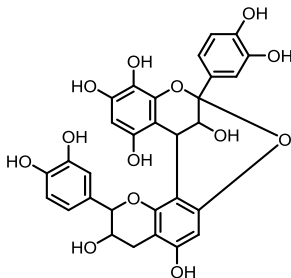
Fig. 11. Inhibitors of PfSUB1 with activity in cell based parasite growth and egress assays.

3. Inhibitors identified by a screening of compound libraries

An interesting SUB1 inhibitor of protein origin was identified by screening the antimalarial activity of the components of venom of the spider *Psalmopoeus cambridgei*. A protein called psalmopeotoxin I (PcFK1) was reported to inhibit the growth of *P. falciparum* parasites with an EC_{50} of 116 μ M.³¹ The sequence of PcFK1 was compared to the PfSUB1 autocatalytic cleavage sequence as well as to cleavage site sequences within SERA family members and merozoite surface proteins. Two regions of PcFK1 were found to share structural similarities (called site 1 and 2). Through computational analysis, the authors concluded that site 2 most likely interacts with the enzyme to mediate inhibitory activity. In rPfSUB1 and rPvSUB1 enzymatic assays, PcFK1 displayed inhibition constants (K_i) of 29.3 μ M and 36.3 μ M, respectively, supporting the hypothesis that SUB1 is a target of the spider venom protein.

To discover small molecule inhibitors of PfSUB1, a fluorescence-based assay³² was used to screen more than 170000 low molecular weight compounds from a range of sources.⁷ This identified a natural product **18** (called MRT12113, Fig. 12), which inhibited PfSUB1 with an $IC_{50} = 0.3$ μ M. Further characterisation revealed that **18** is a highly selective inhibitor of PfSUB1, showing no inhibition of several other tested proteases at concentrations up to 50 μ M. More detailed experiments showed that **18** prevented egress

of *P. falciparum* merozoites *in vitro* and prevented RBC invasion (ED_{50} against schizont rupture around 108 μM and invasion 25 μM). Crucially, the compound was found to prevent maturation of SERA family proteins, but also processing of merozoite surface proteins, shedding the first insights into the endogenous substrates of SUB1.



18; $IC_{50} = 0.3 \mu\text{M}$ (PfsUB1)

Fig. 12. Natural product MRT12113 (**18**) identified by screening.

In a separate study, a screen of a library containing around 1200 irreversible small-molecule protease inhibitors identified a number of specific serine and cysteine protease inhibitors.³³ All these compounds were characterised for their purity, stability, and effects on different stages of the *P. falciparum* blood stage parasite life cycle. The final set of hit compounds were tested for their general toxicity. From these, chloroisocoumarin **19** (Fig. 13) was selected as the best inhibitor of PfSUB1 with an $IC_{50} = 18 \mu\text{M}$, and an $EC_{50} = 22 \mu\text{M}$. The authors searched for analogues of this compound to establish a structure activity relationship; however none of the six follow up compounds **20–25** showed improved activity compared to the parent inhibitor **19**.

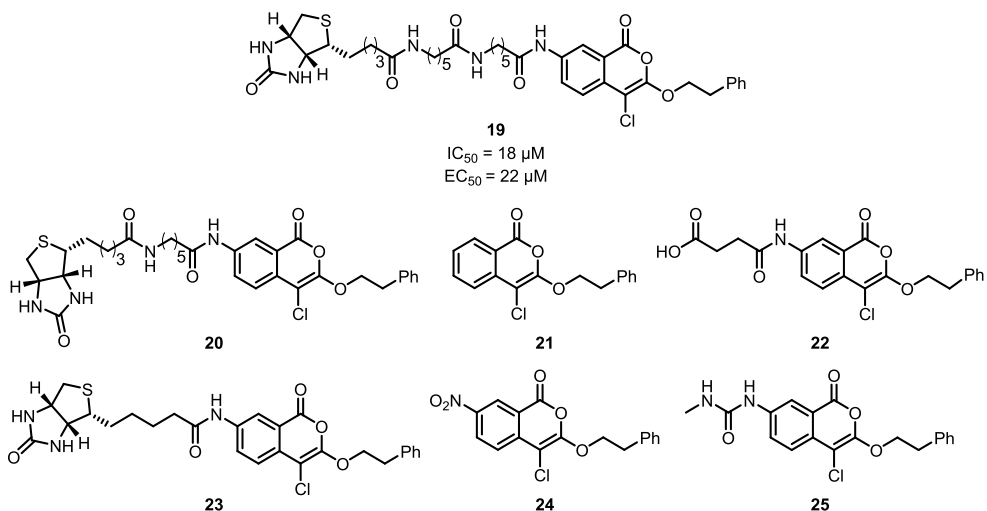


Fig. 13. Chloroisocoumarin containing SUB1 inhibitor **19** and its analogues **20–25**.

A screening of a library comprising ~450 peptidic and non-peptidic compounds was performed. This resulted in identification of the quinolyhydrazone **26** (Fig. 14) as an inhibitor of PfSUB1 with an $IC_{50} = 20 \mu M$.³⁴ Analogues of the hit compound were prepared to investigate SAR and improve potency. First, substituents at the arylidene moiety were explored. The results indicated that hydrogen bond acceptor/donor groups do not improve inhibitory potency. From the analogues bearing electron-withdrawing groups at the arylidene, only compound **27** bearing a cyano group showed potency, although slightly reduced with respect to the original compound **26**. Second, substituents at the quinoline moiety were explored. The results suggested that the fused dioxolane ring can be replaced with a 6-methoxy group, though inhibitory potency was somewhat decreased (**28**, $IC_{50} = 20\text{--}30 \mu M$) compared to **26**. Other modifications, such as replacement of the quinoline with pyridine, benzimidazole, or tetrahydroacridine generated less potent PfSUB1 inhibitors. Substitution of the hydrazone linker with other linkers also did not improve the inhibitory potency. The authors hypothesised that quinolyhydrazones could be covalent inhibitors through attack of the active site serine by the relatively electrophilic bezylidene carbon. However, the enzyme recovered its activity after removal of the inhibitor **26** implying either a competitive or covalent reversible inhibition mechanism.

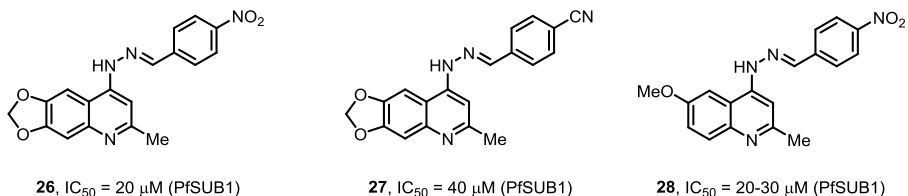


Fig. 14. Quinolyhydrazone containing inhibitors.

In silico screening against a PvSUB1 model and assaying of the inhibitory potency for the most promising compounds resulted in a set of 5 compounds (Fig. 15) displaying inhibitory potency at low micromolar concentrations, which provides a good starting point for further development.³⁵ Compounds **29–31** showed improved activity against PvSUB1 and also against both the *P. falciparum* chloroquine-sensitive 3D7 and chloroquine-resistant Dd2 clones. Dose-dependent reduction of processing of the endogenous PfSUB1 substrate SERA5 demonstrated that the most promising compound **30** is able to inhibit endogenous PfSUB1. Compounds **32** and **33** showed activity against recombinant PvSUB1, however did not inhibit *P. falciparum* growth *in vitro* ($EC_{50} > 50 \mu M$). According to the docking pose of compound **30** into a model of PvSUB1 the inhibitor almost completely occupies the PvSUB1 catalytic groove. The indole carboxamide part of

the inhibitor forms two hydrogen bonds in the S4 subpocket while the aniline moiety resides in the S1 subpocket, forming three hydrogen bonds.

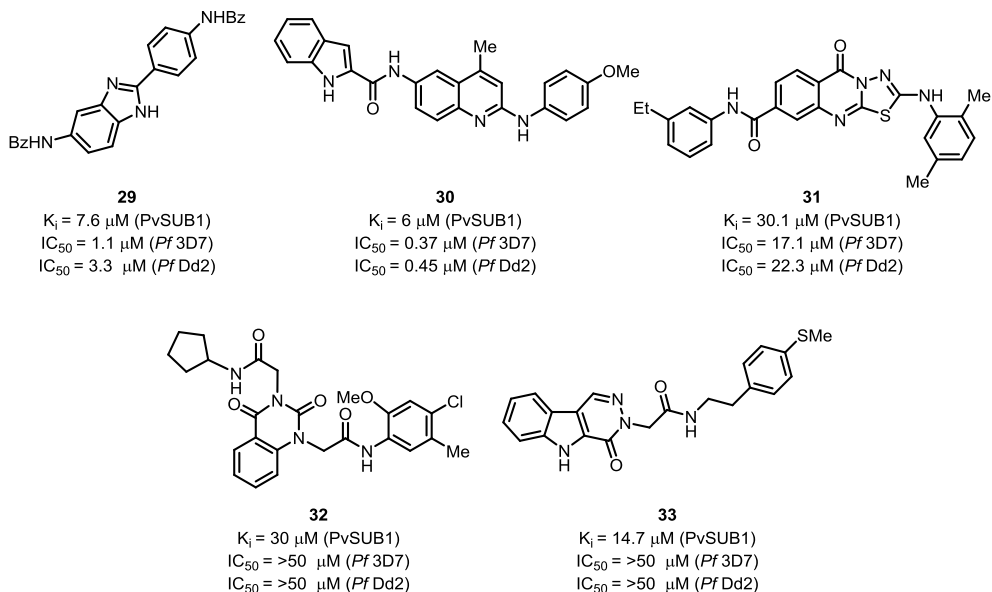


Fig. 15. SUB1 inhibitors identified by virtual screening.

To search for non-peptidic inhibitors of *Pf*SUB1, the Malaria Box (a collection of 400 compounds with confirmed antimalarial activity) was screened³⁶ using the *Pf*SUB1 enzyme assay.¹⁸ The screen identified a quinoxaline derivative **34** as a hit compound with an $\text{IC}_{50} = 10 \mu\text{M}$ (Fig. 16). A range of analogues was prepared by varying R substituents; however, none of them gave improved activity. In fact, only the disubstituted (3-Cl-4-Br) quinoxaline analogue **35** possessed similar activity with respect to the hit compound **34**. The substitution pattern in the quinoxaline moiety was briefly explored. The results indicated that one of the hydrogen atoms at the quinoxaline can be replaced with chloride and another with an amino or mesylamino group to obtain inhibitors **36** and **37** with the potency very similar to that of the parent inhibitor **34**.

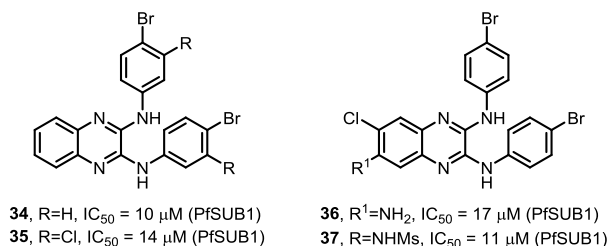


Fig. 16. Malaria Box quinoxaline derivatives as *Pf*SUB1 inhibitors.

Maslinic acid **38** (MA), a natural pentacyclic triterpene with known potential to inhibit intra-erythrocytic stages of *P. falciparum* was tested on four different representative proteases of the classes known to be expressed in the *Plasmodium* parasite life cycle.³⁷ *Bacillus licheniformis* subtilisin A was used as model serine protease and was found to be inhibited by MA with an $IC_{50} = 59 \mu\text{M}$ (fig. 17). Given the similarity of PfSUB1 to subtilisin A, the effects of MA on maturation of merozoite surface proteins in parasite cultures (mediated by PfSUB1) were examined. Although inhibition of MSP1 processing by MA was observed, the compound had no effect on parasite replication. In contrast, the previously reported highly specific PfSUB1 inhibitor⁷ showed no apparent effect on parasite pre-schizont stages, but rather very specific inhibition of schizont rupture and reduced invasion of the released merozoites. Cultures treated with MA displayed an increased fraction of ring, trophozoite or schizont stages, leading the authors to suggest that MA might have additional targets in the intra-erythrocytic stages, possibly through inhibition of parasite metalloproteases.

Two other natural pentacyclic triterpenes – ursolic acid and betulinic acid – and their analogues were presented as potential SUB1 inhibitory compounds (Fig. 17), although these have not been tested in a SUB1 enzymatic assay.³⁸ From the analogues investigated for ability to inhibit parasite growth *in vitro* the most active compound was betulinic acid condensed with butanoic acid at C-3 (compound **39**) which demonstrated an IC_{50} value of $3.4 \mu\text{M}$ against the *P. falciparum* W2 clone.

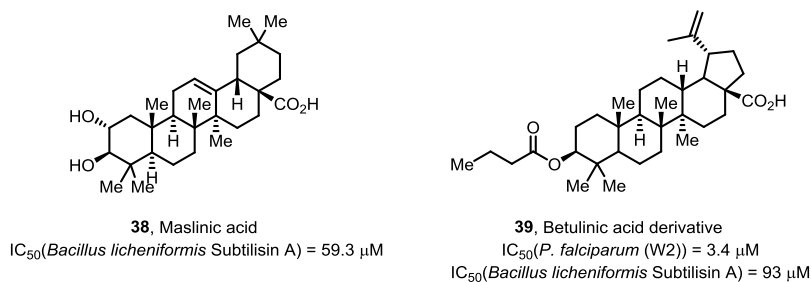


Fig. 17. Pentacyclic triterpenes as putative SUB1 inhibitors.

Docking of compound **39** into the active site of the PfSUB1 model revealed a binding energy -7.02 kcal/mol . The most important contribution for this binding stems from interactions between the carboxylic acid and ester groups of compound **39** with the target protein. Possible inhibition of PfSUB1 by compound **39** *in vitro* was analysed using *Bacillus licheniformis* subtilisin A as a model protein, but this revealed only relatively low inhibitory potency ($IC_{50} = 93 \mu\text{M}$). The antimalarial activity of the compound may result

from targeting other parasite proteins, or alternatively compound **39** could exhibit higher potency against PfSUB1 than against subtilisin A.

Results and discussion

In the previous studies of our group, a SUB1 inhibitor was developed, which was based on SUB1 natural substrate SERA4 cleavage site 1 decapeptide sequence (KITAQ↓DDEES) where the scissile bond was replaced with α -ketoamide substructure²¹ (Fig. 18). Studies of structure activity relationships led to an analogue **4** that possessed sub-micromolar inhibitory potency against recombinant PfSUB1.

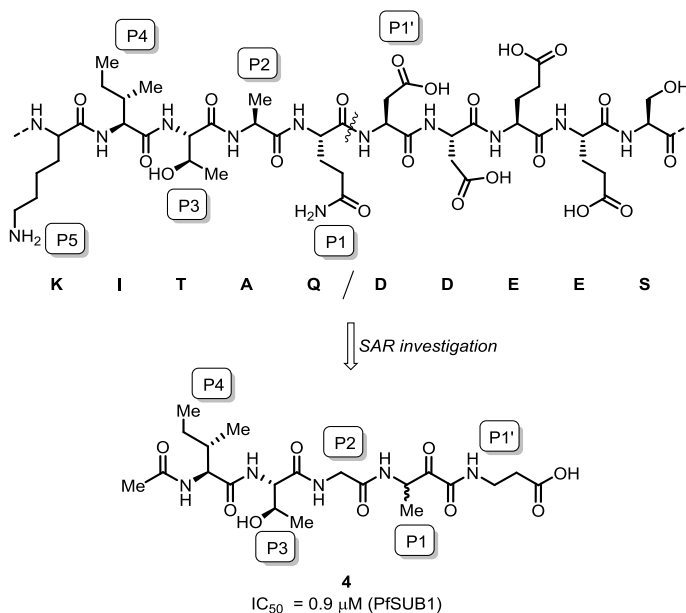


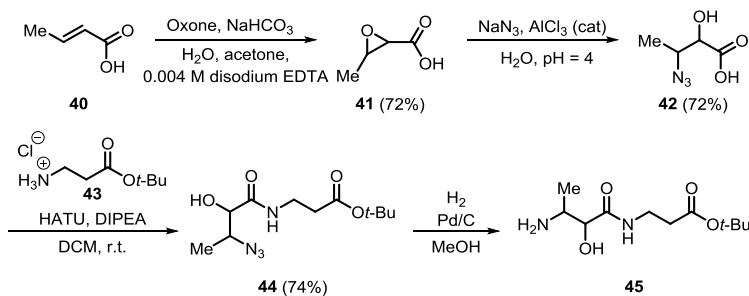
Fig. 18. Sub-micromolar ketoamide inhibitor **4** derived from SUB1 natural substrate.

Unfortunately, compound **4** and related α -ketoamides showed no anti-parasite activity in cell based assays. This was perhaps unsurprising due to the polar nature of these compounds, including the presence of a carboxylic acid moiety which was designed to mimic endogenous PfSUB1 substrate by interacting with the basic S' surface of the PfSUB1 active-site cleft. The polar inhibitors like **4** presumably had poor membrane-permeability properties. In our work we decided to modify the structure of compound **4** at P4 position as the previous substrate scanning studies¹⁷ showed that hydrophobic substituents are preferred at this position.

1. Synthesis and inhibitory potency of peptidic α -ketoamide inhibitors

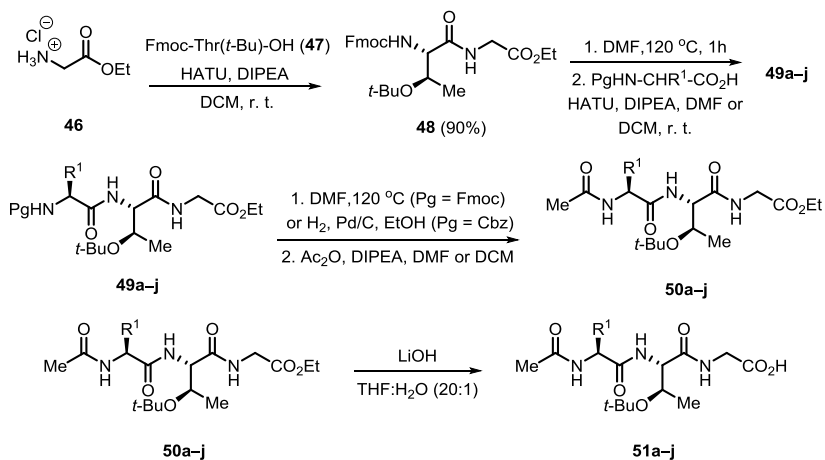
The synthesis of peptidic α -ketoamide inhibitors with modified P4 position were performed in analogy to the described literature procedures.²¹ First, building block **45** was

prepared starting from *trans*-crotonic acid (**40**) (Scheme 1). In the presence of oxone it was epoxidized to 2,3-epoxybutyric acid (**41**). AlCl₃ catalyzed epoxide opening reaction with sodium azide gave α -hydroxy, β -azidobutyric acid (**42**), which was subjected to the coupling with β -alanine *tert*-butyl ester hydrochloride (**43**) to give amide **44**. Azide reduction with Pd/C, H₂ in the intermediate **44** gave amine **45**, which was used in the next reaction step without purification.



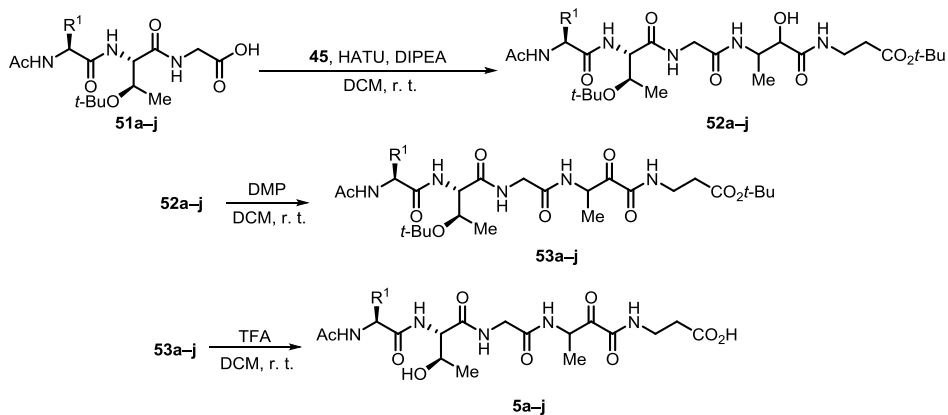
Scheme 1. The synthesis of amine **45**.

Non-prime peptidic part of the inhibitors was synthesized by coupling *N*-Fmoc-, *O*-*tert*-butyl-protected L-threonine (**47**) with glycine ethyl ester hydrochloride (**46**) to form amide **48** (Scheme 2). According to the Fmoc-solution phase peptide synthesis,³⁹ the protecting group was initially cleaved with 4-(aminomethyl)piperidine followed by extraction of the reaction mixture with phosphate buffer of pH 5.5 to get the free amine. Unfortunately, the following coupling reaction yielded very low amount of the desired product **49**. The cleavage of Fmoc- protecting group by heating the starting material in DMF avoiding the extractive work-up turned out to be more productive.⁴⁰ The resulting amine was coupled with different natural and non-natural amino acids to get intermediates **49a–j**. Depending on the protecting group at nitrogen in compounds **49a–j**, either DMF, 120 °C or Pd/C, H₂ was used for the deprotection. The resulting free amines were *N*-acetylated using acetic anhydride in the presence of DIPEA to give intermediates **50a–j**. Finally, ethyl ester was hydrolyzed with lithium hydroxide providing acids **51a–j** (see Table 1 for yields).



Scheme 2. The synthesis of peptidic scaffolds **51a-j**.

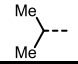
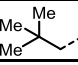
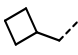
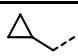
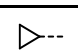
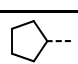
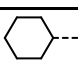
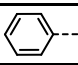
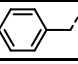
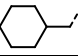
Building blocks **51a-j** and **45** were coupled by using HATU as a coupling agent to provide products **53a-j** (Scheme 3). After oxidation of hydroxyl group with DMP and the cleavage of *tert*-butyl groups with TFA, the final compounds **5a-j** were obtained as a mixture of diastereomers (see Table 1 for yields).



Scheme 3. The synthesis of α -ketoamide inhibitors **5a-j** from peptidic scaffolds **51a-j**.

Table 1

Substituents and reaction yields

Entry	R ¹	Yield, %					
		49	50	51	52	53	5
1.	a 	69	84	38	74	73	99
2.	b 	85	87	95	64	74	99
3.	c 	68	73	97	84	19	89
4.	d 	84	82	36	66	74	77
5.	e 	83	60	55	69	78	99
6.	f 	88	63	91	84	60	98
7.	g 	23	53	n.i. ^a	63	63	76
8.	h 	52	68	99	83	53	99
9.	i 	55	77	93	60	68	99
10.	j 	77	84	91	59	78	94

^an.i. not isolated

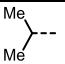
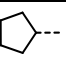
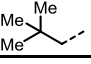
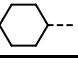
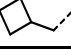
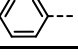
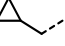
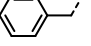
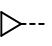
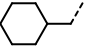
Proteolytic potency^a of all synthesized compounds (see Table 2) was tested by monitoring the cleavage of the peptidic fluorogenic substrate SERA4st1F-6R12 (Ac-CKITAQDDEESC-OH possessing tetramethylrhodamine labeling of both cysteine residues) in the presence of recombinant PfSUB1. When an inhibitor was added to the mixture at 10 μ M concentration, the subsequent fluorescence increase was continuously monitored and the degree of substrate cleavage inhibition was determined.

Results indicated that inhibitors bearing phenyl **5i** or cyclohexylalanine **5j** (Table 2, entries 9 and 10) at P4 position showed reduced potency, also the inhibitor **5e** with cyclopropylglycine (entry 5) at P4 showed poor inhibition, presumably due to insufficient interaction with hydrophobic S4 pocket. Most of all other tested compounds (entries 1–4, 7–8) showed moderate to very good activity at 10 μ M concentration, particularly when isoleucine was replaced with cyclopentylglycine **5f** (entry 6). An IC₅₀ value for compound **5f** was determined to be 370 \pm 3.35 nM, it was 2-fold increase compared to the parent inhibitor **4**.

^a In collaboration with M. J. Blackman, C. Withers-Martinez *et al.*, Malaria Biochemistry Laboratory, The Francis Crick Institute.

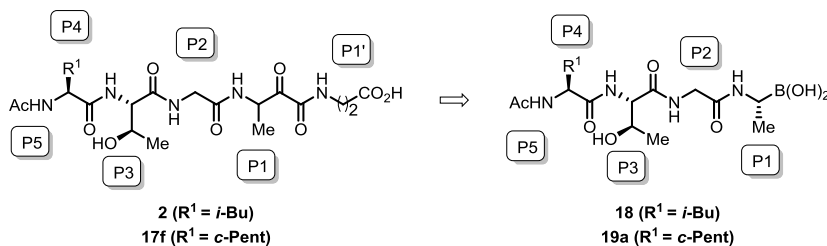
Table 2

Inhibitory potency of α -ketoamide inhibitors **5a–j**^a

Entry	R ¹	Degree of rPfSUB1 inhibition at 10 μ M, %	Entry	R ¹	Degree of rPfSUB1 inhibition at 10 μ M, %		
1.	5a		78	6.	5f		97
2.	5b		71	7.	5g		75
3.	5c		73	8.	5h		56
4.	5d		78	9.	5i		38
5.	5e		45	10.	5j		23

2. Synthesis and inhibitory activity of peptidic boronic acid inhibitors

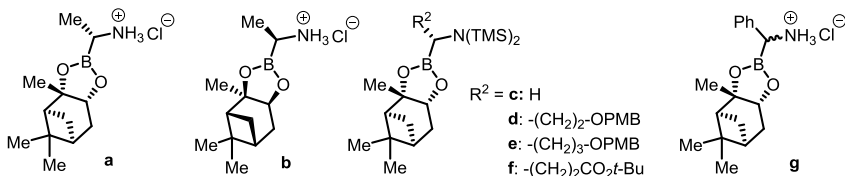
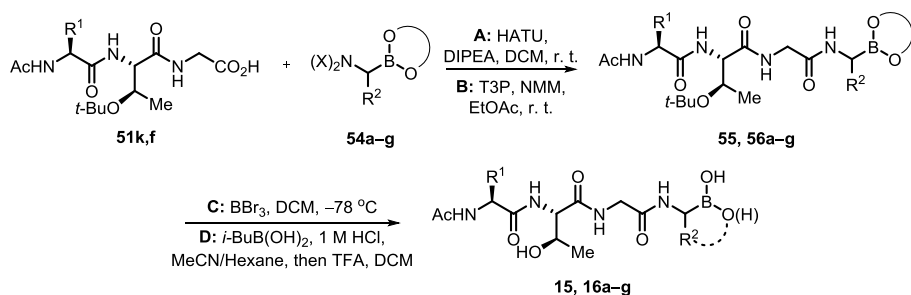
Boronic acids are known as efficient warheads for covalent reversible inhibitors of serine proteases^{10,28,29} which prompted us to investigate them as substructures for SUB1 inhibitors. α -Ketoamide moiety in compounds **4**, **5f** (R¹ = 2-butyl or cyclopentyl) was replaced with boronic acid moiety (Fig. 19) and the compounds **15**, **16a** were selected as a base for further development of PfSUB1 inhibitors by modifying P1, P3 and P5 positions.

Fig. 19. Covalent reversible serine binding group as an alternative to α -ketoamide.

2.1 Synthesis of peptidic boronic acids with a modified P1 position²²

To evaluate SAR of P1 amino acid side chain, boronic acid derivatives were synthesized bearing different cyclic or acyclic boronic acid moieties at P1 position (Scheme 4). Building blocks **51k,f** and **54a–g** were coupled by using HATU or T3P as coupling agents to provide the products **55**, **56a–g**. Protecting groups were cleaved either by BBr₃ in DCM at -78 °C or by treatment with isobutylboronic acid followed by TFA in DCM. It gave free boronic acids **15**, **16a–g** in moderate to good yields (see Table 3).

^a Single measurement for each compound; in collaboration with M. J. Blackman, C. Withers-Martinez *et al.*, Malaria Biochemistry Laboratory, The Francis Crick Institute.



Scheme 4. Synthesis of the peptidic boronic acids with a modified P1 position.

Table 3

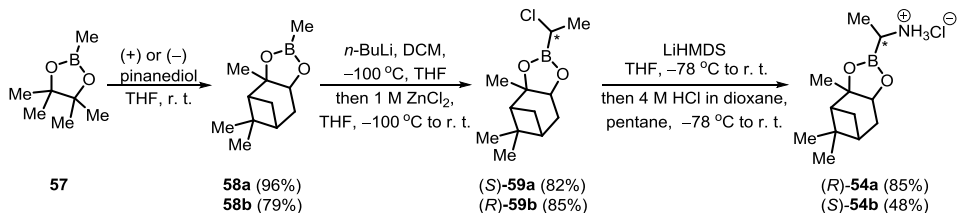
Substituents and reaction yields

Entry	R ²	R ¹	Yield, %	
			55/56	15/16
1.	a		55 (A)	85 (B)
2.	a		64 (C)	49 (D)
3.	b		59 (C)	47 (D)
4.	c		31 (C)	75 (D)

Entry	R ²	R ¹	Yield, %	
			56	16
5.	d		35 (C)	93 (D)
6.	e		22 (C)	81 (D)
7.	f		52 (C)	66 (D)
8.	g		70 (C)	90 (D)

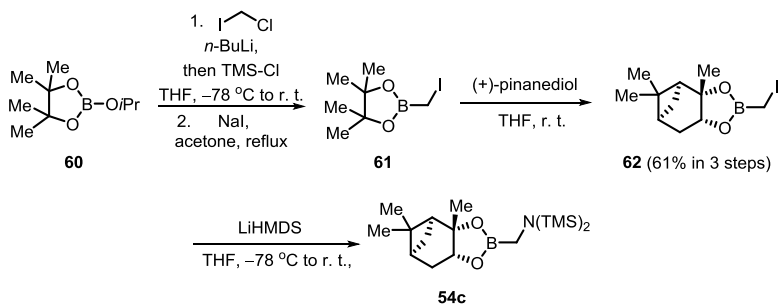
The synthesis of boronic acid building blocks **54a–g** was performed as described in schemes 5–8. To synthesize the corresponding α -amino boronic acid derivative **54a** that resembles L-alanine stereochemistry, the Matteson homologation⁴¹ was used (Scheme 5). First, methylboronic acid pinacol ester (**57**) was converted to (+)-pinanediol ester **58a** in an excellent yield. Second, dichloromethyl lithium species was generated *in situ* at $-100\text{ }^{\circ}\text{C}$ and to this the boronic ester **58a** was added. Zinc(II) chloride promoted rearrangement of the intermediate ate-complex gave the desired α -chloro boronic acid ester **59a**. This was subjected to $\text{S}_{\text{N}}2$ reaction with LiHMDS to give bis-TMS protected α -amino boronic acid ester. After addition of 4 M HCl in dioxane, the desired building block **54a** was isolated as hydrochloride salt (85% yield).

To obtain the stereoisomer **54b** the same pathway as described above was employed (Scheme 5), but (–)-pinanediol was used to prepare a chiral boronic ester **58b**. It was transformed to chloride (*R*)-**59b** which was used to make the compound **54b** where α -amino boronic acid moiety resembles D-alanine stereochemistry.



Scheme 5. The synthesis of boronic acid containing building blocks **54a,b**.

To optimize the synthesis of the building blocks **54c–f**, the key intermediate **62** was prepared (Scheme 6). Isopropoxyboronic acid pinacol ester (**60**) was subjected to homologation with chloromethyl lithium species. According to GC-MS analysis the reaction mixture contained iodo-/chloro-substituted products in a 1 : 5 ratio, thus, the crude product was dissolved in acetone and sodium iodide was added to get a full conversion to iodomethylboronic acid pinacol ester (**61**). Transesterification of the pinacol ester **61** with (+)-pinanediol led to an intermediate **62**, which was converted to a building block **54c** by the treatment with LiHMDS.

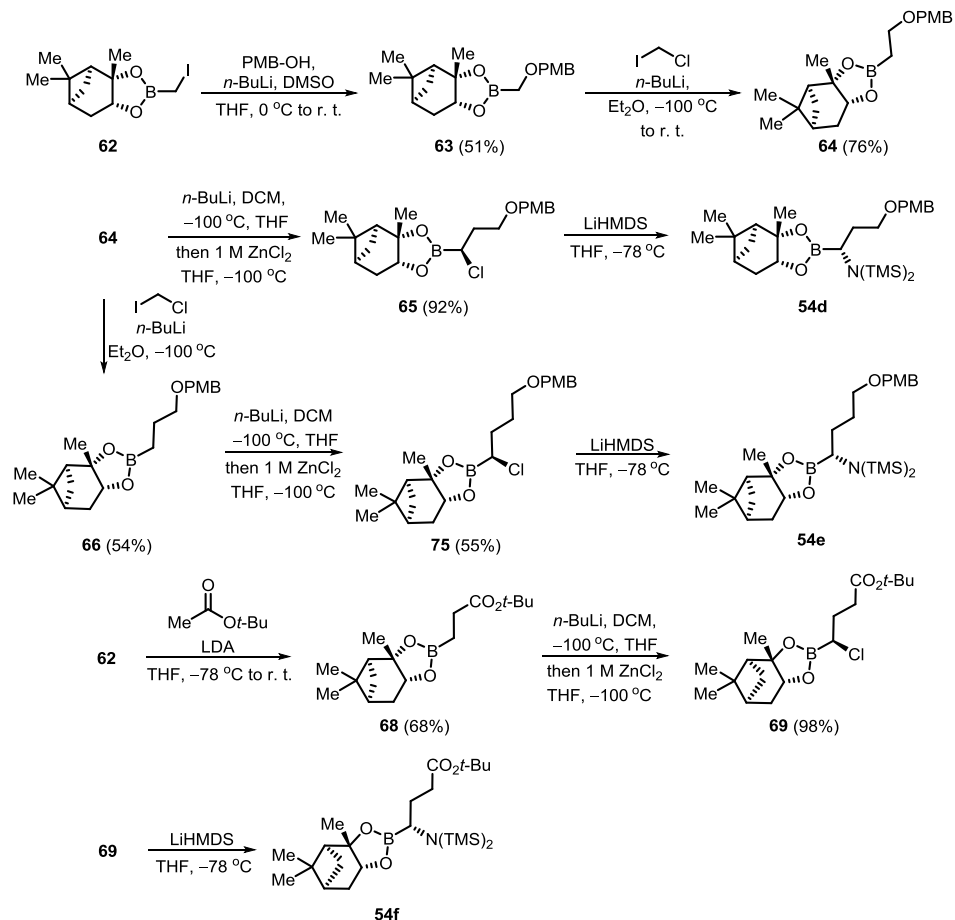


Scheme 6. The synthesis of boronic acid containing building blocks **54c**.

p-Methoxybenzyl alcohol was deprotonated with *n*-BuLi and then added to the building block **62** to get substitution product **63** in a moderate yield (Scheme 7). The synthesis of α -chloro boronic acid ester **65** involved the two subsequent homologation reactions. First, compound **64** was synthesized by the reaction of intermediate **63** with chloromethyl lithium. Next, the compound was added to *in situ* generated dichloromethyl lithium species to get the desired intermediate **65**. Conversion of chloride **65** to bis-TMS protected amine **54d** was performed as previously described (see

Scheme 5). To avoid the loss of valuable building block, it was decided not to cleave TMS groups, but to use the compound in the coupling step as an *N,N*-bis-TMS protected intermediate **54d**.

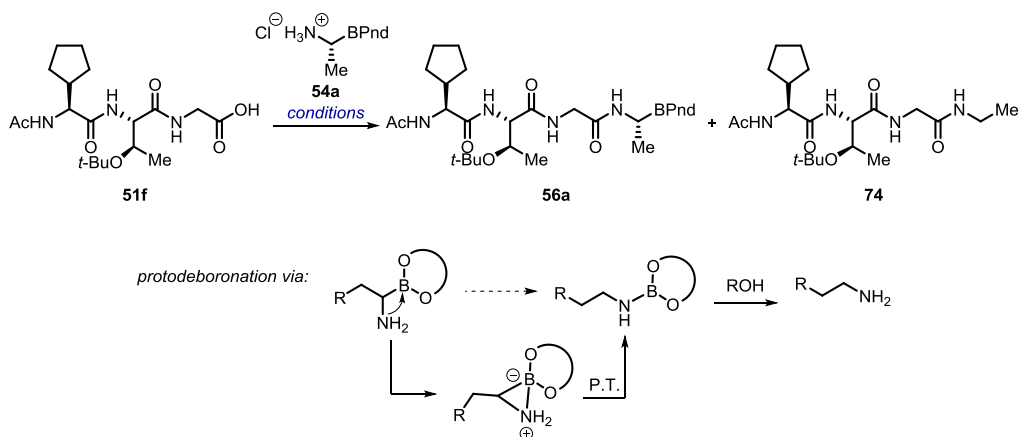
Homologue **54e** was obtained by the same homologation and substitution sequence starting from compound **64** (Scheme 7).



Scheme 7. The synthesis of boronic acid containing building blocks **54d–f**.

To obtain amino boronic acid building block **54f** containing a carboxylic acid moiety in the side chain, the synthesis was started with *tert*-butyl acetate and iodomethaneboronate **62** (Scheme 7). Addition of freshly generated LDA at $-78\text{ }^\circ\text{C}$ gave boronate **68** in a good yield. The Matteson homologation gave α -chloro boronic acid ester **69** in excellent yield, which was then converted to bis-TMS protected amine **54f**.

Finally, the compound **54g** containing a phenyl group alpha to the boronic acid was synthesized. Unfortunately, the previously used Matteson homologation reaction



Scheme 9. Plausible route towards protodeboronated product **74**.

2.2 PfSUB1 inhibitory potency and selectivity of peptidic boronic acids with a modified P1 position^a

When α -ketoamide functionality in compound **4** was replaced with boronic acid, it resulted in compound **15**, which showed \sim sevenfold increase in PfSUB1 inhibitory potency compared to the best α -ketoamide inhibitor **5f** (Table 4, entry 1). Combination of the known features from the α -ketoamide series (cyclopentane at P4) and boronic acid moiety resulted in **16a** displaying low nanomolar potency (entry 2). To examine the importance of the stereochemistry of the aminoboronic acid substructure at the P1 position, the PfSUB1 inhibitory potency of boronic acid epimer **16b** was tested (entry 3). It was discovered that **16b** is significantly less potent than **16a**, indicating the requirement for amino boronic acid to match the configuration of the L-amino acid in native substrates of SUB1. Removal of the methyl side chain at the P1 sub-site (compound **16c**, entry 4) reduced the potency. On the other hand, attempts to improve the potency by exploring extended alkyl or phenyl substituents at the P1 sub-site (compounds **16d–g**, entries 5–8) met with only limited success, only **16d** bearing a hydroxyethyl substituent displayed *ca* twofold increased potency compared to compound **16a**.

^a In collaboration with M. J. Blackman, C. Withers-Martinez *et al.*, Malaria Biochemistry Laboratory, The Francis Crick Institute.

Table 4

Inhibitory Potency and Growth Inhibition of Peptidic Boronic Acids

Entry	Structure	IC ₅₀ nM (rPfSUB1)	EC ₅₀ (μM) (parasite growth)
1. 15		69.4 ± 1.2	1.8 ± 0.6
2. 16a		9.3 ± 0.5	2.3 ± 1.4
3. 16b		60.1 ± 2.1	18.4 ± 1.8
4. 16c		54.3 ± 1.1	1.9 ± 0.4
5. 16d		4.6 ± 0.1	15.0 ± 3.6
6. 16e		204.2 ± 7.5	N.D.
7. 16f		18.7 ± 1.3	N.D.
8. 16g		112.0 ± 2.3	N.D.

IC₅₀ values were determined by quantifying inhibition of rPfSUB1-mediated proteolytic cleavage of a fluorogenic peptide substrate. Values are mean averages from at least three independent measurements ± SD.

EC₅₀ values were obtained by quantifying inhibition of *P. falciparum* growth *in vitro* over a period of 96 h (two erythrocytic growth cycles) using the DNA binding fluorescent dye SYBR Green I to measure parasite replication. Values are mean averages from at least three independent measurements ± SD. N.D., not determined

The capacity of the compounds to interfere with parasite replication was accessed by *in vitro* growth assay to measure parasite proliferation in human RBCs (Table 4). This experiment showed that compounds **15**, **16a,c** (entries 1, 2 and 4) inhibited parasite replication with EC₅₀ values of ~2 μM. However, there was a poor correlation between growth inhibition and the PfSUB1 enzyme inhibitory potency of the compounds. It was

concluded that this set of compounds suffered from poor access to PfSUB1 within the intracellular parasite.

PfSUB1 inhibitors **16c–g** were tested also in human proteasome counter assay^{a,b} at 500 nM concentration (Fig. 20). Preliminary results showed that only compound **16f** bearing glutamic acid side chain did not present an off-target effect against proteasome. Other compounds **16c–e**, **16g** showed a mild off-target effect. These compounds were compared with bortezomib which is known to inhibit the chymotryptic-like proteolytic activity of the proteasome, localized within the β_5 subunit of the 20S core ($IC_{50} = 3–5 \text{ nM}^{43}$).

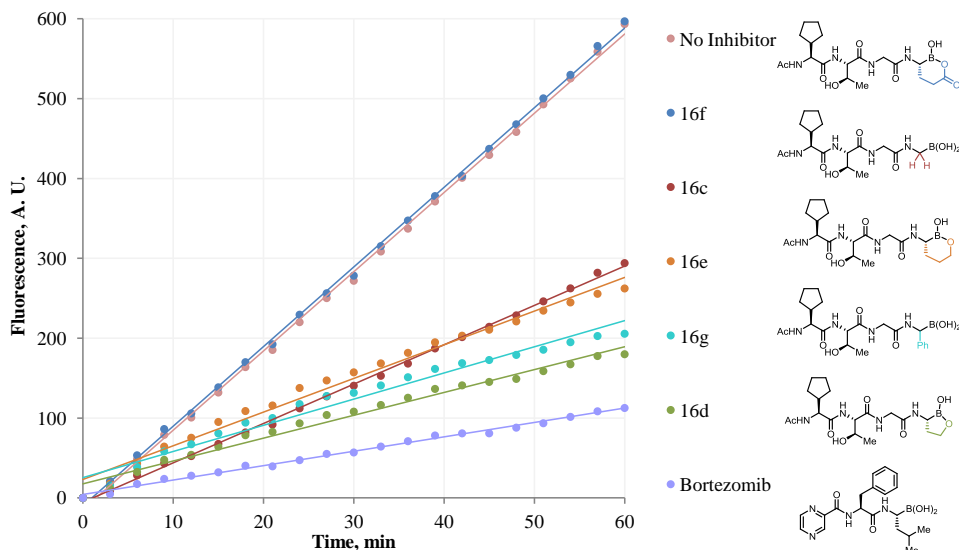


Fig. 20. PfSUB1 inhibitors **16c–g** in human proteasome inhibition assay ($R^2 \geq 0.97$).

2.3 Synthesis of the peptidic boronic acids with a modified P3 position

Although previous attempts to replace threonine at the P3 position with alanine in α -ketoamide series led to decreased inhibitory potency²¹ it was decided to investigate the possible variations of the side chains in more detail. The docking of a compound **16a** into X-ray crystal structure derived model of PfSUB1^a (Fig. 21) revealed that the P3 side chain of the bound inhibitor **16a** is extended into solvent area, with no significant contacts with the molecular surface of the PfSUB1 catalytic domain. However, the docking results

^a In collaboration with M. J. Blackman, C. Withers-Martinez *et al.*, Malaria Biochemistry Laboratory, The Francis Crick Institute.

^b Preliminary results, single measurement for each compound was done.

showed a potential for modifying and/or extending the P3 amino acid side chain in order to promote hydrophobic interactions with the S3 pocket (L461 residue).

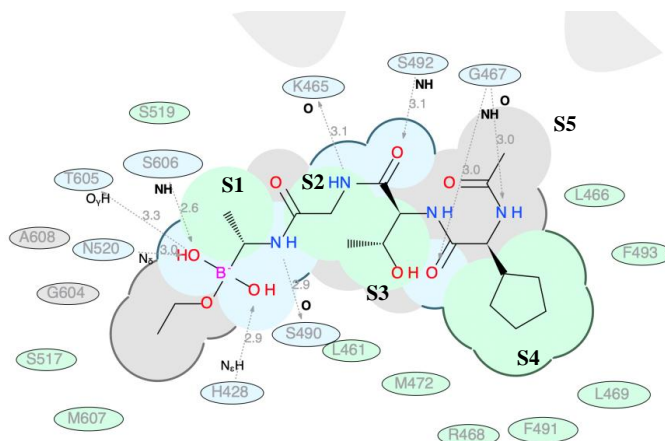
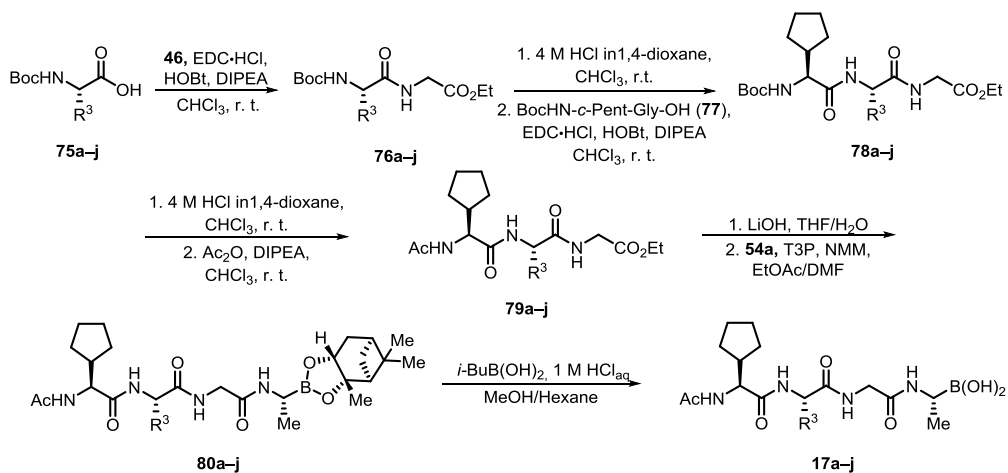


Fig. 21. Compound **16a** into X-ray crystal structure derived model of PfSUB1.^a

The synthesis of inhibitors was performed according to Scheme 10. EDC·HCl, HOBT and DIPEA activating system was used to incorporate different lipophilic amino acid residues in the structure of inhibitors. In this scheme, Boc group was selected as a protecting group for amino acids **76a-j**, thus, for deprotection reactions 4 M HCl in dioxane was chosen followed by coupling with an *N*-Boc-cyclopentyl glycine (**77**) to give the intermediates **78a-j**. After the deprotection of Boc group, the *N*-terminus was acetylated to give tripeptides **79a-j**. Hydrolysis of the ester group in tripeptides and coupling of the resulting acid with an α -amino boronic acid ester building block **54a** gave the desired intermediates **80a-j**. The last step involved the transesterification reaction with isobutylboronic acid to get free boronic acids **17a-j** (see Table 5 for yields).

^a In collaboration with M. J. Blackman, C. Withers-Martinez *et al.*, Malaria Biochemistry Laboratory, The Francis Crick Institute.



Scheme 10. The synthesis of peptidic boronic acids **17a-j**.

Table 5

Substituents and reaction yields

Entry	R ³	Yield, %					
		76	78	79	80	17	
1.	a	Me---	82	58	69	48	75
2.	b		96	69	73	50	77
3.	c		81	88	86	47	74
4.	d		59	71	76	35	75
5.	e		88	74	81	24	59
6.	f		86	69	95	30	54
7.	g		95	74	87	52	82
8.	h		92	84	61	33	81
9.	i		66	78	85	41	79
10.	j		79	76	86	38	81

2.4 PfSUB1 inhibitory potency and selectivity of peptidic boronic acids with a modified P3 position^a

The first two examples with alanine and valine side chains at the P3 position (compounds **17a** and **17b**) showed low nanomolar potency, which was similar to inhibitor **16a** with threonine side chain. Importantly, both compounds **17a** and **17b** with more lipophilic side chains showed increased sub-micromolar potency to inhibit the parasite growth in cell based assays²² (Fig. 22).

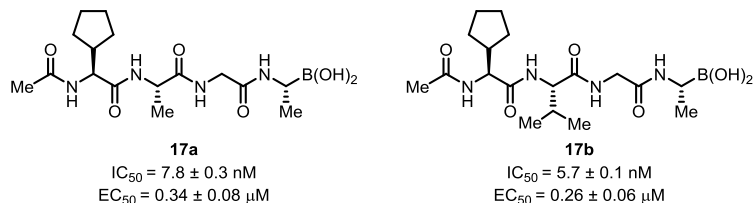


Fig. 22. Inhibitors of PfSUB1 with activity in cell based parasite growth and egress assays.

The inhibitory potency of peptidic boronic acids **17c–j** were determined (Fig. 23). The results indicated that the least active compound **17g** was with *tert*-butyl alanine side chain at P3 position. Derivatives bearing leucine, cyclopentyl, cyclohexyl or phenylalanine side chains (**17i,e,f,j**) showed similar potency to inhibit SUB1. Boronic acids possessing *tert*-butyl (**17c**), phenylglycine (**17d**) and isoleucine (**17h**) side chains at P3 position were slightly better SUB1 inhibitors.

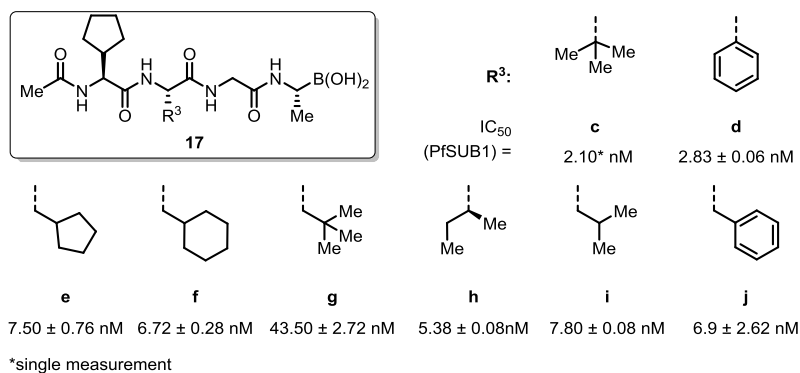


Fig. 23. Inhibitory potency of peptidic boronic acids **17c–j**.

Examination of the inhibitory potency of compound **17b** against the mammalian trypsin-family serine proteases trypsin, chymotrypsin, and elastase revealed a high degree

^a In collaboration with M. J. Blackman, C. Withers-Martinez *et al.*, Malaria Biochemistry Laboratory, The Francis Crick Institute.

of selectivity for PfSUB1.^a The estimated IC₅₀ value was determined to be 822 nM (>>100-fold) against mammalian elastase, while for trypsin and chymotrypsin the approximate IC₅₀ value was >>10 μM and >200 μM, respectively.²² This encouraged us to focus our subsequent work on this and related compounds.

P. falciparum cultures containing synchronous, highly mature schizonts were supplemented with compounds **17a** and **17b**. Microscopic examination of the cultures revealed schizonts arrested by these compounds, confirming inhibition of schizont rupture (Fig. 24).²²

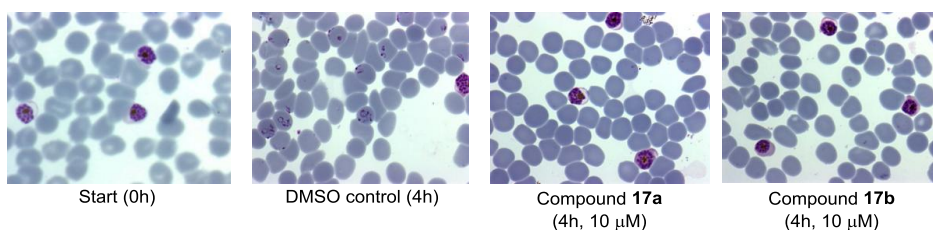
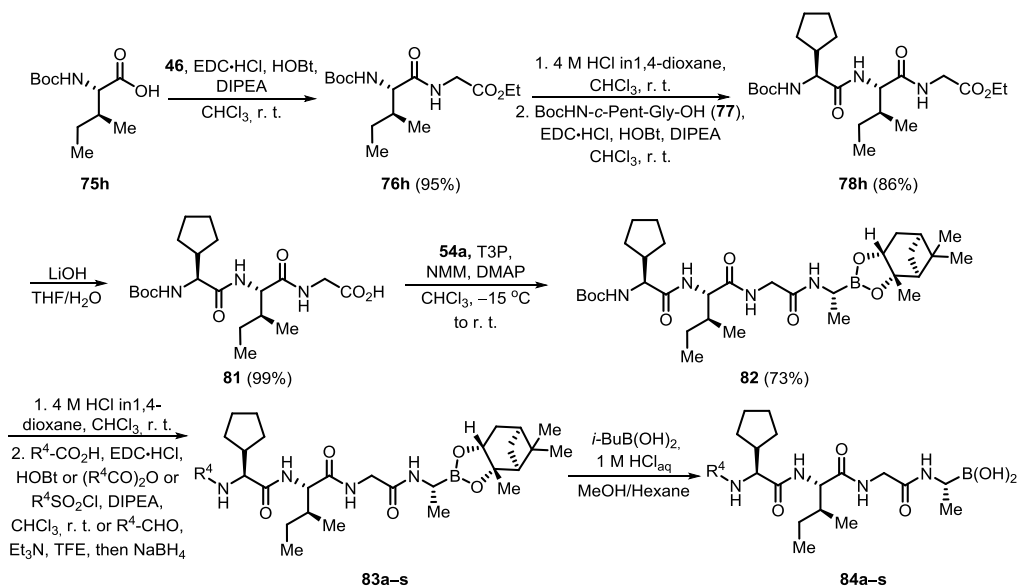


Fig. 24. Light micrographs of Giemsa-stained thin films prepared from highly mature 3D7 schizonts with RBCs (Scale bar, 20 μm).²²

2.5 Synthesis of the peptidic boronic acids with a modified P5 position

Combining all the known SAR results from previous modifications of the parent boronic acid based inhibitors, a set of new inhibitors with different *N*-capping groups (P5 position) was synthesized (Scheme 11). First, compound **81** was obtained using previously described peptide synthesis which involved the same coupling procedure as in the Scheme 10. Slightly different method for coupling of an acid **81** with α -amino boronic acid building block **54a** was applied.⁴⁴ The key intermediate **82** was deprotected and either coupled with an acid, acylated, sulfonylated or substituted to *N*-monoalkylated amine via reductive amination. The last step to give products **84a–s** was carried out as described before by using transesterification reaction with isobutylboronic acid (see Table 6 for yields).

^a In collaboration with M. J. Blackman, C. Withers-Martinez *et al.*, Malaria Biochemistry Laboratory, The Francis Crick Institute.



Scheme 11. The synthesis of peptidic boronic acids **84a-s**.

Table 6

Yields for boronic acid esters **83** and boronic acids **84**

Entry	R ⁴	Yield, %	
		83	84
1. a		75	66
2. b		67	53
3. c		74	81
4. d		55	80
5. e		62	67
6. f		54	71

Entry	R ⁴	Yield, %	
		83	84
10. j		84	54
11. k		64	70
12. l		63	74
13. m		69	67
14. n		56	80
15. o		81	75

Table 6 (cont.)

7.	g		64	70
8.	h		69	82
9.	i		81	72
16.	p		49	65
17.	r		59	62
18.	s		50	83

2.6 PfSUB1 inhibitory potency and selectivity of peptidic boronic acids with a modified P5 position^a

PfSUB1 inhibitory potency for compounds **84a–s** is shown in the Fig. 25. The results indicated that compounds with *N*-acyl groups bearing aliphatic, aromatic and heteroaromatic substituents at P5 position displayed inhibitory potency at low nanomolar concentrations comparable to the parent inhibitor **17h**. Interestingly, sulfonlated analogue **84o** with less peptidic nature gave similar activity compared to acylated analogues. When carbonyl group was replaced with methylene group, the SUB1 inhibitory potency decreased (**84e** vs **84p**; **84j** vs **84r**; **84i** vs **84s**).

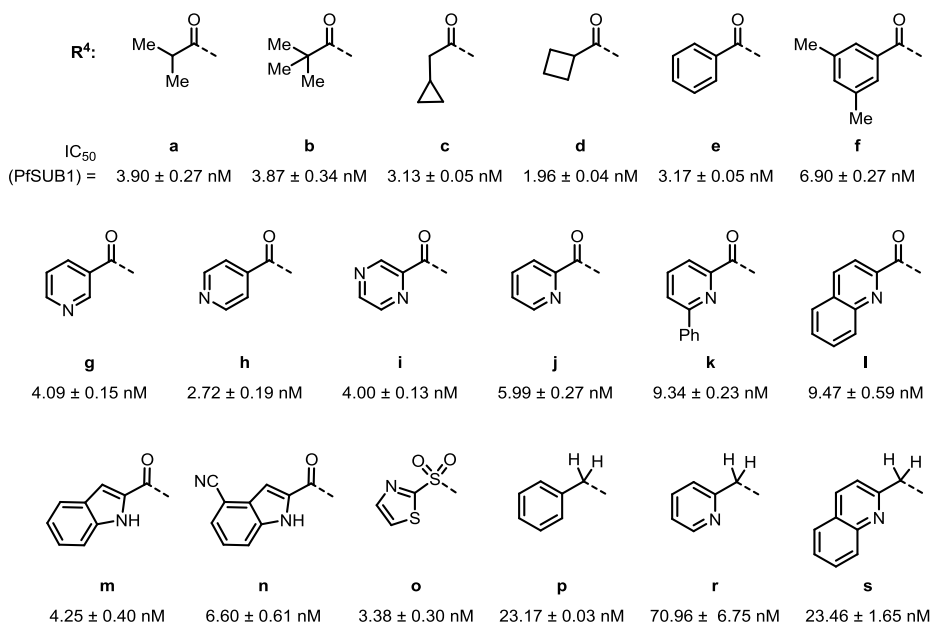


Fig. 25. Inhibitory potencies of peptidic boronic acids **84a–s**.^b

^a In collaboration with M. J. Blackman, C. Withers-Martinez et al., Malaria Biochemistry Laboratory, The Francis Crick Institute.

^b Values are mean average from two independent measurements ± SD.

Compounds **84f,k,l** were tested in human proteasome assay^{a,b} at 500 nM concentration. The proteasome inhibition potency was compared to inhibitors **16d** and **17b** (Fig. 26). Compounds **84f,k,l** demonstrated increased inhibition of human proteasome although their IC₅₀ (PfsUB1) values were similar to compound **17b**. These results suggested that modification at P5 position can lead to decreased SUB1 vs human proteasome selectivity.

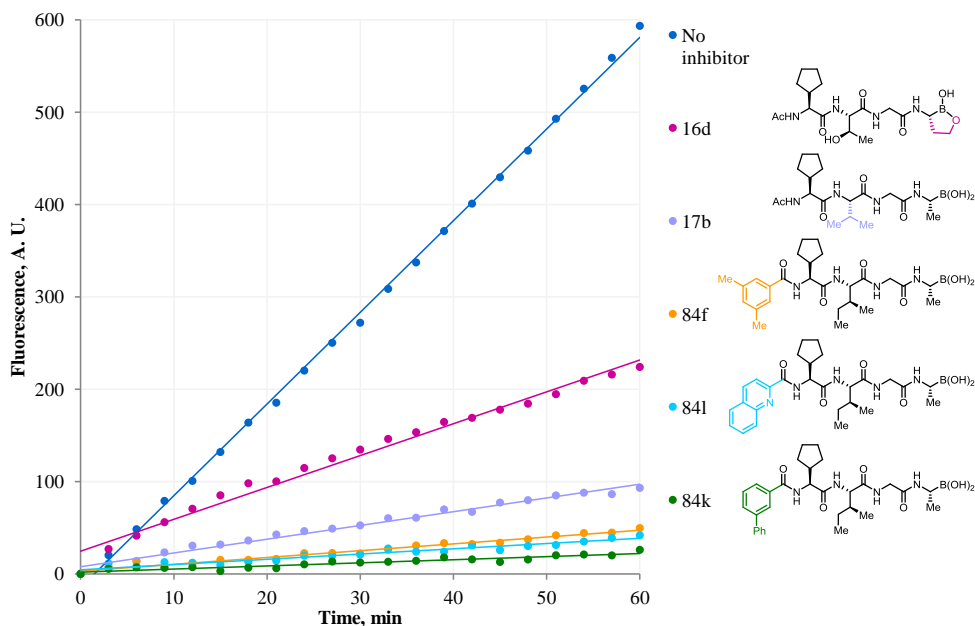


Fig. 26. PfsUB1 inhibitors in human proteasome inhibition assay ($R^2 \geq 0.90$).

2.7 Synthesis of peptidic boronic acids with a modified P5 and P1 positions

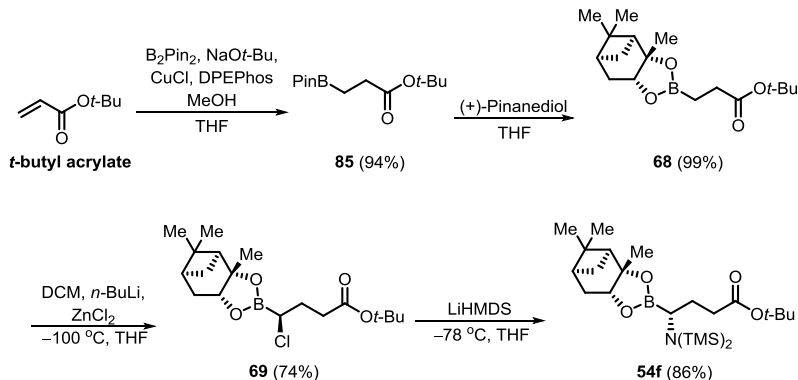
To improve selectivity for inhibition of SUB1 and to avoid the off-target effects against human proteasome, the selectivity inducing features from previous SAR studies were taken into account (section 2.2, Fig. 20). The base for the design of the next set of inhibitors was compound **16f** containing glutamic acid at P1 position which showed remarkable SUB1 inhibition selectivity versus proteasome inhibition.

Even though the key amino boronic acid building block **54f** was synthesized before (see Scheme 7), an alternative, more productive synthetic pathway was developed (Scheme 12). *tert*-Butyl acrylate was treated with bis(pinacolato)diboron in the presence of

^a In collaboration with M. J. Blackman, C. Withers-Martinez *et al.*, Malaria Biochemistry Laboratory, The Francis Crick Institute.

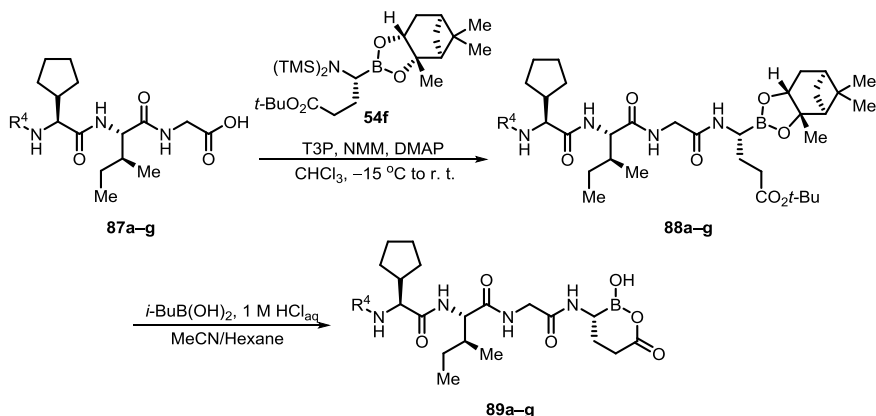
^b Preliminary results, single measurement for each compound was done.

copper(I) chloride, sodium *tert*-butoxide and bis[(2-diphenylphosphino)phenyl] ether (DPEPhos) to form β -borylated product **85** in excellent yield.⁴⁵ After transesterification with (+)-pinanediol and the Matteson homologation the desired chloride **69** was obtained which was transformed to bis(trimethylsilyl)amine derivative **54f**.



Scheme 12. Alternative route to boronic acid building block **54f**.

The building block **54f** was used in the coupling reaction with previously synthesized peptides **87a–g** with modified P5 position to give intermediates **88a–g** (Scheme 13). Finally, compounds **88a–g** were subjected to transesterification reaction with isobutyl boronic acid to get the final products **89a–g**. In this case, it was important to avoid methanol as a solvent for the last step since it tended to form methyl ester of cyclic boronic acid; thus, MeCN was used instead (see Table 7 for yields)



Scheme 13. The synthesis of peptidic boronic acid inhibitors **89a–g**.

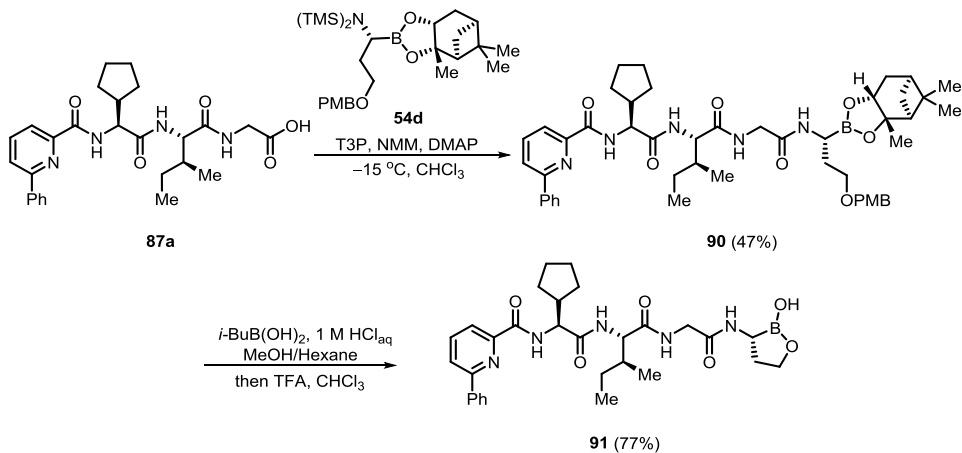
Table 7

Yields for boronic acid esters **88** and boronic acids **89**

Entry	R ⁴	Yield, %	
		88	89
1.		39	93
2.		55	82
3.		36	88
4.		36	79

Entry	R ⁴	Yield, %	
		88	89
5.		37	75
6.		39	89
7.		46	82

Peptidic building block **87a** was also coupled with boronic acid building block **54d** containing PMB-protected hydroxyethyl substituent to give compound **90**, which after transesterification and PMB cleavage with TFA yielded cyclic boronic acid **91** (Scheme 14).

Scheme 14. The synthesis of peptidic boronic acid inhibitor **91**.

2.8 PfSUB1 inhibitory potency and selectivity of peptidic boronic acids with a modified P5 and P1 positions

The PfSUB1 inhibitory potencies^a of compounds **89a–g** are presented in Fig. 27. In general, it is decreased compared to series of compounds **84** with the same substituent at P5 position; however the inhibitory potencies are still in low nanomolar concentrations. As an exception, compound **91** with hydroxyethyl substituent showed increased inhibitory potency against recombinant PfSUB1 if compared to the compound **84k**.

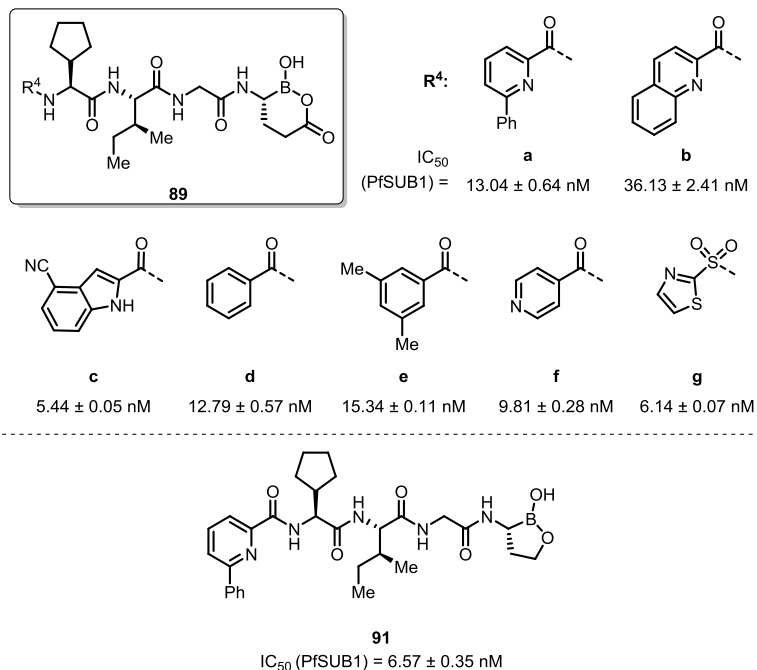


Fig. 27. Inhibitory potencies of peptidic boronic acids **89a–g** and **91**.^b

The effect on substituent at P1 to proteasome inhibition selectivity is depicted in the Fig. 28.^{a,c} Reference compounds **16f** did not show inhibition of human proteasome while boronic acid **84i** showed high inhibition of human proteasome. When the peptidic part from one and boronic acid moiety from other were combined, it resulted in product **89b** with lower SUB1 inhibition potency but with remarkable decrease of inhibition of human proteasome at 50 nM and 500 nM concentrations.

^a In collaboration with M. J. Blackman, C. Withers-Martinez *et al.*, Malaria Biochemistry Laboratory, The Francis Crick Institute.

^b Values are mean average from two independent measurements \pm SD.

^c Preliminary results.

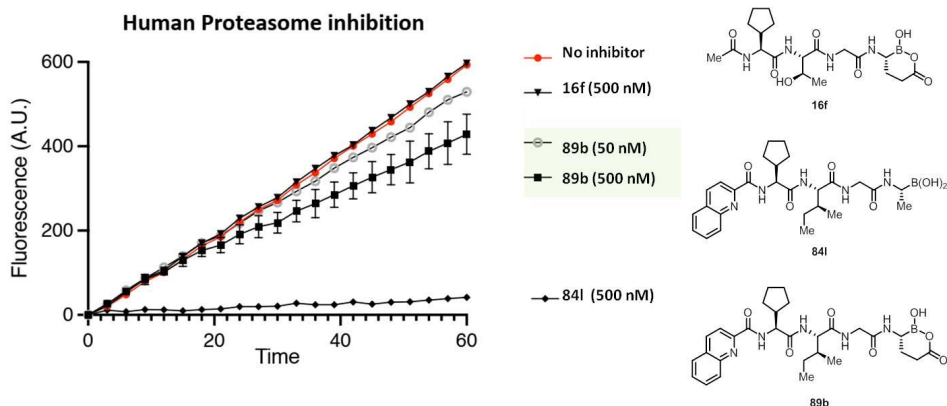
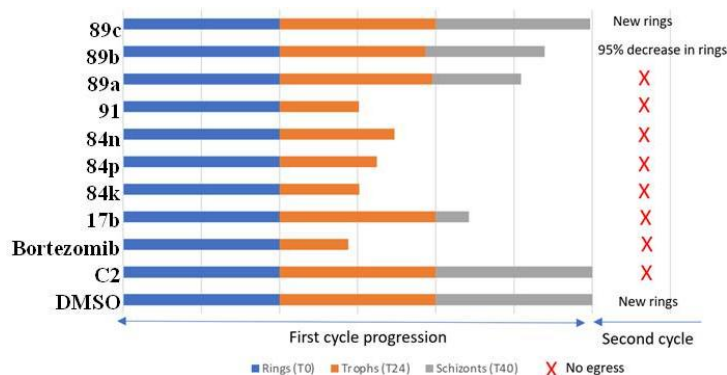


Fig. 28. Compounds with modified P5 and P1 position in human proteasome inhibition assay.

A set of synthesized compounds were tested in the parasite growth assay^a (Fig. 29). Reference compound **17b** stopped the progression of the parasite growth at early schizont stage. Analogues **84n,p,k** and **91** blocked the progression at trophozoite stage, like Bortezomib. It indicated that parasite growth effect of these compounds is due to off-target effects since it is known that SUB1 is discharged at schizont stage, before the egress.



Drugs at 1 μ M. Time point taken over 72 h. Data taken from FACS and Giemsa-stained smears

Fig. 29. SUB1 inhibitors in the parasite growth assay.

Compounds **89a** bearing glutamic acid arrested the parasite at late schizonts, while **89b** showed an impaired egress with decrease in amount of new ring formation. Compound **89c** showed similar phenotype as DMSO, no egress defect was observed. C2 is the reversible protein kinase G (PKG) inhibitor. A cGMP-dependent parasite protein kinase G is required for discharge of SUB1 from exoemes.

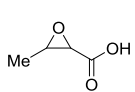
^a In collaboration with M. J. Blackman, C. Withers-Martinez *et al.*, Malaria Biochemistry Laboratory, The Francis Crick Institute.

Experimental part

1. General information

Reagents and starting materials were obtained from commercial sources and used as received. The solvents were purified and dried by standard procedures prior to use. Flash chromatography was carried out using silica gel (230–400 mesh). Thin layer chromatography was performed on TLC silica gel 60 F₂₅₄ (Supelco) and was visualized by UV lamp or staining with KMnO₄. NMR spectra were recorded on 300 and 400 MHz spectrometers with chemical shift values (δ) in parts per million using the residual chloroform, dimethylsulfoxide, acetonitrile or methanol signal as the internal standard. Conversion of starting material was detected with UPLC Waters Acquity, column: Acquity UPLC BEH-C18, 1.7 μ m, 2.1mm x 50 mm, column temperature (30.0 \pm 5.0) °C, gradient: 0.01% TFA in water/CH₃CN 90%/10% – 5%/95%; flow: 0.500 mL/min; time: 8 min; detector: PDA, 220 – 320 nm, SQ detector with an electrospray ion source (ESI/APCI). Gas chromatographic (GC) analysis was performed on Agilent Technologies gas chromatographer with triple-axis detector, heating range 40 – 280 °C, column 30 m x 0.25 mm, 0.25 μ m, 7 inch cage. Exact molecular masses (HRMS) were determined on a hybrid quadrupole time-of-flight mass spectrometer equipped with an electrospray ion source. For reversed phase column chromatography Biotage KP-C18-HS SNAP cartridge was used (gradient – water/CH₃CN).

2. Synthesis of α -ketoamides 5a–j and intermediates

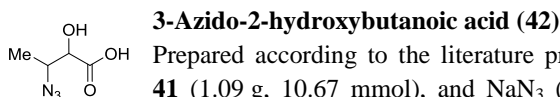


3-Methyloxirane-2-carboxylic acid (**41**)

According to literature procedure⁴⁶: stirred slurry of crotonic acid **40** (2 g, 23.2 mol) in acetone (10 mL) was treated first with NaHCO₃ (8.5 g, 101.2 mol, 4.4 equiv) and then carefully with water (10 mL). The resulting thick mixture was treated dropwise, over 1.5 h, with a solution of Oxone monopersulfate compound (13 g, contains 1.82 equiv of KHSO₅) in 4 \times 10⁻⁴ M aqueous disodium EDTA (52 mL). During this addition, the reaction temperature was maintained at 24–27 °C by using a water bath and the reaction pH at ca. 7.4. After the addition was complete the mixture was stirred an additional 0.5 h and then cooled in ice-water bath. The reaction was acidified with concentrated HCl to pH 2 and then treated with EtOAc (50 mL) followed by rapid stirring. The aqueous layer was extracted with EtOAc (50 mL), and the combined organic layers were washed once with saturated aqueous NaCl (25 mL), dried over MgSO₄, and concentrated in vacuo to give **41** (1.71 g, 72%).

¹H NMR (300 MHz, Chloroform-*d*) δ 9.30 (broad s, 1H), 3.28 (qd, *J* = 5.1, 1.9 Hz, 1H), 3.24 (d, *J* = 1.9 Hz, 1H), 1.43 (d, *J* = 5.1 Hz, 3H).

NMR data corresponds to the literature.⁴⁷

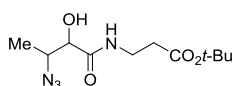


Prepared according to the literature procedure⁴⁸: α,β -epoxycarboxylic acid **41** (1.09 g, 10.67 mmol), and NaN_3 (3.46 g, 53.22 mmol, 5 equiv) were dissolved in water (20 mL) with stirring at room temperature. 0.5 M AlCl_3 aqueous solution (210 μL) was added and the pH adjusted to 4.0 by adding 50 % H_2SO_4 solution. The mixture was stirred for 3.5 h. At the end mixture was cooled to 0 °C, acidified to pH 2, extracted with Et_2O to give **42** (1.114 g, 72%).

^1H NMR (400 MHz, Chloroform-*d*) δ 6.95 (broad s, 1H), 4.40 (d, J = 3.1 Hz, 1H), 3.86 (qd, J = 6.8, 3.1 Hz, 1H), 1.36 (d, J = 6.8 Hz, 3H).

IR (thin film): 2122 cm^{-1} (for azide)

NMR data corresponds to the literature.²¹

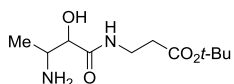


tert-Butyl 3-(3-azido-2-hydroxybutanamido)propanoate (44)

A mixture of **42** (800 mg, 5.5 mmol, 1.0 equiv), β -alanine *t*-butyl ester (**43**) (1.055 g, 5.5 mmol, 1.0 equiv), HATU (2.52 g, 6.63 mmol, 1.2 equiv) and DIPEA (2.86 mL, 16.5 mmol, 3.0 equiv) in DCM (50 mL) were stirred for 4 h at room temperature. The reaction mixture was washed with H_2O (2x20 mL) and then with brine (20 mL). Organic phase was dried over Na_2SO_4 , filtered and evaporated in vacuo. The residue was purified by flash chromatography on silica gel eluting with hexane:EtOAc to provide **44** (1.114 g, 74%) as a white solid.

^1H NMR (400 MHz, Chloroform-*d*) δ 7.13 (s, 1H), 4.14 (t, J = 4.2 Hz, 1H), 3.91 (qd, J = 6.6, 4.1 Hz, 1H), 3.52 (qd, J = 6.3, 2.5 Hz, 3H), 3.03 (d, J = 4.4 Hz, 1H), 2.51 – 2.43 (m, 3H), 1.46 (s, 9H), 1.25 (d, J = 6.6 Hz, 3H).

NMR data corresponds to the literature.²¹



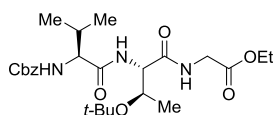
tert-Butyl 3-(3-amino-2-hydroxybutanamido)propanoate (45)

A mixture of **44** (447 mg, 1.64 mmol) was dissolved in methanol, 10% Pd/C (50 mg) was added, and then the balloon filled with H_2 was attached to the flask. Reaction mixture was stirred at room temperature until full conversion, filtered through the pad of celite and evaporated to provide the product **45** in quantitative yield.

^1H NMR (400 MHz, Chloroform-*d*) δ 7.59 (s, 1H), 3.85 (d, J = 5.0 Hz, 1H), 3.60 – 3.42 (m, 2H), 3.36 – 3.28 (m, 1H), 2.46 (t, J = 6.2 Hz, 3H), 1.45 (s, 10H), 1.03 (d, J = 6.5 Hz, 3H).

NMR data corresponds to the literature.²¹

The synthesis of compounds **48**, **49f,k**, **50f,k**, **51f,k** are described in the reference.²²



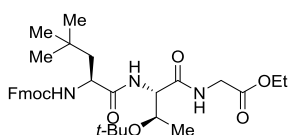
Ethyl N-(((benzyloxy)carbonyl)-L-valyl)-O-(tert-butyl)-L-threonylglycinate (49a)

According to the literature procedure⁴⁰ compound **48** (95 mg, 0.197 mmol) was dissolved in DMF (3 mL) under an argon atmosphere and stirred at 120 °C until full cleavage of Fmoc- group (UPLC-MS control).

Under an argon atmosphere a mixture of amine, Cbz-Val-OH (107 mg, 0.426 mmol) and HATU (195 mg, 0.513 mmol, 1.2 equiv) and DIPEA (220 μ L, 1.28 mmol, 3.0 equiv) in DMF were stirred at room temperature. The reaction mixture was diluted with EtOAc, washed with H₂O (2 \times) and then with brine. Organic phase was dried over Na₂SO₄, filtered and evaporated in vacuo. The residue was purified by flash chromatography on silica gel eluting with hexane:EtOAc to obtain product. Yield: 145 mg (69%).

¹H NMR (400 MHz, Chloroform-*d*) δ 7.64 (t, *J* = 5.1 Hz, 1H), 7.41 – 7.26 (m, 5H), 6.96 (d, *J* = 5.8 Hz, 1H), 5.40 (d, *J* = 8.4 Hz, 1H), 5.11 (s, 2H), 4.40 – 4.33 (m, 1H), 4.26 – 4.15 (m, 3H), 4.13 – 3.97 (m, 3H), 2.19 – 2.08 (m, 1H), 1.31 – 1.26 (m, 12H), 1.03 (d, *J* = 6.4 Hz, 3H), 0.97 (d, *J* = 6.8 Hz, 3H), 0.92 (d, *J* = 6.9 Hz, 3H).

¹³C NMR (101 MHz, Chloroform-*d*) δ 171.1, 169.6, 169.5, 156.5, 136.4, 128.6, 128.3, 128.2, 75.7, 67.2, 66.1, 61.6, 60.4, 57.6, 41.7, 31.5, 28.3, 19.3, 17.8, 17.2, 14.3.



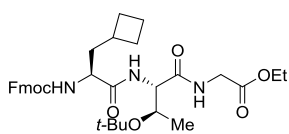
Ethyl *N*-((*S*)-2-(((9*H*-fluoren-9-yl)methoxy)carbonyl)amino)-4,4-dimethylpentanoyl)-*O*-(*tert*-butyl)-*L*-threonylglycinate (49b)

Compound was prepared in analogues way as **49a**: compound **48** (147 mg, 0.305 mmol) in DMF (4 mL).

Coupling: Fmoc-*t*-Bu-Ala-OH (111 mg, 0.305 mmol), HATU (138 mg, 0.364 mmol, 1.2 equiv) and DIPEA (158 μ L, 0.910 mmol, 3.0 equiv) in DMF. Yield: 157 mg (85%).

¹H NMR (400 MHz, Chloroform-*d*) δ 7.78 – 7.73 (m, 2H), 7.67 – 7.59 (m, 1H), 7.59 (d, *J* = 6.7 Hz, 2H), 7.42 – 7.36 (m, 2H), 7.30 (tt, *J* = 7.4, 1.0 Hz, 2H), 7.08 (d, *J* = 5.7 Hz, 1H), 5.14 (d, *J* = 8.2 Hz, 1H), 4.48 (dd, *J* = 10.6, 7.2 Hz, 1H), 4.39 – 4.30 (m, 2H), 4.29 – 4.18 (m, 5H), 4.11 – 3.98 (m, 2H), 1.86 (dd, *J* = 14.5, 3.6 Hz, 1H), 1.47 (dd, *J* = 14.5, 8.8 Hz, 1H), 1.28 (s, 9H), 1.27 (t, *J* = 7.2 Hz, 3H), 1.03 (d, *J* = 6.4 Hz, 3H), 0.97 (s, 9H).

¹³C NMR (101 MHz, Chloroform-*d*) δ 172.7, 169.7, 169.5, 155.9, 144.0, 143.8, 141.4, 127.8, 127.2, 125.2, 120.1, 75.7, 67.2, 66.0, 61.6, 57.7, 53.2, 47.3, 46.3, 41.7, 30.7, 29.8, 28.3, 17.3, 14.3.

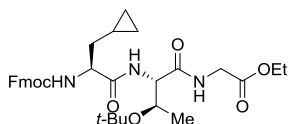


Ethyl *N*-((*S*)-2-(((9*H*-fluoren-9-yl)methoxy)carbonyl)amino)-3-cyclobutylpropanoyl)-*O*-(*tert*-butyl)-*L*-threonylglycinate (49c)

Compound was prepared in analogues way as **49a**: compound **48** (183 mg, 0.379 mmol) in DMF (3 mL). Coupling: Fmoc-*c*Butyl-Ala-OH (137 mg, 0.375 mmol) and HATU (170 mg, 0.447 mmol, 1.2 equiv) and DIPEA (195 μ L, 1.12 mmol, 3.0 equiv) in DMF (4 mL). Yield: 155 mg (68%).

¹H NMR (400 MHz, Chloroform-*d*) δ 7.76 (d, *J* = 7.5 Hz, 2H), 7.66 (t, *J* = 5.3 Hz, 1H), 7.60 (d, *J* = 7.6 Hz, 2H), 7.40 (t, *J* = 7.4 Hz, 2H), 7.31 (t, *J* = 7.4 Hz, 2H), 6.95 (d, *J* = 5.6 Hz, 1H), 5.32 (d, *J* = 7.9 Hz, 1H), 4.44 (dd, *J* = 10.6, 7.3 Hz, 1H), 4.40 – 4.31 (m, 2H), 4.26 – 4.13 (m, 5H), 4.15 – 3.97 (m, 2H), 2.35 (p, *J* = 7.9 Hz, 1H), 2.11 – 1.99 (m, 2H), 1.97 – 1.85 (m, 2H), 1.85 – 1.73 (m, 2H), 1.72 – 1.62 (m, 2H), 1.30 (s, 9H), 1.28 (t, *J* = 7.1 Hz, 3H), 1.04 (d, *J* = 6.4 Hz, 3H).

^{13}C NMR (101 MHz, Chloroform-*d*) δ 171.7, 169.6, 169.5, 156.0, 144.1, 143.9, 141.46, 141.45, 127.8, 127.2, 125.3, 125.2, 120.12, 120.10, 75.8, 67.1, 66.1, 61.6, 57.7, 54.0, 47.3, 41.7, 40.2, 32.6, 28.5, 28.5, 28.3, 18.8, 17.2, 14.3.

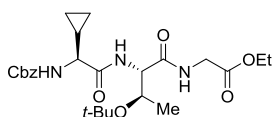


Ethyl *N*-((*S*)-2-(((9*H*-fluoren-9-yl)methoxy)carbonyl)amino)-3-cyclopropylpropanoyl)-*O*-(*tert*-butyl)-*L*-threonylglycinate (49d)

Compound was prepared in analogues way as **49a**: compound **48** (183 mg, 0.379 mmol) in DMF (3 mL). Coupling: Fmoc-*c*Propyl-Ala-OH (153 mg, 0.435 mmol) and HATU (190 mg, 0.500 mmol, 1.2 equiv) and DIPEA (215 μL , 1.24 mmol, 3.0 equiv) in DMF (3 mL). Yield: 206 mg (84%).

^1H NMR (400 MHz, Chloroform-*d*) δ 7.76 (d, $J = 7.5$ Hz, 2H), 7.67 (d, $J = 5.4$ Hz, 1H), 7.61 (d, $J = 6.6$ Hz, 2H), 7.40 (tt, $J = 7.5, 1.4$ Hz, 2H), 7.31 (tt, $J = 7.5, 1.5$ Hz, 2H), 7.06 (d, $J = 5.3$ Hz, 1H), 5.53 (d, $J = 8.2$ Hz, 1H), 4.48 – 4.27 (m, 4H), 4.26 – 4.17 (m, 4H), 4.13 – 3.97 (m, 2H), 1.78 – 1.58 (m, 2H), 1.32 – 1.24 (m, 12H), 1.05 (d, $J = 6.4$ Hz, 3H), 0.76 – 0.64 (m, 1H), 0.50 (d, $J = 8.1$ Hz, 2H), 0.11 (d, $J = 5.7$ Hz, 2H).

^{13}C NMR (101 MHz, Chloroform-*d*) δ 171.6, 169.6, 169.5, 156.0, 144.1, 143.9, 141.45, 141.43, 127.8, 127.19, 127.17, 125.3, 125.2, 120.11, 120.10, 75.8, 67.2, 66.1, 61.6, 57.8, 55.6, 47.3, 41.7, 38.1, 28.3, 17.2, 14.3, 7.3, 4.8, 4.3.

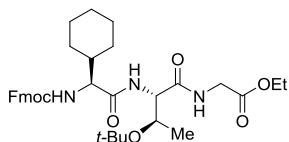


Ethyl *N*-((*S*)-2-((benzyloxy)carbonyl)amino)-2-cyclopropylacetyl)-*O*-(*tert*-butyl)-*L*-threonylglycinate (49e)

Compound was prepared in analogues way as **49a**: compound **48** (95 mg, 0.197 mmol) was dissolved in DMF (3 mL). Coupling: Cbz-*c*Propyl-Gly-OH (49 mg, 0.197 mmol), HATU (90 mg, 0.237 mmol, 1.2 equiv) and DIPEA (100 μL , 0.589 mmol, 3.0 equiv) in DMF (3 mL). Yield: 80 mg (83%).

^1H NMR (400 MHz, Chloroform-*d*) δ 7.64 (t, $J = 5.2$ Hz, 1H), 7.39 – 7.28 (m, 5H), 7.08 (s, 1H), 5.52 (s, 1H), 5.11 (s, 2H), 4.36 (t, $J = 4.7$ Hz, 1H), 4.27 – 4.18 (m, 3H), 4.13 – 3.97 (m, 2H), 3.63 (t, $J = 8.3$ Hz, 1H), 1.31 – 1.26 (m, 12H), 1.17 – 1.05 (m, 1H), 1.05 (d, $J = 6.5$ Hz, 3H), 0.75 – 0.65 (m, 1H), 0.62 – 0.48 (m, 3H).

^{13}C NMR (101 MHz, Chloroform-*d*) δ 171.0, 169.7, 169.5, 156.3, 136.4, 128.6, 128.3, 128.2, 75.7, 67.2, 66.1, 61.6, 59.0, 57.8, 41.7, 28.3, 17.4, 15.0, 14.3, 3.9, 3.3.



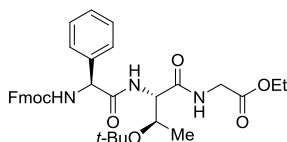
Ethyl *N*-((*S*)-2-(((9*H*-fluoren-9-yl)methoxy)carbonyl)amino)-2-cyclohexylacetyl)-*O*-(*tert*-butyl)-*L*-threonylglycinate (49g)

According to the literature procedure³⁹ the starting Fmoc-protected compound **48** (1 g, 2.07 mmol) was dissolved in (30 mL) and 4-(aminomethyl)piperidine (2 mL, 20.5 mmol, 10 equiv) was added. Reaction was stirred until full cleavage of Fmoc- group (UPLC-MS control). DCM was then washed with 10% (w/v) aqueous phosphate buffer (pH 5.5, 3 x 5 mL). Organic phase was separated, dried over Na_2SO_4 , filtered and evaporated in vacuo to obtain crude amine (100 mg, 18%).

Under an argon atmosphere a mixture of amine, Fmoc-cHex-Gly-OH (100 mg, 0.26 mmol) and HATU (219 mg, 0.58 mmol, 1.1 equiv) and DIPEA (200 μ L, 1.16 mmol, 3.0 equiv) in DCM were stirred at room temperature. The reaction mixture was washed with H₂O (2 \times) and then with brine. Organic phase was dried over Na₂SO₄, filtered and evaporated in vacuo. The residue was purified by flash chromatography on silica gel eluting with *n*-hexane:EtOAc to obtain product **49g** (38 mg, 23%).

¹H NMR (400 MHz, Chloroform-*d*) δ 7.76 (d, *J* = 7.5 Hz, 2H), 7.66 (t, *J* = 5.0 Hz, 1H), 7.61 (d, *J* = 7.5 Hz, 2H), 7.45 – 7.36 (m, 2H), 7.35 – 7.28 (m, 2H), 6.91 (d, *J* = 5.6 Hz, 1H), 5.40 (d, *J* = 8.4 Hz, 1H), 4.46 (dd, *J* = 10.6, 7.3 Hz, 1H), 4.40 – 4.30 (m, 2H), 4.26 – 4.16 (m, 4H), 4.13 – 3.97 (m, 3H), 1.82 – 1.59 (m, 7H), 1.32 – 1.25 (m, 12H), 1.19 – 0.98 (m, 7H).

¹³C NMR (101 MHz, Chloroform-*d*) δ 171.1, 169.6, 169.5, 156.4, 144.1, 143.9, 141.5, 127.8, 127.2, 125.3, 125.2, 120.13, 120.09, 75.8, 67.1, 66.1, 61.6, 60.1, 57.6, 47.4, 41.7, 41.2, 29.8, 28.4, 28.3, 26.2, 26.1, 17.2, 14.3.

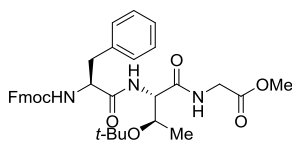


Ethyl *N*-((*S*)-2-(((9*H*-fluoren-9-yl)methoxy)carbonyl)amino)-2-phenylacetyl)-*O*-(*tert*-butyl)-*L*-threonylglycinate (49h**)**

Compound was prepared in analogues way as **49a**: compound **48** (187 mg, 0.388 mmol) in DMF (3 mL). Coupling: Fmoc-PhGly-OH (145 mg, 0.388 mmol) and HATU (177 mg, 0.466 mmol) and DIPEA (200 μ L, 1.16 mmol, 3.0 equiv) in DMF (3 mL). Yield: 125 mg (52%).

¹H NMR (400 MHz, Chloroform-*d*) δ 7.75 (d, *J* = 7.5 Hz, 2H), 7.59 (d, *J* = 7.4 Hz, 2H), 7.50 (t, *J* = 5.3 Hz, 1H), 7.42 – 7.27 (m, 9H), 6.93 (s, 1H), 6.14 (s, 1H), 5.26 (d, *J* = 6.4 Hz, 1H), 4.37 (d, *J* = 7.0 Hz, 2H), 4.31 – 4.24 (m, 2H), 4.23 – 4.15 (m, 3H), 4.02 (dd, *J* = 18.2, 5.1 Hz, 1H), 3.94 (dd, *J* = 18.4, 5.3 Hz, 1H), 1.29 (s, 9H), 1.27 (t, *J* = 7.2 Hz, 3H), 1.07 (d, *J* = 6.3 Hz, 3H).

¹³C NMR (101 MHz, Chloroform-*d*) δ 169.7, 169.4, 169.3, 155.7, 144.0, 143.9, 141.38, 141.36, 129.4, 128.8, 127.8, 127.2, 127.1, 125.2, 120.1, 120.0, 75.8, 67.3, 65.9, 61.6, 59.2, 57.9, 47.2, 41.6, 28.2, 17.3, 14.3.



Methyl *N*-(((9*H*-fluoren-9-yl)methoxy)carbonyl)-*L*-phenylalanyl)-*O*-(*tert*-butyl)-*L*-threonylglycinate (49i**)**

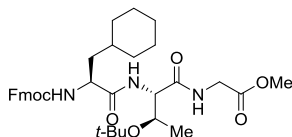
Compound was prepared in analogues way as **49a**: compound **S1^a** (183 mg, 0.390 mmol) in DMF (5 mL). Coupling: Fmoc-PhAla-OH (154 mg, 0.390 mmol) and HATU (222 mg, 0.585 mmol, 1.5 equiv) and DIPEA (200 μ L, 1.17 mmol, 3.0 equiv) in DMF (5 mL). Yield: 131 mg (55%).

¹H NMR (400 MHz, Chloroform-*d*) δ 7.76 (d, *J* = 7.5 Hz, 2H), 7.54 (t, *J* = 7.2 Hz, 2H), 7.48 (t, *J* = 5.2 Hz, 1H), 7.40 (t, *J* = 7.5 Hz, 2H), 7.33 – 7.21 (m, 5H), 7.17 (d, *J* = 7.3 Hz, 2H), 6.97 (s, 1H), 5.32 (d, *J* = 7.9 Hz, 1H), 4.55 – 4.48 (m, 1H), 4.44 (dd, *J* = 10.6, 7.2 Hz,

^a Compound **48** with methyl ester instead of ethyl ester. See the synthesis in supporting information of appendix I²²

1H), 4.31 (q, $J = 6.2, 5.5$ Hz, 2H), 4.20 (q, $J = 7.1$ Hz, 2H), 4.03 (d, $J = 5.2$ Hz, 2H), 3.75 (s, 3H), 3.15 – 3.07 (m, 2H), 1.28 (s, 9H), 0.97 (d, $J = 6.3$ Hz, 3H).

^{13}C NMR (101 MHz, Chloroform- d) δ 170.8, 169.9, 169.5, 156.0, 144.0, 143.8, 141.4, 136.1, 129.4, 128.9, 127.8, 127.3, 127.2, 125.3, 125.2, 120.11, 120.09, 75.7, 67.3, 66.0, 57.8, 56.2, 52.4, 47.2, 41.5, 38.6, 28.3, 17.4.



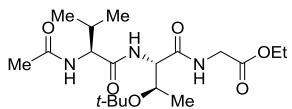
Methyl *N*-(((*S*)-2-(((9*H*-fluoren-9-yl)methoxy)carbonyl)-amino)-3-cyclohexylpropanoyl)-*O*-(*tert*-butyl)-*L*-threoninyl-glycinate (49j**)**

Compound was prepared in analogues way as **49a**: compound **S1** (163 mg, 0.348 mmol) in DMF (5 mL).

Coupling: Fmoc-cHex-Ala-OH (153 mg, 0.390 mmol) and HATU (222 mg, 0.585 mmol, 1.5 equiv) and DIPEA (200 μL , 1.17 mmol, 3.0 equiv) in DMF (5 mL). Yield: 186 mg (77%).

^1H NMR (300 MHz, Chloroform- d) δ 7.76 (dd, $J = 7.5, 1.1$ Hz, 2H), 7.68 – 7.54 (m, 3H), 7.44 – 7.36 (m, 2H), 7.31 (tt, $J = 7.4, 1.1$ Hz, 2H), 7.01 (d, $J = 5.8$ Hz, 1H), 5.24 (d, $J = 7.9$ Hz, 1H), 4.49 – 4.32 (m, 3H), 4.33 – 4.17 (m, 3H), 4.07 (d, $J = 5.1$ Hz, 2H), 3.75 (s, 3H), 1.87 – 1.46 (m, 7H), 1.40 – 1.09 (m, 13H), 1.03 (d, $J = 6.4$ Hz, 3H), 1.00 – 0.81 (m, 2H).

^{13}C NMR (101 MHz, Chloroform- d) δ 172.3, 170.0, 169.7, 156.2, 144.0, 143.9, 141.43, 141.42, 127.8, 127.2, 125.2, 120.12, 120.10, 75.7, 67.3, 66.0, 57.7, 53.1, 52.4, 47.3, 41.5, 40.6, 34.2, 33.8, 32.7, 28.3, 26.5, 26.3, 26.1, 17.3.



Ethyl *N*-(acetyl-*L*-valyl)-*O*-(*tert*-butyl)-*L*-threoninyl-glycinate (50a**)**

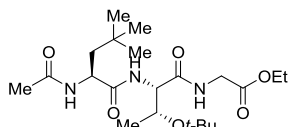
A mixture of **49a** (145 mg, 0.294 mmol) was dissolved in ethanol (10 mL), 10% Pd/C (14 mg) was added, and then the

balloon filled with H_2 was attached to the flask. Reaction mixture was stirred at room temperature until full conversion. Mixture was filtered through the pad of celite and evaporated.

Under an argon atmosphere acetic anhydride (42 μL , 0.441 mmol) and DIPEA (100 μL , 0.590 mmol) were added to the solution of amine (1 equiv) in DCM (10 mL). Reaction mixture was stirred at room temperature, then diluted with DCM, washed with H_2O (2 \times) and brine. Organic phase was dried over Na_2SO_4 , filtered and evaporated in vacuo. The residue was purified by flash chromatography on silica gel eluting with hexane:EtOAc. Yield: 99 mg (84%).

^1H NMR (300 MHz, Chloroform- d) δ 7.64 (t, $J = 5.2$ Hz, 1H), 6.84 (d, $J = 5.8$ Hz, 1H), 6.09 (d, $J = 8.4$ Hz, 1H), 4.40 – 4.33 (m, 2H), 4.28 – 3.96 (m, 5H), 2.15 – 2.06 (m, 1H), 2.05 (s, 3H), 1.31 (s, 9H), 1.29 (t, $J = 7.2$ Hz, 3H), 1.05 (d, $J = 6.4$ Hz, 3H), 0.96 (d, $J = 6.9$ Hz, 3H), 0.95 (d, $J = 6.9$ Hz, 3H).

^{13}C NMR (101 MHz, Chloroform- d) δ 171.2, 170.2, 169.6, 169.5, 75.7, 66.3, 61.6, 58.4, 57.6, 41.7, 31.7, 28.3, 23.4, 19.3, 18.2, 17.2, 14.3.

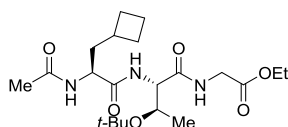


Ethyl *N*-((*S*)-2-acetamido-4,4-dimethylpentanoyl)-*O*-(*tert*-butyl)-*L*-threonylglycinate (50b**)**

Cleavage of the Fmoc- group was done in analogues way as for **49a**: compound **49b** (156 mg, 0.256 mmol) in DMF (4 mL). Acylation was done in analogous to compound **50a**: acetic anhydride (36 μ L, 0.384 mmol) and DIPEA (90 μ L, 0.512 mmol) in DMF (4 mL). Yield: 96 mg (87%).

$^1\text{H NMR}$ (400 MHz, Chloroform-*d*) δ 7.62 (t, J = 5.2 Hz, 1H), 7.02 (d, J = 5.9 Hz, 1H), 6.09 (d, J = 8.0 Hz, 1H), 4.50 (td, J = 8.4, 3.8 Hz, 1H), 4.30 (dd, J = 5.9, 3.7 Hz, 1H), 4.24 – 4.15 (m, 3H), 4.11 – 3.96 (m, 2H), 1.99 (s, 3H), 1.81 (dd, J = 14.6, 3.9 Hz, 1H), 1.47 (dd, J = 14.5, 8.7 Hz, 1H), 1.30 – 1.25 (m, 12H), 1.04 (d, J = 6.4 Hz, 3H), 0.95 (s, 9H).

$^{13}\text{C NMR}$ (101 MHz, Chloroform-*d*) δ 172.7, 169.9, 169.6, 169.5, 75.7, 66.1, 61.6, 57.7, 51.3, 46.2, 41.7, 30.7, 29.8, 28.3, 23.3, 17.3, 14.3.

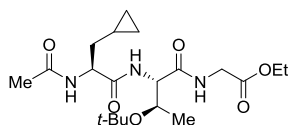


Ethyl *N*-((*S*)-2-acetamido-3-cyclobutylpropanoyl)-*O*-(*tert*-butyl)-*L*-threonylglycinate (50c**)**

Compound was prepared in analogues way as **50b**: compound **49c** (155 mg, 0.255 mmol) in DMF (3 mL). Acylation: acetic anhydride (36 μ L, 0.383 mmol) and DIPEA (90 μ L, 0.510 mmol) in DMF (3 mL). Yield: 80 mg (73%).

$^1\text{H NMR}$ (400 MHz, Chloroform-*d*) δ 7.65 (t, J = 5.2 Hz, 1H), 6.89 (d, J = 5.6 Hz, 1H), 6.04 (d, J = 7.7 Hz, 1H), 4.39 (q, J = 6.9 Hz, 1H), 4.32 (dd, J = 5.7, 3.9 Hz, 1H), 4.27 – 4.16 (m, 3H), 4.14 – 3.97 (m, 2H), 2.34 (p, J = 7.9 Hz, 1H), 2.11 – 2.02 (m, 2H), 2.00 (s, 3H), 1.95 – 1.82 (m, 2H), 1.82 – 1.71 (m, 2H), 1.70 – 1.61 (m, 2H), 1.33 – 1.25 (m, 12H), 1.04 (d, J = 6.4 Hz, 3H).

$^{13}\text{C NMR}$ (101 MHz, Chloroform-*d*) δ 171.8, 169.8, 169.53, 169.47, 76.8, 75.7, 66.1, 61.6, 57.7, 52.3, 41.7, 40.1, 32.6, 28.6, 28.5, 28.3, 23.3, 18.8, 17.1, 14.3.

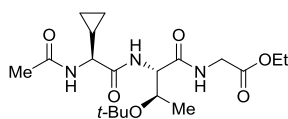


Ethyl *N*-((*S*)-2-acetamido-3-cyclopropylpropanoyl)-*O*-(*tert*-butyl)-*L*-threonylglycinate (50d**)**

Compound was prepared in analogues way as **50b**: compound **49d** (188 mg, 0.317 mmol) in DMF (3 mL). Acylation: acetic anhydride (45 μ L, 0.477 mmol) and DIPEA (110 μ L, 0.636 mmol) in DMF (3 mL). Yield: 107 mg (82%).

$^1\text{H NMR}$ (400 MHz, Chloroform-*d*) δ 7.64 (t, J = 5.3 Hz, 1H), 7.02 (d, J = 5.7 Hz, 1H), 6.32 (d, J = 7.6 Hz, 1H), 4.53 (q, J = 6.9 Hz, 1H), 4.35 (dd, J = 5.6, 3.8 Hz, 1H), 4.26 – 4.16 (m, 3H), 4.14 – 3.95 (m, 2H), 2.01 (s, 3H), 1.74 – 1.55 (m, 2H), 1.34 – 1.23 (m, 12H), 1.05 (d, J = 6.4 Hz, 3H), 0.75 – 0.63 (m, 1H), 0.54 – 0.43 (m, 2H), 0.16 – 0.02 (m, 2H).

$^{13}\text{C NMR}$ (101 MHz, Chloroform-*d*) δ 171.7, 169.8, 169.54, 169.47, 75.7, 66.2, 61.6, 57.7, 53.9, 41.7, 37.9, 28.3, 23.4, 17.2, 14.3, 7.4, 4.8, 4.2.



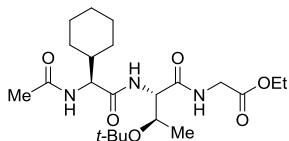
Ethyl *N*-((*S*)-2-acetamido-2-cyclopropylacetyl)-*O*-(*tert*-butyl)-*L*-threonylglycinate (50e**)**

Compound was prepared in analogues way as **50a**: compound **49e** (80 mg, 0.163 mmol), 10% Pd/C (8 mg) in ethanol

(5 mL). Acylation: acetic anhydride (23 μ L, 0.244 mmol) and DIPEA (56 μ L, 0.325 mmol) were added to the solution of amine in DCM (5 mL). Yield: 39 mg (60%)

^1H NMR (400 MHz, Chloroform-*d*) δ 7.63 (t, J = 5.3 Hz, 1H), 7.08 (d, J = 5.7 Hz, 1H), 6.34 (d, J = 7.4 Hz, 1H), 4.38 – 4.34 (m, 1H), 4.25 – 4.16 (m, 3H), 4.13 – 3.96 (m, 2H), 3.93 – 3.87 (m, 1H), 2.02 (s, 3H), 1.28 (s, 9H), 1.27 (t, J = 6.9 Hz, 3H), 1.14 – 1.06 (m, 1H), 1.05 (d, J = 6.4 Hz, 3H), 0.73 – 0.64 (m, 1H), 0.59 – 0.48 (m, 3H).

^{13}C NMR (101 MHz, Chloroform-*d*) δ 171.2, 170.1, 169.7, 169.5, 75.7, 66.1, 61.6, 57.8, 57.0, 41.7, 28.3, 23.3, 17.4, 14.9, 14.3, 4.0, 3.4.



Ethyl *N*-((*S*)-2-acetamido-2-cyclohexylacetyl)-*O*-(*tert*-butyl)-*L*-threonylglycinate (50g)

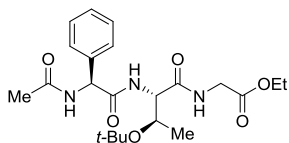
Compound was prepared in analogues way as **50b**: compound **49g** (38 mg, 0.061 mmol) in DMF (3 mL).

Acylation: acetic anhydride (8.5 μ L, 1.5 equiv) and DIPEA

(21 μ L, 2.0 equiv) in DMF. Yield: 14 mg (53%).

^1H NMR (300 MHz, Chloroform-*d*) δ 7.64 (t, J = 5.1 Hz, 1H), 6.87 (d, J = 5.7 Hz, 1H), 6.15 (d, J = 8.4 Hz, 1H), 4.40 – 4.30 (m, 2H), 4.27 – 4.13 (m, 4H), 4.16 – 3.98 (m, 2H), 2.03 (s, 3H), 1.82 – 1.57 (m, 8H), 1.31 – 1.27 (m, 12H), 1.12 – 0.99 (m, 5H).

^{13}C NMR (101 MHz, Chloroform-*d*) δ 171.1, 170.1, 169.52, 169.48, 75.7, 66.2, 61.6, 58.2, 57.6, 41.7, 41.2, 29.7, 28.7, 28.3, 26.14, 26.08, 26.0, 23.4, 17.1, 14.3.



Ethyl *N*-((*S*)-2-acetamido-2-phenylacetyl)-*O*-(*tert*-butyl)-*L*-threonylglycinate (50h)

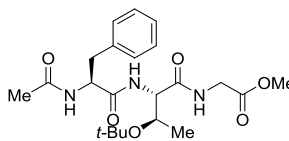
Compound was prepared in analogues way as **50b**: compound **49h** (51 mg, 0.083 mmol) in DMF (3 mL).

Acylation: acetic anhydride (12 μ L, 0.126 mmol) and DIPEA

(30 μ L, 0.168 mmol) in DMF (3 mL). Yield: 25 mg (68%)

^1H NMR (400 MHz, Chloroform-*d*) δ 7.48 (t, J = 5.3 Hz, 1H), 7.40 – 7.28 (m, 5H), 6.98 (d, J = 5.4 Hz, 1H), 6.86 (d, J = 6.8 Hz, 1H), 5.50 (d, J = 6.8 Hz, 1H), 4.29 – 4.25 (m, 1H), 4.25 – 4.22 (m, 1H), 4.18 (q, J = 7.2 Hz, 2H), 4.00 (dd, J = 18.3, 5.1 Hz, 1H), 3.92 (dd, J = 18.3, 5.4 Hz, 1H), 2.02 (s, 3H), 1.28 – 1.23 (m, 12H), 1.06 (d, J = 6.3 Hz, 3H).

^{13}C NMR (101 MHz, Chloroform-*d*) δ 170.0, 169.7, 169.4, 169.3, 137.7, 129.3, 128.7, 127.3, 75.7, 66.0, 61.5, 57.9, 57.5, 41.6, 28.2, 23.2, 17.4, 14.3.



Methyl *N*-(acetyl-*L*-phenylalanyl)-*O*-(*tert*-butyl)-*L*-threonylglycinate (50i)

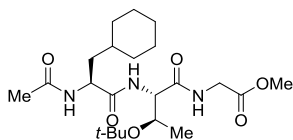
Compound was prepared in analogues way as **50b**: compound **49i** (131 mg, 0.213 mmol) in DMF (4 mL).

Acylation: acetic anhydride (30 μ L, 0.320 mmol) and

DIPEA (74 μ L, 0.427 mmol) in DMF (4 mL). Yield: 72 mg (77%)

^1H NMR (400 MHz, Chloroform-*d*) δ 7.42 (t, J = 5.2 Hz, 1H), 7.34 – 7.19 (m, 3H), 7.20 – 7.14 (m, 2H), 6.88 (d, J = 5.9 Hz, 1H), 6.13 (d, J = 7.5 Hz, 1H), 4.74 (q, J = 6.8 Hz, 1H), 4.28 (dd, J = 5.9, 3.5 Hz, 1H), 4.24 – 4.16 (m, 1H), 4.03 (dd, J = 5.3, 2.0 Hz, 2H), 3.76 (s, 3H), 3.09 (d, J = 6.5 Hz, 2H), 1.98 (s, 3H), 1.27 (s, 9H), 1.00 (d, J = 6.4 Hz, 3H).

¹³C NMR (101 MHz, Chloroform-*d*) δ 170.9, 170.1, 169.9, 169.5, 136.2, 129.3, 128.9, 127.3, 75.6, 66.0, 57.8, 54.5, 52.4, 41.5, 38.4, 28.3, 23.3, 17.6.



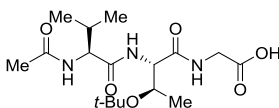
Methyl *N*-((*S*)-2-acetamido-3-cyclohexylpropanoyl)-*O*-(*tert*-butyl)-*L*-threonylglycinate (50j**)**

Compound was prepared in analogues way as **50b**: compound **49j** (186 mg, 0.299 mmol) in DMF (5 mL).

Acylation: acetic anhydride (43 μL, 0.450 mmol) and DIPEA (104 μL, 0.600 mmol) in DMF (5 mL). Yield: 112 mg (84%)

¹H NMR (400 MHz, Chloroform-*d*) δ 7.64 (t, *J* = 5.2 Hz, 1H), 6.97 (d, *J* = 5.8 Hz, 1H), 6.09 (d, *J* = 7.8 Hz, 1H), 4.51 (td, *J* = 8.5, 5.4 Hz, 1H), 4.33 (dd, *J* = 5.8, 3.7 Hz, 1H), 4.19 (qd, *J* = 6.4, 3.9 Hz, 1H), 4.15 – 3.98 (m, 2H), 3.76 (s, 3H), 2.02 (s, 3H), 1.81 – 1.75 (m, 1H), 1.72 – 1.57 (m, 5H), 1.56 – 1.43 (m, 1H), 1.28 (s, 9H), 1.24 – 1.09 (m, 4H), 1.04 (d, *J* = 6.4 Hz, 3H), 0.99 – 0.83 (m, 2H).

¹³C NMR (101 MHz, Chloroform-*d*) δ 172.4, 170.1, 170.0, 169.7, 75.7, 66.1, 57.7, 52.4, 51.4, 41.5, 40.5, 34.2, 33.8, 32.8, 28.3, 26.5, 26.3, 26.1, 23.3, 17.2.

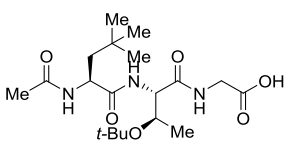


***N*-(acetyl-*L*-valyl)-*O*-(*tert*-butyl)-*L*-threonylglycine (**51a**)**

Starting material **50a** (120 mg, 0.299 mmol) was dissolved in the mixture of THF and H₂O (20:1, 7 mL), then LiOH (72 mg, 2.99 mmol) was added and the reaction mixture was stirred at room temperature until full conversion (UPLC-MS control). Water was added and the reaction mixture was acidified to pH≈2 by the addition of 1 M HCl and the aqueous layer was extracted with EtOAc (4x). Organic phase was washed with brine, dried over Na₂SO₄, filtered and evaporated in vacuo to provide product **51a** (42 mg, 38%).

¹H NMR (400 MHz, Chloroform-*d*) δ 7.66 (t, *J* = 5.0 Hz, 1H), 7.61 (d, *J* = 6.7 Hz, 1H), 6.75 (d, *J* = 8.8 Hz, 1H), 4.54 (dd, *J* = 8.9, 6.3 Hz, 1H), 4.48 (dd, *J* = 6.7, 3.7 Hz, 1H), 4.17 – 4.04 (m, 3H), 2.09 – 1.99 (m, 4H), 1.27 (s, 9H), 1.01 (d, *J* = 6.4 Hz, 3H), 0.94 (d, *J* = 6.7 Hz, 3H), 0.92 (d, *J* = 6.8 Hz, 3H).

¹³C NMR (101 MHz, Chloroform-*d*) δ 171.7, 171.6, 171.2, 170.0, 75.7, 66.5, 58.4, 57.8, 42.0, 31.9, 28.3, 23.3, 19.2, 18.2, 17.4.

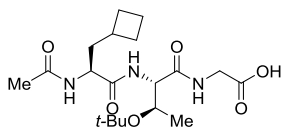


***N*-((*S*)-2-acetamido-4,4-dimethylpentanoyl)-*O*-(*tert*-butyl)-*L*-threonylglycine (**51b**)**

Prepared in analogues way as **51a**: compound **50b** (96 mg, 0.223 mmol) and LiOH (54 mg, 2.23 mmol) in the mixture of THF and H₂O (20:1, 5 mL). Yield: 85 mg (95%)

¹H NMR (400 MHz, Chloroform-*d*) δ 7.65 (t, *J* = 5.0 Hz, 1H), 7.51 (d, *J* = 6.5 Hz, 1H), 6.79 (d, *J* = 8.4 Hz, 1H), 4.69 (td, *J* = 8.6, 3.9 Hz, 1H), 4.38 (dd, *J* = 6.5, 3.7 Hz, 1H), 4.20 – 4.02 (m, 3H), 2.00 (s, 3H), 1.73 (dd, *J* = 14.4, 3.8 Hz, 1H), 1.53 (dd, *J* = 14.4, 8.8 Hz, 1H), 1.25 (s, 9H), 1.01 (d, *J* = 6.4 Hz, 3H), 0.94 (s, 9H).

¹³C NMR (101 MHz, Chloroform-*d*) δ 173.4, 171.8, 170.7, 169.7, 75.6, 66.3, 57.9, 51.3, 46.3, 41.8, 30.8, 29.8, 28.3, 23.2, 17.4.

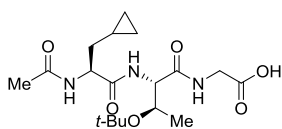


***N*-((*S*)-2-acetamido-3-cyclobutylpropanoyl)-*O*-(*tert*-butyl)-*L*-threonylglycine (**51c**)**

Prepared in analogues way as **51a**: compound **50c** (104 mg, 0.243 mmol) and LiOH (60 mg, 2.51 mmol) in the mixture of THF and H₂O (20:1, 5 mL). Yield: 94 mg (97%)

¹H NMR (400 MHz, Chloroform-*d*) δ 7.67 (t, *J* = 5.1 Hz, 1H), 7.52 (d, *J* = 6.2 Hz, 1H), 6.59 (d, *J* = 8.1 Hz, 1H), 4.59 (q, *J* = 7.7 Hz, 1H), 4.40 (dd, *J* = 6.1, 3.9 Hz, 1H), 4.26 – 4.01 (m, 3H), 2.39 – 2.29 (m, 1H), 2.07 – 1.98 (m, 5H), 1.92 – 1.81 (m, 2H), 1.81 – 1.71 (m, 2H), 1.69 – 1.56 (m, 2H), 1.28 (s, 9H), 1.01 (d, *J* = 6.4 Hz, 3H).

¹³C NMR (101 MHz, Chloroform-*d*) δ 172.1, 171.5, 170.8, 169.9, 75.8, 66.4, 57.9, 52.3, 42.0, 40.3, 32.6, 30.5, 28.6, 28.6, 28.3, 23.3, 18.8, 17.3.

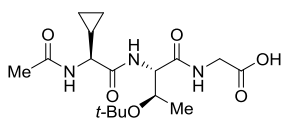


***N*-((*S*)-2-acetamido-3-cyclopropylpropanoyl)-*O*-(*tert*-butyl)-*L*-threonylglycine (**51d**)**

Prepared in analogues way as **51a**: compound **50d** (104 mg, 0.251 mmol) and LiOH (60 mg, 2.51 mmol) in the mixture of THF and H₂O (20:1, 5 mL). Yield: 35 mg (36%)

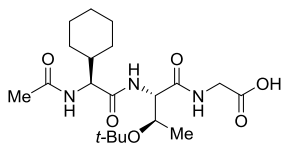
¹H NMR (300 MHz, Chloroform-*d*) δ 7.71 – 7.60 (m, 2H), 6.82 (d, *J* = 8.0 Hz, 1H), 4.81 – 4.67 (m, 1H), 4.44 (dd, *J* = 6.4, 3.7 Hz, 1H), 4.24 – 4.00 (m, 3H), 2.04 (s, 3H), 1.62 (t, *J* = 6.8 Hz, 2H), 1.27 (s, 9H), 1.03 (d, *J* = 6.4 Hz, 3H), 0.78 – 0.59 (m, 1H), 0.52 – 0.37 (m, 2H), 0.11 – 0.00 (m, 2H).

¹³C NMR (101 MHz, Chloroform-*d*) δ 172.1, 171.5, 170.8, 169.9, 75.8, 66.5, 57.9, 53.9, 42.0, 38.1, 28.3, 23.3, 17.4, 7.3, 4.6, 4.3.



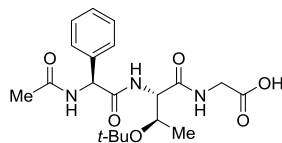
***N*-((*S*)-2-acetamido-2-cyclopropylacetyl)-*O*-(*tert*-butyl)-*L*-threonylglycine (**51e**)**

Prepared in analogues way as **51a**: compound **50e** (74 mg, 0.185 mmol) and LiOH (44 mg, 1.84 mmol) in the mixture of THF and H₂O (20:1, 4.2 mL). Yield: 38 mg (55%). Compound was submitted to the next reaction without identification.



***N*-((*S*)-2-acetamido-2-cyclohexylacetyl)-*O*-(*tert*-butyl)-*L*-threonylglycine (**51g**)**

Prepared in analogues way as **51a**: compound **50g** (14 mg, 0.032 mmol) and LiOH (7.6 mg, 0.32 mmol) in the mixture of THF and H₂O (20:1, 2 mL). Crude mixture was submitted to the next reaction without identification.

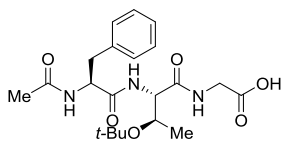


***N*-((*S*)-2-acetamido-2-phenylacetyl)-*O*-(*tert*-butyl)-*L*-threonylglycine (**51h**)**

Prepared in analogues way as **51a**: compound **50h** (78 mg, 0.180 mmol) and LiOH (43 mg, 1.80 mmol) in the mixture of THF and H₂O (20:1, 5 mL). Yield: 72 mg (99%, mixture of diastereomers, dr 2 : 1).

¹H NMR (400 MHz, Chloroform-*d*) δ 7.67 (t, *J* = 5.3 Hz, 0.66H), 7.51 (t, *J* = 5.2 Hz, 0.34H), 7.47 – 7.16 (m, 6H, overlaps with solvent), 5.67 (d, *J* = 7.3 Hz, 0.34H), 5.64 (d, *J* = 7.0 Hz, 0.66H), 4.39 (dd, *J* = 6.5, 3.4 Hz, 0.66H), 4.35 (dd, *J* = 6.2, 3.6 Hz, 0.34H), 4.24 – 3.90 (m, 4H), 2.03 (s, 1H), 2.00 (s, 2H), 1.24 (s, 3H), 1.19 (s, 6H), 1.06 (d, *J* = 6.4 Hz, 1H), 0.78 (d, *J* = 6.3 Hz, 2H).

¹³C NMR (101 MHz, Chloroform-*d*) δ 172.0, 171.8, 170.8, 170.7, 170.6, 170.4, 170.1, 169.8, 137.5, 137.3, 129.24, 129.16, 128.7, 128.6, 127.3, 127.2, 75.7, 75.5, 66.3, 65.8, 58.2, 58.1, 57.4, 57.3, 41.6, 28.24, 28.23, 23.1, 23.0, 17.9, 17.7.

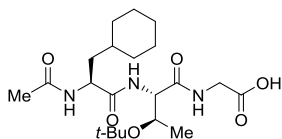


***N*-(acetyl-*L*-phenylalanyl)-*O*-(*tert*-butyl)-*L*-threonylglycine (51i)**

Prepared in analogues way as **51a**: compound **50i** (72 mg, 0.165 mmol) and LiOH (40 mg, 1.65 mmol) in the mixture of THF and H₂O (20:1, 5 mL). Yield: 65 mg (93%)

¹H NMR (400 MHz, Chloroform-*d*) δ 7.54 (d, *J* = 6.6 Hz, 1H), 7.49 (t, *J* = 5.1 Hz, 1H), 7.25 – 7.14 (m, 3H), 7.13 – 7.07 (m, 2H), 6.70 (d, *J* = 8.1 Hz, 1H), 4.97 – 4.89 (m, 1H), 4.40 (dd, *J* = 6.5, 3.6 Hz, 1H), 4.19 – 4.09 (m, 1H), 4.06 (d, *J* = 5.1 Hz, 2H), 3.06 (dd, *J* = 13.9, 6.0 Hz, 1H), 2.98 (dd, *J* = 13.9, 7.3 Hz, 1H), 1.96 (s, 3H), 1.25 (s, 9H), 1.00 (d, *J* = 6.4 Hz, 3H).

¹³C NMR (101 MHz, Chloroform-*d*) δ 171.8, 171.5, 170.9, 169.9, 136.1, 129.3, 128.7, 127.2, 75.7, 66.4, 58.0, 54.4, 41.9, 38.8, 28.3, 23.1, 17.6.

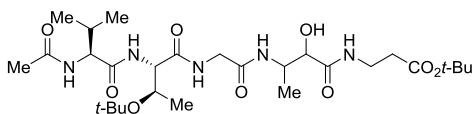


***N*-((*S*)-2-acetamido-3-cyclohexylpropanoyl)-*O*-(*tert*-butyl)-*L*-threonylglycine (51j)**

Prepared in analogues way as **51a**: compound **50j** (112 mg, 0.254 mmol) and LiOH (61 mg, 2.54 mmol) in the mixture of THF and H₂O (20:1, 5 mL). Yield: 99 mg (91%)

¹H NMR (400 MHz, Chloroform-*d*) δ 7.65 (t, *J* = 5.1 Hz, 1H), 7.43 (s, 1H), 6.54 (s, 1H), 4.72 – 4.63 (m, 1H), 4.40 (dd, *J* = 6.4, 3.7 Hz, 1H), 4.18 – 4.13 (m, 1H), 4.13 – 4.07 (m, 2H), 2.04 (s, 3H), 1.80 – 1.72 (m, 1H), 1.71 – 1.48 (m, 6H), 1.27 (s, 9H), 1.23 – 1.08 (m, 4H), 1.02 (d, *J* = 6.4 Hz, 3H), 0.96 – 0.80 (m, 2H).

¹³C NMR (101 MHz, Chloroform-*d*) δ 172.8, 171.7, 170.9, 169.9, 75.7, 66.3, 57.9, 51.5, 41.8, 40.6, 34.2, 33.8, 32.7, 28.3, 26.5, 26.3, 26.1, 23.3, 17.4.



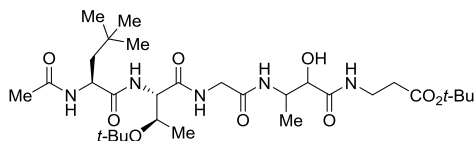
***tert*-Butyl (4*S*,7*S*)-7-((*R*)-1-(*tert*-butoxy)-ethyl)-14-hydroxy-4-isopropyl-13-methyl-2,5,8,11,15-pentaoxo-3,6,9,12,16-penta-azonadecan-19-oate (52a)**

A mixture of an acid **51a** (42 mg, 0.113 mmol), amine **45** (28 mg, 0.114 mmol, 1.01 equiv), HATU (51 mg, 0.134 mmol) and DIPEA (60 μL, 0.34 mmol) in DCM (10 mL) were stirred for 4 h at room temperature. The reaction mixture was washed with H₂O (2×20 mL) and then with brine (20 mL). Organic phase was dried over Na₂SO₄, filtered and evaporated in vacuo. The residue was purified by flash chromatography on

silica gel eluting with 0–5% MeOH in EtOAc to get the product **52a** (50 mg, 74%, mixture of diastereomers).

^1H NMR (400 MHz, Chloroform-*d*) δ 8.13 – 7.94 (m, 1H), 7.93 – 7.80 (m, 1H), 7.45 – 7.30 (m, 2H), 6.77 – 6.65 (m, 1H), 5.32 (s, 1H), 4.70 – 4.58 (m, 1H), 4.48 – 4.40 (m, 1H), 4.39 – 4.29 (m, 1H), 4.23 – 4.17 (m, 1H), 4.17 – 3.98 (m, 3H), 3.57 – 3.39 (m, 2H), 2.44 (t, $J = 6.2$ Hz, 2H), 2.10 – 2.00 (m, 4H), 1.43 (s, 9H), 1.24 (d, $J = 4.1$ Hz, 9H), 1.10 (dd, $J = 6.5, 3.8$ Hz, 3H), 1.00 (dd, $J = 11.3, 6.4$ Hz, 3H), 0.95 – 0.87 (m, 6H).

^{13}C NMR (101 MHz, Chloroform-*d*) δ 171.52, 171.47, 171.43, 171.36, 171.3, 171.2, 169.9, 169.01, 168.96, 81.2, 75.4, 75.3, 74.6, 74.5, 66.7, 58.5, 58.4, 49.4, 49.3, 43.14, 43.07, 35.5, 34.92, 34.87, 32.1, 31.9, 28.3, 28.2, 23.4, 23.3, 18.7, 18.34, 18.30, 14.0, 13.9.

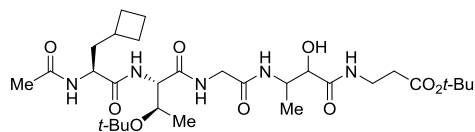


***tert*-Butyl (4*S*,7*S*)-7-((*R*)-1-(*tert*-butoxy)ethyl)-14-hydroxy-13-methyl-4-neopentyl-2,5,8,11,15-pentaoxo-3,6,9,12,16-pentaaza-nonadecan-19-oate (52b)**

The same procedure was used as for **52a**: an acid **51b** (85 mg, 0.212 mmol), amine **45** hydrochloride salt (63 mg, 0.223 mmol, 1.05 equiv), HATU (105 mg, 0.275 mmol) and DIPEA (110 μL , 0.64 mmol) in DCM (10 mL). Yield: 85 mg (64%, mixture of diastereomers)

^1H NMR (400 MHz, Chloroform-*d*) δ 7.59 (dt, $J = 32.8, 5.6$ Hz, 1H), 7.40 (dd, $J = 25.8, 5.9$ Hz, 1H), 7.32 (t, $J = 5.7$ Hz, 1H), 7.06 (dd, $J = 16.6, 7.9$ Hz, 1H), 6.53 (d, $J = 6.1$ Hz, 1H), 5.20 (dd, $J = 21.9, 3.9$ Hz, 1H), 4.42 – 4.06 (m, 6H), 3.84 – 3.65 (m, 1H), 3.59 – 3.38 (m, 2H), 2.47 – 2.41 (m, 2H), 2.07 (d, $J = 3.2$ Hz, 3H), 1.81 (dd, $J = 14.5, 3.0$ Hz, 1H), 1.56 (dd, $J = 14.5, 8.9$ Hz, 1H), 1.43 (s, 9H), 1.17 (d, $J = 3.7$ Hz, 9H), 1.10 (dd, $J = 6.4, 3.4$ Hz, 6H), 0.97 (s, 9H).

^{13}C NMR (101 MHz, Chloroform-*d*) δ 174.12, 174.06, 171.9, 171.51, 171.46, 171.3, 170.3, 169.4, 169.2, 81.2, 75.2, 75.1, 74.4, 74.3, 66.2, 59.8, 53.1, 52.9, 49.4, 49.2, 45.7, 43.1, 43.0, 35.5, 34.9, 30.92, 30.89, 29.74, 29.70, 28.3, 28.2, 23.23, 23.17, 20.3, 20.0, 14.0, 13.8.

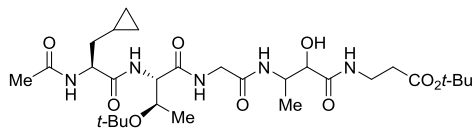


***tert*-Butyl (4*S*,7*S*)-7-((*R*)-1-(*tert*-butoxy)ethyl)-14-(cyclobutylmethyl)-14-hydroxy-13-methyl-2,5,8,11,15-pentaoxo-3,6,9,12,16-pentaaza-nonadecan-19-oate (52c)**

The same procedure was used as for **52a**: an acid **51c** (94 mg, 0.235 mmol), amine **45** (58 mg, 0.235 mmol, 1 equiv), HATU (107 mg, 0.281 mmol) and DIPEA (120 μL , 0.705 mmol) in DCM (10 mL). Yield: 124 mg (84%, mixture of diastereomers)

^1H NMR (400 MHz, Chloroform-*d*) δ 7.97 (d, $J = 31.2$ Hz, 1H), 7.78 (d, $J = 5.4$ Hz, 1H), 7.33 (s, 2H), 6.68 (s, 1H), 4.64 (d, $J = 24.6$ Hz, 1H), 4.35 (s, 2H), 4.21 (dd, $J = 9.5, 2.3$ Hz, 1H), 4.19 – 3.92 (m, 3H), 3.57 – 3.41 (m, 2H), 2.46 – 2.41 (m, 2H), 2.40 – 2.30 (m, 1H), 2.08 – 1.97 (m, 5H), 1.91 – 1.70 (m, 4H), 1.68 – 1.53 (m, 2H), 1.43 (s, 9H), 1.23 (d, $J = 6.0$ Hz, 9H), 1.11 (dd, $J = 6.9, 4.6$ Hz, 3H), 1.00 (dd, $J = 11.1, 6.3$ Hz, 3H).

^{13}C NMR (101 MHz, Chloroform-*d*) δ 172.3, 172.1, 171.5, 171.4, 171.3, 171.2, 171.0, 169.82, 169.81, 168.94, 168.91, 81.14, 81.12, 75.4, 75.3, 74.6, 74.5, 66.5, 58.8, 58.7, 53.0, 52.7, 49.4, 49.3, 43.14, 43.08, 40.5, 40.4, 35.5, 34.90, 34.88, 32.52, 32.50, 28.72, 28.70, 28.69, 28.67, 28.3, 28.2, 23.35, 23.29, 18.8, 18.4, 14.0, 13.9.

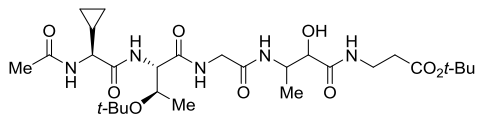


tert-Butyl (4*S*,7*S*)-7-((*R*)-1-(*tert*-butoxy)-ethyl)-4-(cyclopropylmethyl)-14-hydroxy-13-methyl-2,5,8,11,15-pentaoxo-3,6,9,12,16-pentaaza-nonadecan-19-oate (52d)

The same procedure was used as for **52a**: an acid **51d** (35 mg, 0.091 mmol), amine **45** (23 mg, 0.093 mmol, 1.03 equiv), HATU (41.5 mg, 0.109 mmol) and DIPEA (47 μL , 0.272 mmol) in DCM (5 mL). Yield: 37 mg (66%, mixture of diastereomers)

^1H NMR (400 MHz, Chloroform-*d*) δ 7.85 (d, $J = 27.9$ Hz, 1H), 7.76 – 7.68 (m, 1H), 7.34 – 7.22 (m, 2H), 6.72 (d, $J = 6.1$ Hz, 1H), 5.32 – 5.19 (m, 1H) 4.77 – 4.63 (m, 1H), 4.39 – 4.28 (m, 2H), 4.24 – 4.20 (m, 2H), 4.20 – 3.88 (m, 2H), 3.59 – 3.40 (m, 2H), 2.44 (t, $J = 6.3$ Hz, 2H), 2.07 (s, 3H), 1.71 – 1.57 (m, 2H), 1.44 (s, 9H), 1.24 (d, $J = 6.5$ Hz, 9H), 1.11 (d, $J = 6.9$ Hz, 3H), 1.03 (dd, $J = 9.5, 6.4$ Hz, 3H), 0.74 – 0.65 (m, 1H), 0.49 – 0.40 (m, 2H), 0.09 – 0.00 (m, 2H).

^{13}C NMR (101 MHz, Chloroform-*d*) δ 172.2, 172.1, 171.51, 171.47, 171.4, 171.24, 171.18, 171.1, 170.0, 169.0, 81.18, 81.16, 75.4, 75.3, 74.6, 74.5, 66.5, 59.0, 54.4, 49.5, 49.4, 43.1, 38.0, 35.5, 34.9, 28.3, 28.2, 23.3, 19.0, 18.6, 14.0, 13.9, 7.2, 4.5.

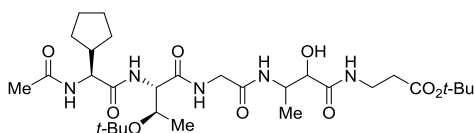


tert-Butyl (4*S*,7*S*)-7-((*R*)-1-(*tert*-butoxy)-ethyl)-4-cyclopropyl-14-hydroxy-13-methyl-2,5,8,11,15-pentaoxo-3,6,9,12,16-pentaaza-nonadecan-19-oate (52e)

The same procedure was used as for **52a**: an acid **51e** (38 mg, 0.102 mmol), amine **45** (26 mg, 0.106 mmol, 1.03 equiv), HATU (47 mg, 0.123 mmol) and DIPEA (50 μL , 0.31 mmol) in DCM (5 mL). Yield: 43 mg (69%, mixture of diastereomers)

^1H NMR (400 MHz, Chloroform-*d*) δ 7.81 – 7.28 (m, 2H), 7.11 – 6.97 (m, 1H), 6.85 – 6.61 (m, 2H), 4.38 – 4.07 (m, 5H), 3.74 – 3.37 (m, 4H), 2.48 – 2.41 (m, 2H), 2.11 – 1.97 (m, 3H), 1.44 (s, 9H), 1.22 – 1.04 (m, 15H), 0.72 – 0.55 (m, 3H), 0.53 – 0.37 (m, 2H).

^{13}C NMR (101 MHz, Chloroform-*d*) δ 173.8, 173.6, 172.0, 171.9, 171.85, 171.6, 171.54, 171.48, 171.3, 171.2, 170.64, 170.57, 170.4, 170.3, 169.6, 169.4, 169.2, 81.3, 81.2, 81.1, 75.2, 75.1, 75.0, 74.4, 74.2, 66.2, 65.8, 65.7, 60.6, 60.4, 59.9, 59.8, 59.7, 59.6, 59.1, 49.39, 49.35, 49.0, 43.3, 43.2, 43.0, 35.50, 35.46, 34.93, 34.90, 34.88, 28.44, 28.41, 28.35, 28.2, 23.2, 23.1, 22.9, 22.8, 21.03, 20.98, 20.4, 20.0, 13.93, 13.92, 13.8, 13.6, 12.9, 4.0, 3.9, 3.8, 3.7, 3.43, 3.35.



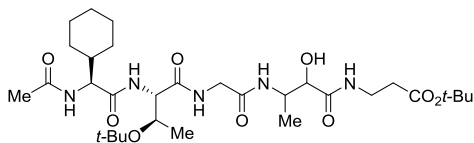
***tert*-Butyl (4*S*,7*S*)-7-((*R*)-1-(*tert*-butoxy)-ethyl)-4-cyclopentyl-14-hydroxy-13-methyl-2,5,8,11,15-pentaoxo-3,6,9,12,16-pentaaza-**

nonadecan-19-oate (52f)

The same procedure was used as for **52a**: an acid **51f** (102 mg, 0.255 mmol), amine **45** (63 mg, 0.256 mmol, 1 equiv), HATU (117 mg, 0.306 mmol) and DIPEA (130 μ L, 0.766 mmol) in DCM (10 mL). Yield: 135 mg (84%, mixture of diastereomers)

^1H NMR (400 MHz, Chloroform-*d*) δ 8.17 – 7.83 (m, 2H), 7.43 (s, 1H), 7.33 (s, 1H), 6.88 – 6.62 (m, 1H), 5.40 (d, J = 25.4 Hz, 1H), 4.77 – 4.63 (m, 1H), 4.49 – 4.40 (m, 1H), 4.40 – 4.30 (m, 1H), 4.24 – 4.15 (m, 2H), 4.06 – 3.93 (m, 2H), 3.60 – 3.40 (m, 2H), 2.44 (t, J = 6.3 Hz, 2H), 2.15 (p, J = 8.2 Hz, 1H), 2.06 (s, 3H), 1.67 (d, J = 15.1 Hz, 1H), 1.64 – 1.54 (m, 3H), 1.52 – 1.46 (m, 2H), 1.43 (d, J = 0.7 Hz, 9H), 1.40 – 1.29 (m, 2H), 1.23 (d, J = 1.5 Hz, 9H), 1.10 (td, J = 7.0, 1.4 Hz, 3H), 1.01 (dd, J = 12.3, 6.3 Hz, 3H).

^{13}C NMR (101 MHz, Chloroform-*d*) δ 172.0, 171.9, 171.4, 171.3, 171.2, 169.9, 169.0, 168.8, 81.1, 75.2, 74.6, 74.5, 66.9, 58.4, 57.0, 56.8, 49.3, 49.2, 43.9, 43.2, 43.0, 35.5, 34.9, 29.2, 29.1, 28.4, 28.3, 28.2, 25.2, 24.9, 23.35, 23.32, 18.8, 18.6, 14.0, 13.9.

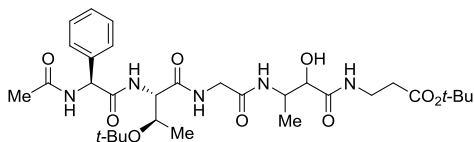


***tert*-Butyl (4*S*,7*S*)-7-((*R*)-1-(*tert*-butoxy)-ethyl)-4-cyclohexyl-14-hydroxy-13-methyl-2,5,8,11,15-pentaoxo-3,6,9,12,16-pentaaza-nonadecan-19-oate (52g)**

The same procedure was used as for **52a**: an acid **51g** (31 mg, 0.076 mmol), amine **45** (20 mg, 0.081 mmol, 1.07 equiv), HATU (35 mg, 0.092 mmol) and DIPEA (40 μ L, 0.23 mmol) in DCM (5 mL). Yield: 31 mg (63%, mixture of diastereomers)

^1H NMR (400 MHz, Chloroform-*d*) δ 8.10 – 7.76 (m, 2H), 7.49 – 7.28 (m, 2H), 6.79 – 6.52 (m, 1H), 5.31 (s, 1H), 4.61 (s, 1H), 4.47 – 4.28 (m, 2H), 4.24 – 4.12 (m, 2H), 4.10 – 3.94 (m, 2H), 3.59 – 3.38 (m, 2H), 2.44 (t, J = 6.3 Hz, 2H), 2.06 (s, 3H), 1.79 – 1.56 (m, 6H), 1.43 (s, 9H), 1.23 (s, 9H), 1.22 – 0.94 (m, 11H).

^{13}C NMR (101 MHz, Chloroform-*d*) δ 171.5, 171.44, 171.43, 171.37, 171.3, 171.2, 169.93, 169.86, 169.1, 168.9, 81.1, 75.3, 74.6, 74.5, 66.7, 58.5, 58.4, 58.3, 49.4, 49.2, 43.2, 43.1, 41.7, 41.6, 35.5, 34.9, 29.8, 29.6, 28.8, 28.3, 28.2, 26.2, 26.1, 23.4, 18.8, 18.6, 14.1, 13.9.



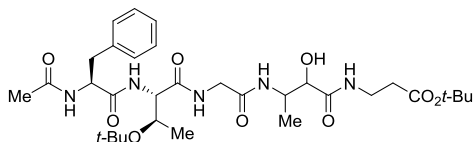
***tert*-Butyl (4*S*,7*S*)-7-((*R*)-1-(*tert*-butoxy)-ethyl)-14-hydroxy-13-methyl-2,5,8,11,15-pentaoxo-4-phenyl-3,6,9,12,16-pentaaza-nonadecan-19-oate (52h)**

The same procedure was used as for **52a**: an acid **51h** (72 mg, 0.177 mmol), amine **45** (44 mg, 0.179 mmol, 1.01 equiv), HATU (81 mg, 0.212 mmol) and DIPEA (92 μ L, 0.53 mmol) in DCM (5 mL). Yield: 93 mg (83%, mixture of diastereomers)

^1H NMR (300 MHz, Chloroform-*d*) δ 7.79 – 7.59 (m, 1H), 7.48 – 7.28 (m, 7H), 7.12 – 6.93 (m, 2H), 5.60 – 5.49 (m, 1H), 5.24 – 5.05 (m, 1H), 4.33 – 4.00 (m, 5H), 3.87 – 3.67

(m, 1H), 3.52 (d, $J = 6.5$ Hz, 1H), 3.45 – 3.35 (m, 1H), 2.49 – 2.37 (m, 2H), 2.06 – 1.99 (m, 3H), 1.43 (s, 9H), 1.14 (s, 9H), 1.07 – 1.02 (m, 3H), 0.95 – 0.87 (m, 3H).

^{13}C NMR (101 MHz, Chloroform- d) δ 171.9, 171.7, 171.5, 169.7, 129.4, 129.3, 129.2, 127.5, 81.3, 75.2, 66.0, 59.8, 58.2, 49.2, 49.0, 43.3, 35.4, 34.9, 28.3, 28.3, 28.2, 23.0, 22.9, 19.8, 14.3, 13.8.

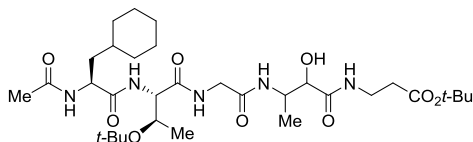


tert-Butyl (4*S*,7*S*)-4-benzyl-7-((*R*)-1-(*tert*-butoxy)ethyl)-14-hydroxy-13-methyl-2,5,8,11,15-pentaoxo-3,6,9,12,16-pentaaza-nonadecan-19-oate (52i)

The same procedure was used as for **52a**: an acid **51i** (65 mg, 0.154 mmol), amine **45** hydrochloride salt (46 mg, 0.163 mmol, 1.05 equiv), HATU (76 mg, 0.200 mmol) and DIPEA (80 μL , 0.46 mmol) in DCM (7 mL). Yield: 60 mg (60%, mixture of diastereomers)

^1H NMR (400 MHz, Chloroform- d) 7.80 – 7.65 (m, 1H), 7.59 – 7.50 (m, 1H), 7.33 – 7.17 (m, 3H), 7.18 – 7.09 (m, 3H), 6.47 (d, $J = 6.8$ Hz, 1H), 5.17 (dd, $J = 16.8, 4.3$ Hz, 1H), 4.97 – 4.84 (m, 1H), 4.39 – 4.27 (m, 2H), 4.24 – 4.13 (m, 2H), 4.12 – 3.79 (m, 3H), 3.59 – 3.39 (m, 2H), 3.18 – 3.07 (m, 1H), 3.09 – 2.95 (m, 1H), 2.45 (td, $J = 6.4, 2.0$ Hz, 2H), 1.99 (s, 3H), 1.44 (d, $J = 1.0$ Hz, 9H), 1.20 (d, $J = 6.8$ Hz, 9H), 1.12 (dd, $J = 6.9, 3.1$ Hz, 3H), 1.01 (dd, $J = 6.4, 4.7$ Hz, 3H).

^{13}C NMR (101 MHz, Chloroform- d) δ 171.53, 171.51, 171.5, 171.4, 171.2, 171.11, 171.06, 170.0, 169.0, 168.9, 136.07, 136.05, 129.4, 129.3, 128.83, 128.77, 127.4, 127.3, 81.2, 81.1, 75.4, 75.3, 74.6, 74.5, 66.4, 59.1, 59.0, 54.9, 54.8, 49.4, 43.2, 39.1, 38.9, 35.50, 35.48, 34.91, 34.88, 28.3, 28.2, 23.23, 23.20, 19.1, 18.8, 14.1, 14.0.

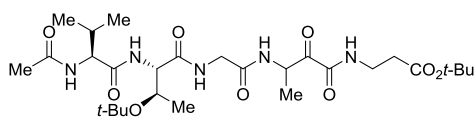


tert-Butyl (4*S*,7*S*)-7-((*R*)-1-(*tert*-butoxy)ethyl)-4-(cyclohexylmethyl)-14-hydroxy-13-methyl-2,5,8,11,15-pentaoxo-3,6,9,12,16-pentaaza-nonadecan-19-oate (52j)

The same procedure was used as for **52a**: an acid **51j** (99 mg, 0.232 mmol), amine **45** hydrochloride salt (69 mg, 0.244 mmol, 1.05 equiv), HATU (115 mg, 0.302 mmol) and DIPEA (120 μL , 0.69 mmol) in DCM (10 mL). Yield: 90 mg (59%, mixture of diastereomers)

^1H NMR (400 MHz, Chloroform- d) δ 7.66 (d, $J = 22.7$ Hz, 1H), 7.54 (d, $J = 36.6$ Hz, 1H), 7.31 (q, $J = 6.2$ Hz, 1H), 7.10 (d, $J = 6.9$ Hz, 1H), 6.57 (d, $J = 6.4$ Hz, 1H), 5.24 (dd, $J = 29.9, 4.4$ Hz, 1H), 4.58 – 4.42 (m, 1H), 4.34 (dt, $J = 16.5, 8.4$ Hz, 1H), 4.29 – 4.04 (m, 4H), 3.93 – 3.71 (m, 1H), 3.61 – 3.37 (m, 2H), 2.44 (td, $J = 6.6, 2.9$ Hz, 2H), 2.07 (d, $J = 2.7$ Hz, 3H), 1.80 – 1.51 (m, 7H), 1.44 (s, 9H), 1.39 – 1.15 (m, 13H), 1.14 – 1.03 (m, 6H), 1.00 – 0.80 (m, 2H).

^{13}C NMR (101 MHz, Chloroform- d) δ 173.4, 173.3, 171.9, 171.7, 171.50, 171.45, 171.3, 171.2, 170.3, 170.2, 169.2, 169.1, 81.15, 81.13, 75.24, 75.15, 74.5, 74.4, 66.3, 59.4, 59.3, 52.9, 52.5, 49.4, 49.3, 43.1, 43.0, 40.3, 40.1, 35.5, 34.9, 34.2, 33.83, 33.78, 32.6, 28.3, 28.2, 26.4, 26.2, 26.0, 23.25, 23.18, 19.9, 19.5, 14.0, 13.9.

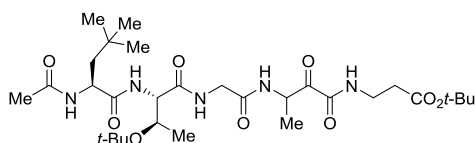


***tert*-Butyl (4*S*,7*S*)-7-((*R*)-1-(*tert*-butoxy)ethyl)-4-isopropyl-13-methyl-2,5,8,11,14,15-hexaoxo-3,6,9,12,16-pentaazonadecan-19-oate (53a)**

Starting material **52a** (50 mg, 0.083 mmol) was dissolved in dry DCM (3 mL), and then DMP (0.4 M, 620 μ L, 0.248 mmol, 3 equiv) was added to the solution. Reaction was stirred at room temperature until full conversion (UPLC-MS control). Mixture was washed with $\text{Na}_2\text{S}_2\text{O}_3$, NaHCO_3 and brine, dried over Na_2SO_4 , filtered and evaporated in vacuo. The residue was purified by flash chromatography on silica gel eluting with 0–10 % MeOH in EtOAc. Yield: 36 mg (73%, mixture of diastereomers)

^1H NMR (400 MHz, Chloroform-*d*) δ 7.98 (s, 1H), 7.81 – 7.66 (m, 2H), 7.59 – 7.51 (m, 1H), 6.42 (s, 1H), 5.47 – 5.33 (m, 1H), 4.81 – 4.72 (m, 1H), 4.48 – 4.42 (m, 1H), 4.33 – 4.02 (m, 3H), 3.56 – 3.50 (m, 2H), 2.51 – 2.45 (m, 2H), 2.08 – 1.96 (m, 4H), 1.47 – 1.40 (m, 12H), 1.29 (s, 9H), 0.98 – 0.87 (m, 9H).

^{13}C NMR (101 MHz, Chloroform-*d*) δ 196.7, 196.4, 171.3, 171.1, 170.4, 170.3, 169.5, 169.4, 168.2, 159.0, 81.51, 81.48, 75.6, 66.5, 57.9, 50.3, 43.2, 35.2, 35.1, 34.9, 32.4, 28.3, 28.2, 23.6, 19.2, 18.3, 17.5, 17.4, 17.3.



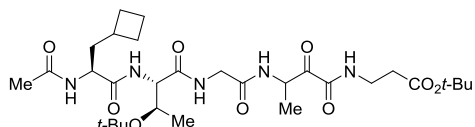
***tert*-Butyl (4*S*,7*S*)-7-((*R*)-1-(*tert*-butoxy)ethyl)-13-methyl-4-neopentyl-2,5,8,11,14,15-hexaoxo-3,6,9,12,16-pentaazonadecan-19-oate (53b)**

The same procedure was used as for **53a**:

compound **52b** (85 mg, 0.135 mmol) and DMP (0.4 M, 1 mL, 0.405 mmol) in dry DCM (10 mL). Yield: 63 mg (74%, mixture of diastereomers).

^1H NMR (400 MHz, Chloroform-*d*) δ 7.80 – 7.47 (m, 4H), 6.21 (d, J = 8.2 Hz, 1H), 5.53 – 5.35 (m, 1H), 4.80 – 4.70 (m, 1H), 4.38 – 4.32 (m, 1H), 4.22 – 4.03 (m, 3H), 3.57 – 3.50 (m, 2H), 2.52 – 2.45 (m, 2H), 2.02 (s, 3H), 1.80 – 1.72 (m, 1H), 1.51 (dd, J = 14.5, 8.5 Hz, 1H), 1.48 – 1.39 (m, 12H), 1.27 (s, 9H), 0.98 (t, J = 6.8 Hz, 3H), 0.93 (d, J = 2.0 Hz, 9H).

^{13}C NMR (101 MHz, Chloroform-*d*) δ 196.8, 196.4, 173.0, 172.9, 171.1, 170.0, 169.6, 169.5, 168.24, 168.18, 159.1, 159.0, 81.5, 81.4, 75.6, 66.31, 66.27, 58.24, 58.16, 51.39, 51.36, 50.4, 46.93, 46.91, 43.2, 35.3, 35.2, 34.95, 34.92, 30.8, 29.8, 28.3, 28.2, 23.5, 17.9, 17.8, 17.7, 17.6.



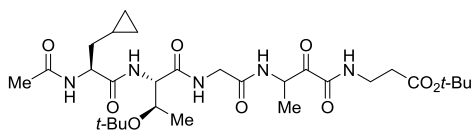
***tert*-Butyl (4*S*,7*S*)-7-((*R*)-1-(*tert*-butoxy)ethyl)-4-(cyclobutylmethyl)-13-methyl-2,5,8,11,14,15-hexaoxo-3,6,9,12,16-pentaazonadecan-19-oate (53c)**

The same procedure was used as for **53a**: compound **52c** (124 mg, 0.198 mmol) and DMP (0.4 M, 1.48 mL, 0.592 mmol) in dry DCM (7 mL). Yield: 24 mg (19%, mixture of diastereomers).

^1H NMR (400 MHz, Chloroform-*d*) δ 8.02 (s, 1H), 7.84 – 7.64 (m, 2H), 7.56 – 7.47 (m, 1H), 6.41 (s, 1H), 5.46 – 5.34 (m, 1H), 4.86 – 4.76 (m, 1H), 4.41 – 4.37 (m, 1H), 4.26 –

4.04 (m, 3H), 3.59 – 3.48 (m, 2H), 2.48 (t, $J = 5.4$ Hz, 2H), 2.41 – 2.28 (m, 1H), 2.06 – 1.99 (m, 5H), 1.89 – 1.72 (m, 4H), 1.65 – 1.53 (m, 2H), 1.49 – 1.39 (m, 12H), 1.29 (s, 9H), 0.94 (t, $J = 6.6$ Hz, 3H).

^{13}C NMR (101 MHz, Chloroform- d) δ 196.6, 196.3, 172.0, 171.9, 171.17, 171.15, 170.09, 170.06, 169.4, 169.3, 168.20, 168.16, 159.0, 81.54, 81.51, 75.6, 66.4, 66.3, 58.12, 58.08, 52.1, 50.3, 43.2, 41.1, 35.15, 35.12, 34.93, 34.91, 32.6, 28.72, 28.66, 28.3, 28.2, 23.5, 18.8, 17.5, 17.4, 17.3.

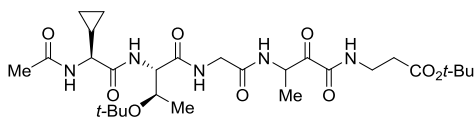


***tert*-Butyl (4*S*,7*S*)-7-((*R*)-1-(*tert*-butoxy)ethyl)-4-(cyclopropylmethyl)-13-methyl-2,5,8,11,14,15-hexaoxo-3,6,9,12,16-pentaaza-nonadecan-19-oate (53d)**

The same procedure was used as for **53a**: compound **52d** (36.5 mg, 0.0595 mmol) and DMP (0.4 M, 450 μL , 0.180 mmol) in dry DCM (4 mL). Yield: 27 mg (74%, mixture of diastereomers).

^1H NMR (400 MHz, Chloroform- d) δ 8.01 (t, $J = 5.4$ Hz, 1H), 7.74 – 7.63 (m, 2H), 7.50 (q, $J = 6.1$ Hz, 1H), 6.53 (dd, $J = 8.0, 3.3$ Hz, 1H), 5.47 – 5.31 (m, 1H), 4.95 (q, $J = 6.7$ Hz, 1H), 4.43 – 4.38 (m, 1H), 4.22 – 4.04 (m, 3H), 3.56 – 3.49 (m, 2H), 2.51 – 2.45 (m, 2H), 2.03 (d, $J = 1.2$ Hz, 3H), 1.71 – 1.62 (m, 1H), 1.60 – 1.50 (m, 1H), 1.48 – 1.38 (m, 12H), 1.29 (d, $J = 1.1$ Hz, 9H), 0.95 (dd, $J = 6.5, 5.2$ Hz, 3H), 0.72 – 0.63 (m, 1H), 0.42 – 0.37 (m, 2H), 0.02 – -0.04 (m, 2H).

^{13}C NMR (101 MHz, Chloroform- d) δ 196.5, 196.3, 171.9, 171.8, 171.2, 171.1, 170.02, 169.97, 169.5, 169.4, 168.19, 168.16, 159.0, 81.52, 81.50, 75.6, 66.44, 66.40, 58.2, 58.1, 53.6, 53.5, 50.3, 43.22, 43.20, 38.85, 38.79, 35.13, 35.10, 34.9, 28.3, 28.2, 23.5, 17.5, 17.44, 17.39, 17.3, 7.3, 7.2, 4.6, 4.3.

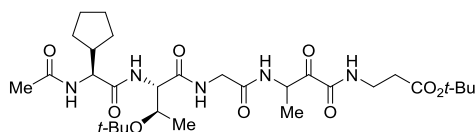


***tert*-Butyl (4*S*,7*S*)-7-((*R*)-1-(*tert*-butoxy)ethyl)-4-cyclopropyl-13-methyl-2,5,8,11,14,15-hexaoxo-3,6,9,12,16-pentaazanonadecan-19-oate (53e)**

The same procedure was used as for **53a**: compound **52e** (42.6 mg, 0.071 mmol) and DMP (0.4 M, 530 μL , 0.213 mmol) in dry DCM (4 mL). Yield: 33 mg (78%, mixture of diastereomers).

^1H NMR (400 MHz, Chloroform- d) δ 7.80 – 7.61 (m, 2H), 7.53 – 7.47 (m, 1H), 7.21 – 7.07 (m, 1H), 6.47 (dd, $J = 25.0, 6.8$ Hz, 1H), 5.41 – 5.28 (m, 1H), 4.43 – 4.04 (m, 5H), 3.94 – 3.73 (m, 1H), 3.58 – 3.48 (m, 2H), 2.52 – 2.43 (m, 2H), 2.06 – 1.98 (m, 3H), 1.44 (s, 12H), 1.30 – 0.95 (m, 13H), 0.66 – 0.42 (m, 4H).

^{13}C NMR (101 MHz, Chloroform- d) δ 196.6, 196.5, 196.3, 196.1, 172.4, 172.0, 171.41, 171.37, 171.33, 171.26, 171.2, 171.13, 171.10, 170.8, 170.45, 170.35, 170.2, 170.0, 169.7, 169.6, 168.6, 168.4, 168.25, 168.21, 159.3, 159.2, 159.14, 159.06, 81.52, 81.50, 75.50, 75.49, 75.3, 75.2, 66.3, 65.70, 65.68, 60.5, 59.4, 58.9, 58.5, 58.3, 57.9, 56.8, 56.7, 50.32, 50.30, 43.3, 43.15, 43.09, 35.13, 35.10, 34.9, 28.4, 28.3, 28.2, 23.4, 23.1, 23.0, 21.7, 21.2, 19.6, 19.0, 18.1, 17.9, 17.40, 17.35, 17.1, 15.1, 15.0, 14.3, 14.2, 13.8, 3.6, 3.5, 3.42, 3.40, 3.38, 3.3.

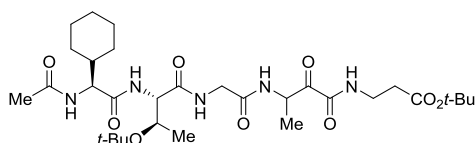


tert-Butyl (4*S*,7*S*)-7-((*R*)-1-(*tert*-butoxy)-ethyl)-4-cyclopentyl-13-methyl-2,5,8,11,14,15-hexaoxo-3,6,9,12,16-penta-azanonadecan-19-oate (53f)

The same procedure was used as for **53a**: compound **52f** (135 mg, 0.215 mmol) and DMP (0.4 M, 1.61 mL, 0.644 mmol) in dry DCM (8 mL). Yield: 80 mg (60%, mixture of diastereomers).

^1H NMR (400 MHz, Chloroform-*d*) δ 8.01 (t, J = 6.0 Hz, 1H), 7.81 – 7.68 (m, 2H), 7.59 – 7.51 (m, 1H), 6.48 – 6.40 (m, 1H), 5.48 – 5.34 (m, 1H), 4.79 (t, J = 8.4 Hz, 1H), 4.48 – 4.40 (m, 1H), 4.30 – 4.01 (m, 3H), 3.59 – 3.48 (m, 2H), 2.52 – 2.43 (m, 2H), 2.18 – 2.09 (m, 1H), 2.04 (s, 3H), 1.72 – 1.53 (m, 4H), 1.51 – 1.39 (m, 13H), 1.34 – 1.21 (m, 12H), 0.94 (t, J = 6.9 Hz, 3H).

^{13}C NMR (101 MHz, Chloroform-*d*) δ 196.7, 196.4, 171.84, 171.81, 171.15, 171.14, 170.3, 170.2, 169.5, 169.4, 168.24, 168.21, 159.1, 159.0, 81.51, 81.48, 75.62, 75.60, 66.51, 66.47, 57.92, 57.89, 56.22, 56.21, 50.31, 50.29, 44.21, 44.20, 43.2, 35.2, 35.1, 34.94, 34.92, 29.2, 29.01, 28.98, 28.3, 28.2, 25.2, 24.9, 23.6, 17.6, 17.41, 17.37, 17.36.

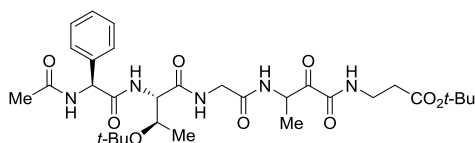


tert-Butyl (4*S*,7*S*)-7-((*R*)-1-(*tert*-butoxy)-ethyl)-4-cyclohexyl-13-methyl-2,5,8,11,14,15-hexaoxo-3,6,9,12,16-penta-azanonadecan-19-oate (53g)

The same procedure was used as for **53a**: compound **52g** (30.6 mg, 0.048 mmol) and DMP (0.4 M, 360 μL , 0.144 mmol) in dry DCM (7 mL). Yield: 19 mg (63%, mixture of diastereomers)

^1H NMR (400 MHz, Chloroform-*d*) δ 7.81 – 7.65 (m, 2H), 7.62 – 7.48 (m, 2H), 6.27 (d, J = 8.4 Hz, 1H), 5.48 – 5.34 (m, 1H), 4.66 (q, J = 8.2, 7.8 Hz, 1H), 4.41 (dd, J = 6.1, 3.8 Hz, 1H), 4.24 – 4.05 (m, 3H), 3.58 – 3.50 (m, 2H), 2.51 – 2.45 (m, 2H), 2.06 (s, 3H), 11.76 – 1.59 (m, 7H), 1.45 (s, 9H), 1.30 (s, 9H), 1.25 – 0.99 (m, 7H), 0.95 (t, J = 6.8 Hz, 3H).

^{13}C NMR (101 MHz, Chloroform-*d*) δ 196.7, 196.3, 171.24, 171.19, 171.17, 171.15, 170.34, 170.30, 169.53, 169.45, 168.21, 168.19, 159.04, 159.01, 81.55, 81.52, 75.67, 75.66, 66.32, 66.29, 58.01, 57.98, 57.9, 50.4, 50.3, 43.31, 43.30, 41.9, 35.2, 35.1, 34.9, 31.1, 29.6, 28.8, 28.3, 28.2, 26.19, 26.16, 23.6, 17.61, 17.58, 17.52, 17.49.

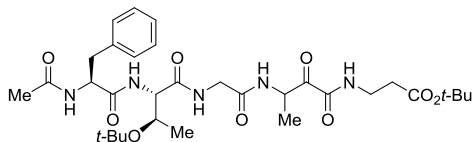


tert-Butyl (4*S*,7*S*)-7-((*R*)-1-(*tert*-butoxy)-ethyl)-13-methyl-2,5,8,11,14,15-hexaoxo-4-phenyl-3,6,9,12,16-penta-azanonadecan-19-oate (53h)

The same procedure was used as for **53a**: compound **52h** (75 mg, 0.118 mmol) and DMP (0.4 M, 885 μL , 0.354 mmol) in dry DCM (5 mL). Yield: 40 mg (53%, mixture of diastereomers).

^1H NMR (400 MHz, Chloroform-*d*) δ 7.80 – 7.68 (m, 1H), 7.56 – 7.25 (m, 9H), 7.10 – 6.88 (m, 2H), 5.88 – 5.67 (m, 1H), 5.40 – 5.27 (m, 1H), 4.41 – 4.32 (m, 1H), 4.20 – 3.94 (m, 4H), 3.57 – 3.46 (m, 2H), 2.50 – 2.42 (m, 2H), 2.09 – 2.00 (m, 3H), 1.45 – 1.42 (m, 9H), 1.27 – 1.21 (m, 9H), 1.04 (t, J = 6.1 Hz, 1H), 0.80 – 0.74 (m, 2H).

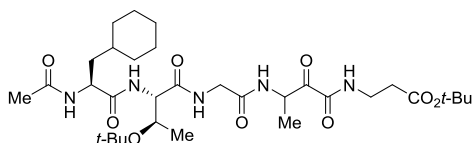
^{13}C NMR (101 MHz, Chloroform-*d*) δ 196.5, 196.3, 171.2, 171.1, 170.7, 170.5, 170.3, 170.2, 170.0, 169.6, 169.5, 168.2, 168.1, 159.2, 159.1, 138.0, 137.6, 129.14, 129.11, 129.09, 129.0, 128.7, 128.6, 127.0, 126.9, 81.53, 81.50, 75.6, 75.53, 75.49, 65.5, 58.6, 58.3, 57.4, 57.2, 50.4, 43.2, 35.1, 34.90, 34.88, 28.3, 28.24, 28.20, 23.19, 23.15, 18.1, 17.6, 17.33, 17.29.



***tert*-Butyl (4*S*,7*S*)-4-benzyl-7-((*R*)-1-(*tert*-butoxy)ethyl)-13-methyl-2,5,8,11,14,15-hexaaxo-3,6,9,12,16-pentaazanonadecan-19-oate (53i)**

The same procedure was used as for **53a**: compound **52i** (59 mg, 0.091 mmol) and DMP (0.4 M, 680 μL , 0.272 mmol) in dry DCM (7 mL). Yield: 40 mg (68%, mixture of diastereomers).

^1H NMR (400 MHz, Chloroform-*d*) δ 7.55 – 7.45 (m, 2H), 7.42 – 7.29 (m, 2H), 7.28 – 7.09 (m, 5H), 6.22 (dd, $J = 7.6, 2.0$ Hz, 1H), 5.38 (p, $J = 7.2$ Hz, 1H), 4.98 (p, $J = 6.9$ Hz, 1H), 4.35 – 4.26 (m, 1H), 4.16 – 3.94 (m, 3H), 3.57 – 3.50 (m, 2H), 3.13 – 3.00 (m, 2H), 2.48 (t, $J = 5.9$ Hz, 2H), 1.99 (d, $J = 2.7$ Hz, 3H), 1.47 – 1.40 (m, 12H), 1.24 (d, $J = 7.9$ Hz, 9H), 0.97 (d, $J = 6.3$ Hz, 3H).

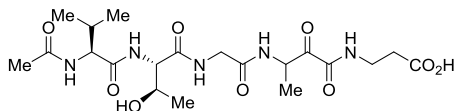


***tert*-Butyl (4*S*,7*S*)-7-((*R*)-1-(*tert*-butoxy)ethyl)-4-(cyclohexylmethyl)-13-methyl-2,5,8,11,14,15-hexaaxo-3,6,9,12,16-pentaazanonadecan-19-oate (53j)**

The same procedure was used as for **53a**: compound **52j** (90 mg, 0.137 mmol) and DMP (0.4 M, 1 mL, 0.412 mmol) in dry DCM (10 mL). Yield: 70 mg (78%, mixture of diastereomers).

^1H NMR (400 MHz, Chloroform-*d*) δ 7.80 – 7.46 (m, 4H), 6.27 (d, $J = 8.1$ Hz, 1H), 5.52 – 5.34 (m, 1H), 4.85 – 4.72 (m, 1H), 4.41 – 4.33 (m, 1H), 4.24 – 4.01 (m, 3H), 3.59 – 3.48 (m, 2H), 2.53 – 2.44 (m, 2H), 2.03 (s, 3H), 1.78 – 1.56 (m, 7H), 1.45 – 1.41 (m, 12H), 1.28 (d, $J = 1.6$ Hz, 9H), 1.21 – 1.09 (m, 4H), 0.97 (dd, $J = 8.1, 6.4$ Hz, 3H), 0.92 – 0.80 (m, 2H).

^{13}C NMR (101 MHz, Chloroform-*d*) δ 196.8, 196.4, 172.60, 172.56, 171.1, 170.3, 169.6, 169.5, 168.20, 168.15, 159.1, 159.0, 81.5, 81.4, 75.6, 66.31, 66.27, 58.2, 58.1, 51.4, 51.3, 50.44, 50.41, 43.2, 41.1, 35.3, 35.2, 34.94, 34.92, 34.2, 33.8, 33.7, 32.9, 28.3, 28.2, 26.4, 26.3, 26.1, 23.5, 17.74, 17.70, 17.66, 17.5.



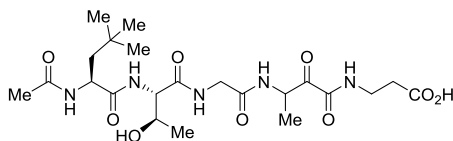
(4*S*,7*S*)-7-((*R*)-1-hydroxyethyl)-4-isopropyl-13-methyl-2,5,8,11,14,15-hexaaxo-3,6,9,12,16-pentaazanonadecan-19-oic acid (5a)

Starting material **53a** (36 mg, 0.0604 mmol) was dissolved in DCM (2 mL), then TFA (500 μL) was added and the reaction was stirred at room temperature. After the reaction is complete, solvent was evaporated in vacuo. Crude mixture was treated with Et_2O (3 \times 5 mL,

the precipitate was separated by centrifugation after each addition) to give the product **5a** (29 mg, 99%, mixture of diastereomers)

¹H NMR (400 MHz, Methanol-*d*₄) δ 4.39 – 4.28 (m, 1H), 4.28 – 4.12 (m, 3H), 3.98 – 3.76 (m, 2H), 3.53 – 3.43 (m, 2H), 2.61 – 2.50 (m, 2H), 2.19 – 2.07 (m, 1H), 2.06 – 1.99 (m, 3H), 1.24 – 1.15 (m, 3H), 1.16 – 1.05 (m, 3H), 1.03 – 0.94 (m, 6H).

¹³C NMR (101 MHz, Methanol-*d*₄) δ 175.3, 174.2, 172.8, 172.3, 170.8, 68.23, 68.16, 68.1, 61.0, 60.95, 60.86, 60.8, 60.4, 60.3, 60.0, 52.4, 52.0, 51.9, 43.7, 43.6, 36.5, 36.4, 34.44, 34.37, 31.4, 31.3, 22.4, 19.98, 19.96, 19.9, 19.8, 19.75, 18.7, 18.6, 15.3, 15.2, 14.8, 14.7.

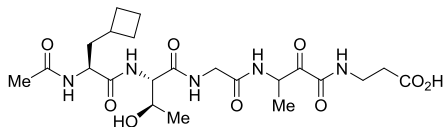


(4*S*,7*S*)-7-((*R*)-1-hydroxyethyl)-13-methyl-4-neopentyl-2,5,8,11,14,15-hexaoxo-3,6,9,12,16-pentaazonadecan-19-oic acid (5b**)**

Prepared in analogy to **5a**: starting material **53b** (63 mg, 0.100 mmol) and TFA (500 μL) in DCM (2 mL). Yield: 51 mg (99%, mixture of diastereomers)

¹H NMR (400 MHz, Acetonitrile-*d*₃) δ 7.59 – 6.88 (m, 5H), 5.11 – 4.94 (m, 1H), 4.35 (s, 1H), 4.25 – 4.06 (m, 2H), 3.81 (d, *J* = 17.2 Hz, 2H), 3.52 – 3.39 (m, 2H), 2.54 (td, *J* = 6.3, 2.0 Hz, 2H), 1.96 (s, 3H, overlaps with solvent), 1.83 – 1.73 (m, 1H), 1.52 (dd, *J* = 14.6, 8.9 Hz, 1H), 1.37 – 1.28 (m, 3H), 1.12 (d, *J* = 5.5 Hz, 3H), 0.94 (s, 9H).

¹³C NMR (101 MHz, Acetonitrile-*d*₃) δ 197.3, 174.5, 173.7, 172.4, 172.1, 170.2, 161.3, 67.8, 59.9, 52.7, 51.0, 50.9, 44.9, 43.0, 35.7, 33.8, 31.0, 29.8, 22.9, 19.6, 16.3.

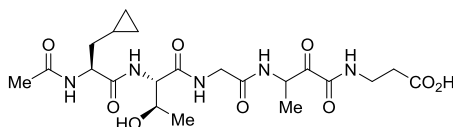


(4*S*,7*S*)-4-(cyclobutylmethyl)-7-((*R*)-1-hydroxyethyl)-13-methyl-2,5,8,11,14,15-hexaoxo-3,6,9,12,16-pentaazonadecan-19-oic acid (5c**)**

Prepared in analogy to **5a**: starting material **53c** (24 mg, 0.0441 mmol) and TFA (500 μL) in DCM (2 mL). Yield: 18 mg (89%, mixture of diastereomers)

¹H NMR (400 MHz, Acetonitrile-*d*₃) δ 7.52 – 7.46 (m, 1H), 7.35 – 7.22 (m, 2H), 7.17 – 7.08 (m, 1H), 6.94 – 6.83 (m, 1H), 5.00 (h, *J* = 7.2 Hz, 1H), 4.26 – 4.06 (m, 4H), 3.86 – 3.77 (m, 1H), 3.49 – 3.43 (m, 2H), 2.56 – 2.51 (m, 2H), 2.39 (p, *J* = 7.8 Hz, 1H), 2.08 – 1.98 (m, 2H), 1.94 – 1.91 (m, 3H, overlaps with solvent), 1.89 – 1.78 (m, 3H), 1.72 – 1.60 (m, 3H), 1.32 (dd, *J* = 7.2, 4.5 Hz, 3H), 1.17 – 1.08 (m, 3H).

¹³C NMR (101 MHz, Acetonitrile-*d*₃) δ 197.5, 173.9, 173.7, 172.1, 170.2, 161.37, 161.35, 67.8, 59.9, 53.92, 53.89, 50.9, 43.0, 38.8, 35.7, 33.8, 33.7, 33.6, 29.1, 29.0, 28.7, 22.89, 22.88, 19.1, 16.4.

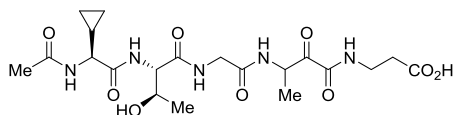


(4*S*,7*S*)-4-(cyclopropylmethyl)-7-((*R*)-1-hydroxyethyl)-13-methyl-2,5,8,11,14,15-hexaoxo-3,6,9,12,16-pentaazonadecan-19-oic acid (5d**)**

Prepared in analogy to **5a**: starting material **53d** (27 mg, 0.0441 mmol) and TFA (500 μL) in DCM (2 mL). Yield: 17 mg (77%, mixture of diastereomers)

^1H NMR (400 MHz, Methanol- d_4) δ 4.46 – 4.40 (m, 1H), 4.36 – 4.13 (m, 3H), 3.96 – 3.76 (m, 2H), 3.52 – 3.41 (m, 2H), 2.60 – 2.46 (m, 2H), 2.03 – 2.00 (m, 3H), 1.75 – 1.58 (m, 2H), 1.22 – 1.17 (m, 3H), 1.14 – 1.07 (m, 3H), 0.86 – 0.77 (m, 1H), 0.55 – 0.41 (m, 2H), 0.20 – 0.08 (m, 2H).

^{13}C NMR (101 MHz, Methanol- d_4) δ 175.3, 174.8, 173.8, 173.0, 172.8, 171.4, 170.6, 68.3, 60.3, 60.0, 55.9, 52.3, 51.9, 43.7, 43.2, 37.5, 36.5, 36.4, 34.4, 22.4, 19.9, 14.8, 8.6, 5.3, 4.7.

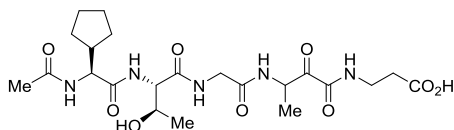


(4*S*,7*S*)-4-cyclopropyl-7-((*R*)-1-hydroxyethyl)-13-methyl-2,5,8,11,14,15-hexaoxo-3,6,9,12,16-pentaazanonadecan-19-oic acid (5e)

Prepared in analogy to **5a**: starting material **53e** (33 mg, 0.055 mmol) and TFA (500 μL) in DCM (2 mL). Yield: 26 mg (quant., mixture of diastereomers)

^1H NMR (400 MHz, Methanol- d_4) δ 4.46 – 4.15 (m, 3H), 3.99 – 3.82 (m, 2H), 3.65 – 3.54 (m, 1H), 3.52 – 3.45 (m, 2H), 2.60 – 2.51 (m, 2H), 2.04 – 1.96 (m, 3H), 1.43 – 1.37 (m, 1H), 1.24 – 1.06 (m, 6H), 0.70 – 0.54 (m, 3H), 0.46 – 0.34 (m, 1H).

^{13}C NMR (101 MHz, Methanol- d_4) δ 196.9, 175.3, 175.0, 173.7, 170.8, 68.2, 67.5, 66.9, 60.8, 60.4, 60.2, 60.0, 52.3, 52.0, 43.9, 43.7, 43.4, 36.4, 36.1, 34.4, 34.1, 22.3, 22.2, 20.3, 20.2, 19.9, 15.4, 15.2, 14.8, 13.8, 13.7, 4.6, 4.2, 3.9, 3.6.

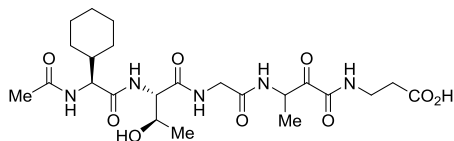


(4*S*,7*S*)-4-cyclopentyl-7-((*R*)-1-hydroxyethyl)-13-methyl-2,5,8,11,14,15-hexaoxo-3,6,9,12,16-pentaazanododecan-19-oic acid (5f)

Prepared in analogy to **5a**: starting material **53f** (80 mg, 0.128 mmol) and TFA (500 μL) in DCM (2 mL). Yield: 64 mg (98% mixture of diastereomers)

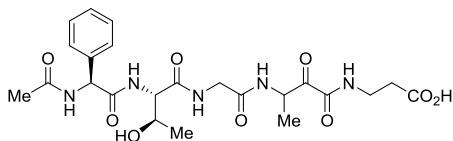
^1H NMR (400 MHz, Acetonitrile- d_3) δ 7.48 – 7.41 (m, 1H), 7.32 – 7.17 (m, 2H), 7.11 – 7.01 (m, 1H), 6.93 – 6.84 (m, 1H), 5.05 – 4.94 (m, 1H), 4.26 – 4.18 (m, 1H), 4.17 – 4.07 (m, 2H), 3.91 – 3.72 (m, 2H), 3.51 – 3.39 (m, 2H), 2.56 – 2.50 (m, 2H), 2.30 – 2.19 (m, 1H), 1.95 (s, 3H, overlaps with solvent), 1.81 – 1.74 (m, 1H), 1.72 – 1.49 (m, 5H), 1.39 – 1.28 (m, 5H), 1.14 – 1.09 (m, 3H).

^{13}C NMR (101 MHz, Acetonitrile- d_3) δ 196.5, 172.6, 171.5, 171.0, 169.1, 168.4, 66.8, 58.2, 49.9, 42.0, 41.1, 34.7, 32.8, 29.0, 28.9, 28.8, 25.0, 24.8, 21.84, 21.80, 18.7, 15.7, 15.3.



(4*S*,7*S*)-4-cyclohexyl-7-((*R*)-1-hydroxyethyl)-13-methyl-2,5,8,11,14,15-hexaoxo-3,6,9,12,16-pentaazanododecan-19-oic acid (5g)

Prepared in analogy to **5a**: starting material **53g** (10 mg, 0.0156 mmol) and TFA (2 mL) in DCM (2 mL). Yield: 6 mg (76%, mixture of diastereomers)

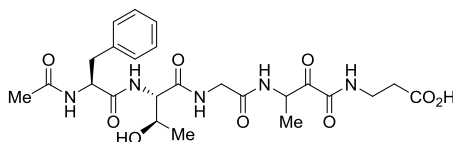


(4*S*,7*S*)-7-((*R*)-1-hydroxyethyl)-13-methyl-2,5,8,11,14,15-hexaoxo-4-phenyl-3,6,9,12,16-pentaazanonadecan-19-oic acid (5h)

Prepared in analogy to **5a**: starting material **53h** (40 g, 0.062 mmol) and TFA (500 μ L) in DCM (2 mL). Yield: 32 mg (98%, mixture of diastereomers)

^1H NMR (400 MHz, Methanol- d_4) δ 7.55 – 7.29 (m, 5H), 5.57 – 5.48 (m, 1H), 4.38 – 4.12 (m, 3H), 4.01 – 3.72 (m, 2H), 3.54 – 3.42 (m, 2H), 2.60 – 2.51 (m, 2H), 2.07 – 1.99 (m, 3H), 1.25 – 0.91 (m, 6H).

^{13}C NMR (101 MHz, Methanol- d_4) δ 175.4, 173.7, 173.53, 173.45, 173.33, 173.27, 173.1, 172.6, 172.0, 170.8, 138.3, 138.2, 129.92, 129.88, 129.86, 129.6, 129.5, 129.05, 129.01, 128.97, 128.9, 67.82, 67.78, 60.5, 60.4, 59.5, 43.9, 43.6, 36.5, 36.4, 34.4, 34.1, 22.4, 22.3, 20.0, 19.94, 19.86, 15.4, 15.2, 14.8.

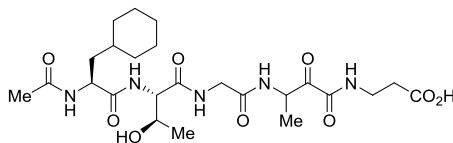


(4*S*,7*S*)-4-benzyl-7-((*R*)-1-hydroxyethyl)-13-methyl-2,5,8,11,14,15-hexaoxo-3,6,9,12,16-pentaazanonadecan-19-oic acid (5i)

Prepared in analogy to **5a**: starting material **53i** (40 mg, 0.062 mmol) and TFA (500 μ L) in DCM (2 mL). Yield: 33 mg (97%, mixture of diastereomers).

^1H NMR (400 MHz, Acetonitrile- d_3) δ 7.53 – 7.45 (m, 1H), 7.33 – 7.13 (m, 7H), 7.10 – 7.03 (m, 1H), 6.95 (d, J = 7.3 Hz, 1H), 5.09 – 4.95 (m, 1H), 4.66 – 4.58 (m, 1H), 4.25 – 4.13 (m, 2H), 3.88 – 3.79 (m, 1H), 3.79 – 3.71 (m, 1H), 3.51 – 3.40 (m, 2H), 3.18 – 3.09 (m, 1H), 2.92 (dd, J = 14.1, 8.9 Hz, 1H), 2.53 (td, J = 6.4, 1.9 Hz, 2H), 1.88 – 1.84 (m, 3H), 1.31 (dd, J = 8.1, 7.3 Hz, 3H), 1.09 (dd, J = 6.3, 1.3 Hz, 3H).

^{13}C NMR (101 MHz, Acetonitrile- d_3) δ 197.38, 197.36, 173.63, 173.60, 173.12, 173.06, 172.20, 172.18, 171.94, 171.91, 170.1, 170.0, 161.23, 161.21, 138.3, 138.2, 130.2, 129.4, 127.6, 67.9, 67.8, 59.82, 59.79, 56.0, 51.0, 50.9, 43.0, 37.69, 37.67, 35.7, 33.77, 33.75, 22.7, 19.6, 16.40, 16.35.



(4*S*,7*S*)-4-(cyclohexylmethyl)-7-((*R*)-1-hydroxyethyl)-13-methyl-2,5,8,11,14,15-hexaoxo-3,6,9,12,16-pentaazanonadecan-19-oic acid (5j)

Prepared in analogy to **5a**: starting material **53j** (70 mg, 0.107 mmol) and TFA (500 μ L) in DCM (2 mL). Yield: 55 mg (94%, mixture of diastereomers)

^1H NMR (400 MHz, Acetonitrile- d_3) δ 7.58 – 7.48 (m, 1H), 7.43 – 7.06 (m, 2H), 6.98 (dd, J = 30.0, 6.7 Hz, 1H), 5.08 – 4.95 (m, 1H), 4.39 – 4.27 (m, 2H), 4.28 – 4.06 (m, 2H), 3.93 – 3.74 (m, 2H), 3.53 – 3.39 (m, 2H), 2.54 (t, J = 6.2 Hz, 2H), 1.96 (s, 3H), 1.81 – 1.47 (m, 7H), 1.45 – 1.28 (m, 4H), 1.29 – 1.14 (m, 3H), 1.12 (d, J = 5.3 Hz, 3H), 1.03 – 0.82 (m, 2H).

^{13}C NMR (101 MHz, Acetonitrile- d_3) δ 197.3, 174.37, 174.36, 173.73, 173.71, 172.84, 172.81, 172.11, 172.10, 170.24, 170.22, 161.3, 67.9, 67.8, 59.8, 53.0, 51.0, 50.9, 43.0, 39.3, 35.7, 34.8, 34.4, 33.8, 33.0, 27.1, 27.0, 26.8, 22.8, 19.7, 16.4.

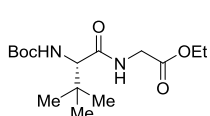
3. Synthesis of peptidic boronic acids and intermediates

3.1 Synthesis of the peptidic boronic acids with a modified P1 position

The synthesis of building blocks **55a–g**, compounds **55**, **56a–g**, **15**, **16a–g** are described in the publication.²²

3.2 Synthesis of the peptidic boronic acids with a modified P3 position

The synthesis of peptidic boronic acids **17a,b** and their intermediates are described in the publication.²²



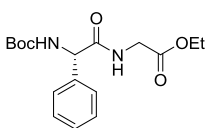
Ethyl (S)-(2-((*tert*-butoxycarbonyl)amino)-3,3-dimethylbutanoyl) glycinate (**76c**)

A mixture of glycine ethyl ester hydrochloride (**46**) (243 mg, 1.74 mmol, 1.0 equiv), *N*-Boc-*L*-*tert*-leucine (402 mg, 1.74 mmol, 1.0 equiv), HOBt (258 mg, 1.91 mmol, 1.1 equiv), EDC·HCl (400 mg, 2.09 mmol, 1.2 equiv) and DIPEA (0.90 mL, 5.20 mmol, 3.0 equiv) in DCM (30 mL) were stirred overnight at room temperature. The reaction mixture was washed with 1 M HCl (15 mL) and then with brine (10 mL). Organic phase was dried over Na_2SO_4 , filtered and evaporated in vacuo. The residue was purified by flash chromatography on silica gel eluting with hexane:EtOAc (4:1 – 2:1) to provide **76c** (445 mg, 81%) as a white solid.

^1H NMR (400 MHz, Chloroform- d) δ 6.46 (t, J = 5.4 Hz, 1H), 5.27 (s, 1H), 4.25 – 4.10 (m, 3H), 3.97 – 3.82 (m, 2H), 1.42 (s, 9H), 1.27 (t, J = 7.2 Hz, 3H), 1.01 (s, 9H).

^{13}C NMR (101 MHz, Chloroform- d) δ 171.3, 169.7, 155.9, 79.8, 62.4, 61.6, 41.4, 34.7, 28.4, 26.7, 14.3.

HR-MS (ESI/TOF) calcd for $\text{C}_{15}\text{H}_{28}\text{N}_2\text{O}_5\text{Na}$ [$\text{M}+\text{Na}$] $^+$ 339.1896, found 339.1913



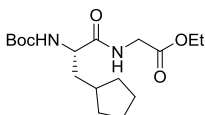
Ethyl (S)-(2-((*tert*-butoxycarbonyl)amino)-2-phenylacetyl) glycinate (**76d**)

Prepared in analogues way as **76c**: glycine ethyl ester hydrochloride (**46**) (248 mg, 1.78 mmol), *N*-Boc-*L*-phenylglycine (447 mg, 1.78 mmol), HOBt (264 mg, 1.95 mmol), EDC·HCl (410 mg, 2.14 mmol) and DIPEA (0.92 mL, 5.32 mmol) in DCM (30 mL). Yield: 354 mg (59%)

^1H NMR (400 MHz, Chloroform- d) δ 7.45 – 7.28 (m, 5H), 6.33 (t, J = 5.3 Hz, 1H), 5.72 (s, 1H), 5.20 (s, 1H), 4.17 (q, J = 7.2 Hz, 2H), 4.05 (dd, J = 18.3, 5.3 Hz, 1H), 3.95 (dd, J = 18.4, 5.1 Hz, 1H), 1.41 (s, 9H), 1.24 (t, J = 7.2 Hz, 3H).

^{13}C NMR (101 MHz, Chloroform- d) δ 170.4, 169.5, 155.2, 138.2, 129.2, 128.6, 127.5, 80.3, 61.8, 58.8, 41.7, 28.4, 14.2.

HR-MS (ESI/TOF) calcd for $\text{C}_{17}\text{H}_{24}\text{N}_2\text{O}_5\text{Na}$ [$\text{M}+\text{Na}$] $^+$ 359.1583, found 359.1590



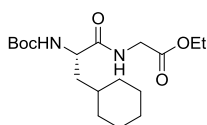
Ethyl (S)-(2-((tert-butoxycarbonyl)amino)-3-cyclopentyl)propanoate (76e)

Prepared in analogues way as **76c**: glycine ethyl ester hydrochloride (**46**) (206 mg, 1.48 mmol), *N*-Boc-L-cyclopentylalanine (380 mg, 1.48 mmol), HOBT (220 mg, 1.63 mmol), EDC·HCl (340 mg, 1.77 mmol) and DIPEA (0.78 mL, 4.51 mmol) in DCM (30 mL). Yield: 447 mg (88%)

¹H NMR (400 MHz, Chloroform-*d*) δ 6.59 (s, 1H), 4.91 (s, 1H), 4.21 (q, *J* = 7.2 Hz, 2H), 4.16 – 4.07 (m, 1H), 4.02 (d, *J* = 5.2 Hz, 2H), 1.92 – 1.73 (m, 4H), 1.65 – 1.56 (m, 3H), 1.56 – 1.47 (m, 2H), 1.44 (s, 9H), 1.28 (t, *J* = 7.2 Hz, 3H), 1.19 – 1.07 (m, 2H).

¹³C NMR (101 MHz, Chloroform-*d*) δ 172.6, 169.7, 155.7, 80.2, 61.5, 54.2, 41.3, 38.6, 36.6, 32.8, 32.5, 28.3, 25.2, 25.0, 14.1.

HR-MS (ESI/TOF) calcd for C₁₇H₃₀N₂O₅Na [M+Na]⁺ 365.2052, found 365.2059



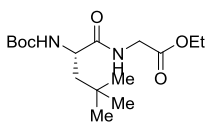
Ethyl (S)-(2-((tert-butoxycarbonyl)amino)-3-cyclohexyl)propanoate (76f)

Prepared in analogues way as **76c**: glycine ethyl ester hydrochloride (**46**) (250 mg, 1.79 mmol), *N*-Boc-L-cyclohexylalanine (486 mg, 1.79 mmol), HOBT (266 mg, 1.97 mmol), EDC·HCl (412 mg, 2.15 mmol) and DIPEA (0.93 mL, 5.38 mmol) in DCM (35 mL). Yield: 549 mg (86%)

¹H NMR (400 MHz, Chloroform-*d*) δ 6.59 (s, 1H), 4.83 (s, 1H), 4.30 – 4.16 (m, 3H), 4.02 (d, *J* = 5.2 Hz, 2H), 1.84 – 1.62 (m, 6H), 1.54 – 1.41 (m, 10H), 1.40 – 1.32 (m, 1H), 1.28 (t, *J* = 7.2 Hz, 3H), 1.25 – 1.07 (m, 3H), 1.04 – 0.82 (m, 2H).

¹³C NMR (101 MHz, Chloroform-*d*) δ 173.0, 169.8, 155.9, 80.4, 61.7, 52.4, 41.5, 40.0, 34.2, 33.8, 32.6, 28.4, 26.5, 26.4, 26.2, 14.3.

HR-MS (ESI/TOF) calcd for C₁₈H₃₂N₂O₅Na [M+Na]⁺ 379.2209, found 379.2212



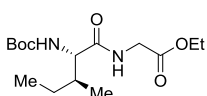
Ethyl (S)-(2-((tert-butoxycarbonyl)amino)-4,4-dimethyl)pentanoate (76g)

Prepared in analogues way as **76c**: glycine ethyl ester hydrochloride (**46**) (204 mg, 1.45 mmol), *N*-Boc-L-*tert*-butylalanine (354 mg, 1.44 mmol), HOBT (215 mg, 1.59 mmol), EDC·HCl (332 mg, 1.73 mmol) and DIPEA (0.75 mL, 4.33 mmol) in DCM (25 mL). Yield: 455 mg (95%)

¹H NMR (400 MHz, Chloroform-*d*) δ 6.72 (t, *J* = 5.5 Hz, 1H), 4.85 (d, *J* = 8.5 Hz, 1H), 4.27 – 4.14 (m, 3H), 4.00 (dd, *J* = 5.4, 1.7 Hz, 2H), 1.92 (dd, *J* = 14.5, 3.6 Hz, 1H), 1.44 (s, 9H), 1.39 (dd, *J* = 14.5, 8.9 Hz, 1H), 1.27 (t, *J* = 7.2 Hz, 3H), 0.96 (s, 9H).

¹³C NMR (101 MHz, Chloroform-*d*) δ 173.3, 169.8, 155.6, 80.4, 61.6, 52.3, 45.7, 41.5, 30.6, 29.8, 28.5, 14.3.

HR-MS (ESI/TOF) calcd for C₁₆H₃₀N₂O₅Na [M+Na]⁺ 353.2052, found 353.2057



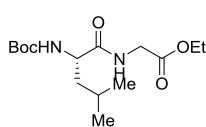
Ethyl (tert-butoxycarbonyl)-L-isoleucylglycinate (76h)

Prepared in analogues way as **76c**: glycine ethyl ester hydrochloride (**46**) (200 mg, 1.42 mmol), *N*-Boc-L-isoleucine (330 mg, 1.43 mmol), HOBT (211 mg, 1.56 mmol), EDC·HCl (326 mg, 1.70 mmol) and DIPEA (0.74 mL, 4.28 mmol) in DCM (30 mL). Yield: 412 mg (92%)

¹H NMR (400 MHz, Chloroform-*d*) δ 6.54 (t, *J* = 5.3 Hz, 1H), 5.05 (d, *J* = 8.2 Hz, 1H), 4.20 (q, *J* = 7.2 Hz, 2H), 4.12 – 3.92 (m, 3H), 1.96 – 1.86 (m, 1H), 1.56 – 1.46 (m, 1H), 1.43 (s, 9H), 1.27 (t, *J* = 7.2 Hz, 3H), 1.20 – 1.06 (m, 1H), 0.94 (d, *J* = 6.9 Hz, 3H), 0.91 (t, *J* = 7.4 Hz, 3H).

¹³C NMR (101 MHz, Chloroform-*d*) δ 172.0, 169.8, 155.9, 80.1, 61.7, 59.3, 41.4, 37.4, 28.4, 24.8, 15.7, 14.3, 11.6.

HR-MS (ESI/TOF) calcd for C₁₅H₂₈N₂O₅Na [M+Na]⁺ 339.1896, found 339.1911



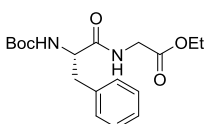
Ethyl (*tert*-butoxycarbonyl)-L-leucylglycinate (**76i**)

Prepared in analogues way as **76c**: glycine ethyl ester hydrochloride (**46**) (200 mg, 1.42 mmol), *N*-Boc-L-leucine (328 mg, 1.42 mmol), HOBt (211 mg, 1.56 mmol), EDC·HCl (326 mg, 1.70 mmol) and DIPEA (0.74 mL, 4.28 mmol) in DCM (30 mL). Yield: 297 mg (66%)

¹H NMR (400 MHz, Chloroform-*d*) δ 6.66 (t, *J* = 5.5 Hz, 1H), 4.91 (d, *J* = 7.4 Hz, 1H), 4.24 – 4.12 (m, 3H), 4.01 (dd, *J* = 5.3, 1.4 Hz, 2H), 1.74 – 1.64 (m, 2H), 1.48 (dd, *J* = 9.5, 8.2 Hz, 1H), 1.44 (s, 9H), 1.27 (t, *J* = 7.2 Hz, 3H), 0.94 (d, *J* = 4.2 Hz, 3H), 0.93 (d, *J* = 3.9 Hz, 3H).

¹³C NMR (101 MHz, Chloroform-*d*) δ 173.0, 169.8, 155.8, 80.3, 61.6, 53.1, 41.4, 28.4, 24.9, 23.1, 22.0, 14.3.

HR-MS (ESI/TOF) calcd for C₁₅H₂₈N₂O₅Na [M+Na]⁺ 339.1896, found 339.1906



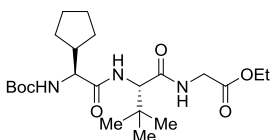
Ethyl (*tert*-butoxycarbonyl)-L-phenylalanyl-glycinate (**76j**)

Prepared in analogues way as **76c**: glycine ethyl ester hydrochloride (**46**) (200 mg, 1.42 mmol), *N*-Boc-L-phenylalanine (376 mg, 1.42 mmol), HOBt (211 mg, 1.56 mmol), EDC·HCl (326 mg, 1.70 mmol) and DIPEA (0.74 mL, 4.28 mmol) in DCM (30 mL). Yield: 394 mg (79%)

¹H NMR (400 MHz, Chloroform-*d*) δ 7.33 – 7.27 (m, 2H), 7.26 – 7.19 (m, 3H), 6.47 – 6.40 (m, 1H), 5.01 (s, 1H), 4.46 – 4.33 (m, 1H), 4.19 (q, *J* = 7.1 Hz, 2H), 4.02 (dd, *J* = 18.3, 5.4 Hz, 1H), 3.91 (dd, *J* = 18.4, 5.0 Hz, 1H), 3.16 – 3.00 (m, 2H), 1.39 (s, 9H), 1.26 (t, *J* = 7.2 Hz, 3H).

¹³C NMR (101 MHz, Chloroform-*d*) δ 171.6, 169.5, 155.5, 136.7, 129.4, 128.8, 127.1, 80.4, 61.7, 55.8, 41.5, 38.5, 28.4, 14.3.

HR-MS (ESI/TOF) calcd for C₁₈H₂₆N₂O₅Na [M+Na]⁺ 373.1739, found 373.1740



Ethyl ((*S*)-2-((*S*)-2-((*tert*-butoxycarbonyl)amino)-2-cyclopentylacetamido)-3,3-dimethylbutanoyl)glycinate (**78c**)

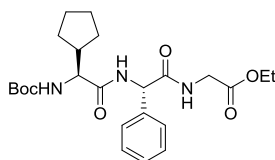
Starting material **76c** (435 mg, 1.37 mmol, 1.0 equiv) in DCM (10 mL) was treated with 4 M HCl in dioxane (1.4 mL, 4 equiv) while stirring under inert atmosphere. After a full conversion of the starting material, solvent was evaporated and the residue was utilized in the next step without purification. The residue (347 mg, 1.37 mmol based on a theoretical yield of a 100%) was dissolved in DCM (40 mL), *N*-Boc-cyclopentyl-Gly-OH (**77**) (334 mg, 1.37 mmol, 1.0 equiv), EDC·HCl (316 mg, 1.65 mmol, 1.2 equiv), HOBt

(204 mg, 1.51 mmol, 1.1 equiv) and DIPEA (0.72 mL, 4.16 mmol, 3.0 equiv) were added and mixture was stirred overnight at room temperature, then washed with 1 M HCl (20 mL) and brine (20 mL). Organic phase was dried over Na₂SO₄, filtered and evaporated in vacuo. The residue was purified by flash chromatography on silica gel eluting with hexane:EtOAc (2:1 – 1:1) to provide **78c** (532 mg, 88%) as a white solid.

¹H NMR (400 MHz, Chloroform-*d*) δ 6.88 – 6.74 (m, 2H), 5.21 (d, *J* = 8.1 Hz, 1H), 4.36 (d, *J* = 9.2 Hz, 1H), 4.25 – 4.08 (m, 3H), 3.94 (t, *J* = 8.9 Hz, 1H), 3.86 (dd, *J* = 18.2, 4.7 Hz, 1H), 2.21 (h, *J* = 8.5 Hz, 1H), 1.78 – 1.46 (m, 6H), 1.42 (s, 9H), 1.36 – 1.20 (m, 5H), 1.01 (s, 9H).

¹³C NMR (101 MHz, Chloroform-*d*) δ 172.3, 170.6, 169.7, 156.1, 80.0, 61.6, 60.6, 59.1, 41.9, 41.4, 34.8, 29.6, 29.0, 28.4, 26.7, 25.5, 25.2, 14.36.

HR-MS (ESI/TOF) calcd for C₂₂H₃₉N₃O₆Na [M+Na]⁺ 464.2737, found 464.2742



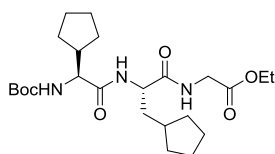
Ethyl ((S)-2-((S)-2-((tert-butoxycarbonyl)amino)-2-cyclopentylacetamido)-2-phenylacetyl)glycinate (78d**)**

Prepared in analogues way as **78c**: starting material **76d** (340 mg, 1.01 mmol) and 4 M HCl in dioxane (1.0 mL) in DCM (5 mL). Coupling: *N*-Boc-cyclopentyl-Gly-OH (**77**) (246 mg, 1.01 mmol), EDC·HCl (233 mg, 1.22 mmol), HOBT (150 mg, 1.11 mmol) and DIPEA (0.52 mL, 3.01 mmol) in DCM (40 mL). Yield: 331 mg (71%, white solid)

¹H NMR (400 MHz, Chloroform-*d*) δ 7.42 – 7.28 (m, 5H), 7.22 (d, *J* = 6.8 Hz, 1H), 6.73 (s, 1H), 5.55 (d, *J* = 7.0 Hz, 1H), 5.12 (d, *J* = 7.4 Hz, 1H), 4.16 (q, *J* = 7.2 Hz, 2H), 4.10 – 3.89 (m, 3H), 2.21 (h, *J* = 6.9, 6.2 Hz, 1H), 1.74 – 1.46 (m, 6H), 1.40 (s, 9H), 1.36 – 1.27 (m, 2H), 1.23 (t, *J* = 7.2 Hz, 3H).

¹³C NMR (101 MHz, Chloroform-*d*) δ 171.7, 170.0, 169.5, 156.1, 137.5, 129.1, 128.6, 127.5, 80.2, 61.7, 58.5, 57.3, 42.3, 41.7, 29.5, 28.7, 28.4, 25.5, 25.2, 14.2.

HR-MS (ESI/TOF) calcd for C₂₂H₃₉N₃O₆Na [M+Na]⁺ 464.2424, found 484.2433



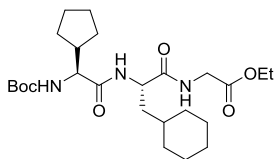
Ethyl ((S)-2-((S)-2-((tert-butoxycarbonyl)amino)-2-cyclopentylacetamido)-3-cyclopentylpropanoyl)glycinate (78e**)**

Prepared in analogues way as **78c**: starting material **76e** (416 mg, 1.21 mmol) and 4 M HCl in dioxane (1.2 mL) in DCM (10 mL). Coupling: *N*-Boc-cyclopentyl-Gly-OH (**77**) (296 mg, 1.21 mmol), EDC·HCl (280 mg, 1.46 mmol), HOBT (181 mg, 1.34 mmol) and DIPEA (0.64 mL, 3.70 mmol) in DCM (30 mL). Yield: 421 mg (74%, white solid).

¹H NMR (400 MHz, Chloroform-*d*) δ 6.90 (t, *J* = 5.5 Hz, 1H), 6.62 (d, *J* = 8.1 Hz, 1H), 5.12 (d, *J* = 8.0 Hz, 1H), 4.48 (td, *J* = 8.5, 5.3 Hz, 1H), 4.18 (q, *J* = 7.2 Hz, 2H), 4.02 – 3.96 (m, 2H), 3.91 (t, *J* = 7.9 Hz, 1H), 2.22 (h, *J* = 8.6 Hz, 1H), 1.93 – 1.63 (m, 7H), 1.65 – 1.46 (m, 8H), 1.42 (s, 9H), 1.36 – 1.22 (m, 5H), 1.19 – 1.04 (m, 2H).

¹³C NMR (101 MHz, Chloroform-*d*) δ 172.3, 172.1, 169.7, 156.2, 80.3, 61.5, 59.0, 52.8, 42.0, 41.5, 38.2, 36.6, 32.9, 32.5, 29.5, 28.9, 28.4, 25.5, 25.3, 25.2, 25.1, 14.3.

HR-MS (ESI/TOF) calcd for C₂₄H₄₂N₃O₆ [M+H]⁺ 468.3074, found 468.3077



Ethyl ((S)-2-((S)-2-((tert-butoxycarbonyl)amino)-2-cyclopentylacetamido)-3-cyclohexylpropanoyl)glycinate (78f)

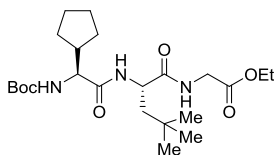
Prepared in analogues way as **78c**: starting material **76f** (530 mg, 1.49 mmol) and 4 M HCl in dioxane (1.5 mL) in DCM (10 mL). Coupling: *N*-Boc-cyclopentyl-Gly-OH (**77**)

(362 mg, 1.49 mmol), EDC·HCl (342 mg, 1.78 mmol), HOBT (222 mg, 1.64 mmol) and DIPEA (0.78 mL, 4.51 mmol) in DCM (30 mL). Yield: 496 mg (69%, white solid).

¹H NMR (400 MHz, Chloroform-*d*) δ 6.90 (s, 1H), 6.51 (d, *J* = 8.3 Hz, 1H), 5.07 (d, *J* = 7.0 Hz, 1H), 4.55 (ddd, *J* = 9.5, 8.3, 5.4 Hz, 1H), 4.18 (q, *J* = 7.2 Hz, 2H), 3.97 (d, *J* = 5.5 Hz, 2H), 3.90 (t, *J* = 7.7 Hz, 1H), 2.22 (h, *J* = 8.2, 7.7 Hz, 1H), 1.83 – 1.48 (m, 14H), 1.43 (s, 9H), 1.37 – 1.23 (m, 6H), 1.21 – 1.07 (m, 2H), 1.03 – 0.81 (m, 2H).

¹³C NMR (101 MHz, Chloroform-*d*) δ 172.4, 172.3, 169.7, 156.2, 80.4, 61.5, 59.1, 50.8, 42.1, 41.5, 39.3, 34.1, 33.8, 32.5, 29.5, 28.9, 28.4, 26.5, 26.3, 26.1, 25.5, 25.2, 14.3.

HR-MS (ESI/TOF) calcd for C₂₅H₄₄N₃O₆ [M+H]⁺ 482.3230, found 482.3230



Ethyl ((S)-2-((S)-2-((tert-butoxycarbonyl)amino)-2-cyclopentylacetamido)-4,4-dimethylpentanoyl)glycinate (78g)

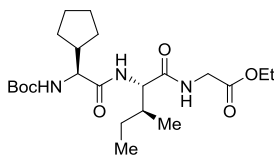
Prepared in analogues way as **78c**: starting material **76g** (440 mg, 1.33 mmol, 1.1 equiv) and 4 M HCl in dioxane (1.4 mL) in DCM (20 mL). Coupling: *N*-Boc-cyclopentyl-Gly-OH (**77**)

(294 mg, 1.21 mmol), EDC·HCl (300 mg, 1.56 mmol), HOBT (200 mg, 1.48 mmol) and DIPEA (0.70 mL, 4.05 mmol) in DCM (30 mL). Yield: 405 mg (74%, white solid).

¹H NMR (400 MHz, Chloroform-*d*) δ 7.07 – 7.00 (m, 1H), 6.73 (d, *J* = 8.3 Hz, 1H), 5.19 (d, *J* = 7.9 Hz, 1H), 4.53 (td, *J* = 8.4, 3.7 Hz, 1H), 4.17 (q, *J* = 7.2 Hz, 2H), 4.03 – 3.87 (m, 3H), 2.22 (h, *J* = 8.8 Hz, 1H), 1.97 (dd, *J* = 14.5, 3.8 Hz, 1H), 1.78 – 1.50 (m, 6H), 1.47 (dd, *J* = 14.5, 8.4 Hz, 1H), 1.41 (s, 9H), 1.34 – 1.22 (m, 5H), 0.93 (s, 9H).

¹³C NMR (101 MHz, Chloroform-*d*) δ 172.7, 172.2, 169.7, 156.2, 80.3, 61.5, 59.2, 50.7, 45.4, 41.9, 41.5, 30.6, 29.7, 29.5, 29.1, 28.4, 25.5, 25.2, 14.3.

HR-MS (ESI/TOF) calcd for C₂₃H₄₁N₃O₆Na [M+Na]⁺ 478.2893, found 478.2900



Ethyl ((S)-2-((tert-butoxycarbonyl)amino)-2-cyclopentyl-acetyl)-L-isoleucylglycinate (78h)

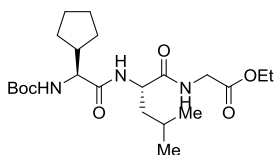
Prepared in analogues way as **78c**: starting material **76h** (400 mg, 1.26 mmol) and 4 M HCl in dioxane (1.3 mL) in DCM (20 mL). Coupling: *N*-Boc-cyclopentyl-Gly-OH (**77**)

(308 mg, 1.27 mmol), EDC·HCl (291 mg, 1.52 mmol), HOBT (188 mg, 1.39 mmol) and DIPEA (0.66 mL, 3.81 mmol) in DCM (40 mL). Yield: 471 mg (84%, white solid).

¹H NMR (400 MHz, Chloroform-*d*) δ 6.91 – 6.82 (m, 1H), 6.69 (d, *J* = 8.8 Hz, 1H), 5.13 (d, *J* = 6.9 Hz, 1H), 4.38 (dd, *J* = 8.8, 6.3 Hz, 1H), 4.18 (q, *J* = 7.2 Hz, 2H), 4.08 – 3.87 (m, 3H), 2.24 (h, *J* = 8.5 Hz, 1H), 2.03 – 1.93 (m, 1H), 1.78 – 1.66 (m, 2H), 1.65 – 1.47 (m, 5H), 1.42 (s, 9H), 1.36 – 1.23 (m, 5H), 1.19 – 1.05 (m, 1H), 0.93 (d, *J* = 6.8 Hz, 3H), 0.89 (t, *J* = 7.4 Hz, 3H).

^{13}C NMR (101 MHz, Chloroform-*d*) δ 172.3, 171.4, 169.7, 156.2, 80.4, 61.6, 59.2, 57.8, 41.8, 41.4, 36.9, 29.6, 28.9, 28.4, 25.5, 25.3, 24.7, 15.6, 14.3, 11.5.

HR-MS (ESI/TOF) calcd for $\text{C}_{22}\text{H}_{39}\text{N}_3\text{O}_6\text{Na}$ $[\text{M}+\text{Na}]^+$ 464.2737, found 464.2758



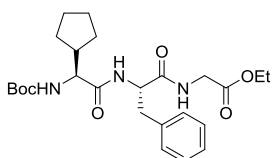
Ethyl ((S)-2-((tert-butoxycarbonyl)amino)-2-cyclopentyl-acetyl)-L-leucylglycinate (78i)

Prepared in analogues way as **78c**: starting material **76i** (287 mg, 0.90 mmol) and 4 M HCl in dioxane (0.92 mL) in DCM (20 mL). Coupling: *N*-Boc-cyclopentyl-Gly-OH (**77**) (220 mg, 0.90 mmol), EDC-HCl (208 mg, 1.08 mmol), HOBt (135 mg, 1.00 mmol) and DIPEA (0.47 mL, 2.72 mmol) in DCM (40 mL). Yield: 313 mg (78%, white solid).

^1H NMR (400 MHz, Chloroform-*d*) δ 6.91 (t, $J = 5.8$ Hz, 1H), 6.57 (d, $J = 8.2$ Hz, 1H), 5.10 (d, $J = 8.1$ Hz, 1H), 4.52 (ddd, $J = 9.5, 8.2, 5.2$ Hz, 1H), 4.18 (q, $J = 7.2$ Hz, 2H), 3.97 (d, $J = 5.4$ Hz, 2H), 3.89 (t, $J = 8.0$ Hz, 1H), 2.23 (h, $J = 8.6$ Hz, 1H), 1.79 – 1.48 (m, 9H), 1.42 (s, 9H), 1.26 (t, $J = 7.2$ Hz, 5H), 0.92 (d, $J = 6.4$ Hz, 3H), 0.90 (d, $J = 6.2$ Hz, 3H).

^{13}C NMR (101 MHz, Chloroform-*d*) δ 172.4, 172.2, 169.7, 156.2, 80.4, 61.5, 59.1, 51.6, 41.9, 41.4, 40.8, 29.5, 28.9, 28.4, 25.5, 25.3, 24.8, 23.1, 21.9, 14.3.

HR-MS (ESI/TOF) calcd for $\text{C}_{22}\text{H}_{39}\text{N}_3\text{O}_6\text{Na}$ $[\text{M}+\text{Na}]^+$ 464.2737, found 464.2741



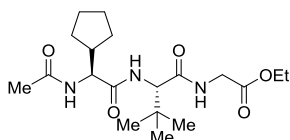
Ethyl ((S)-2-((tert-butoxycarbonyl)amino)-2-cyclopentyl-acetyl)-L-phenylalanylglycinate (78j)

Prepared in analogues way as **78c**: starting material **76j** (377 mg, 1.08 mmol) and 4 M HCl in dioxane (1.1 mL) in DCM (20 mL). Coupling: *N*-Boc-cyclopentyl-Gly-OH (**77**) (262 mg, 1.08 mmol), EDC-HCl (248 mg, 1.30 mmol), HOBt (160 mg, 1.18 mmol) and DIPEA (0.56 mL, 3.24 mmol) in DCM (40 mL). Yield: 391 mg (76%, white solid).

^1H NMR (400 MHz, Chloroform-*d*) δ 7.33 – 7.25 (m, 2H), 7.24 – 7.19 (m, 3H), 6.76 (s, 1H), 6.54 (d, $J = 8.2$ Hz, 1H), 4.91 (d, $J = 6.2$ Hz, 1H), 4.76 (q, $J = 7.0$ Hz, 1H), 4.17 (q, $J = 7.2$ Hz, 2H), 4.00 (dd, $J = 17.9, 5.5$ Hz, 1H), 3.91 – 3.81 (m, 2H), 3.18 (dd, $J = 14.0, 6.6$ Hz, 1H), 3.08 (dd, $J = 14.0, 7.3$ Hz, 1H), 2.13 – 2.02 (m, 1H), 1.65 – 1.43 (m, 6H), 1.40 (s, 9H), 1.25 (t, $J = 7.2$ Hz, 3H), 1.23 – 1.12 (m, 2H).

^{13}C NMR (101 MHz, Chloroform-*d*) δ 172.0, 171.1, 169.4, 156.2, 136.7, 129.4, 128.8, 127.1, 80.6, 61.5, 59.2, 54.0, 42.0, 41.5, 37.9, 29.3, 28.6, 28.4, 25.4, 25.1, 14.3.

HR-MS (ESI/TOF) calcd for $\text{C}_{25}\text{H}_{37}\text{N}_3\text{O}_6\text{Na}$ $[\text{M}+\text{Na}]^+$ 498.2580, found 498.2580



Ethyl ((S)-2-((S)-2-acetamido-2-cyclopentylacetamido)-3,3-dimethylbutanoyl)glycinate (79c)

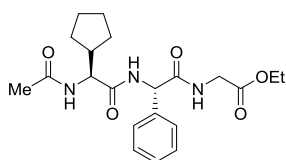
Starting material **78c** (507 mg, 1.15 mmol, 1.0 equiv) in DCM (10 mL) was treated with 4 M HCl in dioxane (1.2 mL, 4 equiv.) while stirring under inert atmosphere. After full conversion of the starting material, solvent was evaporated and the residue was utilized in the next step without purification. The residue (434 mg, 1.15 mmol based on a theoretical yield of a 100%) was dissolved in DCM (30 mL), acetic anhydride (160 μL , 1.70 mmol, 1.5 equiv) and DIPEA (600 μL , 3.47 mmol, 3.0 equiv) were added. Reaction mixture was

stirred at room temperature, and then washed with 1 M HCl (20 mL) and brine (20 mL). Organic phase was dried over Na₂SO₄, filtered and evaporated in vacuo. The crude mixture was purified by flash chromatography on silica gel eluting with Hexane:EtOAc (1:1) – EtOAc to provide **79c** (379 mg, 86%) as a white solid.

¹H NMR (400 MHz, Chloroform-*d*) δ 7.31 – 7.27 (m, 1H), 7.18 (d, *J* = 9.4 Hz, 1H), 6.80 (d, *J* = 8.8 Hz, 1H), 4.51 (t, *J* = 8.9 Hz, 1H), 4.49 (d, *J* = 9.3 Hz, 1H), 4.24 – 4.15 (m, 3H), 3.82 (dd, *J* = 18.2, 4.5 Hz, 1H), 2.15 (h, *J* = 8.9 Hz, 1H), 2.00 (s, 3H), 1.75 – 1.44 (m, 6H), 1.27 (t, *J* = 7.2 Hz, 5H), 1.00 (s, 9H).

¹³C NMR (101 MHz, Chloroform-*d*) δ 172.2, 170.8, 170.4, 170.0, 61.6, 60.7, 57.2, 43.0, 41.4, 34.6, 29.4, 29.3, 26.7, 25.5, 25.0, 23.2, 14.3.

HR-MS (ESI/TOF) calcd for C₁₉H₃₃N₃O₅Na [M+Na]⁺ 406.2318, found 406.2325



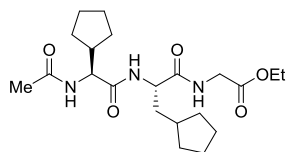
Ethyl ((S)-2-((S)-2-acetamido-2-cyclopentylacetamido)-2-phenylacetyl)glycinate (79d**)**

Prepared in analogues way as **79c**: starting material **78d** (315 mg, 0.68 mmol) and 4 M HCl in dioxane (0.70 mL) in DCM (10 mL). Acylation: acetic anhydride (100 μL, 1.06 mmol) and DIPEA (360 μL, 2.08 mmol) in DCM (15 mL). Yield: 210 mg (76%, white solid).

¹H NMR (400 MHz, Dimethylsulfoxide-*d*₆) δ 8.68 (t, *J* = 5.9 Hz, 1H), 8.39 (d, *J* = 8.2 Hz, 1H), 8.01 (d, *J* = 8.5 Hz, 1H), 7.44 – 7.39 (m, 2H), 7.37 – 7.24 (m, 3H), 5.53 (d, *J* = 8.1 Hz, 1H), 4.28 (t, *J* = 8.5 Hz, 1H), 4.04 (q, *J* = 7.1 Hz, 2H), 3.92 – 3.77 (m, 2H), 2.12 (h, *J* = 8.6 Hz, 1H), 1.83 (s, 3H), 1.68 – 1.37 (m, 6H), 1.35 – 1.18 (m, 2H), 1.13 (t, *J* = 7.1 Hz, 3H).

¹³C NMR (101 MHz, Dimethylsulfoxide-*d*₆) δ 171.1, 170.2, 169.5, 169.3, 138.4, 128.2, 127.6, 127.2, 60.5, 56.0, 55.7, 41.8, 40.9, 28.7, 28.6, 24.9, 24.6, 22.5, 14.0.

HR-MS (ESI/TOF) calcd for C₂₁H₂₉N₃O₅Na [M+Na]⁺ 426.2005, found 426.2019



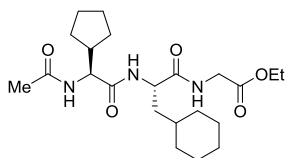
Ethyl ((S)-2-((S)-2-acetamido-2-cyclopentylacetamido)-3-cyclopentylpropanoyl)glycinate (79e**)**

Prepared in analogues way as **79c**: starting material **78e** (404 mg, 0.86 mmol) and 4 M HCl in dioxane (0.90 mL) in DCM (20 mL). Acylation: acetic anhydride (120 μL, 1.27 mmol) and DIPEA (460 μL, 2.66 mmol) in DCM (30 mL). Yield: 288 mg (81%, white solid).

¹H NMR (400 MHz, Dimethylsulfoxide-*d*₆) δ 8.27 (t, *J* = 5.9 Hz, 1H), 7.94 (d, *J* = 8.5 Hz, 1H), 7.88 (d, *J* = 8.2 Hz, 1H), 4.28 (td, *J* = 8.9, 5.7 Hz, 1H), 4.16 (t, *J* = 8.5 Hz, 1H), 4.07 (q, *J* = 7.2 Hz, 2H), 3.85 (dd, *J* = 17.3, 6.0 Hz, 1H), 3.75 (dd, *J* = 17.3, 5.8 Hz, 1H), 2.11 (h, *J* = 8.5 Hz, 1H), 1.84 (s, 3H), 1.83 – 1.68 (m, 2H), 1.68 – 1.48 (m, 9H), 1.48 – 1.40 (m, 4H), 1.34 – 1.14 (m, 5H), 1.14 – 1.00 (m, 2H).

¹³C NMR (101 MHz, Dimethylsulfoxide-*d*₆) δ 172.3, 171.2, 169.6, 169.2, 60.4, 56.1, 51.8, 41.8, 40.7, 38.2, 36.0, 32.3, 31.7, 28.6, 28.5, 24.9, 24.8, 24.6, 24.5, 22.5, 14.0.

HR-MS (ESI/TOF) calcd for C₂₁H₃₆N₃O₅ [M+H]⁺ 410.2655, found 410.2654



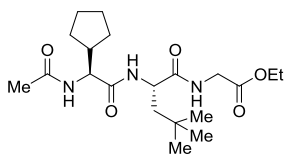
Ethyl ((S)-2-((S)-2-acetamido-2-cyclopentylacetamido)-3-cyclohexylpropanoyl)glycinate (79f)

Prepared in analogues way as **79c**: starting material **78f** (480 mg, 1.00 mmol) and 4 M HCl in dioxane (1 mL) in DCM (20 mL). Acylation: acetic anhydride (140 μ L, 1.48 mmol) and DIPEA (520 μ L, 3.00 mmol) in DCM (30 mL). Yield: 400 mg (95%, white solid).

¹H NMR (400 MHz, Dimethylsulfoxide-*d*₆) δ 8.21 (t, *J* = 5.9 Hz, 1H), 7.96 (d, *J* = 8.5 Hz, 1H), 7.85 (d, *J* = 8.3 Hz, 1H), 4.41 – 4.30 (m, 1H), 4.13 (t, *J* = 8.5 Hz, 1H), 4.07 (q, *J* = 7.2 Hz, 2H), 3.84 (dd, *J* = 17.3, 6.0 Hz, 1H), 3.74 (dd, *J* = 17.3, 5.9 Hz, 1H), 2.11 (h, *J* = 8.3 Hz, 1H), 1.84 (s, 3H), 1.73 – 1.39 (m, 14H), 1.34 – 1.20 (m, 3H), 1.18 (t, *J* = 7.1 Hz, 3H), 1.14 – 1.06 (m, 2H), 0.96 – 0.75 (m, 2H).

¹³C NMR (101 MHz, Dimethylsulfoxide-*d*₆) δ 172.5, 171.2, 169.6, 169.2, 60.4, 56.3, 49.9, 41.7, 40.7, 33.2, 31.7, 28.6, 28.5, 26.1, 25.8, 25.6, 24.9, 24.5, 22.5, 14.0.

HR-MS (ESI/TOF) calcd for C₂₂H₃₈N₃O₅ [M+H]⁺ 424.2811, found 424.2812



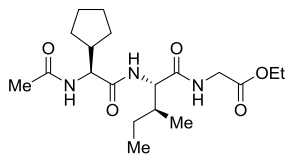
Ethyl ((S)-2-((S)-2-acetamido-2-cyclopentylacetamido)-4,4-di-methylpentanoyl)glycinate (79g)

Prepared in analogues way as **79c**: starting material **78f** (389 mg, 0.85 mmol) and 4 M HCl in dioxane (0.86 mL) in DCM (20 mL). Acylation: acetic anhydride (120 μ L, 1.27 mmol) and DIPEA (440 μ L, 2.54 mmol) in DCM (30 mL). Yield: 297 mg (87%, white solid).

¹H NMR (400 MHz, Chloroform-*d*) δ 7.46 (d, *J* = 8.5 Hz, 1H), 7.33 (t, *J* = 5.5 Hz, 1H), 6.78 (d, *J* = 8.8 Hz, 1H), 4.59 (td, *J* = 8.3, 4.4 Hz, 1H), 4.44 (t, *J* = 9.2 Hz, 1H), 4.17 (q, *J* = 7.2 Hz, 2H), 4.04 (dd, *J* = 18.0, 5.8 Hz, 1H), 3.87 (dd, *J* = 18.1, 5.1 Hz, 1H), 2.21 (h, *J* = 9.0 Hz, 1H), 1.99 (s, 3H), 1.93 – 1.84 (m, 2H), 1.79 – 1.44 (m, 7H), 1.26 (t, *J* = 7.2 Hz, 5H), 0.91 (s, 9H).

¹³C NMR (101 MHz, Chloroform-*d*) δ 172.8, 171.9, 170.4, 169.8, 61.4, 57.3, 50.8, 45.3, 42.9, 41.5, 30.5, 29.7, 29.4, 29.4, 25.5, 25.0, 23.1, 14.3.

HR-MS (ESI/TOF) calcd for C₂₀H₃₅N₃O₅Na [M+Na]⁺ 420.2474, found 420.2473



Ethyl ((S)-2-acetamido-2-cyclopentylacetyl)-L-isoleucyl-glycinate (79h)

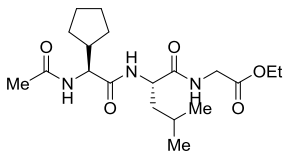
Prepared in analogues way as **79c**: starting material **78h** (456 mg, 1.03 mmol) and 4 M HCl in dioxane (1.05 mL) in DCM (20 mL). Acylation: acetic anhydride (150 μ L, 1.59 mmol) and DIPEA (540 μ L, 3.12 mmol) in DCM (20 mL). Yield: 240 mg (61%, white solid).

¹H NMR (400 MHz, Dimethylsulfoxide-*d*₆) δ 8.35 (t, *J* = 5.8 Hz, 1H), 7.98 (d, *J* = 8.6 Hz, 1H), 7.69 (d, *J* = 8.9 Hz, 1H), 4.23 – 4.14 (m, 2H), 4.07 (q, *J* = 7.1 Hz, 2H), 3.85 (dd, *J* = 17.3, 6.0 Hz, 1H), 3.76 (dd, *J* = 17.3, 5.8 Hz, 1H), 2.11 (h, *J* = 8.2 Hz, 1H), 1.84 (s, 3H),

1.75 – 1.66 (m, 1H), 1.66 – 1.36 (m, 7H), 1.32 – 1.13 (m, 5H), 1.12 – 1.00 (m, 1H), 0.90 – 0.74 (m, 6H).

¹³C NMR (101 MHz, Dimethylsulfoxide-*d*₆) δ 171.4, 171.3, 169.6, 169.2, 60.4, 56.5, 56.2, 41.6, 40.7, 36.8, 28.7, 28.6, 24.9, 24.6, 24.2, 22.5, 15.2, 14.0, 11.1.

HR-MS (ESI/TOF) calcd for C₁₉H₃₃N₃O₅Na [M+Na]⁺ 406.2318, found 406.2328



Ethyl ((S)-2-acetamido-2-cyclopentylacetyl)-L-leucylglycinate (79i)

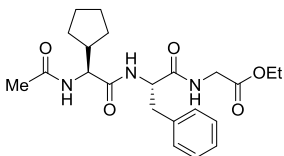
Prepared in analogues way as **79c**: starting material **78i** (313 mg, 0.71 mmol) and 4 M HCl in dioxane (0.71 mL) in DCM (25 mL). Acylation: acetic anhydride (100 μL,

1.06 mmol) and DIPEA (370 μL, 2.14 mmol) in DCM (20 mL). Yield: 232 mg (85%, white solid).

¹H NMR (400 MHz, Dimethylsulfoxide-*d*₆) δ 8.26 (t, *J* = 5.9 Hz, 1H), 7.94 (d, *J* = 8.5 Hz, 1H), 7.88 (d, *J* = 8.3 Hz, 1H), 4.32 (q, *J* = 7.9 Hz, 1H), 4.15 (t, *J* = 8.5 Hz, 1H), 4.07 (q, *J* = 7.0 Hz, 2H), 3.84 (dd, *J* = 17.3, 5.9 Hz, 1H), 3.75 (dd, *J* = 17.3, 5.8 Hz, 1H), 2.10 (h, *J* = 8.6 Hz, 1H), 1.84 (s, 3H), 1.70 – 1.40 (m, 9H), 1.34 – 1.20 (m, 2H), 1.17 (t, *J* = 7.1 Hz, 3H), 0.88 (d, *J* = 6.6 Hz, 3H), 0.83 (d, *J* = 6.6 Hz, 3H).

¹³C NMR (101 MHz, Dimethylsulfoxide-*d*₆) δ 172.4, 171.3, 169.6, 169.2, 60.4, 56.1, 50.6, 41.8, 41.0, 40.7, 28.6, 28.5, 24.9, 24.5, 24.0, 23.0, 22.5, 21.7, 14.0.

HR-MS (ESI/TOF) calcd for C₁₉H₃₃N₃O₅Na [M+Na]⁺ 406.2318, found 406.2322



Ethyl ((S)-2-acetamido-2-cyclopentylacetyl)-L-phenylalanyl-glycinate (79j)

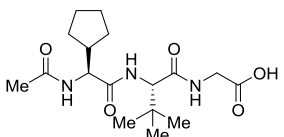
Prepared in analogues way as **79c**: starting material **78j** (391 mg, 0.82 mmol) and 4 M HCl in dioxane (0.82 mL) in DCM (30 mL). Acylation: acetic anhydride (110 μL,

1.16 mmol) and DIPEA (430 μL, 2.48 mmol) in DCM (20 mL). Yield: 297 mg (86%, white solid).

¹H NMR (300 MHz, Dimethylsulfoxide-*d*₆) δ 8.36 (t, *J* = 5.9 Hz, 1H), 7.93 (d, *J* = 8.6 Hz, 1H), 7.87 (d, *J* = 8.5 Hz, 1H), 7.28 – 7.14 (m, 5H), 4.55 (td, *J* = 9.7, 4.5 Hz, 1H), 4.19 – 4.03 (m, 3H), 3.94 – 3.73 (m, 2H), 3.03 (dd, *J* = 13.9, 4.6 Hz, 1H), 2.79 (dd, *J* = 13.9, 9.7 Hz, 1H), 2.08 – 1.92 (m, 1H), 1.81 (s, 3H), 1.62 – 1.28 (m, 6H), 1.25 – 1.09 (m, 5H).

¹³C NMR (101 MHz, Dimethylsulfoxide-*d*₆) δ 171.5, 171.2, 169.6, 169.2, 137.7, 129.2, 128.0, 126.2, 60.4, 56.3, 53.4, 41.8, 40.8, 37.5, 28.6, 28.5, 24.8, 24.5, 22.5, 14.1.

HR-MS (ESI/TOF) calcd for C₂₂H₃₁N₃O₅Na [M+Na]⁺ 440.2161, found 440.2167



((S)-2-((S)-2-acetamido-2-cyclopentylacetamido)-3,3-dimethylbutanoyl)glycine (S2c)

Starting material **79c** (369 mg, 0.96 mmol, 1.0 equiv) was dissolved in THF:H₂O (20:1, 10.5 mL), then LiOH (230 mg, 9.6 mmol, 10 equiv) was added and the reaction was stirred

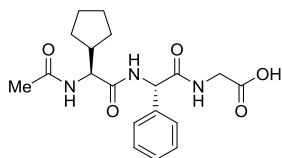
for 20 h at room temperature. Water (3 mL) was added and the reaction mixture was acidified by the addition of 1 M HCl solution and the product was extracted with CHCl₃

(4×10 mL). Organic phase was washed with brine, dried over Na₂SO₄, filtered and evaporated in vacuo to provide product **S2c** (300 mg, 88%) as a white solid.

¹H NMR (400 MHz, Methanol-*d*₄) δ 4.37 (s, 1H), 4.31 (d, *J* = 9.5 Hz, 1H), 3.99 (d, *J* = 17.6 Hz, 1H), 3.77 (d, *J* = 17.6 Hz, 1H), 2.17 (h, *J* = 9.0 Hz, 1H), 1.94 (s, 3H), 1.80 – 1.69 (m, 1H), 1.64 – 1.54 (m, 3H), 1.54 – 1.42 (m, 2H), 1.35 – 1.18 (m, 2H), 0.98 (s, 9H).

¹³C NMR (101 MHz, Methanol-*d*₄) δ 173.9, 173.0, 172.7, 172.5, 61.8, 58.9, 43.1, 41.7, 35.5, 30.4, 30.2, 27.1, 26.2, 25.9, 22.4.

HR-MS (ESI/TOF) calcd for C₁₇H₂₉N₃O₅Na [M+Na]⁺ 378.2005, found 378.2009



((S)-2-((S)-2-acetamido-2-cyclopentylacetamido)-2-phenylacetyl)glycine (S2d)

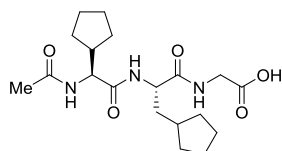
Prepared in analogues way as **S2c**: starting material **79d** (177 mg, 0.44 mmol) and LiOH (105 mg, 4.44 mmol) added to the mixture THF:H₂O (20:1, 10.5 mL). Yield: 120 mg

(73%, white solid).

¹H NMR (400 MHz, Dimethylsulfoxide-*d*₆) δ 12.51 (br s, 1H), 8.56 (t, *J* = 5.8 Hz, 1H), 8.38 (d, *J* = 8.1 Hz, 1H), 8.01 (d, *J* = 8.6 Hz, 1H), 7.50 – 7.37 (m, 2H), 7.37 – 7.23 (m, 3H), 5.54 (d, *J* = 8.1 Hz, 1H), 4.29 (t, *J* = 8.5 Hz, 1H), 3.77 (dd, *J* = 5.8, 2.9 Hz, 2H), 2.20 – 2.06 (m, 1H), 1.84 (s, 3H), 1.65 – 1.49 (m, 4H), 1.49 – 1.37 (m, 2H), 1.33 – 1.17 (m, 2H).

¹³C NMR (101 MHz, Dimethylsulfoxide-*d*₆) δ 171.0, 170.9, 169.9, 169.2, 138.6, 128.2, 127.5, 127.2, 56.0, 55.7, 41.7, 40.8, 28.7, 28.5, 24.9, 24.6, 22.5.

HR-MS (ESI/TOF) calcd for C₁₇H₂₉N₃O₅Na [M+Na]⁺ 398.1692, found 398.1707



((S)-2-((S)-2-acetamido-2-cyclopentylacetamido)-3-cyclopentylpropanoyl)glycine (S2e)

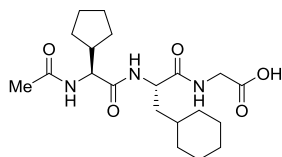
Prepared in analogues way as **S2c**: starting material **79e** (258 mg, 0.63 mmol) and LiOH (151 mg, 6.30 mmol) added to the mixture THF:H₂O (20:1, 30 mL). Yield: 220 mg (92%,

white solid).

¹H NMR (400 MHz, Methanol-*d*₄) δ 4.41 (dd, *J* = 9.3, 5.6 Hz, 1H), 4.14 (d, *J* = 9.2 Hz, 1H), 3.96 (d, *J* = 17.8 Hz, 1H), 3.85 (d, *J* = 17.8 Hz, 1H), 2.21 (h, *J* = 8.9 Hz, 1H), 1.98 (s, 3H), 1.97 – 1.86 (m, 1H), 1.86 – 1.49 (m, 14H), 1.43 – 1.24 (m, 2H), 1.21 – 1.10 (m, 2H).

¹³C NMR (101 MHz, Methanol-*d*₄) δ 174.7, 174.1, 173.5, 172.6, 59.2, 54.0, 43.0, 41.7, 39.1, 37.8, 33.8, 33.1, 30.4, 30.3, 26.2, 26.1, 26.0, 25.9, 22.4.

HR-MS (ESI/TOF) calcd for C₁₉H₃₁N₃O₅Na [M+Na]⁺ 404.2161, found 404.2154



((S)-2-((S)-2-acetamido-2-cyclopentylacetamido)-3-cyclohexylpropanoyl)glycine (S2f)

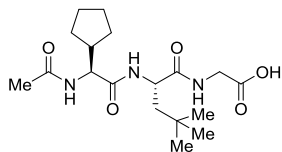
Prepared in analogues way as **S2c**: starting material **79f** (420 mg, 0.99 mmol) and LiOH (238 mg, 9.94 mmol) added to the mixture THF:H₂O (20:1, 30 mL). Yield: 350 mg (89%,

white solid).

^1H NMR (400 MHz, Methanol- d_4) δ 4.50 (dd, $J = 10.2, 5.2$ Hz, 1H), 4.13 (d, $J = 9.1$ Hz, 1H), 3.95 (d, $J = 17.8$ Hz, 1H), 3.85 (d, $J = 17.8$ Hz, 1H), 2.22 (h, $J = 8.9$ Hz, 1H), 1.99 (s, 3H), 1.87 – 1.51 (m, 13H), 1.46 – 1.11 (m, 6H), 1.05 – 0.83 (m, 2H).

^{13}C NMR (101 MHz, Methanol- d_4) δ 175.0, 174.1, 173.5, 172.7, 59.3, 52.0, 43.0, 41.7, 40.3, 35.2, 34.9, 33.3, 30.4, 30.3, 27.6, 27.4, 27.2, 26.2, 25.9, 22.4.

HR-MS (ESI/TOF) calcd for $\text{C}_{20}\text{H}_{33}\text{N}_3\text{O}_5\text{Na}$ [$\text{M}+\text{Na}$] $^+$ 418.2318, found 418.2327



((S)-2-((S)-2-acetamido-2-cyclopentylacetamido)-4,4-dimethylpentanoyl)glycine (S2g)

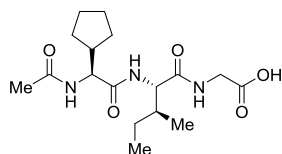
Prepared in analogues way as **S2c**: starting material **79g** (289 mg, 0.73 mmol) and LiOH (174 mg, 7.27 mmol) added to the mixture THF:H₂O (20:1, 21 mL). Yield: 253 mg (94%,

white solid).

^1H NMR (400 MHz, Methanol- d_4) δ 4.50 (dd, $J = 8.9, 3.4$ Hz, 1H), 4.14 (d, $J = 9.4$ Hz, 1H), 4.02 – 3.79 (m, 2H), 2.29 – 2.15 (m, 1H), 1.97 (s, 3H), 1.89 – 1.75 (m, 2H), 1.74 – 1.48 (m, 6H), 1.43 – 1.22 (m, 2H), 0.95 (s, 9H).

^{13}C NMR (101 MHz, Methanol- d_4) δ 175.2, 173.7, 173.5, 172.6, 59.2, 51.9, 46.1, 43.0, 41.8, 31.4, 30.4, 30.3, 30.0, 26.2, 25.9, 22.4.

HR-MS (ESI/TOF) calcd for $\text{C}_{18}\text{H}_{31}\text{N}_3\text{O}_5\text{Na}$ [$\text{M}+\text{Na}$] $^+$ 392.2161, found 392.2177



((S)-2-acetamido-2-cyclopentylacetyl)-L-isoleucylglycine (S2h)

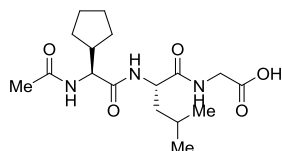
Prepared in analogues way as **S2c**: starting material **79h** (223 mg, 0.58 mmol) and LiOH (140 mg, 5.84 mmol) added to the mixture THF:H₂O (20:1, 21 mL). Yield: 193 mg (93%,

white solid).

^1H NMR (400 MHz, Dimethylsulfoxide- d_6) δ 12.48 (br s, 1H), 8.20 (t, $J = 5.8$ Hz, 1H), 7.99 (d, $J = 8.5$ Hz, 1H), 7.69 (d, $J = 9.1$ Hz, 1H), 4.23 – 4.15 (m, 2H), 3.77 (dd, $J = 17.5, 5.8$ Hz, 1H), 3.69 (dd, $J = 17.5, 5.8$ Hz, 1H), 2.12 (h, $J = 8.4$ Hz, 1H), 1.84 (s, 3H), 1.77 – 1.67 (m, 1H), 1.66 – 1.39 (m, 7H), 1.32 – 1.15 (m, 2H), 1.12 – 0.99 (m, 1H), 0.86 – 0.76 (m, 6H).

^{13}C NMR (101 MHz, Dimethylsulfoxide- d_6) δ 171.3, 171.2, 171.0, 169.1, 56.5, 56.2, 41.6, 40.61, 36.8, 28.7, 28.6, 24.9, 24.6, 24.1, 22.5, 15.2, 11.1.

HR-MS (ESI/TOF) calcd for $\text{C}_{17}\text{H}_{29}\text{N}_3\text{O}_5\text{Na}$ [$\text{M}+\text{Na}$] $^+$ 378.2005, found 378.1999



((S)-2-acetamido-2-cyclopentylacetyl)-L-leucylglycine (S2i)

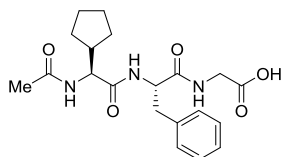
Prepared in analogues way as **S2c**: starting material **79i** (222 mg, 0.58 mmol) and LiOH (140 mg, 5.84 mmol) added to the mixture THF:H₂O (20:1, 50 mL). Yield: 202 mg (98%, white solid).

^1H NMR (400 MHz, Dimethylsulfoxide- d_6) δ 12.39 (br s, 1H), 8.08 (t, $J = 5.8$ Hz, 1H), 7.95 (d, $J = 8.5$ Hz, 1H), 7.88 (d, $J = 8.5$ Hz, 1H), 4.38 – 4.27 (m, 1H), 4.15 (t, $J = 8.5$ Hz, 1H), 3.77 (dd, $J = 17.5, 5.8$ Hz, 1H), 3.68 (dd, $J = 17.5, 5.8$ Hz, 1H), 2.11 (h, $J = 8.5$ Hz,

1H), 1.84 (s, 3H), 1.68 – 1.38 (m, 9H), 1.32 – 1.15 (m, 2H), 0.87 (d, $J = 6.7$ Hz, 3H), 0.82 (d, $J = 6.6$ Hz, 3H).

^{13}C NMR (101 MHz, Dimethylsulfoxide- d_6) δ 172.2, 171.3, 171.1, 169.3, 56.2, 50.7, 41.8, 41.0, 40.6, 28.7, 28.5, 24.9, 24.6, 24.1, 23.1, 22.5, 21.6.

HR-MS (ESI/TOF) calcd for $\text{C}_{17}\text{H}_{29}\text{N}_3\text{O}_5\text{Na}$ [$\text{M}+\text{Na}$] $^+$ 378.2005, found 378.2014



((S)-2-acetamido-2-cyclopentylacetyl)-L-phenylalanyl-glycine (S2j)

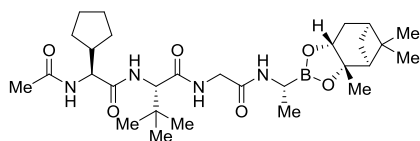
Prepared in analogues way as **S2c**: starting material **79j** (289 mg, 0.69 mmol) and LiOH (166 mg, 6.93 mmol) added to the mixture THF:H₂O (20:1, 50 mL). Yield: 242 mg (90%,

white solid).

^1H NMR (400 MHz, Dimethylsulfoxide- d_6) δ 12.63 (s, 1H), 8.21 (t, $J = 5.8$ Hz, 1H), 7.92 (d, $J = 8.6$ Hz, 1H), 7.88 (d, $J = 8.3$ Hz, 1H), 7.26 – 7.13 (m, 5H), 4.59 – 4.49 (m, 1H), 4.07 (t, $J = 8.5$ Hz, 1H), 3.84 – 3.69 (m, 2H), 3.04 (dd, $J = 13.9, 4.4$ Hz, 1H), 2.78 (dd, $J = 13.9, 9.7$ Hz, 1H), 2.00 (h, $J = 8.6$ Hz, 1H), 1.82 (s, 3H), 1.58 – 1.33 (m, 6H), 1.20 – 1.09 (m, 2H).

^{13}C NMR (101 MHz, Dimethylsulfoxide- d_6) δ 171.3, 171.2, 171.1, 169.3, 137.8, 129.2, 128.0, 126.2, 56.3, 53.5, 41.8, 40.7, 37.5, 28.6, 28.5, 24.8, 24.5, 22.5.

HR-MS (ESI/TOF) calcd for $\text{C}_{20}\text{H}_{27}\text{N}_3\text{O}_5\text{Na}$ [$\text{M}+\text{Na}$] $^+$ 412.1848, found 412.1835



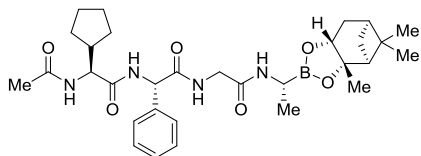
(S)-2-((S)-2-acetamido-2-cyclopentylacetyl)-3,3-dimethyl-N-(2-oxo-2-(((R)-1-(3aS,4S,6S,7aR)-3a,5,5-trimethylhexahydro-4,6-methanobenzo[d][1,3,2]dioxaborol-2-yl)ethyl)-amino)ethyl)-butanamide (80c)

An acid **S2c** (200 mg, 0.56 mmol, 1.0 equiv) was dissolved in 10 mL EtOAc, then *N*-methylmorpholine (200 μL , 1.82 mmol, 3.0 equiv) and a solution of propylphosphonic acid anhydride (670 μL , 2.0 equiv, 50% by weight in EtOAc) was added sequentially. Reaction mixture was stirred for 30 min before **54a** (175 mg, 0.67 mmol, 1.2 equiv) in 1 mL DMF was added. After reaction was complete (UPLC-MS control) it was diluted with 10 mL of H₂O and citric acid was added. Layers were separated and the aqueous layer was extracted with EtOAc (2 \times 10 mL). The combined organic layers were washed with sat. NaHCO₃ (10 mL), brine (10 mL), dried over Na₂SO₄, filtered and concentrated under reduced pressure. Crude mixture was purified by flash chromatography on silica gel eluting with 0–5% MeOH in EtOAc to provide **80c** (148 mg, 47%) as amorphous compound.

^1H NMR (400 MHz, Methanol- d_4) δ 4.23 (d, $J = 9.5$ Hz, 1H), 4.19 – 4.13 (m, 2H), 4.06 (s, 1H), 3.96 (dd, $J = 17.4, 1.0$ Hz, 1H), 2.65 (q, $J = 7.3$ Hz, 1H), 2.39 – 2.27 (m, 1H), 2.23 (h, $J = 8.6$ Hz, 1H), 2.19 – 2.06 (m, 1H), 1.97 (s, 3H), 1.94 (t, $J = 5.5$ Hz, 1H), 1.89 – 1.75 (m, 3H), 1.72 – 1.63 (m, 3H), 1.62 – 1.50 (m, 2H), 1.44 (d, $J = 10.3$ Hz, 1H), 1.38 – 1.27 (m, 8H), 1.16 (d, $J = 7.3$ Hz, 3H), 1.03 (s, 9H), 0.87 (s, 3H).

^{13}C NMR (101 MHz, Methanol- d_4) δ 175.8, 174.8, 173.4, 173.3, 84.3, 77.3, 63.5, 58.9, 53.6, 42.8, 41.4, 39.9 (overlaps with $\underline{\text{CHB}}$ (broad)), 39.2, 37.7, 34.6, 30.5, 30.2, 29.6, 27.8, 27.5, 27.1, 26.3, 26.0, 24.6, 22.3, 16.4.

HR-MS (ESI/TOF) calcd for $\text{C}_{29}\text{H}_{50}\text{BN}_4\text{O}_6$ $[\text{M}+\text{H}]^+$ 561.3823, found 561.3842



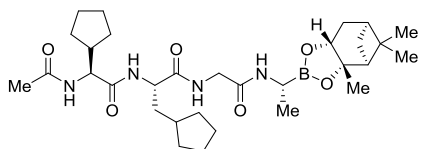
(S)-2-acetamido-2-cyclopentyl-N-((S)-2-oxo-2-((2-oxo-2-(((R)-1-((3a*S*,4*S*,6*S*,7a*R*)-3a,5,5-trimethylhexahydro-4,6-methanobenzo[*d*]-[1,3,2]dioxaborol-2-yl)ethyl)amino)-ethyl)amino)-1-phenyl-ethyl) acetamide (80d)

Prepared in analogy to **80c**: an acid **S2d** (100 mg, 0.27 mmol) and *N*-methylmorpholine (100 μL , 0.91 mmol) were dissolved in EtOAc (5 mL), then propylphosphonic acid anhydride (320 μL , 0.54 mmol) was added sequentially. Reaction mixture was stirred for 30 min before **54a** (83 mg, 0.32 mmol) in 1 mL DMF was added. Yield: 54 mg (35%, amorphous compound).

^1H NMR (400 MHz, Methanol- d_4) δ 7.50 – 7.42 (m, 2H), 7.43 – 7.31 (m, 3H), 5.31 (s, 1H), 4.26 – 4.19 (m, 1H), 4.19 – 4.06 (m, 2H), 3.88 (dd, $J = 17.6, 1.0$ Hz, 1H), 2.67 (q, $J = 7.4$ Hz, 1H), 2.39 – 2.27 (m, 1H), 2.29 – 2.16 (m, 1H), 2.19 – 2.07 (m, 1H), 1.97 (s, 3H), 1.94 (t, $J = 5.5$ Hz, 1H), 1.88 – 1.72 (m, 4H), 1.71 – 1.54 (m, 4H), 1.43 (d, $J = 10.4$ Hz, 1H), 1.39 – 1.24 (m, 8H), 1.17 (d, $J = 7.3$ Hz, 3H), 0.87 (s, 3H).

^{13}C NMR (101 MHz, Methanol- d_4) δ 175.7, 174.4, 173.4, 172.9, 137.4, 129.9, 129.6, 129.0, 84.3, 77.3, 59.6, 58.6, 53.6, 43.1, 41.4, 40.3, 39.8 ($\underline{\text{CHB}}$ (broad)), 39.2, 37.7, 30.3, 30.2, 29.6, 27.8, 27.5, 26.3, 25.9, 24.6, 24.5, 22.3, 16.4.

HR-MS (ESI/TOF) calcd for $\text{C}_{31}\text{H}_{46}\text{BN}_4\text{O}_6$ $[\text{M}+\text{H}]^+$ 581.3510, found 581.3528



(S)-2-((S)-2-acetamido-2-cyclopentylacetamido)-3-cyclopentyl-N-(2-oxo-2-(((R)-1-((3a*S*,4*S*,6*S*,7a*R*)-3a,5,5-trimethylhexahydro-4,6-methanobenzo[*d*]-[1,3,2]dioxaborol-2-yl)ethyl)-amino)ethyl)propan-amide (80e)

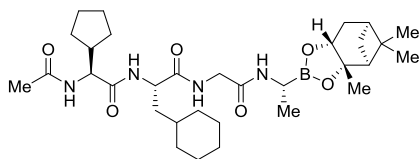
amino)ethyl)propan-amide (80e)

Prepared in analogy to **80c**: an acid **S2e** (200 mg, 0.52 mmol) and *N*-methylmorpholine (170 μL , 1.55 mmol) were dissolved in EtOAc (5 mL), then propylphosphonic acid anhydride (620 μL , 1.04 mmol) was added sequentially. Reaction mixture was stirred for 30 min before **54a** (163 mg, 0.63 mmol) in 1 mL DMF was added. Yield: 75 mg (24%, amorphous compound).

^1H NMR (400 MHz, Methanol- d_4) δ 4.26 – 4.08 (m, 4H), 3.93 (d, $J = 17.6$ Hz, 1H), 2.64 (q, $J = 7.3$ Hz, 1H), 2.38 – 2.28 (m, 1H), 2.26 – 2.15 (m, 1H), 2.18 – 2.07 (m, 1H), 1.98 (s, 3H), 1.95 (t, $J = 5.5$ Hz, 1H), 1.92 – 1.73 (m, 8H), 1.72 – 1.50 (m, 9H), 1.44 (d, $J = 10.3$ Hz, 1H), 1.40 – 1.26 (m, 8H), 1.21 – 1.09 (m, 5H), 0.87 (s, 3H).

^{13}C NMR (101 MHz, Methanol- d_4) δ 175.9, 175.2, 174.9, 173.4, 84.3, 77.3, 58.9, 55.2, 53.6, 43.1, 41.4, 40.1, 39.8 ($\underline{\text{CHB}}$ (broad)), 39.2, 38.4, 37.74, 37.70, 33.8, 33.2, 30.4, 30.2, 29.6, 27.8, 27.5, 26.3, 26.1, 26.0, 25.9, 24.6, 22.3, 16.4.

HR-MS (ESI/TOF) calcd for $\text{C}_{31}\text{H}_{51}\text{BN}_4\text{O}_6\text{Na}$ $[\text{M}+\text{Na}]^+$ 609.3799, found 609.3820



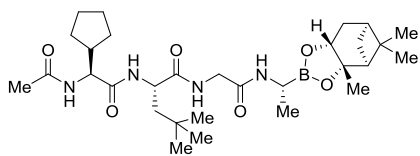
(S)-2-((S)-2-acetamido-2-cyclopentyl-acetamido)-3-cyclohexyl-N-(2-oxo-2-(((R)-1-(3a*S*,4*S*,6*S*,7a*R*)-3a,5,5-trimethylhexahydro-4,6-methanobenzo[*d*][1,3,2]dioxaborol-2-yl)ethyl)-amino)ethyl) propanamide (80f)

Prepared in analogy to **80c**: an acid **S2f** (200 mg, 0.50 mmol) and *N*-methylmorpholine (170 μ L, 1.55 mmol) were dissolved in EtOAc (5 mL), then propylphosphonic acid anhydride (600 μ L, 1.01 mmol) was added sequentially. Reaction mixture was stirred for 30 min before **54a** (158 mg, 0.61 mmol) in 1 mL DMF was added. Yield: 90 mg (30%, amorphous compound).

^1H NMR (400 MHz, Methanol- d_4) δ 4.27 (t, $J = 7.6$ Hz, 1H), 4.21 – 4.10 (m, 3H), 3.93 (dd, $J = 17.6, 1.0$ Hz, 1H), 2.65 (q, $J = 7.2$ Hz, 1H), 2.38 – 2.29 (m, 1H), 2.29 – 2.15 (m, 1H), 2.17 – 2.09 (m, 1H), 1.98 (s, 3H), 1.95 (t, $J = 5.5$ Hz, 1H), 1.90 – 1.84 (m, 1H), 1.82 – 1.52 (m, 14H), 1.44 (d, $J = 10.4$ Hz, 1H), 1.41 – 1.20 (m, 12H), 1.17 (d, $J = 7.3$ Hz, 3H), 1.05 – 0.84 (m, 5H).

^{13}C NMR (101 MHz, Methanol- d_4) δ 175.9, 175.4, 175.0, 173.5, 84.3, 77.3, 59.0, 53.6, 53.1, 43.0, 41.4, 40.1, 39.8 (C_{HB} (broad)), 39.6, 39.2, 37.7, 35.2, 34.8, 33.4, 30.4, 30.2, 29.6, 27.8, 27.6, 27.5, 27.4, 27.2, 26.2, 25.9, 24.6, 22.4, 16.4.

HR-MS (ESI/TOF) calcd for $\text{C}_{32}\text{H}_{54}\text{BN}_4\text{O}_6$ $[\text{M}+\text{H}]^+$ 601.4136, found 601.4150



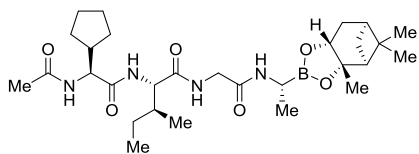
(S)-2-((S)-2-acetamido-2-cyclopentyl-acetamido)-4,4-dimethyl-N-(2-oxo-2-(((R)-1-(3a*S*,4*S*,6*S*,7a*R*)-3a,5,5-trimethylhexahydro-4,6-methanobenzo[*d*][1,3,2]dioxaborol-2-yl)ethyl)-amino)ethyl) pentanamide (80g)

Prepared in analogy to **80c**: an acid **S2g** (210 mg, 0.57 mmol) and *N*-methylmorpholine (200 μ L, 1.82 mmol) were dissolved in EtOAc (7 mL), then propylphosphonic acid anhydride (700 μ L, 1.18 mmol) was added sequentially. Reaction mixture was stirred for 30 min before **54a** (177 mg, 0.68 mmol) in 3 mL DMF was added. Yield: 171 mg (52%, amorphous compound).

^1H NMR (400 MHz, Methanol- d_4) δ 4.26 (dd, $J = 8.0, 4.3$ Hz, 1H), 4.19 – 4.09 (m, 3H), 3.93 (dd, $J = 17.5, 1.0$ Hz, 1H), 2.65 (q, $J = 7.2$ Hz, 1H), 2.39 – 2.28 (m, 1H), 2.28 – 2.15 (m, 1H), 2.17 – 2.08 (m, 1H), 1.97 (s, 3H), 1.95 (t, $J = 5.6$ Hz, 1H), 1.89 – 1.74 (m, 4H), 1.72 – 1.51 (m, 6H), 1.44 (d, $J = 10.4$ Hz, 1H), 1.32 (d, $J = 29.0$ Hz, 8H), 1.17 (d, $J = 7.3$ Hz, 3H), 0.96 (s, 9H), 0.87 (s, 3H).

^{13}C NMR (101 MHz, Methanol- d_4) δ 175.8, 175.6, 174.7, 173.4, 84.3, 77.3, 59.0, 53.6, 52.9, 45.6, 43.0, 41.4, 40.2, 39.8 (C_{HB} (broad)), 39.2, 37.7, 31.3, 30.5, 30.2, 30.0, 29.6, 27.8, 27.5, 26.3, 25.9, 24.5, 22.3, 16.4.

HR-MS (ESI/TOF) calcd for $\text{C}_{30}\text{H}_{52}\text{BN}_4\text{O}_6$ $[\text{M}+\text{H}]^+$ 575.3980, found 575.3998



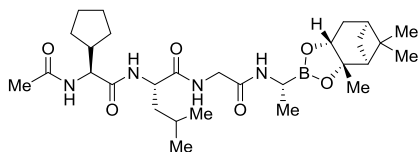
(2*S*,3*S*)-2-((*S*)-2-acetamido-2-cyclopentyl-acetamido)-3-methyl-*N*-(2-oxo-2-(((*R*)-1-(3*aS*,4*S*,6*S*,7*aR*)-3*a*,5,5-trimethylhexahydro-4,6-methanobenzo[*d*][1,3,2]dioxaborol-2-yl)ethyl)-amino)ethyl)pentanamide (80h)

Prepared in analogy to **80c**: an acid **S2h** (180 mg, 0.51 mmol) and *N*-methylmorpholine (170 μ L, 1.55 mmol) were dissolved in EtOAc (10 mL), then propylphosphonic acid anhydride (600 μ L, 1.01 mmol) was added sequentially. Reaction mixture was stirred for 30 min before **54a** (158 mg, 0.61 mmol) in 5 mL DMF was added. Yield: 94 mg (33%, amorphous compound).

^1H NMR (400 MHz, Methanol- d_4) δ 4.24 – 4.13 (m, 3H), 4.02 (d, J = 8.5 Hz, 1H), 3.94 (dd, J = 17.5, 1.0 Hz, 1H), 2.64 (q, J = 7.3 Hz, 1H), 2.40 – 2.29 (m, 1H), 2.28 – 2.15 (m, 1H), 2.18 – 2.07 (m, 1H), 1.97 (s, 3H), 1.94 (t, J = 5.5 Hz, 1H), 1.89 – 1.74 (m, 4H), 1.72 – 1.51 (m, 6H), 1.44 (d, J = 10.4 Hz, 1H), 1.39 – 1.27 (m, 8H), 1.26 – 1.19 (m, 1H), 1.17 (d, J = 7.3 Hz, 3H), 0.97 – 0.90 (m, 6H), 0.87 (s, 3H).

^{13}C NMR (101 MHz, Methanol- d_4) δ 175.8, 175.0, 174.4, 173.3, 84.3, 77.3, 60.2, 58.8, 53.6, 43.0, 41.4, 40.0 (overlaps with CHB (broad)), 39.2, 37.7, 37.2, 30.4, 30.2, 29.6, 27.8, 27.5, 26.3, 26.3, 25.9, 24.6, 22.3, 16.4, 15.8, 11.2.

UPLC (ESI) calcd for $\text{C}_{29}\text{H}_{50}\text{BN}_4\text{O}_6$ $[\text{M}+\text{H}]^+$ 561.53, found 561.85



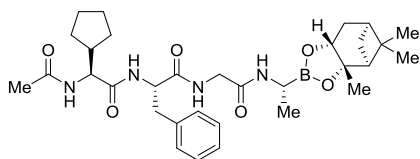
(*S*)-2-((*S*)-2-acetamido-2-cyclopentyl-acetamido)-4-methyl-*N*-(2-oxo-2-(((*R*)-1-(3*aS*,4*S*,6*S*,7*aR*)-3*a*,5,5-trimethylhexahydro-4,6-methanobenzo[*d*][1,3,2]-dioxaborol-2-yl)ethyl)amino)ethyl) pentanamide (80i)

Prepared in analogy to **80c**: an acid **S2i** (174 mg, 0.49 mmol) and *N*-methylmorpholine (160 μ L, 1.45 mmol) were dissolved in EtOAc (6 mL), then propylphosphonic acid anhydride (580 μ L, 0.98 mmol) was added sequentially. Reaction mixture was stirred for 30 min before **54a** (153 mg, 0.59 mmol) in 3 mL DMF was added. Yield: 111 mg (41%, amorphous compound).

^1H NMR (400 MHz, Methanol- d_4) δ 4.27 – 4.09 (m, 4H), 3.94 (dd, J = 17.6, 1.0 Hz, 1H), 2.65 (q, J = 7.3 Hz, 1H), 2.38 – 2.29 (m, 1H), 2.26 – 2.17 (m, 1H), 2.17 – 2.10 (m, 1H), 1.98 (s, 3H), 1.95 (t, J = 5.5 Hz, 1H), 1.89 – 1.75 (m, 3H), 1.73 – 1.52 (m, 8H), 1.44 (d, J = 10.3 Hz, 1H), 1.41 – 1.27 (m, 8H), 1.17 (d, J = 7.3 Hz, 3H), 0.97 (d, J = 6.3 Hz, 3H), 0.93 (d, J = 6.4 Hz, 3H), 0.88 (s, 3H).

^{13}C NMR (101 MHz, Methanol- d_4) δ 175.9, 175.2, 175.0, 173.5, 84.3, 77.3, 59.0, 53.9, 53.6, 43.0, 41.4, 41.0, 40.1, 39.8 (CHB (broad)), 39.2, 37.7, 30.4, 30.2, 29.6, 27.8, 27.5, 26.2, 25.9, 25.8, 24.6, 23.3, 22.3, 22.1, 16.4.

HR-MS (ESI/TOF) calcd for $\text{C}_{29}\text{H}_{50}\text{BN}_4\text{O}_6$ $[\text{M}+\text{H}]^+$ 561.3823, found 561.3846



(S)-2-((S)-2-acetamido-2-cyclopentyl-acetamido)-N-(2-oxo-2-(((R)-1-(3aS,4S,6S,7aR)-3a,5,5-trimethyl-hexahydro-4,6-methanobenzo[d]-[1,3,2]dioxaborol-2-yl)ethyl)amino)ethyl)-3-phenylpropanamide

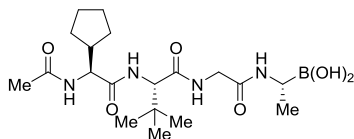
(80j)

Prepared in analogy to **80c**: an acid **S2j** (201 mg, 0.52 mmol) and *N*-methylmorpholine (180 μ L, 1.64 mmol) were dissolved in EtOAc (6 mL), then propylphosphonic acid anhydride (680 μ L, 1.14 mmol) was added sequentially. Reaction mixture was stirred for 30 min before **54a** (176 mg, 0.68 mmol) in 3 mL DMF was added. Yield: 116 mg (38%, amorphous compound).

^1H NMR (400 MHz, Methanol- d_4) δ 7.31 – 7.18 (m, 5H), 4.45 (dd, J = 8.5, 6.8 Hz, 1H), 4.17 – 4.15 (m, 1H), 4.13 (dd, J = 11.8, 2.0 Hz, 1H), 4.07 (d, J = 9.2 Hz, 1H), 3.82 (dd, J = 17.6, 1.0 Hz, 1H), 3.16 (dd, J = 13.8, 6.8 Hz, 1H), 2.99 (dd, J = 13.9, 8.4 Hz, 1H), 2.65 (q, J = 7.6 Hz, 1H), 2.37 – 2.29 (m, 1H), 2.19 – 2.05 (m, 2H), 1.98 – 1.92 (m, 4H), 1.88 – 1.82 (m, 1H), 1.81 – 1.71 (m, 2H), 1.67 – 1.47 (m, 5H), 1.43 (d, J = 10.4 Hz, 1H), 1.35 (s, 3H), 1.29 – 1.20 (m, 5H), 1.16 (d, J = 7.3 Hz, 3H), 0.87 (s, 3H).

^{13}C NMR (101 MHz, Methanol- d_4) δ 175.7, 174.8, 174.1, 173.5, 138.2, 130.3, 129.5, 127.9, 84.4, 77.3, 59.2, 56.8, 53.6, 42.9, 41.3, 40.2, 39.6 ($\underline{\text{CHB}}$ (broad)), 39.2, 37.9, 37.7, 30.4, 30.1, 29.6, 27.8, 27.5, 26.2, 25.8, 24.5, 22.4, 16.4.

HR-MS (ESI/TOF) calcd for $\text{C}_{32}\text{H}_{48}\text{BN}_4\text{O}_6$ $[\text{M}+\text{H}]^+$ 595.3667, found 595.3693



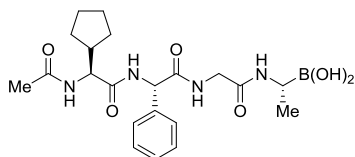
((2R,8S,11S)-8-(tert-butyl)-11-cyclopentyl-4,7,10,13-tetra-oxo-3,6,9,12-tetraazatetradecan-2-yl)boronic acid (17c)

A solution of **80c** (135 mg, 0.24 mmol) in MeOH/*n*-hexane (1:1, 9.2 mL) was treated with isobutylboronic acid (74 mg, 0.72 mmol, 3 equiv) and 1 M HCl (600 μ L). After 18 h at room temperature, the methanolic phase was washed with *n*-hexane (2 \times 5 mL) and the combined *n*-hexane layers were washed with MeOH (2 \times 5 mL). The combined methanol phase was evaporated in vacuo. Crude mixture was purified by flash chromatography on reversed phase silica gel eluting with 10–100% MeCN in H_2O to provide **17c** (76 mg, 74%) as a white solid compound.

^1H NMR (400 MHz, Methanol- d_4) δ 4.24 (d, J = 9.5 Hz, 1H), 4.20 (dd, J = 17.5, 1.6 Hz, 1H), 4.07 (s, 1H), 3.98 (dd, J = 17.4, 1.0 Hz, 1H), 2.66 (q, J = 7.2 Hz, 1H), 2.22 (h, J = 8.9 Hz, 1H), 1.98 (s, 3H), 1.86 – 1.77 (m, 1H), 1.73 – 1.62 (m, 3H), 1.62 – 1.49 (m, 2H), 1.39 – 1.24 (m, 2H), 1.12 (d, J = 7.2 Hz, 3H), 1.04 (s, 9H).

^{13}C NMR (101 MHz, Methanol- d_4) δ 176.2, 174.8, 173.5, 173.4, 63.5, 58.9, 42.9, 41.9 ($\underline{\text{CHB}}$ (broad)), 39.5, 34.6, 30.4, 30.3, 27.0, 26.3, 25.9, 22.3, 15.9

HR-MS (ESI/TOF) calcd for $\text{C}_{19}\text{H}_{35}\text{BN}_4\text{O}_6\text{Na}$ $[\text{M}+\text{Na}]^+$ 449.2547, found 449.2560



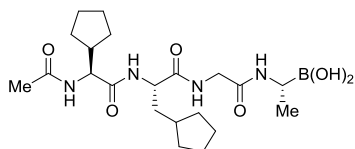
((2*R*,8*S*,11*S*)-11-cyclopentyl-4,7,10,13-tetraoxo-8-phenyl-3,6,9,12-tetraazatetradecan-2-yl)boronic acid (17d**)**

Prepared in analogy to **17c**: a solution of **80d** (50 mg, 0.086 mmol) in MeOH/*n*-hexane (1:1, 3.3 mL) was treated with isobutylboronic acid (27 mg, 0.26 mmol) and 1 M HCl (215 μ L). Yield: 29 mg (75%, white solid).

^1H NMR (400 MHz, Methanol- d_4) δ 7.49 – 7.44 (m, 2H), 7.40 – 7.32 (m, 3H), 5.33 (s, 1H), 4.26 – 4.10 (m, 2H), 3.95 (dd, $J = 17.6, 1.0$ Hz, 1H), 2.67 (q, $J = 7.2$ Hz, 1H), 2.23 (h, $J = 9.0$ Hz, 1H), 1.97 (s, 3H), 1.86 – 1.51 (m, 6H), 1.47 – 1.24 (m, 2H), 1.12 (d, $J = 7.2$ Hz, 3H).

^{13}C NMR (101 MHz, Methanol- d_4) δ 176.2, 174.4, 173.40 173.1, 137.3, 129.9, 129.7, 129.0, 59.4, 58.6, 43.2, 41.9 (C_{HB} (broad)), 39.9, 30.3, 30.2, 26.2, 25.9, 22.3, 15.9.

HR-MS (ESI/TOF) calcd for C₂₁H₃₁BN₄O₆Na [M+Na]⁺ 469.2234, found 469.2235



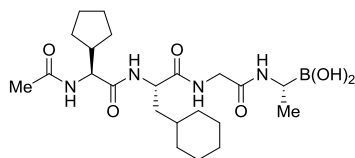
((2*R*,8*S*,11*S*)-11-cyclopentyl-8-(cyclopentylmethyl)-4,7,10,13-tetraoxo-3,6,9,12-tetraazatetradecan-2-yl)boronic acid (17e**)**

Prepared in analogy to **17c**: a solution of **80e** (72 mg, 0.123 mmol) in MeOH/*n*-hexane (1:1, 4.7 mL) was treated with isobutylboronic acid (40 mg, 0.39 mmol) and 1 M HCl (310 μ L). Yield: 33 mg (59%, white solid).

^1H NMR (400 MHz, Methanol- d_4) δ 4.25 – 4.16 (m, 2H), 4.13 (d, $J = 9.2$ Hz, 1H), 3.97 (dd, $J = 17.6, 1.0$ Hz, 1H), 2.66 (q, $J = 7.2$ Hz, 1H), 2.20 (h, $J = 8.9$ Hz, 1H), 1.98 (s, 3H), 1.94 – 1.73 (m, 6H), 1.72 – 1.49 (m, 9H), 1.43 – 1.26 (m, 2H), 1.23 – 1.10 (m, 5H).

^{13}C NMR (101 MHz, Methanol- d_4) δ 176.3, 175.3, 175.0, 173.5, 59.0, 55.1, 43.1, 42.0 (C_{HB} (broad)), 39.8, 38.3, 37.7, 33.7, 33.2, 30.4, 30.2, 26.2, 26.1, 26.0, 25.9, 22.3, 15.9.

HR-MS (ESI/TOF) calcd for C₂₁H₃₇BN₄O₆Na [M+Na]⁺ 475.2704, found 475.2723



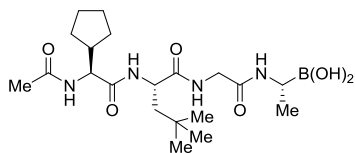
((2*R*,8*S*,11*S*)-8-(cyclohexylmethyl)-11-cyclopentyl-4,7,10,13-tetraoxo-3,6,9,12-tetraazatetradecan-2-yl)boronic acid (17f**)**

Prepared in analogy to **17c**: a solution of **80f** (74 mg, 0.123 mmol) in MeOH/*n*-hexane (1:1, 4.7 mL) was treated with isobutylboronic acid (40 mg, 0.39 mmol) and 1 M HCl (310 μ L). Yield: 31 mg (54%, white solid).

^1H NMR (400 MHz, Methanol- d_4) δ 4.28 (t, $J = 7.7$ Hz, 1H), 4.20 (dd, $J = 17.6, 1.7$ Hz, 1H), 4.13 (d, $J = 9.3$ Hz, 1H), 3.97 (dd, $J = 17.6, 1.0$ Hz, 1H), 2.66 (q, $J = 7.1$ Hz, 1H), 2.21 (h, $J = 8.8$ Hz, 1H), 1.98 (s, 3H), 1.88 – 1.50 (m, 13H), 1.44 – 1.16 (m, 6H), 1.12 (d, $J = 7.2$ Hz, 3H), 1.05 – 0.86 (m, 2H).

^{13}C NMR (101 MHz, Methanol- d_4) δ 176.3, 175.5, 175.0, 173.5, 59.1, 53.1, 43.0, 41.9 (C_{HB} (broad)), 39.8, 39.5, 35.2, 34.8, 33.5, 30.4, 30.2, 27.6, 27.4, 27.2, 26.2, 25.9, 22.4, 16.0.

HR-MS (ESI/TOF) calcd for C₂₂H₃₉BN₄O₆Na [M+Na]⁺ 489.2860, found 489.2850



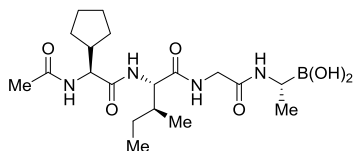
((2R,8S,11S)-11-cyclopentyl-8-neopentyl-4,7,10,13-tetra-oxo-3,6,9,12-tetraazatetradecan-2-yl)boronic acid (17g)

Prepared in analogy to **17c**: a solution of **80g** (151 mg, 0.263 mmol) in MeOH/*n*-hexane (1:1, 10 mL) was treated with isobutylboronic acid (107 mg, 1.05 mmol, 4 equiv) and 1 M HCl (650 μ L). Yield: 95 mg (82%, white solid).

^1H NMR (400 MHz, Methanol- d_4) δ 4.26 (dd, $J = 8.0, 4.3$ Hz, 1H), 4.19 (dd, $J = 17.6, 1.7$ Hz, 1H), 4.11 (d, $J = 9.5$ Hz, 1H), 3.96 (dd, $J = 17.6, 1.0$ Hz, 1H), 2.65 (q, $J = 7.2$ Hz, 1H), 2.21 (h, $J = 8.6$ Hz, 1H), 1.97 (s, 3H), 1.86 – 1.75 (m, 2H), 1.74 – 1.50 (m, 6H), 1.42 – 1.25 (m, 2H), 1.12 (d, $J = 7.2$ Hz, 3H), 0.97 (s, 9H).

^{13}C NMR (101 MHz, Methanol- d_4) δ 176.3, 175.7, 174.7, 173.5, 59.1, 52.9, 45.5, 43.0, 41.8 ($\underline{\text{CHB}}$ (broad)), 39.8, 31.3, 30.5, 30.2, 30.0, 26.3, 25.9, 22.3, 16.0.

HR-MS (ESI/TOF) calcd for $\text{C}_{20}\text{H}_{37}\text{BN}_4\text{O}_6\text{Na}$ [$\text{M}+\text{Na}$] $^+$ 463.2704, found 463.2701



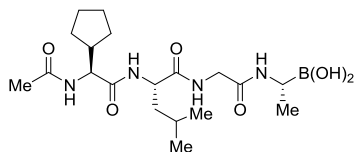
((2R,8S,11S)-8-((S)-*sec*-butyl)-11-cyclopentyl-4,7,10,13-tetraoxo-3,6,9,12-tetraazatetradecan-2-yl)boronic acid (17h)

Prepared in analogy to **17c**: a solution of **80h** (84 mg, 0.150 mmol) in MeOH/*n*-hexane (1:1, 5.8 mL) was treated with isobutylboronic acid (61 mg, 0.598 mmol, 4 equiv) and 1 M HCl (375 μ L). Yield: 52 mg (81%, white solid).

^1H NMR (400 MHz, Methanol- d_4) δ 4.23 (dd, $J = 17.5, 1.7$ Hz, 1H), 4.18 (d, $J = 9.5$ Hz, 1H), 4.04 (d, $J = 8.3$ Hz, 1H), 3.98 (dd, $J = 17.6, 1.0$ Hz, 1H), 2.66 (q, $J = 6.9$ Hz, 1H), 2.28 – 2.13 (m, 1H), 1.98 (s, 3H), 1.89 – 1.76 (m, 2H), 1.72 – 1.50 (m, 6H), 1.41 – 1.27 (m, 2H), 1.26 – 1.17 (m, 1H), 1.12 (d, $J = 7.3$ Hz, 3H), 0.95 (d, $J = 6.8$ Hz, 3H), 0.92 (t, $J = 7.5$ Hz, 3H).

^{13}C NMR (101 MHz, Methanol- d_4) δ 176.3, 175.0, 174.6, 173.3, 60.1, 58.9, 43.1, 41.9 ($\underline{\text{CHB}}$ (broad)), 39.6, 37.2, 30.4, 30.2, 26.29, 26.27, 25.9, 22.3, 15.9, 15.7, 11.2.

HR-MS (ESI/TOF) calcd for $\text{C}_{19}\text{H}_{35}\text{BN}_4\text{O}_6\text{Na}$ [$\text{M}+\text{Na}$] $^+$ 449.2547, found 449.2549

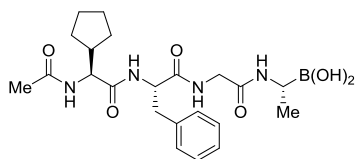


((2R,8S,11S)-11-cyclopentyl-8-isobutyl-4,7,10,13-tetra-oxo-3,6,9,12-tetraazatetradecan-2-yl)boronic acid (17i)

Prepared in analogy to **17c**: a solution of **80i** (97 mg, 0.173 mmol) in MeOH/*n*-hexane (1:1, 6.6 mL) was treated with isobutylboronic acid (71 mg, 0.697 mmol, 4 equiv) and 1 M HCl (425 μ L). Yield: 58 mg (79%, white solid).

^1H NMR (400 MHz, Methanol- d_4) δ 4.27 – 4.17 (m, 2H), 4.12 (d, $J = 9.3$ Hz, 1H), 3.97 (dd, $J = 17.6, 1.0$ Hz, 1H), 2.66 (q, $J = 7.0$ Hz, 1H), 2.20 (h, $J = 8.9$ Hz, 1H), 1.98 (s, 3H), 1.87 – 1.77 (m, 1H), 1.74 – 1.51 (m, 8H), 1.43 – 1.26 (m, 2H), 1.12 (d, $J = 7.2$ Hz, 3H), 0.97 (d, $J = 6.4$ Hz, 3H), 0.93 (d, $J = 6.4$ Hz, 3H).

^{13}C NMR (101 MHz, Methanol- d_4) δ 176.3, 175.4, 175.1, 173.5, 59.0, 53.9, 43.1, 41.9 (CHB (broad)), 40.9, 39.8, 30.4, 30.2, 26.2, 25.9, 25.8, 23.3, 22.3, 22.1, 15.9.
HR-MS (ESI/TOF) calcd for $\text{C}_{19}\text{H}_{35}\text{BN}_4\text{O}_6\text{Na}$ $[\text{M}+\text{Na}]^+$ 449.2547, found 449.2554



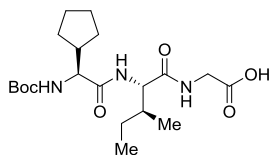
((2R,8S,11S)-8-benzyl-11-cyclopentyl-4,7,10,13-tetra-oxo-3,6,9,12-tetraazatetradecan-2-yl)boronic acid (17j)

Prepared in analogy to **17c**: a solution of **80j** (102 mg, 0.172 mmol) in MeOH/*n*-hexane (1:1, 6.6 mL) was treated with isobutylboronic acid (70 mg, 0.687 mmol, 4 equiv) and 1 M HCl (425 μL). Yield: 59 mg (75%, white solid).

^1H NMR (400 MHz, Methanol- d_4) δ 7.32 – 7.16 (m, 5H), 4.46 (dd, $J = 8.4, 6.9$ Hz, 1H), 4.16 (dd, $J = 17.6, 1.8$ Hz, 1H), 4.06 (d, $J = 9.3$ Hz, 1H), 3.86 (dd, $J = 17.6, 1.0$ Hz, 1H), 3.16 (dd, $J = 13.7, 6.8$ Hz, 1H), 3.00 (dd, $J = 13.8, 8.5$ Hz, 1H), 2.66 (q, $J = 7.0$ Hz, 1H), 2.09 (h, $J = 9.3$ Hz, 1H), 1.96 (s, 3H), 1.81 – 1.71 (m, 1H), 1.66 – 1.46 (m, 5H), 1.29 – 1.20 (m, 2H), 1.11 (d, $J = 7.2$ Hz, 3H).

^{13}C NMR (101 MHz, Methanol- d_4) δ 176.2, 174.8, 174.2, 173.6, 138.2, 130.3, 129.5, 127.9, 59.2, 56.8, 43.0, 41.8 (CHB (broad)), 39.7, 37.8, 30.3, 30.1, 26.1, 25.8, 22.4, 16.0
HR-MS (ESI/TOF) calcd for $\text{C}_{19}\text{H}_{35}\text{BN}_4\text{O}_6\text{Na}$ $[\text{M}+\text{Na}]^+$ 483.2391, found 483.2398

3.3 Synthesis of the peptidic boronic acids with a modified P5 position



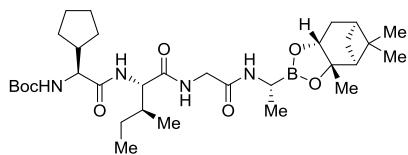
((S)-2-((*tert*-butoxycarbonyl)amino)-2-cyclopentylacetyl)-L-isoleucylglycine (81)

Prepared in analogues way as **S2c**: starting material **78h** (830 mg, 1.88 mmol) and LiOH (450 mg, 18.8 mmol) added to the mixture THF:H₂O (20:1, 52.5 mL). Yield: 769 mg (99%, amorphous solid).

^1H NMR (400 MHz, Methanol- d_4) δ 4.29 (d, $J = 7.7$ Hz, 1H), 3.98 (d, $J = 17.8$ Hz, 1H), 3.91 – 3.79 (m, 2H), 2.24 – 2.10 (m, 1H), 1.92 – 1.73 (m, 2H), 1.70 – 1.51 (m, 6H), 1.44 (s, 9H), 1.38 – 1.26 (m, 2H), 1.26 – 1.14 (m, 1H), 0.97 (d, $J = 6.8$ Hz, 3H), 0.90 (t, $J = 7.4$ Hz, 3H).

^{13}C NMR (101 MHz, Methanol- d_4) δ 174.8, 173.8, 172.5, 158.0, 80.6, 60.3, 58.8, 43.1, 41.7, 38.4, 30.3, 28.7, 26.3, 26.0, 25.7, 15.8, 11.4.

HR-MS (ESI/TOF) calcd for $\text{C}_{20}\text{H}_{35}\text{N}_3\text{O}_6\text{Na}$ $[\text{M}+\text{Na}]^+$ 436.2424, found 436.2425



***tert*-Butyl ((S)-1-cyclopentyl-2-(((2S,3S)-3-methyl-1-oxo-1-((2-oxo-2-(((R)-1-((3a*S*,4*S*,6*S*,7a*R*)-3a,5,5-trimethylhexahydro-4,6-methanobenzo[d][1,3,2]dioxaborol-2-yl)ethyl)amino)ethyl)amino)-pentan-2-yl)amino)-2-oxoethyl) carbamate (82)**

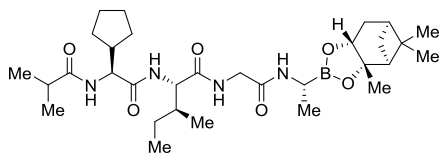
Under argon atmosphere **81** (770 mg, 1.86 mmol) was mixed with **54a** (580 mg, 2.23 mmol, 1.2 equiv) and DMAP (68 mg, 0.56 mmol, 0.3 equiv) in 10 ml of anhydrous CHCl_3 at 20–25°C. The white suspension was cooled to -15°C and then *N*-

methylmorpholine (820 μ l, 7.46 mmol, 4 equiv) was added while the internal temperature was kept at -10°C . T_3P reagent (1.7 mL, 2.84 mmol, 1.50 equiv) was added at the same temperature. The reaction mixture was allowed to warm up from $-10 - -15^{\circ}\text{C}$ to room temperature overnight. It was then diluted with CHCl_3 and equal amount of 5% KHSO_4 and extracted. Organic phase was extracted once more with 5% KHSO_4 . Combined water phase was back extracted with CHCl_3 . Organic phase was washed with brine and dried over Na_2SO_4 , filtered and concentrated under reduced pressure. Crude mixture was purified by flash chromatography on silica gel eluting with 0–5% MeOH in EtOAc to provide **82** (842 mg, 73%) as a solid compound.

^1H NMR (400 MHz, Methanol- d_4) δ 4.22 – 4.13 (m, 2H), 4.08 (d, $J = 8.0$ Hz, 1H), 3.99 – 3.84 (m, 2H), 2.65 (q, $J = 7.3$ Hz, 1H), 2.38 – 2.29 (m, 1H), 2.23 – 2.08 (m, 2H), 1.95 (t, $J = 5.5$ Hz, 1H), 1.89 – 1.72 (m, 4H), 1.71 – 1.50 (m, 6H), 1.47 – 1.40 (m, 10H), 1.35 (s, 3H), 1.34 – 1.17 (m, 6H), 1.16 (d, $J = 7.3$ Hz, 3H), 0.98 – 0.88 (m, 6H), 0.87 (s, 3H).

^{13}C NMR (101 MHz, Methanol- d_4) δ 175.7, 175.5, 174.3, 158.0, 84.3, 80.6, 77.3, 59.9, 53.6, 43.2, 41.3, 40.0 (overlaps with $\underline{\text{CHB}}$ (broad)), 39.2, 37.7, 37.5, 30.2, 29.6, 28.7, 27.8, 27.5, 26.3, 26.2, 26.0, 24.5, 16.4, 15.8, 11.2.

HR-MS (ESI/TOF) calcd for $\text{C}_{32}\text{H}_{56}\text{BN}_4\text{O}_7$ $[\text{M}+\text{H}]^+$ 619.4242, found 619.4258



(2S,3S)-2-((S)-2-cyclopentyl-2-isobutyramido-acetamido)-3-methyl-N-(2-oxo-2-(((R)-1-((3aS,4S,6S,7aR)-3a,5,5-trimethylhexahydro-4,6-methanobenzo[d][1,3,2]-dioxaborol-2-yl)-ethyl)amino)ethyl)-pentanamide (83a)

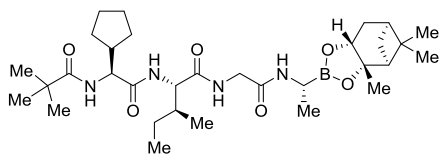
pentanamide (83a)

Starting material **82** (103 mg, 0.17 mmol, 1.0 equiv) in CHCl_3 (2 mL) was treated with 4 M HCl in dioxane (170 μ L, 4 equiv) until full deprotection of the protecting group. After solvent evaporation the crude mixture was utilized in the next step without purification. The residue (0.17 mmol based on a theoretical yield of a 100%) under argon atmosphere was dissolved in dry CHCl_3 (5 mL), isobutyric anhydride (41 μ L, 0.25 mmol, 1.5 equiv) and DIPEA (58 μ L, 0.33 mmol, 2.0 equiv) were added and mixture was stirred for 2 h at room temperature, then washed with 1 M HCl (5 mL), with sat. NaHCO_3 (5 mL), and brine (10 mL). Organic phase was dried over Na_2SO_4 , filtered and evaporated in vacuo. The residue was purified by flash chromatography on silica gel eluting with 0–5% MeOH in EtOAc to provide **83a** (73 mg, 75%) as an amorphous solid.

^1H NMR (400 MHz, Methanol- d_4) δ 4.23 – 4.13 (m, 3H), 4.03 (d, $J = 8.1$ Hz, 1H), 3.94 (dd, $J = 17.5, 1.0$ Hz, 1H), 2.64 (q, $J = 7.2$ Hz, 1H), 2.53 (hept, $J = 6.9$ Hz, 1H), 2.40 – 2.28 (m, 1H), 2.30 – 2.17 (m, 1H), 2.18 – 2.08 (m, 1H), 1.94 (t, $J = 5.5$ Hz, 1H), 1.89 – 1.75 (m, 4H), 1.72 – 1.52 (m, 6H), 1.44 (d, $J = 10.3$ Hz, 1H), 1.35 (s, 3H), 1.33 – 1.19 (m, 6H), 1.17 (d, $J = 7.5$ Hz, 3H), 1.11 (d, $J = 6.9$ Hz, 3H), 1.09 (d, $J = 6.8$ Hz, 3H), 0.94 (d, $J = 6.8$ Hz, 3H), 0.92 (t, $J = 7.4$ Hz, 3H), 0.87 (s, 3H).

^{13}C NMR (101 MHz, Methanol- d_4) δ 180.1, 175.8, 174.9, 174.3, 84.3, 77.3, 60.1, 58.5, 53.6, 42.9, 41.4, 40.0, 39.8 ($\underline{\text{CHB}}$ (broad)), 39.2, 37.7, 37.3, 35.9, 30.4, 30.3, 29.6, 27.8, 27.5, 26.3, 26.3, 26.0, 24.5, 20.1, 19.7, 16.4, 15.8, 11.2.

HR-MS (ESI/TOF) calcd for $\text{C}_{31}\text{H}_{54}\text{BN}_4\text{O}_6$ $[\text{M}+\text{H}]^+$ 589.4136, found 589.4151



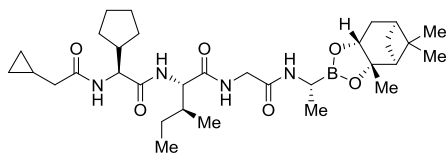
(2*S*,3*S*)-2-((*S*)-2-cyclopentyl-2-pivalamidoacet-amido)-3-methyl-*N*-(2-oxo-2-(((*R*)-1-((3*aS*,4*S*,6*S*,7*aR*)-3*a*,5,5-trimethylhexahydro-4,6-methanobenzo[*d*][1,3,2]dioxaborol-2-yl)-ethyl)amino)ethyl)pentanamide (83b)

Prepared in analogy to **83a**: starting material **82** (92 mg, 0.15 mmol, 1.0 equiv) in CHCl₃ (2 mL) was treated with 4 M HCl in dioxane (150 μL, 4 equiv). Acylation: trimethyl acetic anhydride (45 μL, 0.22 mmol, 1.5 equiv) and DIPEA (52 μL, 0.30 mmol, 2.0 equiv) in dry CHCl₃ (5 mL). Yield: 60 mg (67%, amorphous solid).

¹H NMR (400 MHz, Methanol-*d*₄) δ 4.28 – 4.13 (m, 3H), 4.05 (d, *J* = 8.1 Hz, 1H), 3.95 (dd, *J* = 17.4, 1.0 Hz, 1H), 2.65 (q, *J* = 7.2 Hz, 1H), 2.38 – 2.25 (m, 2H), 2.18 – 2.09 (m, 1H), 1.95 (t, *J* = 5.5 Hz, 1H), 1.89 – 1.73 (m, 4H), 1.72 – 1.52 (m, 6H), 1.44 (d, *J* = 10.4 Hz, 1H), 1.36 (s, 3H), 1.34 – 1.21 (m, 6H), 1.20 (s, 9H), 1.17 (d, *J* = 7.3 Hz, 3H), 0.96 – 0.89 (m, 6H), 0.87 (s, 3H).

¹³C NMR (101 MHz, Methanol-*d*₄) δ 181.1, 175.6, 174.9, 174.2, 84.3, 77.3, 60.0, 58.5, 53.6, 43.1, 41.4, 40.0, 39.8 (overlaps with CHB (broad)), 39.2, 37.7, 37.4, 30.4, 30.3, 29.6, 27.8, 27.5, 26.3, 26.24, 26.0, 24.6, 16.4, 15.8, 11.2.

HR-MS (ESI/TOF) calcd for C₃₂H₅₆BN₄O₆ [M+H]⁺ 603.4293, found 602.4308



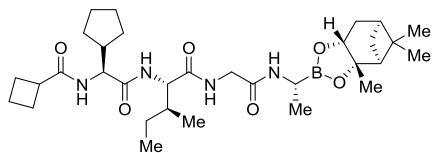
(2*S*,3*S*)-2-((*S*)-2-cyclopentyl-2-(2-cyclopropyl-acetamido)acetamido)-3-methyl-*N*-(2-oxo-2-(((*R*)-1-((3*aS*,4*S*,6*S*,7*aR*)-3*a*,5,5-trimethylhexahydro-4,6-methanobenzo[*d*][1,3,2]-dioxaborol-2-yl)ethyl)amino)ethyl)pentanamide (83c)

Starting material **82** (105 mg, 0.17 mmol, 1.0 equiv) in CHCl₃ (2 mL) was treated with 4 M HCl in dioxane (170 μL, 4 equiv) until full deprotection of the protecting group. After solvent evaporation the crude mixture was utilized in the next step without purification. The residue (0.17 mmol based on a theoretical yield of a 100 %) under argon atmosphere was dissolved in dry CHCl₃ (5 mL), cyclopropane acetic acid (20 μL, 0.20 mmol, 1.2 equiv), EDC·HCl (39 mg, 0.20 mmol, 1.2 equiv), HOBT (26 mg, 0.19 mmol, 1.1 equiv) and DIPEA (90 μL, 0.51 mmol, 3.0 equiv) were added and mixture was stirred 3 h at room temperature, then washed with 1 M HCl (5 mL) and brine (5 mL). Organic phase was dried over Na₂SO₄, filtered and evaporated in vacuo. The residue was purified by flash chromatography on silica gel eluting with 0–5% MeOH in EtOAc to provide **83c** (75 mg, 74%) as an amorphous solid.

¹H NMR (400 MHz, Methanol-*d*₄) δ 4.26 – 4.13 (m, 3H), 4.03 (d, *J* = 8.2 Hz, 1H), 3.94 (dd, *J* = 17.5, 1.0 Hz, 1H), 2.64 (q, *J* = 7.2 Hz, 1H), 2.38 – 2.29 (m, 1H), 2.30 – 2.17 (m, 1H), 2.18 – 2.08 (m, 3H), 1.95 (t, *J* = 5.6 Hz, 1H), 1.89 – 1.75 (m, 4H), 1.72 – 1.53 (m, 6H), 1.44 (d, *J* = 10.3 Hz, 1H), 1.35 (s, 3H), 1.34 – 1.20 (m, 6H), 1.17 (d, *J* = 7.3 Hz, 3H), 1.07 – 0.98 (m, 1H), 0.94 (d, *J* = 6.8 Hz, 3H), 0.92 (t, *J* = 7.5 Hz, 3H), 0.87 (s, 3H), 0.55 – 0.49 (m, 2H), 0.22 – 0.17 (m, 2H).

^{13}C NMR (101 MHz, Methanol- d_4) δ 175.8, 175.6, 174.9, 174.4, 84.3, 77.3, 60.1, 58.4, 53.6, 43.1, 41.6, 41.4, 40.0, 39.7 (CHB (broad)), 39.2, 37.7, 37.3, 30.3, 30.2, 29.6, 27.8, 27.5, 26.3, 26.0, 24.6, 16.4, 15.8, 11.2, 8.7, 4.8.

HR-MS (ESI/TOF) calcd for $\text{C}_{32}\text{H}_{54}\text{BN}_4\text{O}_6$ $[\text{M}+\text{H}]^+$ 601.4136, found 601.4156



***N*-((*S*)-1-cyclopentyl-2-(((2*S*,3*S*)-3-methyl-1-oxo-1-((2-oxo-2-(((*R*)-1-((3*aS*,4*S*,6*S*,7*aR*)-3*a*,5,5-trimethylhexahydro-4,6-methanobenzo[*d*][1,3,2]-dioxaborol-2-yl)ethyl)amino)ethyl)amino)-pentan-2-yl)amino)-2-**

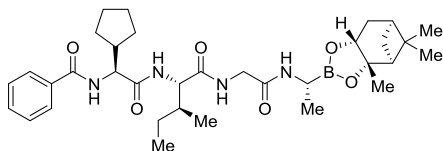
oxoethyl)cyclobutane carboxamide (83d)

Prepared in analogues way as **83c**: starting material **82** (113 mg, 0.183 mmol) and 4 M HCl in dioxane (180 μL) in CHCl_3 (2 mL). Coupling: cyclobutanecarboxylic acid (20 μL , 0.21 mmol), EDC·HCl (42 mg, 0.22 mmol), HOBT (28 mg, 0.21 mmol) and DIPEA (63 μL , 0.37 mmol) in CHCl_3 (5 mL). Yield: 60 mg (55%, amorphous solid).

^1H NMR (400 MHz, Methanol- d_4) δ 4.23 – 4.13 (m, 3H), 4.03 (d, $J = 8.2$ Hz, 1H), 3.94 (dd, $J = 17.6, 1.0$ Hz, 1H), 3.17 (pd, $J = 8.4, 1.1$ Hz, 1H), 2.64 (q, $J = 7.3$ Hz, 1H), 2.38 – 2.29 (m, 1H), 2.27 – 2.18 (m, 3H), 2.18 – 2.08 (m, 3H), 2.05 – 1.91 (m, 2H), 1.90 – 1.73 (m, 5H), 1.71 – 1.50 (m, 6H), 1.44 (d, $J = 10.3$ Hz, 1H), 1.35 (s, 3H), 1.33 – 1.19 (m, 6H), 1.16 (d, $J = 7.3$ Hz, 3H), 0.94 (d, $J = 6.8$ Hz, 3H), 0.92 (t, $J = 7.5$ Hz, 3H), 0.87 (s, 3H).

^{13}C NMR (101 MHz, Methanol- d_4) δ 177.7, 175.8, 175.0, 174.3, 84.3, 77.3, 60.1, 58.6, 53.6, 43.0, 41.4, 40.5, 40.0, 39.8 (CHB (broad)), 39.2, 37.7, 37.3, 30.4, 30.3, 29.6, 27.8, 27.5, 26.3, 26.2, 26.04, 25.96, 24.5, 19.1, 16.4, 15.8, 11.2.

HR-MS (ESI/TOF) calcd for $\text{C}_{32}\text{H}_{54}\text{BN}_4\text{O}_6$ $[\text{M}+\text{H}]^+$ 601.4136, found 601.4141



***N*-((*S*)-1-cyclopentyl-2-(((2*S*,3*S*)-3-methyl-1-oxo-1-((2-oxo-2-(((*R*)-1-((3*aS*,4*S*,6*S*,7*aR*)-3*a*,5,5-trimethylhexahydro-4,6-methanobenzo[*d*]-[1,3,2]dioxaborol-2-yl)ethyl)amino)ethyl)amino)-pentan-2-**

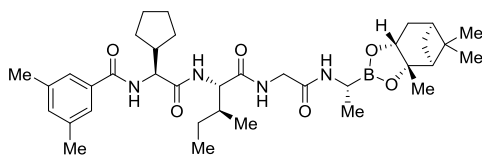
yl)amino)-2-oxoethyl)benzamide (83e)

Prepared in analogues way as **83c**: starting material **82** (100 mg, 0.162 mmol) and 4 M HCl in dioxane (160 μL) in CHCl_3 (3 mL). Coupling: benzoic acid (20 mg, 0.164 mmol, 1 equiv), EDC·HCl (37 mg, 0.193 mmol), HOBT (24 mg, 0.178 mmol) and DIPEA (84 μL , 0.489 mmol) in CHCl_3 (5 mL). Yield: 62 mg (62%, amorphous solid).

^1H NMR (400 MHz, Methanol- d_4) δ 7.84 – 7.79 (m, 2H), 7.58 – 7.52 (m, 1H), 7.50 – 7.44 (m, 2H), 4.41 (d, $J = 10.0$ Hz, 1H), 4.20 (dd, $J = 17.5, 1.6$ Hz, 1H), 4.15 (dd, $J = 8.6, 2.3$ Hz, 1H), 4.07 (d, $J = 8.2$ Hz, 1H), 3.96 (dd, $J = 17.5, 1.0$ Hz, 1H), 2.67 (q, $J = 7.3$ Hz, 1H), 2.47 – 2.27 (m, 2H), 2.17 – 2.09 (m, 1H), 1.95 (t, $J = 5.5$ Hz, 1H), 1.92 – 1.55 (m, 10H), 1.47 – 1.34 (m, 6H), 1.28 (s, 3H), 1.27 – 1.19 (m, 1H), 1.17 (d, $J = 7.4$ Hz, 3H), 0.98 – 0.89 (m, 6H), 0.87 (s, 3H).

^{13}C NMR (101 MHz, Methanol- d_4) δ 175.8, 174.9, 174.3, 170.5, 135.4, 132.8, 129.6, 128.5, 84.3, 77.3, 60.2, 59.6, 53.6, 42.9, 41.4, 40.0, 39.8 (CHB (broad)), 39.2, 37.7, 37.3, 30.8, 30.4, 29.6, 27.8, 27.5, 26.4, 26.3, 26.0, 24.5, 16.4, 15.8, 11.2.

HR-MS (ESI/TOF) calcd for C₃₄H₅₂BN₄O₆ [M+H]⁺ 623.3980, found 623.4008



N-((*S*)-1-cyclopentyl-2-(((2*S*,3*S*)-3-methyl-1-oxo-1-((2-oxo-2-(((*R*)-1-(3*aS*,4*S*,6*S*,7*aR*)-3*a*,5,5-trimethylhexahydro-4,6-methano-benzo[*d*][1,3,2]-dioxaborol-2-yl)ethyl)amino)-

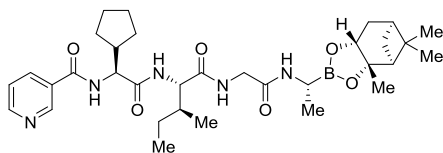
ethyl)amino)pentan-2-yl)amino)-2-oxoethyl)-3,5-dimethylbenzamide (**83f**)

Prepared in analogues way as **83c**: starting material **82** (100 mg, 0.162 mmol) and 4 M HCl in dioxane (160 μ L) in CHCl₃ (3 mL). Coupling: 3,5-dimethylbenzoic acid (25 mg, 0.166 mmol), EDC·HCl (37 mg, 0.193 mmol), HOBT (24 mg, 0.178 mmol) and DIPEA (84 μ L, 0.489 mmol) in CHCl₃ (5 mL). Yield: 57 mg (54%, amorphous solid).

¹H NMR (400 MHz, Methanol-*d*₄) δ 7.45 – 7.40 (m, 2H), 7.22 – 7.17 (m, 1H), 4.40 (d, *J* = 10.0 Hz, 1H), 4.20 (dd, *J* = 17.5, 1.6 Hz, 1H), 4.15 (dd, *J* = 8.6, 2.3 Hz, 1H), 4.07 (d, *J* = 8.2 Hz, 1H), 3.95 (dd, *J* = 17.5, 1.0 Hz, 1H), 2.67 (q, *J* = 7.3 Hz, 1H), 2.44 – 2.28 (m, 8H), 2.17 – 2.09 (m, 1H), 1.94 (t, *J* = 5.6 Hz, 1H), 1.90 – 1.56 (m, 10H), 1.46 – 1.33 (m, 6H), 1.28 (s, 3H), 1.26 – 1.19 (m, 1H), 1.17 (d, *J* = 7.3 Hz, 3H), 0.97 – 0.90 (m, 6H), 0.87 (s, 3H).

¹³C NMR (101 MHz, Methanol-*d*₄) δ 175.7, 175.0, 174.3, 170.8, 139.4, 135.4, 134.3, 126.2, 84.4, 77.3, 60.2, 59.4, 53.6, 43.0, 41.3, 40.0, 39.8 (CHB (broad)), 39.2, 37.7, 37.3, 30.7, 30.4, 29.6, 27.8, 27.5, 26.4, 26.3, 26.0, 24.5, 21.3, 16.4, 15.8, 11.2.

HR-MS (ESI/TOF) calcd for C₃₆H₅₆BN₄O₆ [M+H]⁺ 651.4293, found 651.4313



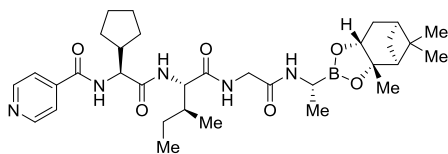
N-((*S*)-1-cyclopentyl-2-(((2*S*,3*S*)-3-methyl-1-oxo-1-((2-oxo-2-(((*R*)-1-(3*aS*,4*S*,6*S*,7*aR*)-3*a*,5,5-trimethylhexahydro-4,6-methano-benzo[*d*][1,3,2]-dioxaborol-2-yl)ethyl)amino)ethyl)amino)pentan-2-yl)amino)-2-oxoethyl)nicotinamide (**83g**)

Prepared in analogues way as **83c**: starting material **82** (103 mg, 0.167 mmol) and 4 M HCl in dioxane (170 μ L) in CHCl₃ (2 mL). Coupling: nicotinic acid (21 mg, 0.171 mmol), EDC·HCl (38 mg, 0.198 mmol), HOBT (25 mg, 0.185 mmol) and DIPEA (60 μ L, 0.347 mmol) in CHCl₃ (5 mL). Yield: 67 mg (64%, amorphous solid).

¹H NMR (400 MHz, Methanol-*d*₄) δ 9.03 – 8.93 (m, 2H), 8.69 (dd, *J* = 4.9, 1.7 Hz, 1H), 8.24 (ddd, *J* = 8.0, 2.3, 1.5 Hz, 1H), 7.55 (ddd, *J* = 7.9, 4.9, 0.8 Hz, 1H), 4.41 (d, *J* = 10.0 Hz, 1H), 4.21 (dd, *J* = 17.5, 1.7 Hz, 1H), 4.15 (dd, *J* = 8.6, 2.3 Hz, 1H), 4.07 (d, *J* = 8.5 Hz, 1H), 3.96 (dd, *J* = 17.5, 1.0 Hz, 1H), 2.66 (q, *J* = 7.3 Hz, 1H), 2.46 – 2.29 (m, 2H), 2.18 – 2.07 (m, 1H), 1.94 (t, *J* = 5.5 Hz, 1H), 1.91 – 1.55 (m, 5H), 1.48 – 1.34 (m, 5H), 1.32 – 1.18 (m, 4H), 1.17 (d, *J* = 7.3 Hz, 3H), 0.97 – 0.89 (m, 6H), 0.87 (s, 3H).

¹³C NMR (101 MHz, Methanol-*d*₄) δ 175.8, 174.7, 174.3, 168.0, 152.7, 149.3, 137.3, 131.9, 125.1, 84.3, 77.3, 60.2, 59.7, 53.6, 42.9, 41.3, 40.0 (overlaps with CHB (broad)), 39.2, 37.7, 37.3, 30.9, 30.4, 29.6, 27.8, 27.5, 26.3, 26.3, 25.9, 24.5, 16.4, 15.8, 11.2.

HR-MS (ESI/TOF) calcd for C₃₂H₅₁BN₅O₆ [M+H]⁺ 624.3932, found 624.3920



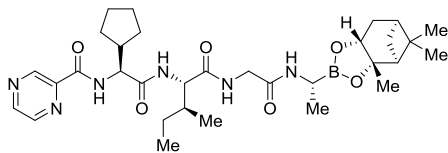
***N*-((*S*)-1-cyclopentyl-2-(((2*S*,3*S*)-3-methyl-1-oxo-1-((2-oxo-2-(((*R*)-1-((3*aS*,4*S*,6*S*,7*aR*)-3*a*,5,5-trimethylhexahydro-4,6-methanobenzo[*d*][1,3,2]-dioxaborol-2-yl)ethyl)amino)ethyl)amino) pentan-2-yl)amino)-2-oxoethyl)isonicotinamide (83h)**

Prepared in analogues way as **83c**: starting material **82** (103 mg, 0.167 mmol) and 4 M HCl in dioxane (170 μ L) in CHCl₃ (2 mL). Coupling: isonicotinic acid (21 mg, 0.171 mmol), EDC·HCl (38 mg, 0.198 mmol), HOBt (25 mg, 0.185 mmol) and DIPEA (60 μ L, 0.347 mmol) in CHCl₃ (5 mL). Yield: 72 mg (69%, amorphous solid).

¹H NMR (400 MHz, Methanol-*d*₄) δ 8.75 – 8.65 (m, 2H), 7.81 – 7.75 (m, 2H), 4.41 (d, *J* = 10.1 Hz, 1H), 4.21 (dd, *J* = 17.5, 1.6 Hz, 1H), 4.15 (dd, *J* = 8.6, 2.4 Hz, 1H), 4.07 (d, *J* = 8.3 Hz, 1H), 3.96 (dd, *J* = 17.4, 1.0 Hz, 1H), 2.66 (q, *J* = 7.2 Hz, 1H), 2.45 – 2.29 (m, 2H), 2.17 – 2.08 (m, 1H), 1.95 (t, *J* = 5.5 Hz, 1H), 1.92 – 1.54 (m, 10H), 1.40 (d, *J* = 36.8 Hz, 6H), 1.28 (s, 3H), 1.27 – 1.17 (m, 1H), 1.17 (d, *J* = 7.3 Hz, 3H), 0.97 – 0.90 (m, 6H), 0.87 (s, 3H).

¹³C NMR (101 MHz, Methanol-*d*₄) δ 175.7, 174.6, 174.3, 168.0, 150.9, 143.7, 123.1, 84.4, 77.3, 60.2, 59.8, 53.6, 42.9, 41.3, 40.0, 39.7 (C_{HB} (broad)), 39.2, 37.7, 37.3, 30.8, 30.3, 29.6, 27.8, 27.5, 26.34, 26.32, 25.9, 24.5, 16.4, 15.8, 11.2.

HR-MS (ESI/TOF) calcd for C₃₂H₅₁BN₅O₆ [M+H]⁺ 624.3932, found 624.3929



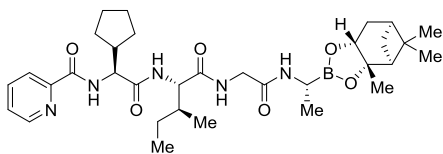
***N*-((*S*)-1-cyclopentyl-2-(((2*S*,3*S*)-3-methyl-1-oxo-1-((2-oxo-2-(((*R*)-1-((3*aS*,4*S*,6*S*,7*aR*)-3*a*,5,5-trimethylhexahydro-4,6-methanobenzo[*d*][1,3,2]-dioxaborol-2-yl)ethyl)amino)ethyl)amino) pentan-2-yl)amino)-2-oxoethyl)pyrazine-2-carboxamide (83i)**

Prepared in analogues way as **83c**: starting material **82** (100 mg, 0.162 mmol) and 4 M HCl in dioxane (160 μ L) in CHCl₃ (2 mL). Coupling: pyrazine-2-carboxylic acid (22 mg, 0.177 mmol), EDC·HCl (38 mg, 0.198 mmol), HOBt (24 mg, 0.178 mmol) and DIPEA (60 μ L, 0.347 mmol) in CHCl₃ (5 mL). Yield: 82 mg (81%, amorphous solid).

¹H NMR (400 MHz, Methanol-*d*₄) δ 9.25 (d, *J* = 1.4 Hz, 1H), 8.81 (d, *J* = 2.5 Hz, 1H), 8.69 (dd, *J* = 2.5, 1.5 Hz, 1H), 4.60 (d, *J* = 8.3 Hz, 1H), 4.23 (dd, *J* = 17.5, 1.5 Hz, 1H), 4.16 (dd, *J* = 8.6, 2.3 Hz, 1H), 4.04 (d, *J* = 8.6 Hz, 1H), 3.93 (dd, *J* = 17.6, 0.9 Hz, 1H), 2.68 (q, *J* = 7.2 Hz, 1H), 2.46 – 2.29 (m, 2H), 2.18 – 2.10 (m, 1H), 1.95 (t, *J* = 5.5 Hz, 1H), 1.89 – 1.73 (m, 5H), 1.70 – 1.54 (m, 5H), 1.49 – 1.33 (m, 6H), 1.28 (s, 3H), 1.26 – 1.17 (m, 4H), 0.96 – 0.89 (m, 6H), 0.87 (s, 3H).

¹³C NMR (101 MHz, Methanol-*d*₄) δ 175.7, 174.34, 174.28, 164.8, 148.9, 145.8, 144.8, 84.4, 77.3, 60.4, 57.8, 53.6, 44.2, 41.3, 40.1, 39.6 (C_{HB} (broad)), 39.2, 37.6, 37.1, 30.2, 29.8, 29.6, 27.8, 27.5, 26.5, 26.3, 26.0, 24.5, 16.3, 15.7, 11.2.

HR-MS (ESI/TOF) calcd for C₃₂H₅₀BN₆O₆ [M+H]⁺ 625.3885, found 625.3895



N-((*S*)-1-cyclopentyl-2-(((2*S*,3*S*)-3-methyl-1-oxo-1-((2-oxo-2-(((*R*)-1-((3*aS*,4*S*,6*S*,7*aR*)-3*a*,5,5-trimethylhexahydro-4,6-methanobenzo[*d*][1,3,2]-dioxaborol-2-yl)ethyl)-amino)ethyl)amino)pentan-2-yl)amino)-2-

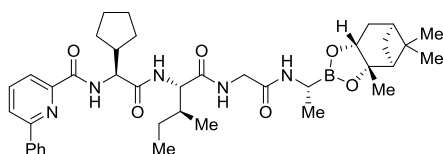
oxoethyl)picolinamide (83j)

Prepared in analogues way as **83c**: starting material **82** (106 mg, 0.171 mmol) and 4 M HCl in dioxane (170 μ L) in CHCl₃ (2 mL). Coupling: 2-picolinic acid (21 mg, 0.171 mmol), EDC·HCl (40 mg, 0.209 mmol), HOBt (26 mg, 0.192 mmol) and DIPEA (60 μ L, 0.347 mmol) in CHCl₃ (5 mL). Yield: 90 mg (84%, amorphous solid).

¹H NMR (400 MHz, Methanol-*d*₄) δ 8.64 (ddd, *J* = 4.8, 1.8, 1.0 Hz, 1H), 8.11 (dt, *J* = 7.9, 1.2 Hz, 1H), 7.97 (td, *J* = 7.7, 1.7 Hz, 1H), 7.57 (ddd, *J* = 7.6, 4.8, 1.3 Hz, 1H), 4.59 (d, *J* = 8.1 Hz, 1H), 4.23 (dd, *J* = 17.5, 1.7 Hz, 1H), 4.16 (dd, *J* = 8.6, 2.3 Hz, 1H), 4.03 (d, *J* = 8.5 Hz, 1H), 3.93 (dd, *J* = 17.6, 0.9 Hz, 1H), 2.69 (q, *J* = 7.5 Hz, 1H), 2.44 – 2.28 (m, 2H), 2.18 – 2.09 (m, 1H), 1.95 (t, *J* = 5.5 Hz, 1H), 1.89 – 1.71 (m, 5H), 1.70 – 1.54 (m, 5H), 1.47 – 1.33 (m, 6H), 1.28 (s, 3H), 1.25 – 1.16 (m, 4H), 0.97 – 0.89 (m, 6H), 0.87 (s, 3H).

¹³C NMR (101 MHz, Methanol-*d*₄) δ 175.7, 174.6, 174.3, 166.1, 150.5, 149.9, 138.9, 128.0, 123.2, 84.4, 77.3, 60.4, 57.6, 53.6, 41.3, 40.1, 39.6 (CHB (broad)), 39.2, 37.7, 37.1, 30.2, 29.7, 29.6, 27.8, 27.5, 26.5, 26.3, 26.0, 24.5, 16.3, 15.7, 11.2.

HR-MS (ESI/TOF) calcd for C₃₂H₅₁BN₅O₆ [M+H]⁺ 624.3932, found 624.3952



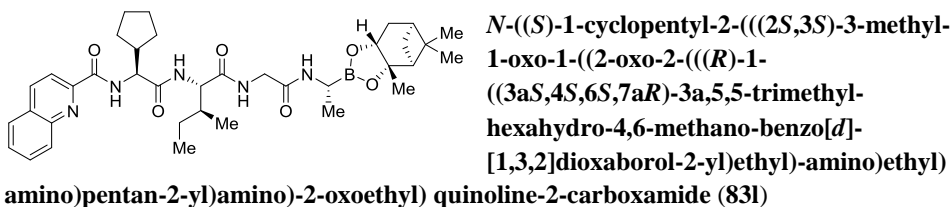
N-((*S*)-1-cyclopentyl-2-(((2*S*,3*S*)-3-methyl-1-oxo-1-((2-oxo-2-(((*R*)-1-((3*aS*,4*S*,6*S*,7*aR*)-3*a*,5,5-trimethylhexahydro-4,6-methanobenzo[*d*][1,3,2]-dioxaborol-2-yl)ethyl)-amino)ethyl)amino)pentan-2-yl)amino)-2-oxoethyl)-6-phenylpicolinamide (83k)

Prepared in analogues way as **83c**: starting material **82** (103 mg, 0.167 mmol) and 4 M HCl in dioxane (170 μ L) in CHCl₃ (2 mL). Coupling: 6-phenylpyridine-2-carboxylic acid (34 mg, 0.171 mmol), EDC·HCl (38 mg, 0.198 mmol), HOBt (25 mg, 0.185 mmol) and DIPEA (60 μ L, 0.347 mmol) in CHCl₃ (5 mL). Yield: 74 mg (64%, amorphous solid).

¹H NMR (400 MHz, Methanol-*d*₄) δ 8.13 – 8.00 (m, 5H), 7.54 – 7.42 (m, 3H), 4.70 (d, *J* = 7.4 Hz, 1H), 4.28 (dd, *J* = 17.6, 1.7 Hz, 1H), 4.15 (dd, *J* = 8.6, 2.3 Hz, 1H), 4.02 (d, *J* = 8.5 Hz, 1H), 3.91 (dd, *J* = 17.6, 0.8 Hz, 1H), 2.69 (q, *J* = 7.2 Hz, 1H), 2.44 (h, *J* = 8.7 Hz, 1H), 2.36 – 2.28 (m, 1H), 2.18 – 2.09 (m, 1H), 1.94 (t, *J* = 5.5 Hz, 1H), 1.88 – 1.74 (m, 5H), 1.71 – 1.57 (m, 5H), 1.52 – 1.41 (m, 3H), 1.35 (s, 3H), 1.27 (s, 3H), 1.26 – 1.20 (m, 1H), 1.14 (d, *J* = 7.3 Hz, 3H), 0.98 – 0.90 (m, 6H), 0.86 (s, 3H).

¹³C NMR (101 MHz, Methanol-*d*₄) δ 175.7, 174.7, 174.4, 166.1, 157.6, 150.2, 139.9, 139.4, 130.7, 130.0, 127.9, 124.6, 121.6, 84.4, 77.3, 60.6, 57.1, 53.6, 44.7, 41.3, 40.1, 39.6 (CHB (broad)), 39.2, 37.6, 36.9, 30.3, 29.6, 29.5, 27.8, 27.5, 26.6, 26.4, 26.1, 24.5, 16.5, 15.7, 11.2.

HR-MS (ESI/TOF) calcd for C₃₉H₅₅BN₅O₆ [M+H]⁺ 700.4245, found 700.4265

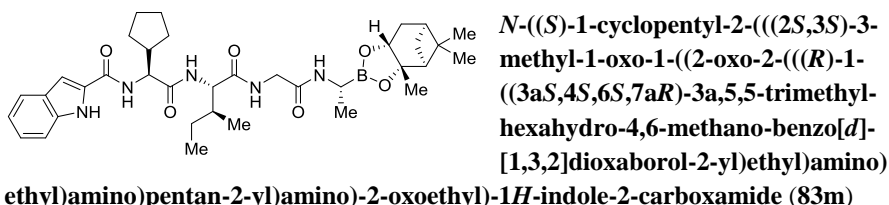


Prepared in analogous way as **83c**: starting material **82** (100 mg, 0.162 mmol) and 4 M HCl in dioxane (160 μ L) in CHCl₃ (3 mL). Coupling: quinaldic acid (28 mg, 0.162 mmol), EDC·HCl (37 mg, 0.193 mmol), HOBT (24 mg, 0.178 mmol) and DIPEA (84 μ L, 0.486 mmol) in CHCl₃ (5 mL). Yield: 69 mg (63%, amorphous solid).

¹H NMR (400 MHz, Methanol-*d*₄) δ 8.48 (dd, *J* = 8.6, 1.0 Hz, 1H), 8.20 (d, *J* = 8.5 Hz, 1H), 8.14 (dd, *J* = 8.6, 1.1 Hz, 1H), 8.00 (dd, *J* = 8.2, 1.7 Hz, 1H), 7.84 (ddd, *J* = 8.5, 6.8, 1.4 Hz, 1H), 7.69 (ddd, *J* = 8.2, 6.9, 1.3 Hz, 1H), 4.66 (d, *J* = 8.0 Hz, 1H), 4.25 (dd, *J* = 17.6, 1.7 Hz, 1H), 4.16 (dd, *J* = 8.6, 2.3 Hz, 1H), 4.05 (d, *J* = 8.5 Hz, 1H), 3.93 (dd, *J* = 17.6, 0.9 Hz, 1H), 2.73 (q, *J* = 7.2 Hz, 1H), 2.46 (h, *J* = 7.7 Hz, 1H), 2.37 – 2.29 (m, 1H), 2.18 – 2.10 (m, 1H), 1.94 (t, *J* = 5.5 Hz, 1H), 1.89 – 1.75 (m, 5H), 1.74 – 1.57 (m, 5H), 1.53 – 1.42 (m, 3H), 1.35 (s, 3H), 1.28 (s, 3H), 1.26 – 1.21 (m, 4H), 0.95 (d, *J* = 6.8 Hz, 3H), 0.92 (t, *J* = 7.4 Hz, 3H), 0.86 (s, 3H).

¹³C NMR (101 MHz, Methanol-*d*₄) δ 175.7, 174.6, 174.4, 166.2, 150.4, 148.0, 139.2, 131.7, 130.9, 130.7, 129.5, 129.1, 119.5, 84.4, 77.4, 60.5, 57.7, 53.6, 44.5, 41.3, 40.1, 39.6 (CHB (broad)), 39.2, 37.6, 37.1, 30.3, 29.8, 29.6, 27.8, 27.5, 26.5, 26.3, 26.1, 24.5, 16.4, 15.7, 11.2.

HR-MS (ESI/TOF) calcd for C₃₇H₅₃BN₅O₆ [M+H]⁺ 674.4089, found 674.4103



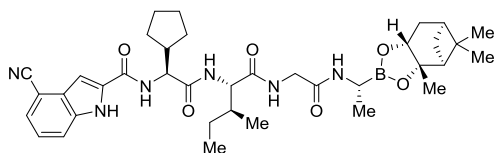
Prepared in analogous way as **83c**: starting material **82** (100 mg, 0.162 mmol) and 4 M HCl in dioxane (160 μ L) in CHCl₃ (3 mL). Coupling: 1*H*-indole-2-carboxylic acid (26 mg, 0.162 mmol), EDC·HCl (37 mg, 0.193 mmol), HOBT (24 mg, 0.178 mmol) and DIPEA (84 μ L, 0.486 mmol) in CHCl₃ (5 mL). Yield: 74 mg (69%, amorphous solid).

¹H NMR (400 MHz, Methanol-*d*₄) δ 7.61 (dt, *J* = 8.0, 1.1 Hz, 1H), 7.44 (dq, *J* = 8.3, 1.0 Hz, 1H), 7.22 (ddd, *J* = 8.2, 6.9, 1.2 Hz, 1H), 7.18 (d, *J* = 1.0 Hz, 1H), 7.06 (ddd, *J* = 8.0, 7.0, 1.0 Hz, 1H), 4.52 (d, *J* = 10.0 Hz, 1H), 4.21 (dd, *J* = 17.4, 1.5 Hz, 1H), 4.15 (dd, *J* = 8.6, 2.3 Hz, 1H), 4.11 (d, *J* = 8.1 Hz, 1H), 3.99 (dd, *J* = 17.4, 1.0 Hz, 1H), 2.69 (q, *J* = 7.2 Hz, 1H), 2.49 – 2.34 (m, 1H), 2.36 – 2.28 (m, 1H), 2.16 – 2.09 (m, 1H), 1.94 (t, *J* = 5.5 Hz, 1H), 1.91 – 1.55 (m, 10H), 1.48 – 1.38 (m, 3H), 1.35 (s, 3H), 1.28 (s, 3H), 1.23 – 1.16 (m, 4H), 0.94 (d, *J* = 6.8 Hz, 3H), 0.90 – 0.85 (m, 6H).

¹³C NMR (101 MHz, Methanol-*d*₄) δ 175.7, 175.0, 174.4, 163.9, 138.5, 131.6, 129.0, 125.2, 122.9, 121.2, 113.1, 105.2, 84.4, 77.4, 60.1, 59.0, 53.6, 43.1, 41.3, 40.1, 39.7 (CHB

(broad)), 39.2, 37.6, 37.4, 30.8, 30.4, 29.6, 27.8, 27.5, 26.4, 26.3, 26.0, 24.5, 16.4, 15.8, 11.3.

HR-MS (ESI/TOF) calcd for C₃₆H₅₃BN₅O₆ [M+H]⁺ 662.4089, found 662.4096



4-Cyano-*N*-((*S*)-1-cyclopentyl-2-(((2*S*,3*S*)-3-methyl-1-oxo-1-((2-oxo-2-(((*R*)-1-((3*aS*,4*S*,6*S*,7*aR*)-3*a*,5,5-trimethylhexahydro-4,6-methanobenzo[*d*][1,3,2]-dioxaborol-2-yl)ethyl)

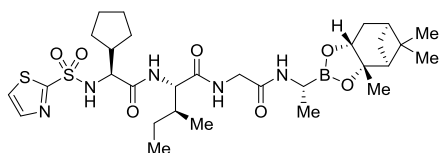
amino)ethyl)amino) pentan-2-yl)amino)-2-oxoethyl)-1*H*-indole-2-carboxamide (83n)

Prepared in analogues way as **83c**: starting material **82** (100 mg, 0.162 mmol) and 4 M HCl in dioxane (200 μ L) in CHCl₃ (3 mL). Coupling: 4-cyano-1*H*-indole-2-carboxylic acid (30 mg, 0.161 mmol), EDC-HCl (38 mg, 0.198 mmol), HOBt (24 mg, 0.178 mmol) and DIPEA (84 μ L, 0.486 mmol) in CHCl₃ (5 mL). Yield: 62 mg (56%, amorphous solid).

¹H NMR (400 MHz, Methanol-*d*₄) δ 7.79 (dt, *J* = 8.5, 1.0 Hz, 1H), 7.53 (dd, *J* = 7.4, 1.0 Hz, 1H), 7.42 (d, *J* = 1.1 Hz, 1H), 7.36 (dd, *J* = 8.3, 7.3 Hz, 1H), 4.57 (d, *J* = 10.1 Hz, 1H), 4.24 – 4.12 (m, 3H), 4.02 (d, *J* = 16.9 Hz, 1H), 2.71 (q, *J* = 7.3 Hz, 1H), 2.43 (h, *J* = 8.0 Hz, 1H), 2.35 – 2.27 (m, 1H), 2.16 – 2.08 (m, 1H), 1.93 (t, *J* = 5.5 Hz, 1H), 1.90 – 1.74 (m, 4H), 1.73 – 1.53 (m, 6H), 1.49 – 1.36 (m, 3H), 1.34 (s, 3H), 1.26 (s, 3H), 1.25 – 1.14 (m, 4H), 0.94 (d, *J* = 6.8 Hz, 3H), 0.89 – 0.83 (m, 6H).

¹³C NMR (101 MHz, Methanol-*d*₄) δ 175.5, 174.8, 174.4, 162.8, 137.9, 134.4, 129.6, 127.1, 124.8, 119.2, 118.7, 104.9, 102.8, 84.5, 77.4, 59.9, 59.3, 53.5, 43.0, 41.3, 40.2, 39.5 (CHB (broad)), 39.1, 37.6, 37.6, 30.9, 30.4, 29.6, 27.8, 27.5, 26.4, 26.3, 26.0, 24.5, 16.4, 15.8, 11.3.

HR-MS (ESI/TOF) calcd for C₃₇H₅₁BN₆O₆Na [M+Na]⁺ 709.3861, found 709.3879



(2*S*,3*S*)-2-((*S*)-2-cyclopentyl-2-(thiazole-2-sulfonamido)acetamido)-3-methyl-*N*-(2-oxo-2-(((*R*)-1-((3*aS*,4*S*,6*S*,7*aR*)-3*a*,5,5-trimethylhexa-hydro-4,6-methanobenzo[*d*]-[1,3,2]dioxaborol-2-yl)ethyl)amino)ethyl)

pentanamide (83o)

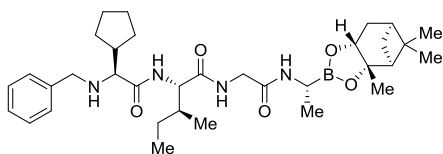
Starting material **82** (100 mg, 0.16 mmol, 1.0 equiv) in CHCl₃ (2 mL) was treated with 4 M HCl in dioxane (160 μ L, 4 equiv) until full deprotection of the protecting group. After solvent evaporation the crude mixture was utilized in the next step without purification. The residue (based on a theoretical yield of a 100%) under argon atmosphere was dissolved in dry CHCl₃ (5 mL), thiazole-2-sulfonyl chloride (35 μ L, 0.25 mmol, 1.5 equiv) and DIPEA (60 μ L, 0.35 mmol, 2.0 equiv) were added and mixture was stirred for 2 h at room temperature, then washed with 5% KHSO₄ (5 mL), with sat. NaHCO₃ (5 mL), and brine (10 mL). Organic phase was dried over Na₂SO₄, filtered and evaporated in vacuo. The residue was purified by flash chromatography on silica gel eluting with 1–5% MeOH in EtOAc to provide **83o** (87 mg, 81%) as an amorphous solid.

¹H NMR (400 MHz, Methanol-*d*₄) δ 7.95 (d, *J* = 3.1 Hz, 1H), 7.92 (d, *J* = 3.1 Hz, 1H), 4.19 (dd, *J* = 17.5, 1.7 Hz, 1H), 4.15 (dd, *J* = 8.6, 2.3 Hz, 1H), 3.97 (d, *J* = 8.6 Hz, 1H),

3.90 (dd, $J = 17.6, 0.9$ Hz, 1H), 3.85 (d, $J = 8.6$ Hz, 1H), 2.62 (q, $J = 7.3$ Hz, 1H), 2.39 – 2.28 (m, 1H), 2.25 – 2.07 (m, 2H), 1.94 (t, $J = 5.6$ Hz, 1H), 1.88 – 1.82 (m, 1H), 1.81 – 1.71 (m, 2H), 1.70 – 1.46 (m, 7H), 1.43 (d, $J = 10.4$ Hz, 1H), 1.40 – 1.33 (m, 4H), 1.28 (s, 3H), 1.23 – 1.13 (m, 5H), 0.93 (t, $J = 7.4$ Hz, 3H), 0.91 (d, $J = 6.8$ Hz, 3H), 0.87 (s, 3H).

^{13}C NMR (101 MHz, Methanol- d_4) δ 175.75, 175.73, 174.2, 174.1, 168.0, 145.1, 126.4, 84.3, 77.3, 61.6, 60.4, 53.6, 44.0, 41.3, 40.0, 39.8 (C_{HB} (broad)), 39.2, 37.7, 37.1, 29.94, 29.86, 29.6, 27.8, 27.5, 26.5, 26.3, 25.8, 24.5, 16.4, 15.7, 11.3.

HR-MS (ESI/TOF) calcd for C₃₀H₄₉BN₅O₇S₂ [M+H]⁺ 666.3166, found 666.3162



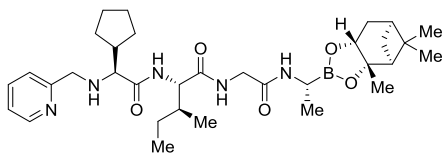
(2*S*,3*S*)-2-((*S*)-2-(benzylamino)-2-cyclopentylacetamido)-3-methyl-*N*-(2-oxo-2-(((*R*)-1-((3*aS*,4*S*,6*S*,7*a**R*)-3*a*,5,5-trimethylhexahydro-4,6-methanobenzo[*d*][1,3,2]-dioxaborol-2-yl)ethyl) amino)ethyl) pentanamide (83p)**

pentanamide (83p)

Starting material **82** (172 mg, 0.13 mmol, 1.0 equiv) in CHCl₃ (5 mL) was treated with 4 M HCl in dioxane (280 μ L, 4 equiv) until full deprotection of the protecting group. After solvent evaporation the crude mixture was utilized in the next step without purification. The residue was dissolved in 2,2,2-trifluoroethanol (2 mL) and cooled to 0 °C, triethylamine (43 μ L, 0.31 mmol, 1.1 equiv) and benzaldehyde (60 μ L, 0.59 mmol, 2.0 equiv) were added and mixture was allowed to warm up to room temperature overnight. Then it was cooled to 0 °C and NaBH₄ (53 mg, 1.40 mmol, 5.0 equiv) was added, followed by few drops of MeOH. Reaction was stirred 1h, then acidified with 5% KHSO₄ and extracted with CHCl₃ (3 \times). Organic phase was dried over Na₂SO₄, filtered and evaporated in vacuo. The residue was purified by flash chromatography on reversed phase silica gel eluting with 10–100% MeOH in H₂O to provide **83p** (83 mg, 49%) as an amorphous solid.

^1H NMR (400 MHz, Chloroform- d) δ 7.73 (d, $J = 7.6$ Hz, 1H), 7.37 – 7.30 (m, 4H), 7.30 – 7.22 (m, 1H), 7.07 (d, $J = 4.3$ Hz, 1H), 6.62 (t, $J = 5.8$ Hz, 1H), 4.25 (dd, $J = 8.8, 2.1$ Hz, 1H), 4.09 (t, $J = 7.4$ Hz, 1H), 4.02 (dd, $J = 17.0, 6.3$ Hz, 1H), 3.90 (dd, $J = 16.9, 5.5$ Hz, 1H), 3.76 (d, $J = 12.9$ Hz, 1H), 3.64 (d, $J = 12.9$ Hz, 1H), 3.05 (qd, $J = 7.3, 4.0$ Hz, 1H), 2.99 (d, $J = 6.9$ Hz, 1H), 2.35 – 2.26 (m, 1H), 2.22 – 2.05 (m, 2H), 2.01 (dd, $J = 6.7, 4.2$ Hz, 1H), 1.96 – 1.80 (m, 5H), 1.73 – 1.46 (m, 7H), 1.39 (s, 3H), 1.31 – 1.25 (m, 5H), 1.21 – 1.10 (m, 4H), 0.95 (d, $J = 6.8$ Hz, 3H), 0.91 (t, $J = 7.4$ Hz, 3H), 0.83 (s, 3H).

HR-MS (ESI/TOF) calcd for C₃₄H₅₄BN₄O₅ [M+H]⁺ 609.4187, found 609.4202



(2*S*,3*S*)-2-((*S*)-2-cyclopentyl-2-((pyridin-2-ylmethyl)amino)acetamido)-3-methyl-*N*-(2-oxo-2-(((*R*)-1-((3*aS*,4*S*,6*S*,7*a**R*)-3*a*,5,5-trimethylhexahydro-4,6-methanobenzo[*d*][1,3,2]-dioxaborol-2-yl)ethyl) amino)ethyl) pentanamide (83r)**

pentanamide (83r)

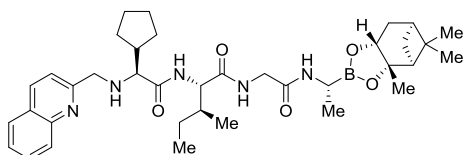
Prepared in analogy to **83p**: starting material **82** (150 mg, 0.24 mmol) in CHCl₃ (5 mL) was treated with 4 M HCl in dioxane (250 μ L, 1 mmol). The residue was dissolved in TFE (2 mL) and cooled to 0 °C, triethylamine (40 μ L, 0.29 mmol) and pyridine-2-

carboxaldehyde (46 μ L, 0.48 mmol) were added. Then NaBH₄ (46 mg, 1.22 mmol) was added. Yield: 87 mg (59%, amorphous solid).

¹H NMR (400 MHz, Methanol-*d*₄) δ 8.48 (ddd, *J* = 4.9, 1.8, 1.0 Hz, 1H), 7.80 (td, *J* = 7.7, 1.8 Hz, 1H), 7.51 (dt, *J* = 7.9, 1.2 Hz, 1H), 7.30 (ddd, *J* = 7.6, 5.0, 1.3 Hz, 1H), 4.20 (dd, *J* = 17.5, 1.6 Hz, 1H), 4.15 (dd, *J* = 8.6, 2.3 Hz, 1H), 4.12 (d, *J* = 8.1 Hz, 1H), 3.95 (dd, *J* = 17.4, 1.0 Hz, 1H), 3.89 (d, *J* = 14.2 Hz, 1H), 3.74 (d, *J* = 14.2 Hz, 1H), 3.00 (d, *J* = 8.0 Hz, 1H), 2.66 (q, *J* = 7.2 Hz, 1H), 2.37 – 2.28 (m, 1H), 2.18 – 2.04 (m, 2H), 1.94 (t, *J* = 5.5 Hz, 1H), 1.88 – 1.75 (m, 4H), 1.69 – 1.49 (m, 6H), 1.44 (d, *J* = 10.3 Hz, 1H), 1.42 – 1.36 (m, 2H), 1.35 (s, 3H), 1.28 (s, 3H), 1.26 – 1.18 (m, 1H), 1.16 (d, *J* = 7.3 Hz, 3H), 1.00 – 0.89 (m, 6H), 0.87 (s, 3H).

¹³C NMR (101 MHz, Methanol-*d*₄) δ 177.4, 175.7, 174.4, 160.6, 149.7, 138.7, 124.2, 123.7, 84.4, 77.3, 67.4, 59.6, 54.0, 53.6, 44.9, 41.3, 40.1, 39.6 (CHB (broad)), 39.2, 37.7, 37.4, 30.5, 30.2, 29.6, 27.8, 27.5, 26.4, 26.2, 26.1, 24.5, 16.4, 15.9, 11.2.

HR-MS (ESI/TOF) calcd for C₃₃H₅₃BN₅O₅ [M+H]⁺ 610.4140, found 610.4152



(2*S*,3*S*)-2-((*S*)-2-cyclopentyl-2-((quinolin-2-yl-methyl)amino)acetamido)-3-methyl-N-(2-oxo-2-(((*R*)-1-((3*aS*,4*S*,6*S*,7*aR*)-3*a*,5,5-trimethyl-hexahydro-4,6-

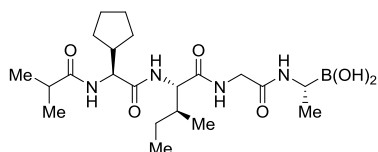
yl)ethyl)amino)ethyl)-pentanamide (83s)

Prepared in analogy to **83p**: starting material **82** (150 mg, 0.24 mmol) in CHCl₃ (5 mL) was treated with 4 M HCl in dioxane (250 μ L, 1 mmol). The residue was dissolved in TFE (2 mL) and cooled to 0 °C, triethylamine (40 μ L, 0.29 mmol) and quinoline-2-carboxaldehyde (76 mg, 0.49 mmol) were added. Then NaBH₄ (46 mg, 1.22 mmol) was added. Yield: 80 mg (50%, amorphous solid).

¹H NMR (400 MHz, Methanol-*d*₄) δ 8.30 (dd, *J* = 8.5, 0.8 Hz, 1H), 8.00 (dq, *J* = 8.5, 0.9 Hz, 1H), 7.91 (dd, *J* = 8.2, 1.7 Hz, 1H), 7.75 (ddd, *J* = 8.5, 6.9, 1.5 Hz, 1H), 7.66 (d, *J* = 8.6 Hz, 1H), 7.57 (ddd, *J* = 8.1, 6.9, 1.2 Hz, 1H), 4.20 (dd, *J* = 17.5, 1.6 Hz, 1H), 4.14 (dd, *J* = 8.6, 2.3 Hz, 1H), 4.12 – 4.06 (m, 2H), 3.99 – 3.90 (m, 2H), 3.05 (d, *J* = 8.1 Hz, 1H), 2.67 (q, *J* = 7.3 Hz, 1H), 2.36 – 2.27 (m, 1H), 2.18 – 2.05 (m, 2H), 1.94 (t, *J* = 5.5 Hz, 1H), 1.90 – 1.73 (m, 4H), 1.70 – 1.50 (m, 6H), 1.48 – 1.38 (m, 3H), 1.35 (s, 3H), 1.27 (s, 3H), 1.23 – 1.09 (m, 4H), 0.94 (d, *J* = 6.9 Hz, 3H), 0.90 (t, *J* = 7.5 Hz, 3H), 0.86 (s, 3H).

¹³C NMR (101 MHz, Methanol-*d*₄) δ 177.4, 175.7, 174.4, 161.6, 148.5, 138.5, 131.0, 129.0, 128.9, 127.6, 122.1, 84.4, 77.3, 67.5, 59.7, 54.6, 53.6, 45.0, 41.3, 40.1, 39.6 (CHB (broad)), 39.2, 37.6, 37.4, 30.6, 30.2, 29.6, 27.8, 27.5, 26.4, 26.3, 26.1, 24.5, 16.4, 15.8, 11.2.

HR-MS (ESI/TOF) calcd for C₃₇H₅₅BN₅O₅ [M+H]⁺ 660.4296, found 660.4304



((2*R*,8*S*,11*S*)-8-((*S*)-*sec*-butyl)-11-cyclopentyl-14-methyl-4,7,10,13-tetraoxo-3,6,9,12-tetraaza-pentadecan-2-yl) boronic acid (84a)

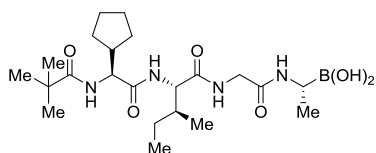
A solution of **83a** (67 mg, 0.11 mmol) in MeOH/*n*-hexane (1:1, 4.4 mL) was treated with

isobutylboronic acid (46 mg, 0.72 mmol, 4 equiv) and 1 M HCl (280 μ L). After 18 h at room temperature, the methanolic phase was washed with *n*-hexane (2 \times 5 mL) and the combined *n*-hexane layers were washed with MeOH (2 \times 5 mL). The combined methanol phase was evaporated in vacuo. Crude mixture was purified by flash chromatography on reversed phase silica gel eluting with 10–100% MeCN in H₂O to provide **84a** (34 mg, 66%) as a white solid compound.

¹H NMR (400 MHz, Methanol-*d*₄) δ 4.23 (dd, *J* = 17.5, 1.7 Hz, 1H), 4.18 (d, *J* = 9.7 Hz, 1H), 4.06 (d, *J* = 8.1 Hz, 1H), 3.99 (dd, *J* = 17.6, 1.0 Hz, 1H), 2.67 (q, *J* = 6.9 Hz, 1H), 2.53 (hept, *J* = 6.9 Hz, 1H), 2.24 (h, *J* = 8.7 Hz, 1H), 1.88 – 1.76 (m, 2H), 1.72 – 1.51 (m, 6H), 1.40 – 1.16 (m, 3H), 1.12 (d, *J* = 7.2 Hz, 3H), 1.11 (d, *J* = 6.8 Hz, 3H), 1.09 (d, *J* = 6.9 Hz, 3H), 0.96 – 0.89 (m, 6H).

¹³C NMR (101 MHz, Methanol-*d*₄) δ 180.2, 176.4, 175.0, 174.5, 59.9, 58.6, 43.0, 42.0 (CHB (broad)), 39.6, 37.4, 35.8, 30.4, 30.3, 26.3, 26.2, 25.9, 20.1, 19.7, 15.9, 15.7, 11.2.

HR-MS (ESI/TOF) calcd for C₂₁H₃₉BN₄O₆Na [M+Na]⁺ 477.2860, found 477.2869



((2*R*,8*S*,11*S*)-8-((*S*)-*sec*-butyl)-11-cyclopentyl-14,14-dimethyl-4,7,10,13-tetraoxo-3,6,9,12-tetraazapenta-decan-2-yl) boronic acid (84b**)**

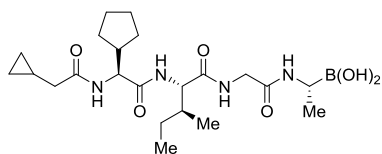
Prepared in analogy to **84a**: a solution of **83b** (58 mg, 0.096 mmol) in MeOH/*n*-hexane (1:1, 3.7 mL)

was treated with isobutylboronic acid (40 mg, 0.39 mmol) and 1 M HCl (240 μ L). Yield: 24 mg (53%, white solid).

¹H NMR (400 MHz, Methanol-*d*₄) δ 4.24 (d, *J* = 9.5 Hz, 1H), 4.22 (dd, *J* = 17.5, 1.7 Hz, 1H), 4.07 (d, *J* = 8.0 Hz, 1H), 3.98 (dd, *J* = 17.5, 1.0 Hz, 1H), 2.67 (q, *J* = 7.2 Hz, 1H), 2.30 (dq, *J* = 16.7, 8.6 Hz, 1H), 1.89 – 1.73 (m, 2H), 1.72 – 1.52 (m, 6H), 1.38 – 1.30 (m, 1H), 1.29 – 1.17 (m, 11H), 1.12 (d, *J* = 7.2 Hz, 3H), 0.97 – 0.87 (m, 6H).

¹³C NMR (101 MHz, Methanol-*d*₄) δ 181.1, 176.3, 174.9, 174.4, 59.9, 58.6, 43.1, 41.9 (CHB (broad)), 39.8, 39.6, 37.5, 30.4, 30.3, 27.8, 26.3, 26.2, 25.9, 15.9, 15.7, 11.2.

HR-MS (ESI/TOF) calcd for C₂₂H₄₁BN₄O₆Na [M+Na]⁺ 491.3030, found 491.3040



((2*R*,8*S*,11*S*)-8-((*S*)-*sec*-butyl)-11-cyclopentyl-14-cyclopropyl-4,7,10,13-tetraoxo-3,6,9,12-tetraaza-tetradecan-2-yl) boronic acid (84c**)**

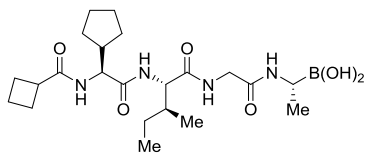
Prepared in analogy to **84a**: a solution of **83c** (73 mg, 0.122 mmol) in MeOH/*n*-hexane (1:1,

4.6 mL) was treated with isobutylboronic acid (50 mg, 0.49 mmol) and 1 M HCl (300 μ L). Yield: 46 mg (81%, white solid).

¹H NMR (400 MHz, Methanol-*d*₄) δ 4.29 – 4.21 (m, 2H), 4.06 (d, *J* = 8.2 Hz, 1H), 4.01 (dd, *J* = 17.5, 1.0 Hz, 1H), 2.69 (q, *J* = 7.2 Hz, 1H), 2.24 (h, *J* = 8.8 Hz, 1H), 2.20 – 2.10 (m, 2H), 1.91 – 1.74 (m, 2H), 1.72 – 1.52 (m, 6H), 1.40 – 1.18 (m, 3H), 1.13 (d, *J* = 7.2 Hz, 3H), 1.07 – 0.98 (m, 1H), 0.98 – 0.89 (m, 6H), 0.55 – 0.49 (m, 2H), 0.23 – 0.17 (m, 2H).

¹³C NMR (101 MHz, Methanol-*d*₄) δ 176.6, 175.7, 174.9, 174.5, 60.0, 58.6, 43.1, 42.3 (CHB (broad)), 41.5, 39.6, 37.3, 30.3, 30.2, 26.3, 26.3, 25.9, 15.8, 15.7, 11.2, 8.7, 4.8.

HR-MS (ESI/TOF) calcd for C₂₂H₃₉BN₄O₆Na [M+Na]⁺ 489.2860, found 489.2854



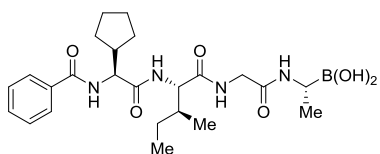
((3S,6S,12R)-6-((S)-sec-butyl)-1-cyclobutyl-3-cyclopentyl-1,4,7,10-tetraoxo-2,5,8,11-tetraazatridecan-12-yl) boronic acid (84d)

Prepared in analogy to **84a**: a solution of **83d** (58 mg, 0.097 mmol) in MeOH/*n*-hexane (1:1, 3.7 mL) was treated with isobutylboronic acid (40 mg, 0.39 mmol) and 1 M HCl (240 μL). Yield: 36 mg (80%, white solid).

¹H NMR (400 MHz, Methanol-*d*₄) δ 4.23 (dd, *J* = 17.6, 1.7 Hz, 1H), 4.18 (d, *J* = 9.5 Hz, 1H), 4.05 (d, *J* = 8.1 Hz, 1H), 3.99 (dd, *J* = 17.6, 1.0 Hz, 1H), 3.17 (pd, *J* = 8.4, 1.0 Hz, 1H), 2.67 (q, *J* = 7.2 Hz, 1H), 2.31 – 2.17 (m, 3H), 2.20 – 2.05 (m, 2H), 2.06 – 1.90 (m, 1H), 1.91 – 1.73 (m, 3H), 1.70 – 1.49 (m, 6H), 1.39 – 1.17 (m, 3H), 1.12 (d, *J* = 7.2 Hz, 3H), 0.94 (d, *J* = 6.8 Hz, 3H), 0.92 (t, *J* = 7.5 Hz, 3H).

¹³C NMR (101 MHz, Methanol-*d*₄) δ 177.7, 176.4, 175.0, 174.5, 60.0, 58.7, 43.0, 42.1 (CHB (broad)), 40.4, 39.6, 37.4, 30.4, 30.3, 26.3, 26.25, 26.22, 26.0, 25.9, 19.1, 15.9, 15.7, 11.2.

HR-MS (ESI/TOF) calcd for C₂₂H₃₉BN₄O₆Na [M+Na]⁺ 489.2860, found 489.2865



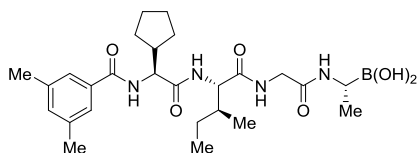
((3S,6S,12R)-6-((S)-sec-butyl)-3-cyclopentyl-1,4,7,10-tetraoxo-1-phenyl-2,5,8,11-tetraazatridecan-12-yl) boronic acid (84e)

Prepared in analogy to **84a**: a solution of **83e** (53 mg, 0.085 mmol) in MeOH/*n*-hexane (1:1, 3.2 mL) was treated with isobutylboronic acid (35 mg, 0.34 mmol) and 1 M HCl (210 μL). Yield: 28 mg (67%, white solid).

¹H NMR (400 MHz, Methanol-*d*₄) δ 7.84 – 7.80 (m, 2H), 7.57 – 7.52 (m, 1H), 7.49 – 7.44 (m, 2H), 4.41 (d, *J* = 10.0 Hz, 1H), 4.22 (dd, *J* = 17.5, 1.7 Hz, 1H), 4.10 (d, *J* = 8.2 Hz, 1H), 3.99 (dd, *J* = 17.5, 1.0 Hz, 1H), 2.67 (q, *J* = 6.7 Hz, 1H), 2.47 – 2.32 (m, 1H), 1.95 – 1.80 (m, 2H), 1.76 – 1.53 (m, 6H), 1.47 – 1.33 (m, 2H), 1.30 – 1.17 (m, 1H), 1.12 (d, *J* = 7.2 Hz, 3H), 0.95 (d, *J* = 6.8 Hz, 3H), 0.92 (t, *J* = 7.5 Hz, 3H).

¹³C NMR (101 MHz, Methanol-*d*₄) δ 176.2, 175.0, 174.5, 170.5, 135.4, 132.8, 129.6, 128.5, 60.1, 59.6, 43.0, 42.0 (CHB (broad)), 39.6, 37.4, 30.8, 30.5, 26.35, 26.26, 25.9, 15.9, 15.7, 11.2.

HR-MS (ESI/TOF) calcd for C₂₄H₃₇BN₄O₆Na [M+Na]⁺ 511.2704, found 511.2705



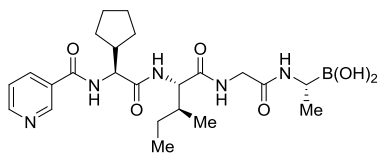
((3S,6S,12R)-6-((S)-sec-butyl)-3-cyclopentyl-1-(3,5-dimethylphenyl)-1,4,7,10-tetraoxo-2,5,8,11-tetra-azatridecan-12-yl) boronic acid (84f)

Prepared in analogy to **84a**: a solution of **83f** (48 mg, 0.074 mmol) in MeOH/*n*-hexane (1:1, 2.8 mL) was treated with isobutylboronic acid (30 mg, 0.29 mmol) and 1 M HCl (185 μL). Yield: 27 mg (71%, white solid).

^1H NMR (400 MHz, Methanol- d_4) δ 7.44 – 7.41 (m, 2H), 7.20 – 7.18 (m, 1H), 4.40 (d, J = 10.0 Hz, 1H), 4.22 (dd, J = 17.5, 1.6 Hz, 1H), 4.10 (d, J = 8.2 Hz, 1H), 4.00 (dd, J = 17.5, 0.9 Hz, 1H), 2.67 (q, J = 7.0 Hz, 1H), 2.45 – 2.31 (m, 7H), 1.93 – 1.80 (m, 2H), 1.77 – 1.54 (m, 6H), 1.47 – 1.32 (m, 2H), 1.30 – 1.17 (m, 1H), 1.12 (d, J = 7.2 Hz, 3H), 0.95 (d, J = 6.8 Hz, 3H), 0.92 (t, J = 7.4 Hz, 3H).

^{13}C NMR (101 MHz, Methanol- d_4) δ 176.3, 175.0, 174.5, 170.8, 139.4, 135.3, 134.3, 126.2, 60.0, 59.5, 43.0, 41.9 ($\underline{\text{CHB}}$ (broad)), 39.6, 37.4, 30.7, 30.5, 26.3, 26.3, 25.9, 21.29, 21.27, 21.2, 15.9, 15.7, 11.2.

HR-MS (ESI/TOF) calcd for $\text{C}_{26}\text{H}_{41}\text{BN}_4\text{O}_6\text{Na}$ [$\text{M}+\text{Na}$] $^+$ 539.3017, found 539.3034



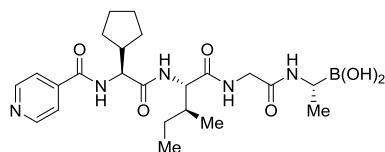
((3S,6S,12R)-6-((S)-sec-butyl)-3-cyclopentyl-1,4,7,10-tetraoxo-1-(pyridin-3-yl)-2,5,8,11-tetraazatridecan-12-yl) boronic acid (84g)

Prepared in analogy to **84a**: a solution of **83g** (66 mg, 0.106 mmol) in MeOH/*n*-hexane (1:1, 4 mL) was treated with isobutylboronic acid (44 mg, 0.43 mmol) and 1 M HCl (265 μL). Yield: 36 mg (70%, white solid).

^1H NMR (400 MHz, Methanol- d_4) δ 8.97 (dd, J = 2.3, 1.0 Hz, 1H), 8.69 (dd, J = 5.0, 1.7 Hz, 1H), 8.24 (ddd, J = 8.0, 2.3, 1.7 Hz, 1H), 7.54 (ddd, J = 8.0, 4.9, 1.0 Hz, 1H), 4.42 (d, J = 10.1 Hz, 1H), 4.23 (d, J = 17.5 Hz, 0H), 4.10 (d, J = 8.3 Hz, 1H), 4.00 (d, J = 17.5 Hz, 0H), 2.67 (q, J = 7.1 Hz, 1H), 2.38 (h, J = 8.6 Hz, 1H), 1.97 – 1.82 (m, 2H), 1.76 – 1.53 (m, 6H), 1.48 – 1.32 (m, 2H), 1.31 – 1.17 (m, 1H), 1.12 (d, J = 7.2 Hz, 3H), 0.96 (d, J = 6.8 Hz, 3H), 0.92 (t, J = 7.5 Hz, 3H).

^{13}C NMR (101 MHz, Methanol- d_4) δ 176.2, 174.8, 174.5, 168.1, 152.8, 149.3, 137.2, 131.8, 125.1, 60.1, 59.8, 43.0, 41.9 ($\underline{\text{CHB}}$ (broad)), 39.6, 37.3, 30.9, 30.4, 26.32, 26.29, 25.9, 16.0, 15.7, 11.2.

HR-MS (ESI/TOF) calcd for $\text{C}_{23}\text{H}_{36}\text{BN}_5\text{O}_6\text{Na}$ [$\text{M}+\text{Na}$] $^+$ 512.2656, found 512.2646



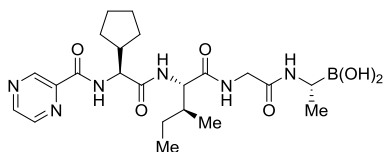
((3S,6S,12R)-6-((S)-sec-butyl)-3-cyclopentyl-1,4,7,10-tetraoxo-1-(pyridin-4-yl)-2,5,8,11-tetraazatridecan-12-yl) boronic acid (84h)

Prepared in analogy to **84a**: a solution of **83h** (70 mg, 0.112 mmol) in MeOH/*n*-hexane (1:1, 4.4 mL) was treated with isobutylboronic acid (46 mg, 0.45 mmol) and 1 M HCl (280 μL). Yield: 45 mg (82%, white solid).

^1H NMR (400 MHz, Methanol- d_4) δ 8.72 – 8.67 (m, 2H), 7.80 – 7.76 (m, 2H), 4.41 (d, J = 10.1 Hz, 1H), 4.23 (d, J = 17.4 Hz, 1H), 4.10 (d, J = 8.3 Hz, 1H), 3.99 (d, J = 17.4 Hz, 1H), 2.67 (q, J = 7.2 Hz, 1H), 2.38 (h, J = 8.7 Hz, 1H), 1.95 – 1.81 (m, 2H), 1.76 – 1.53 (m, 6H), 1.47 – 1.33 (m, 2H), 1.29 – 1.19 (m, 1H), 1.12 (d, J = 7.2 Hz, 3H), 0.96 (d, J = 6.8 Hz, 3H), 0.92 (t, J = 7.4 Hz, 3H).

^{13}C NMR (101 MHz, Methanol- d_4) δ 176.2, 174.6, 174.4, 168.0, 150.9, 143.7, 123.1, 60.1, 59.8, 43.0, 41.9 ($\underline{\text{CHB}}$ (broad)), 39.6, 37.3, 30.8, 30.4, 26.31, 26.29, 25.9, 16.0, 15.7, 11.2.

HR-MS (ESI/TOF) calcd for $\text{C}_{23}\text{H}_{36}\text{BN}_5\text{O}_6\text{Na}$ [$\text{M}+\text{Na}$] $^+$ 512.2656, found 512.2631



((3S,6S,12R)-6-((S)-sec-butyl)-3-cyclopentyl-1,4,7,10-tetraoxo-1-(pyrazin-2-yl)-2,5,8,11-tetraazatridecan-12-yl) boronic acid (84i)

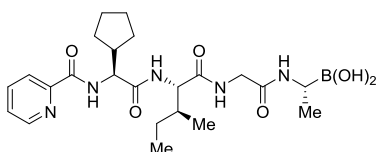
Prepared in analogy to **84a**: a solution of **83i** (80 mg, 0.128 mmol) in MeOH/*n*-hexane (1:1, 5 mL) was treated with isobutylboronic acid (52 mg, 0.51 mmol) and 1 M HCl (320 μ L).

Yield: 45 mg (72%, white solid).

^1H NMR (400 MHz, Methanol- d_4) δ 9.25 (s, 1H), 8.82 (s, 1H), 8.70 (s, 1H), 4.59 (d, J = 8.5 Hz, 1H), 4.25 (dd, J = 17.6, 1.6 Hz, 1H), 4.06 (d, J = 8.3 Hz, 1H), 3.99 (dd, J = 17.6, 1.0 Hz, 1H), 2.70 (q, J = 7.2 Hz, 1H), 2.40 (h, J = 8.7 Hz, 1H), 1.90 – 1.52 (m, 8H), 1.49 – 1.32 (m, 2H), 1.30 – 1.17 (m, 1H), 1.15 (d, J = 7.2 Hz, 3H), 0.95 (d, J = 6.8 Hz, 3H), 0.92 (t, J = 7.4 Hz, 3H).

^{13}C NMR (101 MHz, Methanol- d_4) δ 176.3, 174.5, 174.4, 164.8, 148.8, 145.8, 144.9, 144.8, 60.2, 57.9, 44.2, 42.0 ($\underline{\text{C}}\text{HB}$ (broad)), 39.6, 37.2, 30.2, 29.9, 26.4, 26.3, 25.9, 15.9, 15.7, 11.2.

HR-MS (ESI/TOF) calcd for $\text{C}_{22}\text{H}_{35}\text{BN}_6\text{O}_6\text{Na}$ [$\text{M}+\text{Na}$] $^+$ 513.2609, found 513.2632



((3S,6S,12R)-6-((S)-sec-butyl)-3-cyclopentyl-1,4,7,10-tetraoxo-1-(pyridin-2-yl)-2,5,8,11-tetraazatridecan-12-yl) boronic acid (84j)

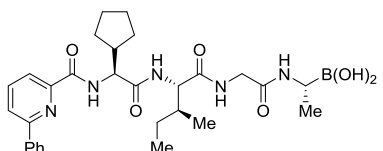
Prepared in analogy to **84a**: a solution of **83j** (88 mg, 0.141 mmol) in MeOH/*n*-hexane (1:1, 5.4 mL) was

treated with isobutylboronic acid (58 mg, 0.57 mmol) and 1 M HCl (350 μ L). Yield: 37 mg (54%, white solid).

^1H NMR (400 MHz, Methanol- d_4) δ 8.64 (ddd, J = 4.8, 1.7, 0.9 Hz, 1H), 8.10 (dt, J = 7.9, 1.2 Hz, 1H), 7.97 (td, J = 7.7, 1.7 Hz, 1H), 7.57 (ddd, J = 7.6, 4.8, 1.3 Hz, 1H), 4.58 (d, J = 8.2 Hz, 1H), 4.25 (dd, J = 17.6, 1.7 Hz, 1H), 4.05 (d, J = 8.5 Hz, 1H), 3.97 (dd, J = 17.5, 1.0 Hz, 1H), 2.69 (q, J = 7.2 Hz, 1H), 2.40 (h, J = 8.3 Hz, 1H), 1.88 – 1.71 (m, 3H), 1.70 – 1.55 (m, 5H), 1.49 – 1.33 (m, 2H), 1.32 – 1.17 (m, 1H), 1.15 (d, J = 7.2 Hz, 3H), 0.95 (d, J = 6.8 Hz, 3H), 0.92 (t, J = 7.4 Hz, 3H).

^{13}C NMR (101 MHz, Methanol- d_4) δ 176.3, 174.6, 174.5, 166.2, 150.5, 149.9, 138.9, 128.0, 123.2, 60.3, 57.7, 44.3, 42.0 ($\underline{\text{C}}\text{HB}$ (broad)), 39.6, 37.1, 30.2, 29.8, 26.4, 26.3, 26.0, 15.9, 15.7, 11.2.

HR-MS (ESI/TOF) calcd for $\text{C}_{23}\text{H}_{36}\text{BN}_5\text{O}_6\text{Na}$ [$\text{M}+\text{Na}$] $^+$ 512.2656, found 512.2657



((3S,6S,12R)-6-((S)-sec-butyl)-3-cyclopentyl-1,4,7,10-tetraoxo-1-(6-phenylpyridin-2-yl)-2,5,8,11-tetraaza-tridecan-12-yl) boronic acid (84k)

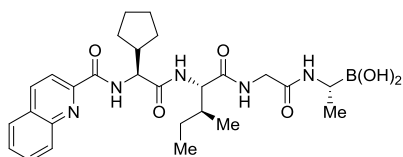
Prepared in analogy to **84a**: a solution of **83k** (130 mg, 0.186 mmol) in MeOH/*n*-hexane (1:1, 7.2 mL) was treated with isobutylboronic acid (76 mg, 0.75 mmol) and 1 M HCl (460 μ L). Yield: 74 mg (70%, white solid).

^1H NMR (400 MHz, Methanol- d_4) δ 8.13 – 7.99 (m, 5H), 7.53 – 7.43 (m, 3H), 4.71 (d, J = 7.6 Hz, 1H), 4.29 (dd, J = 17.6, 1.7 Hz, 1H), 4.06 (d, J = 8.5 Hz, 1H), 3.97 (dd, J = 17.6,

0.9 Hz, 1H), 2.69 (q, $J = 7.2$ Hz, 1H), 2.44 (h, $J = 8.6$ Hz, 1H), 1.90 – 1.72 (m, 3H), 1.71 – 1.53 (m, 5H), 1.53 – 1.41 (m, 2H), 1.31 – 1.17 (m, 1H), 1.11 (d, $J = 7.2$ Hz, 3H), 0.96 (d, $J = 6.8$ Hz, 3H), 0.91 (t, $J = 7.5$ Hz, 3H).

^{13}C NMR (101 MHz, Methanol- d_4) δ 176.2, 174.7, 174.5, 166.1, 157.6, 150.2, 139.9, 139.3, 130.7, 130.0, 127.9, 124.6, 121.6, 60.4, 57.2, 44.7, 41.7 ($\underline{\text{CHB}}$ (broad)), 39.6, 37.0, 30.2, 29.6, 26.5, 26.4, 26.1, 16.1, 15.6, 11.1.

HR-MS (ESI/TOF) calcd for $\text{C}_{29}\text{H}_{40}\text{BN}_5\text{O}_6\text{Na}$ [$\text{M}+\text{Na}$] $^+$ 588.2969, found 588.2975



((3S,6S,12R)-6-((S)-sec-butyl)-3-cyclopentyl-1,4,7,10-tetraoxo-1-(quinolin-2-yl)-2,5,8,11-tetraazatridecan-12-yl) boronic acid (84l)

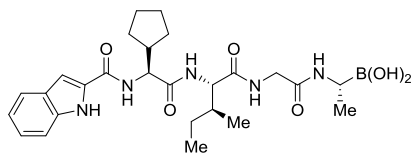
Prepared in analogy to **84a**: a solution of **83l** (59 mg, 0.088 mmol) in MeOH/*n*-hexane (1:1,

3.4 mL) was treated with isobutylboronic acid (36 mg, 0.35 mmol) and 1 M HCl (220 μL). Yield: 35 mg (74%, white solid).

^1H NMR (400 MHz, Methanol- d_4) δ 8.48 (dd, $J = 8.6, 1.0$ Hz, 1H), 8.19 (d, $J = 8.5$ Hz, 1H), 8.13 (dd, $J = 8.5, 1.0$ Hz, 1H), 8.00 (dd, $J = 8.2, 1.8$ Hz, 1H), 7.83 (ddd, $J = 8.5, 6.9, 1.5$ Hz, 1H), 7.69 (ddd, $J = 8.2, 6.9, 1.3$ Hz, 1H), 4.67 (d, $J = 8.1$ Hz, 1H), 4.27 (dd, $J = 17.6, 1.7$ Hz, 1H), 4.08 (d, $J = 8.5$ Hz, 1H), 3.98 (dd, $J = 17.6, 0.9$ Hz, 1H), 2.72 (q, $J = 6.8$ Hz, 1H), 2.53 – 2.39 (m, 1H), 1.89 – 1.74 (m, 3H), 1.73 – 1.54 (m, 5H), 1.53 – 1.40 (m, 2H), 1.29 – 1.21 (m, 1H), 1.19 (d, $J = 7.3$ Hz, 3H), 0.96 (d, $J = 6.9$ Hz, 3H), 0.92 (t, $J = 7.5$ Hz, 3H).

^{13}C NMR (101 MHz, Methanol- d_4) δ 176.3, 174.7, 174.5, 166.2, 150.4, 147.9, 139.2, 131.7, 130.9, 130.7, 129.5, 129.1, 119.5, 60.4, 57.7, 44.5, 41.8 ($\underline{\text{CHB}}$ (broad)), 39.7, 37.1, 30.3, 29.8, 26.4, 26.3, 26.0, 16.0, 15.7, 11.2.

HR-MS (ESI/TOF) calcd for $\text{C}_{27}\text{H}_{38}\text{BN}_5\text{O}_6\text{Na}$ [$\text{M}+\text{Na}$] $^+$ 562.2813, found 562.2822



((3S,6S,12R)-6-((S)-sec-butyl)-3-cyclopentyl-1-(1H-indol-2-yl)-1,4,7,10-tetraoxo-2,5,8,11-tetraazatri-decan-12-yl) boronic acid (84m)

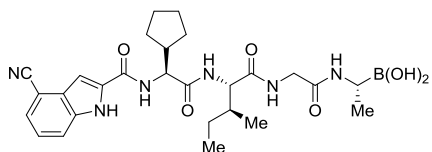
Prepared in analogy to **84a**: a solution of **83m** (64 mg, 0.097 mmol) in MeOH/*n*-hexane (1:1,

3.7 mL) was treated with isobutylboronic acid (40 mg, 0.39 mmol) and 1 M HCl (240 μL). Yield: 34 mg (67%, white solid).

^1H NMR (400 MHz, Methanol- d_4) δ 7.61 (dt, $J = 8.1, 1.0$ Hz, 1H), 7.45 (dq, $J = 8.2, 1.0$ Hz, 1H), 7.22 (ddd, $J = 8.3, 7.0, 1.2$ Hz, 1H), 7.19 (d, $J = 1.0$ Hz, 1H), 7.06 (ddd, $J = 8.1, 7.0, 1.1$ Hz, 1H), 4.56 (d, $J = 10.1$ Hz, 1H), 4.23 (dd, $J = 17.5, 1.6$ Hz, 1H), 4.15 (d, $J = 8.1$ Hz, 1H), 4.04 (dd, $J = 17.5, 1.0$ Hz, 1H), 2.68 (q, $J = 7.1$ Hz, 1H), 2.42 (h, $J = 8.2$ Hz, 1H), 1.96 – 1.80 (m, 2H), 1.76 – 1.52 (m, 6H), 1.49 – 1.34 (m, 2H), 1.28 – 1.15 (m, 1H), 1.13 (d, $J = 7.3$ Hz, 3H), 0.94 (d, $J = 6.8$ Hz, 3H), 0.87 (t, $J = 7.4$ Hz, 3H).

^{13}C NMR (101 MHz, Methanol- d_4) δ 176.2, 175.1, 174.6, 163.9, 138.5, 131.6, 129.0, 125.2, 122.9, 121.2, 113.1, 105.2, 59.9, 59.0, 43.2, 41.9 ($\underline{\text{CHB}}$ (broad)), 39.7, 37.6, 30.8, 30.5, 26.4, 26.3, 26.0, 16.0, 15.7, 11.3.

HR-MS (ESI/TOF) calcd for $\text{C}_{26}\text{H}_{38}\text{BN}_5\text{O}_6\text{Na}$ [$\text{M}+\text{Na}$] $^+$ 550.2813, found 550.2827



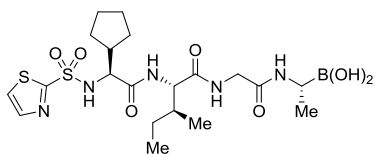
((3S,6S,12R)-6-((S)-sec-butyl)-1-(4-cyano-1H-indol-2-yl)-3-cyclopentyl-1,4,7,10-tetraoxo-2,5,8,11-tetraazatridecan-12-yl) boronic acid (84n)

Prepared in analogy to **84a**: a solution of **83n** (39 mg, 0.057 mmol) in MeOH/*n*-hexane (1:1, 2.2 mL) was treated with isobutylboronic acid (23 mg, 0.23 mmol) and 1 M HCl (140 μ L). Yield: 25 mg (80%, white solid).

^1H NMR (400 MHz, Methanol- d_4) δ 7.78 (dt, J = 8.3, 1.0 Hz, 1H), 7.53 (dd, J = 7.3, 1.0 Hz, 1H), 7.42 (d, J = 1.0 Hz, 1H), 7.36 (dd, J = 8.4, 7.3 Hz, 1H), 4.54 (d, J = 10.3 Hz, 1H), 4.23 (dd, J = 17.5, 1.6 Hz, 1H), 4.17 (d, J = 8.1 Hz, 1H), 4.04 (dd, J = 17.5, 1.0 Hz, 1H), 2.68 (q, J = 7.2 Hz, 1H), 2.43 (h, J = 8.1 Hz, 1H), 1.97 – 1.79 (m, 2H), 1.76 – 1.53 (m, 6H), 1.48 – 1.33 (m, 2H), 1.30 – 1.17 (m, 1H), 1.12 (d, J = 7.2 Hz, 3H), 0.95 (d, J = 6.9 Hz, 3H), 0.88 (t, J = 7.4 Hz, 3H).

^{13}C NMR (101 MHz, Methanol- d_4) δ 176.2, 174.8, 174.6, 162.8, 137.9, 134.4, 129.6, 127.0, 124.7, 119.1, 118.6, 105.0, 102.8, 59.9, 59.3, 43.0, 41.8 (CHB (broad)), 39.7, 37.6, 30.9, 30.5, 26.4, 26.2, 25.9, 16.0, 15.7, 11.2.

HR-MS (ESI/TOF) calcd for $\text{C}_{27}\text{H}_{37}\text{BN}_6\text{O}_6\text{Na}$ [$\text{M}+\text{Na}$] $^+$ 575.2765, found 575.2770



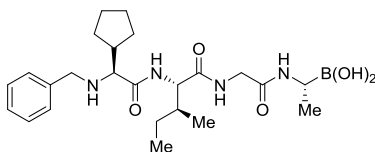
((R)-1-(2-((2S,3S)-2-((S)-2-cyclopentyl-2-(thiazole-2-sulfonamido)acetamido)-3-methylpentanamido)acetamido)ethyl) boronic acid (84o)

Prepared in analogy to **84a**: a solution of **83o** (84 mg, 0.126 mmol) in MeOH/*n*-hexane (1:1, 5 mL) was treated with isobutylboronic acid (52 mg, 0.51 mmol) and 1 M HCl (320 μ L). Yield: 50 mg (75%, white solid).

^1H NMR (400 MHz, Methanol- d_4) δ 7.96 (d, J = 3.2 Hz, 1H), 7.92 (d, J = 3.2 Hz, 1H), 4.22 (dd, J = 17.6, 1.7 Hz, 1H), 3.99 – 3.91 (m, 2H), 3.86 (d, J = 8.5 Hz, 1H), 2.64 (q, J = 7.2 Hz, 1H), 2.17 (h, J = 8.6 Hz, 1H), 1.82 – 1.72 (m, 1H), 1.70 – 1.46 (m, 7H), 1.43 – 1.32 (m, 1H), 1.26 – 1.14 (m, 2H), 1.11 (d, J = 7.3 Hz, 3H), 0.98 – 0.89 (m, 6H).

^{13}C NMR (101 MHz, Methanol- d_4) δ 176.3, 174.4, 174.1, 168.0, 145.1, 126.4, 61.6, 60.3, 44.1, 42.0 (CHB (broad)), 39.6, 37.1, 29.95, 29.91, 26.5, 26.3, 25.8, 15.9, 15.6, 11.3.

HR-MS (ESI/TOF) calcd for $\text{C}_{20}\text{H}_{34}\text{BN}_5\text{O}_7\text{S}_2\text{Na}$ [$\text{M}+\text{Na}$] $^+$ 554.1890, found 554.1889



((3S,6S,12R)-6-((S)-sec-butyl)-3-cyclopentyl-4,7,10-tri-oxo-1-phenyl-2,5,8,11-tetraazatridecan-12-yl) boronic acid (84p)

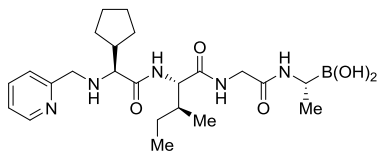
Prepared in analogy to **84a**: a solution of **83p** (83 mg, 0.136 mmol) in MeOH/*n*-hexane (1:1, 5.2 mL) was treated with isobutylboronic acid (56 mg, 0.55 mmol) and 1 M HCl (340 μ L). Yield: 44 mg (65%, white solid).

^1H NMR (400 MHz, Methanol- d_4) δ 7.37 – 7.27 (m, 4H), 7.28 – 7.19 (m, 1H), 4.22 (d, J = 17.5 Hz, 1H), 4.15 (d, J = 8.1 Hz, 1H), 3.99 (d, J = 17.5 Hz, 1H), 3.79 (d, J = 13.1 Hz, 1H), 3.57 (d, J = 13.1 Hz, 1H), 2.99 (d, J = 8.0 Hz, 1H), 2.68 (q, J = 7.2 Hz, 1H), 2.03 (h, J

= 7.6 Hz, 1H), 1.90 – 1.77 (m, 2H), 1.69 – 1.44 (m, 6H), 1.43 – 1.29 (m, 2H), 1.29 – 1.18 (m, 1H), 1.12 (d, $J = 7.3$ Hz, 3H), 1.00 – 0.92 (m, 6H).

^{13}C NMR (101 MHz, Methanol- d_4) δ 177.6, 176.0, 174.5, 140.9, 129.5, 129.4, 128.2, 66.9, 59.4, 53.0, 44.9, 41.7 ($\underline{\text{CHB}}$ (broad)), 39.8, 37.4, 30.6, 30.1, 26.3, 26.2, 26.0, 16.0, 15.8, 11.1.

HR-MS (ESI/TOF) calcd for $\text{C}_{24}\text{H}_{39}\text{BN}_4\text{O}_5\text{Na}$ [$\text{M}+\text{Na}$] $^+$ 497.2911, found 497.2912



((3S,6S,12R)-6-((S)-sec-butyl)-3-cyclopentyl-4,7,10-trioxo-1-(pyridin-2-yl)-2,5,8,11-tetraazatridecan-12-yl) boronic acid (83r)

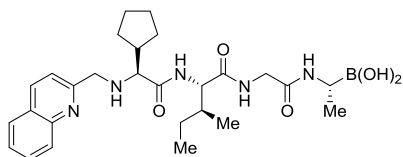
Prepared in analogy to **84a**: a solution of **83r** (78 mg, 0.128 mmol) in MeOH/*n*-hexane (1:1,

5 mL) was treated with isobutylboronic acid (52 mg, 0.51 mmol) and 1 M HCl (320 μL). Yield: 38 mg (62%, white solid).

^1H NMR (400 MHz, Methanol- d_4) δ 8.48 (ddd, $J = 5.0, 1.8, 1.0$ Hz, 1H), 7.80 (td, $J = 7.6, 1.8$ Hz, 1H), 7.51 (dt, $J = 8.0, 1.2$ Hz, 1H), 7.30 (ddd, $J = 7.6, 4.9, 1.4$ Hz, 1H), 4.22 (dd, $J = 17.5, 1.6$ Hz, 1H), 4.14 (d, $J = 7.9$ Hz, 1H), 3.99 (dd, $J = 17.5, 1.0$ Hz, 1H), 3.89 (d, $J = 14.2$ Hz, 1H), 3.74 (d, $J = 14.2$ Hz, 1H), 3.01 (d, $J = 8.1$ Hz, 1H), 2.66 (q, $J = 7.2$ Hz, 1H), 2.15 – 2.01 (m, 1H), 1.90 – 1.79 (m, 2H), 1.68 – 1.49 (m, 6H), 1.44 – 1.35 (m, 2H), 1.27 – 1.17 (m, 1H), 1.11 (d, $J = 7.2$ Hz, 3H), 0.97 (d, $J = 6.8$ Hz, 3H), 0.93 (t, $J = 7.5$ Hz, 3H).

^{13}C NMR (101 MHz, Methanol- d_4) δ 177.4, 176.2, 174.6, 160.6, 149.7, 138.7, 124.2, 123.7, 67.4, 59.6, 54.0, 45.0, 41.8 ($\underline{\text{CHB}}$ (broad)), 39.6, 37.5, 30.5, 30.2, 26.3, 26.2, 26.1, 15.9, 15.8, 11.2.

HR-MS (ESI/TOF) calcd for $\text{C}_{23}\text{H}_{38}\text{BN}_5\text{O}_5\text{Na}$ [$\text{M}+\text{Na}$] $^+$ 498.2864, found 498.2870



((3S,6S,12R)-6-((S)-sec-butyl)-3-cyclopentyl-4,7,10-trioxo-1-(quinolin-2-yl)-2,5,8,11-tetraazatridecan-12-yl) boronic acid (84s)

Prepared in analogy to **84a**: a solution of **83s** (68 mg, 0.103 mmol) in MeOH/*n*-hexane (1:1,

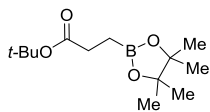
4 mL) was treated with isobutylboronic acid (42 mg, 0.41 mmol) and 1 M HCl (260 μL). Yield: 45 mg (83%, white solid).

^1H NMR (400 MHz, Methanol- d_4) δ 8.30 (dd, $J = 8.6, 0.8$ Hz, 1H), 8.00 (dq, $J = 8.6, 1.0$ Hz, 1H), 7.91 (dd, $J = 8.2, 1.7$ Hz, 1H), 7.75 (ddd, $J = 8.5, 6.9, 1.5$ Hz, 1H), 7.65 (d, $J = 8.6$ Hz, 1H), 7.57 (ddd, $J = 8.1, 6.9, 1.3$ Hz, 1H), 4.22 (dd, $J = 17.5, 1.7$ Hz, 1H), 4.13 – 4.06 (m, 2H), 3.99 (dd, $J = 17.5, 1.0$ Hz, 1H), 3.94 (d, $J = 14.7$ Hz, 1H), 3.06 (d, $J = 8.0$ Hz, 1H), 2.67 (q, $J = 7.2$ Hz, 1H), 2.11 (h, $J = 7.5$ Hz, 1H), 1.95 – 1.84 (m, 1H), 1.84 – 1.74 (m, 1H), 1.69 – 1.50 (m, 6H), 1.49 – 1.37 (m, 2H), 1.26 – 1.12 (m, 1H), 1.12 (d, $J = 7.2$ Hz, 3H), 0.95 (d, $J = 6.9$ Hz, 3H), 0.90 (t, $J = 7.5$ Hz, 3H).

^{13}C NMR (101 MHz, Methanol- d_4) δ 177.5, 176.2, 174.6, 161.6, 148.5, 138.5, 131.0, 129.0, 128.9, 127.6, 122.0, 67.4, 59.6, 54.6, 45.0, 41.8 ($\underline{\text{CHB}}$ (broad)), 39.7, 37.5, 30.6, 30.2, 26.34, 26.25, 26.1, 15.9, 15.8, 11.2.

HR-MS (ESI/TOF) calcd for $\text{C}_{27}\text{H}_{40}\text{BN}_5\text{O}_5\text{Na}$ [$\text{M}+\text{Na}$] $^+$ 548.3020, found 548.2994

3.4 Synthesis of the peptidic boronic acids with a modified P5 and P1 position

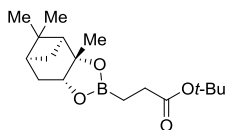


tert-Butyl 3-(4,4,5,5-tetramethyl-1,3,2-dioxaborolan-2-yl)propanoate (**85**)

According to literature procedure⁴⁵: CuCl (21 mg, 0.212 mmol), NaOt-Bu (60 mg, 0.624 mmol) and DPEphos ligand (8.1 mg, 0.015 mmol) were placed in an oven-dried flask and THF (5.5 mL) were added under argon. The reaction mixture was stirred for 30 min at room temperature and then, bis(pinacolato)diboron in THF (4 mL) were added. The reaction mixture was stirred for 10 min and *tert*-butyl acrylate (1 mL, 6.89 mmol) was added, followed by MeOH (600 μ L, 14.83 mmol). The reaction was sealed and stirred until no starting material was detected by TLC. The reaction mixture was filtered through a pad of Celite, concentrated and purified by flash chromatography on silica gel eluting with hexane:EtOAc 8:1 to provide boronic ester **85** as a colorless liquid (1.665 g, 94%).

¹H NMR (300 MHz, Chloroform-*d*) δ 2.34 (t, $J = 7.5$ Hz, 2H), 1.43 (s, 9H), 1.23 (s, 12H), 0.96 (t, $J = 7.5$ Hz, 2H).

The spectral data was identical to that reported in the literature^{49,50}



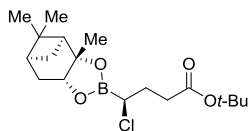
tert-Butyl 3-((3a*S*,4*S*,6*S*,7a*R*)-3a,5,5-trimethylhexahydro-4,6-methanobenzo[*d*][1,3,2]dioxaborol-2-yl)propanoate (**68**)

To the solution of boronic ester **85** (1.353 g, 5.28 mmol, 1.0 equiv) in THF (10 mL) was added (+)-pinanediol (1.35 g, 7.93 mmol, 1.5 equiv). The mixture was stirred for 15 hours at room temperature. Then the solution was evaporated and crude mixture was purified by flash chromatography on silica gel eluting with hexane:EtOAc (20:1) – hexane:EtOAc (8:1) to provide **68** (1.615 g, 99%) as a colorless oil.

¹H NMR (300 MHz, , Chloroform-*d*) δ 4.26 (dd, $J = 8.8, 2.0$ Hz, 1H), 2.40 – 2.26 (m, 3H), 2.24 – 2.14 (m, 1H), 2.05 – 1.99 (m, 1H), 1.93 – 1.78 (m, 2H), 1.43 (s, 9H), 1.37 (s, 3H), 1.28 (s, 3H), 1.18 (d, $J = 10.8$ Hz, 1H), 1.02 (t, $J = 7.5$ Hz, 2H), 0.83 (s, 3H).

¹³C NMR (101 MHz, Chloroform-*d*) δ 174.2, 85.7, 80.0, 77.9, 51.4, 39.6, 38.3, 35.6, 30.2, 28.7, 28.3, 27.2, 26.5, 24.2.

Spectral data are in accordance with those reported in the literature²²



(+)-Pinanediol (1*S*)-(1-chloro)-3-(*tert*-butoxycarbonyl)propyl boronate (**69**)

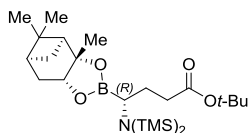
Slightly modified Matteson homologation procedure was used to synthesise α -chlorinated boronates⁵¹. A stirred solution of anhydrous dichloromethane (1.4 mL, 21.8 mmol, 5.0 equiv) in anhydrous tetrahydrofuran (25 mL) was cooled in liquid nitrogen/ethanol bath to -100 °C and treated with 2.5 M *n*-buthyllithium (2.6 mL, 6.5 mmol, 1.5 equiv) over a period of 30 min (under argon). After 20 min to the resulting mixture a solution of pinanediol alkylboronate **68** (1.318 g, 4.28 mmol, 1.0 equiv) in anhydrous tetrahydrofuran (15 mL) was added dropwise and the reaction mixture was stirred for 30 min at -100 °C. Then 1 M ZnCl₂ (7.7 mL, 7.7 mmol,

1.8 equiv) was added slowly. The cooling bath was removed and the reaction was allowed to warm to room temperature. After stirring overnight diethyl ether was added to the reaction mixture and the suspension obtained was washed with a saturated ammonium chloride solution. The solvent was evaporated and the oily residue was dissolved in diethyl ether, washed with brine and organic phase was dried over Na₂SO₄, filtered and evaporated in vacuo. The residue was purified by flash chromatography on silica gel eluting with Hexane:EtOAc (20:1) – Hexane:EtOAc (8:1) to provide boronate **69** (1.124 g, 74%) as a colorless oil

¹H NMR (400 MHz, Chloroform-*d*) δ 4.36 (dd, *J* = 8.8, 2.0 Hz, 1H), 3.52 (dd, *J* = 9.2, 5.2 Hz, 1H), 2.53 – 2.41 (m, 2H), 2.40 – 2.30 (m, 1H), 2.28 – 2.13 (m, 2H), 2.10 – 2.00 (m, 2H), 1.95 – 1.86 (m, 2H), 1.44 (s, 9H), 1.42 (s, 3H), 1.29 (s, 3H), 1.16 (d, *J* = 11.1 Hz, 1H), 0.84 (s, 3H).

¹³C NMR (101 MHz, Chloroform-*d*) δ 172.3, 86.8, 80.4, 78.6, 51.2, 42.5 (C_{HB} (broad)), 39.4, 38.2, 35.2, 33.0, 29.3, 28.4, 28.1, 27.0, 26.4, 26.3, 24.0.

Spectral data are in accordance with those reported in the literature²²

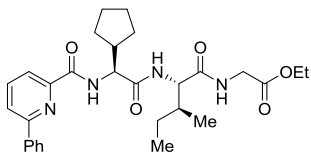


(+)-Pinanediol (1R)-(1-bistrimethylsilylamino)-3-(tert-butoxycarbonyl) propyl boronate (54f)

To the solution of α-chloroboronic acid ester **69** (1.124 g, 3.15 mmol, 1 equiv) in anhydrous tetrahydrofuran (20 mL) 1 M lithium bis(trimethylsilyl)amide (3.5 mL, 3.5 mmol, 1.1 equiv) was slowly added at –78 °C. The mixture was allowed to warm up and stirred overnight at room temperature. The solvent was removed in vacuo and hexane (50 mL) was added to the residue. The inorganic precipitates were filtered off through a pad of Celite, and then washed with additional amount of hexane, and filtrate was evaporated to provide **54f** (1.31 g, 86%) as a colourless oil.

¹H NMR (400 MHz, Chloroform-*d*) δ 4.28 (dd, *J* = 8.7, 1.9 Hz, 1H), 2.55 (dd, *J* = 9.1, 6.8 Hz, 1H), 2.44 – 2.14 (m, 4H), 2.02 (dd, *J* = 6.1, 4.9 Hz, 1H), 1.99 – 1.92 (m, 1H), 1.92 – 1.81 (m, 2H), 1.77 – 1.66 (m, 1H), 1.44 (s, 9H), 1.37 (s, 3H), 1.28 (s, 3H), 1.11 (d, *J* = 10.8 Hz, 1H), 0.83 (s, 3H), 0.11 (s, 18H).

¹³C NMR (101 MHz, Chloroform-*d*) δ 173.8, 85.6, 79.9, 78.5, 51.5, 39.6, 38.3, 35.5, 33.8, 30.5, 28.5, 28.3, 27.2, 26.5, 24.1, 3.1. (C_{HB} not visible)



Ethyl ((S)-2-cyclopentyl-2-(6-phenylpicolinamido) acetyl)-L-isoleucylglycinate (86a)

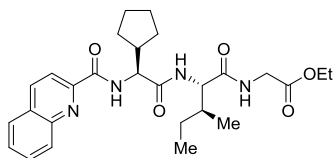
Starting material **78h** (400 mg, 0.91 mmol, 1.0 equiv) in CHCl₃ (5 mL) was treated with 4 M HCl in dioxane (900 μL, 3.6 mmol 4 equiv) until full deprotection of the protecting group. After solvent evaporation the crude mixture was utilized in the next step without purification. The residue (based on a theoretical yield of a 100%) under argon atmosphere was dissolved in dry CHCl₃ (15 mL), 6-phenylpicolinic acid (181 mg, 0.91 mmol, 1.0 equiv), EDC·HCl (208 mg, 1.09 mmol, 1.2 equiv), HOBt (135 mg, 1.0 mmol, 1.1 equiv) and DIPEA (470 μL, 2.72 mmol, 3.0 equiv) were added and mixture was stirred 3 h at room temperature, then diluted with chloroform, washed with 5%

KHSO₄ and brine. Organic phase was dried over Na₂SO₄, filtered and evaporated in vacuo. The residue was purified by flash chromatography on silica gel eluting with 1:1:1 Hex:EtOAc:CHCl₃ – 1:1 EtOAc:CHCl₃ to provide **86** (380 mg, 80%) as an amorphous solid.

¹H NMR (400 MHz, Chloroform-*d*) δ 8.68 (d, *J* = 8.1 Hz, 1H), 8.13 (dd, *J* = 7.1, 1.5 Hz, 1H), 8.04 – 7.97 (m, 2H), 7.97 – 7.86 (m, 2H), 7.54 – 7.43 (m, 3H), 6.93 (d, *J* = 8.6 Hz, 1H), 6.76 (t, *J* = 5.4 Hz, 1H), 4.54 (t, *J* = 8.2 Hz, 1H), 4.40 (dd, *J* = 8.6, 6.3 Hz, 1H), 4.19 (q, *J* = 7.1 Hz, 2H), 4.13 – 3.95 (m, 2H), 2.55 (h, *J* = 8.3 Hz, 1H), 2.03 – 1.95 (m, 1H), 1.90 – 1.79 (m, 2H), 1.71 – 1.55 (m, 4H), 1.52 – 1.36 (m, 3H), 1.26 (t, *J* = 7.2 Hz, 3H), 1.16 – 1.04 (m, 1H), 0.91 (d, *J* = 6.8 Hz, 3H), 0.83 (t, *J* = 7.4 Hz, 3H).

¹³C NMR (101 MHz, Chloroform-*d*) δ 171.7, 171.3, 169.7, 165.1, 156.3, 149.1, 138.5, 138.3, 129.7, 129.1, 127.1, 123.5, 120.9, 61.6, 57.95, 57.90, 41.9, 41.5, 36.8, 29.8, 29.1, 25.6, 25.4, 24.8, 15.6, 14.3, 11.5.

HR-MS (ESI/TOF) calcd for C₂₉H₃₉N₄O₅ [M+H]⁺ 523.2920, found 523.2925



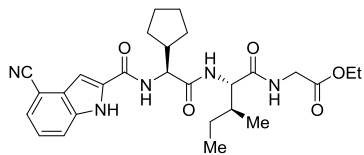
Ethyl ((S)-2-cyclopentyl-2-(quinoline-2-carboxamido)acetyl)-L-isoleucylglycinate (86b**)**

Prepared in analogues way as **86a**: starting material **78h** (400 mg, 0.91 mmol) and 4 M HCl in dioxane (1 mL) in CHCl₃ (5 mL). Coupling: quinoline-2-carboxylic acid (157 mg, 0.91 mmol), EDC·HCl (208 mg, 1.09 mmol), HOBt (135 mg, 1 mmol) and DIPEA (470 μL, 2.72 mmol) in CHCl₃ (20 mL). Yield: 358 mg (80%, amorphous solid).

¹H NMR (400 MHz, Chloroform-*d*) δ 8.75 (d, *J* = 8.2 Hz, 1H), 8.31 (dd, *J* = 8.5, 0.7 Hz, 1H), 8.28 (d, *J* = 8.5 Hz, 1H), 8.13 (dd, *J* = 8.5, 1.1 Hz, 1H), 7.87 (dd, *J* = 8.2, 1.8 Hz, 1H), 7.77 (ddd, *J* = 8.5, 6.8, 1.4 Hz, 1H), 7.62 (ddd, *J* = 8.1, 6.9, 1.3 Hz, 1H), 6.93 (d, *J* = 8.6 Hz, 1H), 6.75 (t, *J* = 5.4 Hz, 1H), 4.56 (t, *J* = 8.4 Hz, 1H), 4.41 (dd, *J* = 8.6, 6.3 Hz, 1H), 4.19 (q, *J* = 7.2 Hz, 2H), 4.13 – 3.95 (m, 2H), 2.57 (h, *J* = 8.5 Hz, 1H), 2.03 – 1.94 (m, 1H), 1.92 – 1.80 (m, 2H), 1.72 – 1.54 (m, 4H), 1.53 – 1.38 (m, 3H), 1.26 (t, *J* = 7.2 Hz, 3H), 1.17 – 1.04 (m, 1H), 0.90 (d, *J* = 6.8 Hz, 3H), 0.81 (t, *J* = 7.4 Hz, 3H).

¹³C NMR (101 MHz, Chloroform-*d*) δ 171.8, 171.3, 169.7, 165.1, 149.1, 146.7, 137.7, 130.3, 130.1, 129.6, 128.2, 127.8, 118.9, 61.6, 58.1, 58.0, 42.0, 41.5, 36.8, 29.8, 29.2, 25.6, 25.3, 24.8, 15.6, 14.3, 11.5.

HR-MS (ESI/TOF) calcd for C₂₇H₃₇N₄O₅ [M+H]⁺ 497.2764, found 497.2770



Ethyl ((S)-2-(4-cyano-1H-indole-2-carboxamido)-2-cyclopentylacetyl)-L-isoleucylglycinate (86c**)**

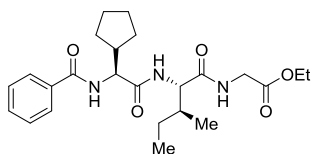
Prepared in analogues way as **86a**: starting material **78h** (218 mg, 0.49 mmol) and 4 M HCl in dioxane (500 μL) in CHCl₃ (3 mL). Coupling: 4-cyano-1H-indole-2-carboxylic acid (97 mg, 0.49 mmol), EDC·HCl (114 mg, 0.59 mmol), HOBt (74 mg, 0.55 mmol) and DIPEA (260 μL, 1.50 mmol) in CHCl₃ (15 mL). Yield: 169 mg (67%, amorphous solid).

¹H NMR (400 MHz, Chloroform-*d*) δ 11.92 (br s, 1H), 9.33 (br s, 1H), 8.78 (br s, 1H), 8.26 (d, *J* = 9.7 Hz, 1H), 7.77 (d, *J* = 8.2 Hz, 1H), 7.44 (dd, *J* = 7.3, 1.0 Hz, 1H), 7.39 (d, *J* = 2.0 Hz, 1H), 7.38 – 7.30 (m, 1H), 5.34 (t, *J* = 9.9 Hz, 1H), 4.93 (t, *J* = 9.7 Hz, 1H), 4.80

(dd, $J = 18.5, 7.8$ Hz, 1H), 4.41 (q, $J = 7.1$ Hz, 2H), 3.97 (dd, $J = 18.8, 2.2$ Hz, 1H), 2.39 – 2.27 (m, 1H), 1.85 – 1.42 (m, 10H), 1.37 (t, $J = 7.2$ Hz, 3H), 1.30 – 1.20 (m, 1H), 0.51 (br s, 3H), 0.19 (br s, 3H).

^{13}C NMR (101 MHz, Chloroform- d) δ 173.5, 172.3, 171.0, 160.9, 136.7, 132.5, 128.6, 126.1, 124.0, 118.6, 118.0, 104.0, 101.5, 62.5, 57.4, 56.9, 43.8, 41.7, 37.5, 29.6, 29.5, 25.5, 25.2, 24.9, 15.0, 14.3, 11.5.

HR-MS (ESI/TOF) calcd for $\text{C}_{27}\text{H}_{36}\text{N}_5\text{O}_5$ $[\text{M}+\text{H}]^+$ 510.2716, found 510.2714



Ethyl ((S)-2-benzamido-2-cyclopentylacetyl)-L-isoleucyl-glycinate (86d)

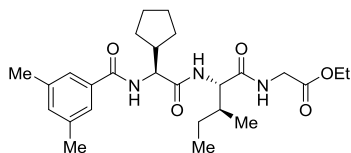
Prepared in analogues way as **86a**: starting material **78h** (250 mg, 0.57 mmol) and 4 M HCl in dioxane (580 μL) in CHCl_3 (5 mL). Coupling: benzoic acid (73 mg,

0.60 mmol), EDC·HCl (130 mg, 0.68 mmol), HOBt (84 mg, 0.62 mmol) and DIPEA (300 μL , 1.73 mmol) in CHCl_3 (10 mL). Yield: 242 mg (96%, amorphous solid).

^1H NMR (400 MHz, Methanol- d_4) δ 7.79 – 7.75 (m, 2H), 7.52 – 7.46 (m, 1H), 7.44 – 7.37 (m, 2H), 4.48 – 4.42 (m, 1H), 4.26 – 4.22 (m, 1H), 4.15 (q, $J = 7.2$ Hz, 2H), 4.03 (d, $J = 17.8$ Hz, 1H), 3.84 (d, $J = 17.8$ Hz, 1H), 2.30 (h, $J = 8.7$ Hz, 1H), 1.89 – 1.73 (m, 2H), 1.72 – 1.58 (m, 3H), 1.58 – 1.43 (m, 3H), 1.38 – 1.26 (m, 2H), 1.23 (t, $J = 7.2$ Hz, 3H), 1.18 – 1.05 (m, 1H), 0.90 (d, $J = 6.8$ Hz, 3H), 0.82 (t, $J = 7.5$ Hz, 3H).

^{13}C NMR (101 MHz, Methanol- d_4) δ 172.5, 171.9, 169.5, 168.3, 133.6, 131.6, 128.3, 127.0, 61.2, 57.8, 57.6, 42.1, 40.9, 36.6, 29.16, 29.12, 25.1, 24.7, 24.4, 14.9, 13.7, 10.6.

HR-MS (ESI/TOF) calcd for $\text{C}_{24}\text{H}_{36}\text{N}_3\text{O}_5$ $[\text{M}+\text{H}]^+$ 446.2655, found 446.2666



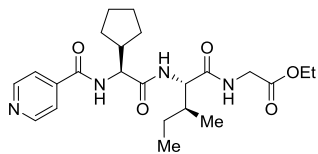
Ethyl ((S)-2-cyclopentyl-2-(3,5-dimethylbenzamido)acetyl)-L-isoleucyl-glycinate (86e)

Prepared in analogues way as **86a**: starting material **78h** (300 mg, 0.68 mmol) and 4 M HCl in dioxane (680 μL) in CHCl_3 (5 mL). Coupling: 3,5-dimethylbenzoic acid (102 mg, 0.68 mmol), EDC·HCl (156 mg, 0.81 mmol), HOBt (101 mg, 0.75 mmol) and DIPEA (350 μL , 2.02 mmol) in CHCl_3 (20 mL). Yield: 302 mg (94%, amorphous solid).

^1H NMR (400 MHz, Chloroform- d) δ 7.37 (s, 2H), 7.13 (s, 1H), 6.85 (d, $J = 8.7$ Hz, 1H), 6.80 (d, $J = 8.1$ Hz, 1H), 6.69 (t, $J = 5.4$ Hz, 1H), 4.54 (t, $J = 8.6$ Hz, 1H), 4.39 (dd, $J = 8.6, 6.4$ Hz, 1H), 4.20 (q, $J = 7.2$ Hz, 2H), 4.10 (dd, $J = 18.2, 5.6$ Hz, 1H), 3.97 (dd, $J = 18.3, 4.9$ Hz, 1H), 2.43 – 2.30 (m, 7H), 2.00 – 1.90 (m, 1H), 1.84 – 1.74 (m, 2H), 1.68 – 1.46 (m, 5H, overlaps with H_2O in CHCl_3), 1.43 – 1.32 (m, 2H), 1.27 (t, $J = 7.2$ Hz, 3H), 1.19 – 1.06 (m, 1H), 0.91 (d, $J = 6.8$ Hz, 3H), 0.85 (t, $J = 7.4$ Hz, 3H).

^{13}C NMR (101 MHz, Chloroform- d) δ 172.0, 171.2, 169.7, 168.2, 138.5, 134.0, 133.5, 125.0, 61.7, 58.0, 57.9, 42.4, 41.5, 37.1, 29.8, 29.2, 25.5, 25.2, 24.9, 21.3, 15.6, 14.3, 11.5.

HR-MS (ESI/TOF) calcd for $\text{C}_{26}\text{H}_{40}\text{N}_3\text{O}_5$ $[\text{M}+\text{H}]^+$ 474.2968, found 474.2951



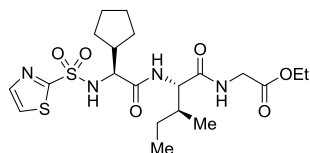
Ethyl ((S)-2-cyclopentyl-2-(isonicotinamido)acetyl)-L-isoleucylglycinate (86f)

Prepared in analogues way as **86a**: starting material **78h** (250 mg, 0.57 mmol) and 4 M HCl in dioxane (570 μ L) in CHCl_3 (5 mL). Coupling: isonicotinic acid (75 mg, 0.61 mmol), EDC·HCl (130 mg, 0.68 mmol), HOBt (84 mg, 0.62 mmol) and DIPEA (300 μ L, 1.73 mmol) in CHCl_3 (20 mL). Yield: 240 mg (95%, amorphous solid).

^1H NMR (400 MHz, Methanol- d_4) δ 8.73 – 8.65 (m, 2H), 7.82 – 7.76 (m, 2H), 4.43 (d, J = 10.0 Hz, 1H), 4.31 (d, J = 8.0 Hz, 1H), 4.17 (q, J = 7.1 Hz, 2H), 4.02 (d, J = 17.5 Hz, 1H), 3.85 (d, J = 17.5 Hz, 1H), 2.44 – 2.29 (m, 1H), 1.93 – 1.82 (m, 2H), 1.76 – 1.53 (m, 6H), 1.46 – 1.32 (m, 2H), 1.26 (t, J = 7.2 Hz, 3H), 1.23 – 1.14 (m, 1H), 0.97 (d, J = 6.9 Hz, 3H), 0.89 (t, J = 7.5 Hz, 3H).

^{13}C NMR (101 MHz, Methanol- d_4) δ 173.9, 173.7, 170.9, 167.9, 150.9, 143.7, 123.1, 62.2, 60.0, 59.0, 43.0, 42.0, 38.2, 30.9, 30.5, 26.3, 25.9, 25.8, 15.8, 14.5, 11.3.

HR-MS (ESI/TOF) calcd for $\text{C}_{23}\text{H}_{35}\text{N}_4\text{O}_5$ $[\text{M}+\text{H}]^+$ 447.2607, found 447.2612



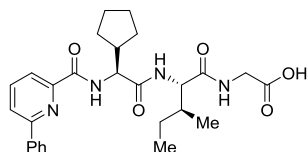
Ethyl ((S)-2-cyclopentyl-2-(thiazole-2-sulfonamido)acetyl)-L-isoleucylglycinate (86g)

Prepared in analogues way as **83o**: starting material **78h** (250 mg, 0.57 mmol) and 4 M HCl in dioxane (600 μ L) in CHCl_3 (5 mL). Sulfonation: thiazole-2-sulfonyl chloride (156 mg, 0.85 mmol) and DIPEA (300 μ L, 1.73 mmol) in CHCl_3 (10 mL). Yield: 246 mg (89%, amorphous solid).

^1H NMR (400 MHz, Dimethylsulfoxide- d_6) δ 8.61 (d, J = 8.9 Hz, 1H), 8.31 (t, J = 5.9 Hz, 1H), 8.06 (d, J = 3.1 Hz, 1H), 7.95 (d, J = 3.1 Hz, 1H), 7.88 (d, J = 8.7 Hz, 1H), 4.10 – 4.03 (m, 3H), 3.92 – 3.81 (m, 2H), 3.73 (dd, J = 17.3, 5.7 Hz, 1H), 2.07 (h, J = 8.2 Hz, 1H), 1.66 – 1.58 (m, 1H), 1.56 – 1.27 (m, 8H), 1.17 (t, J = 7.1 Hz, 3H), 1.13 – 1.07 (m, 1H), 1.06 – 0.96 (m, 1H), 0.84 – 0.77 (m, 6H).

^{13}C NMR (101 MHz, Dimethylsulfoxide- d_6) δ 176.3, 175.2, 174.8, 171.3, 149.2, 131.0, 65.6, 65.1, 61.7, 47.6, 45.9, 42.0, 33.49, 33.46, 30.0, 29.6, 29.4, 20.3, 19.2, 16.3.

HR-MS (ESI/TOF) calcd for $\text{C}_{20}\text{H}_{33}\text{N}_4\text{O}_6\text{S}$ $[\text{M}+\text{H}]^+$ 489.1842, found 489.1860



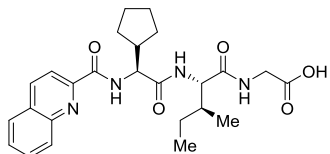
((S)-2-cyclopentyl-2-(6-phenylpicolinamido)acetyl)-L-isoleucylglycine (87a)

Prepared in analogues way as **S2c**: starting material **86a** (295 mg, 0.56 mmol) and LiOH (124 mg, 5.18 mmol) added to the mixture THF:H₂O (20:1, 11 mL). Yield: 273 mg (98%, white solid).

^1H NMR (400 MHz, Methanol- d_4) δ 8.16 – 8.11 (m, 2H), 8.10 – 8.01 (m, 3H), 7.55 – 7.43 (m, 3H), 4.61 (d, J = 8.3 Hz, 1H), 4.32 (d, J = 8.0 Hz, 1H), 3.99 (d, J = 17.6 Hz, 1H), 3.83 (d, J = 17.6 Hz, 1H), 2.45 (h, J = 8.3 Hz, 1H), 1.93 – 1.74 (m, 4H), 1.71 – 1.54 (m, 4H), 1.52 – 1.41 (m, 2H), 1.25 – 1.13 (m, 1H), 0.97 (d, J = 6.8 Hz, 3H), 0.88 (t, J = 7.5 Hz, 3H).

^{13}C NMR (101 MHz, Methanol- d_4) δ 173.8, 173.7, 172.9, 166.2, 157.6, 150.3, 139.9, 139.4, 130.7, 129.9, 128.0, 124.5, 121.6, 59.1, 58.2, 44.2, 42.0, 38.1, 30.4, 30.0, 26.4, 26.1, 25.9, 15.8, 11.3.

HR-MS (ESI/TOF) calcd for $\text{C}_{27}\text{H}_{35}\text{N}_4\text{O}_5$ $[\text{M}+\text{H}]^+$ 495.2607, found 495.2619



((S)-2-cyclopentyl-2-(quinoline-2-carboxamido)acetyl)-L-isoleucylglycine (87b)

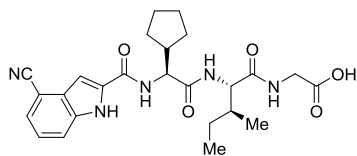
Prepared in analogues way as **S2c**: starting material **86b** (345 mg, 0.69 mmol) and LiOH (166 mg, 6.93 mmol) added to the mixture THF:H₂O (20:1, 10.5 mL). Yield:

314 mg (97%, white solid).

^1H NMR (400 MHz, Methanol- d_4) δ 8.48 (d, J = 8.6 Hz, 1H), 8.18 (t, J = 8.5 Hz, 1H), 8.00 (dd, J = 8.2, 1.7 Hz, 1H), 7.84 (ddd, J = 8.5, 6.9, 1.5 Hz, 1H), 7.69 (ddd, J = 8.2, 6.9, 1.2 Hz, 1H), 4.60 (d, J = 8.7 Hz, 1H), 4.32 (d, J = 8.0 Hz, 1H), 3.98 (d, J = 17.6 Hz, 1H), 3.84 (d, J = 17.6 Hz, 1H), 2.46 (h, J = 8.6 Hz, 1H), 1.93 – 1.82 (m, 2H), 1.81 – 1.66 (m, 3H), 1.66 – 1.54 (m, 3H), 1.54 – 1.42 (m, 2H), 1.25 – 1.13 (m, 1H), 0.96 (d, J = 6.8 Hz, 3H), 0.88 (t, J = 7.5 Hz, 3H).

^{13}C NMR (101 MHz, Methanol- d_4) δ 173.8, 173.7 (overlaps two C=O), 166.3, 150.5, 148.0, 139.1, 131.6, 130.9, 130.8, 129.4, 129.0, 119.5, 59.1, 58.6, 44.2, 42.2, 38.1, 30.4, 30.2, 26.3, 26.0, 25.9, 15.8, 11.3.

HR-MS (ESI/TOF) calcd for $\text{C}_{25}\text{H}_{33}\text{N}_4\text{O}_5$ $[\text{M}+\text{H}]^+$ 469.2451, found 469.2449



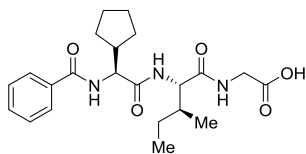
((S)-2-(4-cyano-1H-indole-2-carboxamido)-2-cyclopentylacetyl)-L-isoleucylglycine (87c)

Prepared in analogues way as **S2c**: starting material **86c** (156 mg, 0.31 mmol) and LiOH (73 mg, 3.06 mmol) added to the mixture THF:H₂O (20:1,

10.5 mL). Yield: 132 mg (90%, white solid).

After evaporation compound was used in the next reaction without characterization.

UPLC-MS (ESI) calcd for $\text{C}_{19}\text{H}_{36}\text{N}_3\text{O}_6$ $[\text{M}+\text{H}]^+$ 402.51, found 402.55



((S)-2-benzamido-2-cyclopentylacetyl)-L-isoleucylglycine (87d)

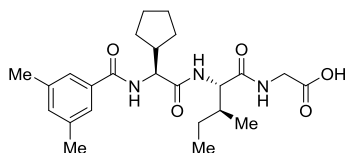
Prepared in analogues way as **S2c**: starting material **86d** (230 mg, 0.52 mmol) and LiOH (124 mg, 5.18 mmol) added to the mixture THF:H₂O (20:1, 42 mL). Yield:

179 mg (83%, white solid).

^1H NMR (400 MHz, Methanol- d_4) δ 7.88 – 7.79 (m, 2H), 7.57 – 7.51 (m, 1H), 7.45 (t, J = 7.6 Hz, 2H), 4.44 (d, J = 9.9 Hz, 1H), 4.32 (d, J = 7.9 Hz, 1H), 4.04 – 3.96 (m, 1H), 3.88 – 3.81 (m, 1H), 2.38 (h, J = 8.2 Hz, 1H), 1.94 – 1.83 (m, 2H), 1.78 – 1.64 (m, 3H), 1.63 – 1.54 (m, 3H), 1.48 – 1.32 (m, 2H), 1.21 – 1.13 (m, 1H), 0.96 (d, J = 6.8 Hz, 3H), 0.88 (t, J = 7.4 Hz, 3H).

^{13}C NMR (101 MHz, Methanol- d_4) δ 174.2, 173.9, 172.5, 170.3, 135.4, 132.8, 129.5, 128.5, 59.8, 59.0, 43.0, 41.8, 38.3, 30.8, 30.5, 26.3, 25.9, 25.8, 15.8, 11.4.

HR-MS (ESI/TOF) calcd for $C_{22}H_{31}N_3O_5Na$ $[M+Na]^+$ 440.2161, found 440.2168



((S)-2-cyclopentyl-2-(3,5-dimethylbenzamido)acetyl)-L-isoleucylglycine (87e)

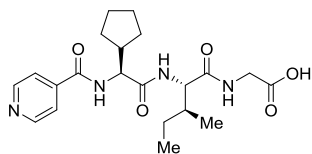
Prepared in analogues way as **S2c**: starting material **86e** (282 mg, 0.60 mmol) and LiOH (143 mg, 5.97 mmol) added to the mixture THF:H₂O (20:1, 31.5 mL). Yield:

225 mg (85%, white solid).

¹H NMR (400 MHz, Dimethylsulfoxide-*d*₆) δ 12.50 (s, 1H), 8.35 (d, *J* = 8.5 Hz, 1H), 8.27 (t, *J* = 5.8 Hz, 1H), 7.75 (d, *J* = 9.1 Hz, 1H), 7.44 (d, *J* = 1.7 Hz, 2H), 7.16 (s, 1H), 4.32 (dd, *J* = 9.7, 8.4 Hz, 1H), 4.24 (dd, *J* = 9.1, 7.2 Hz, 1H), 3.79 (dd, *J* = 17.5, 5.9 Hz, 1H), 3.70 (dd, *J* = 17.5, 5.8 Hz, 1H), 2.38 – 2.27 (m, 7H), 1.79 – 1.66 (m, 2H), 1.64 – 1.53 (m, 3H), 1.52 – 1.40 (m, 3H), 1.40 – 1.31 (m, 1H), 1.31 – 1.19 (m, 1H), 1.15 – 1.01 (m, 1H), 0.83 (d, *J* = 6.8 Hz, 3H), 0.79 (t, *J* = 7.4 Hz, 3H).

¹³C NMR (101 MHz, Dimethylsulfoxide-*d*₆) δ 171.2, 171.1, 171.0, 166.6, 137.4, 134.4, 132.5, 125.2, 57.7, 56.4, 41.3, 40.6, 37.0, 29.3, 28.9, 25.0, 24.6, 24.1, 20.8, 15.2, 11.0.

HR-MS (ESI/TOF) calcd for $C_{24}H_{36}N_3O_5$ $[M+H]^+$ 446.2655, found 446.2655



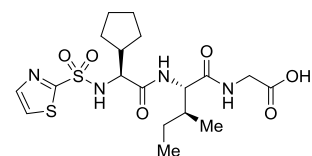
((S)-2-cyclopentyl-2-(isonicotinamido)acetyl)-L-isoleucylglycine (87f)

Prepared in analogues way as **S2c**: starting material **86f** (230 mg, 0.51 mmol) and LiOH (124 mg, 5.18 mmol) added to the mixture THF:H₂O (20:1, 31.5 mL). Yield:

213 mg (99%, white solid).

¹H NMR (300 MHz, Dimethylsulfoxide-*d*₆) δ 12.53 (s, 1H), 8.88 (d, *J* = 8.4 Hz, 1H), 8.76 – 8.68 (m, 2H), 8.30 (t, *J* = 6.0 Hz, 1H), 7.99 – 7.88 (m, 1H), 7.82 – 7.74 (m, 2H), 4.34 (dd, *J* = 9.8, 8.4 Hz, 1H), 4.22 (dd, *J* = 8.9, 7.4 Hz, 1H), 3.86 – 3.59 (m, 2H), 2.43 – 2.28 (m, 1H), 1.82 – 1.68 (m, 2H), 1.65 – 1.33 (m, 1H), 1.30 – 1.19 (m, 0H), 1.16 – 1.01 (m, 1H), 0.84 (d, *J* = 6.8 Hz, 3H), 0.79 (t, *J* = 7.4 Hz, 3H).

UPLC-MS (ESI) calcd for $C_{21}H_{31}N_4O_5$ $[M+H]^+$ 419.50, found 419.62



((S)-2-cyclopentyl-2-(thiazole-2-sulfonamido)acetyl)-L-isoleucylglycine (87g)

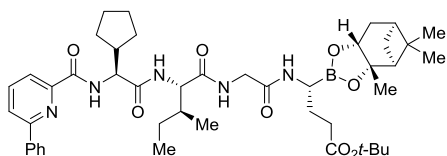
Prepared in analogues way as **S2c**: starting material **86g** (235 mg, 0.48 mmol) and LiOH (115 mg, 4.81 mmol) added to the mixture THF:H₂O (20:1, 21 mL). Yield:

213 mg (98%, white solid).

¹H NMR (400 MHz, Methanol-*d*₄) δ 7.95 (d, *J* = 3.1 Hz, 1H), 7.90 (d, *J* = 3.2 Hz, 1H), 4.14 (d, *J* = 7.9 Hz, 1H), 3.99 (d, *J* = 8.3 Hz, 1H), 3.97 (d, *J* = 17.6 Hz, 1H), 3.81 (d, *J* = 17.8 Hz, 1H), 2.18 (h, *J* = 8.7 Hz, 1H), 1.84 – 1.73 (m, 1H), 1.70 – 1.46 (m, 7H), 1.44 – 1.34 (m, 1H), 1.23 – 1.06 (m, 2H), 0.96 – 0.86 (m, 6H).

¹³C NMR (101 MHz, Methanol-*d*₄) δ 173.6, 173.2, 172.4, 168.0, 145.1, 126.4, 61.9, 59.0, 44.2, 41.7, 38.2, 30.0, 29.8, 26.2, 25.9, 25.8, 15.7, 11.5.

HR-MS (ESI/TOF) calcd for $C_{18}H_{29}N_4O_6S_2$ $[M+H]^+$ 461.1529, found 461.1527



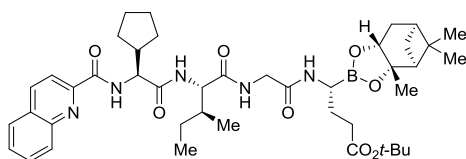
***tert*-Butyl (3*S*,6*S*,12*R*)-6-((*S*)-*sec*-butyl)-3-cyclopentyl-1,4,7,10-tetraoxo-1-(6-phenylpyridin-2-yl)-12-((3*aS*,4*S*,6*S*,7*aR*)-3*a*,5,5-trimethyl-hexa-hydro-4,6-methanobenzo[*d*][1,3,2]dioxaborol-2-yl)-2,5,8,11-tetraazapenta-decan-15-oate (88a)**

Prepared in analogy to **82**: **87a** (100 mg, 0.202 mmol) was mixed with **54f** (100 mg, 0.208 mmol) and DMAP (8 mg, 0.066 mmol) in anhydrous CHCl₃ (3 mL). The white suspension was cooled to -15 °C and then *N*-methylmorpholine (70 μL, 0.637 mmol, 3 equiv) and T₃P reagent (240 μL, 0.401 mmol, 2 equiv) was added. Yield: 64 mg (39%, amorphous solid).

¹H NMR (400 MHz, Methanol-*d*₄) δ 8.16 – 8.01 (m, 5H), 7.55 – 7.41 (m, 3H), 4.66 (d, *J* = 8.1 Hz, 1H), 4.34 (dd, *J* = 17.8, 1.7 Hz, 1H), 4.15 (dd, *J* = 8.7, 2.4 Hz, 1H), 3.98 (d, *J* = 8.6 Hz, 1H), 3.91 (d, *J* = 17.6 Hz, 1H), 2.61 – 2.54 (m, 1H), 2.51 – 2.44 (m, 1H), 2.41 – 2.28 (m, 3H), 2.19 – 2.07 (m, 1H), 1.95 (t, *J* = 5.5 Hz, 1H), 1.90 – 1.74 (m, 6H), 1.74 – 1.55 (m, 6H), 1.52 – 1.42 (m, 3H), 1.36 (s, 3H), 1.33 – 1.09 (m, 13H), 0.95 (dd, *J* = 7.1, 3.9 Hz, 6H), 0.86 (s, 3H).

¹³C NMR (101 MHz, Methanol-*d*₄) δ 176.4, 174.8, 174.4, 174.3, 166.3, 157.7, 150.5, 139.9, 139.5, 130.7, 130.0, 128.1, 124.6, 121.6, 84.3, 81.1, 77.3, 60.9, 57.6, 53.6, 44.4, 44.0 (CHB (broad)), 41.4, 40.0, 39.2, 37.7, 36.8, 34.4, 30.3, 29.9, 29.7, 28.3, 28.0, 27.8, 27.7, 26.7, 26.4, 26.1, 24.6, 15.7, 11.1.

HR-MS (ESI/TOF) calcd for C₄₅H₆₅BN₅O₈ [M+H]⁺ 814.4926, found 814.4910



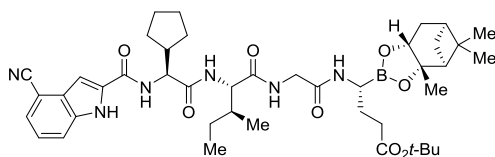
***tert*-Butyl (3*S*,6*S*,12*R*)-6-((*S*)-*sec*-butyl)-3-cyclopentyl-1,4,7,10-tetraoxo-1-(quinolin-2-yl)-12-((3*aS*,4*S*,6*S*,7*aR*)-3*a*,5,5-trimethyl-hexa-hydro-4,6-methanobenzo[*d*][1,3,2]-dioxaborol-2-yl)-2,5,8,11-tetraazapenta-decan-15-oate (88b)**

Prepared in analogy to **82**: **87b** (120 mg, 0.256 mmol) was mixed with **54f** (154 mg, 0.320 mmol) and DMAP (10 mg, 0.077 mmol) in anhydrous CHCl₃ (3 mL). The white suspension was cooled to -15 °C and then *N*-methylmorpholine (90 μL, 0.819 mmol) and T₃P reagent (310 μL, 0.518 mmol) was added. Yield: 111 mg (55%, amorphous solid).

¹H NMR (400 MHz, Methanol-*d*₄) δ 8.47 (dd, *J* = 8.6, 0.9 Hz, 1H), 8.19 (d, *J* = 8.6 Hz, 1H), 8.14 (dd, *J* = 8.5, 1.1 Hz, 1H), 8.02 – 7.97 (m, 1H), 7.83 (ddd, *J* = 8.5, 6.8, 1.4 Hz, 1H), 7.68 (ddd, *J* = 8.1, 6.9, 1.2 Hz, 1H), 4.65 (d, *J* = 8.6 Hz, 1H), 4.33 (dd, *J* = 17.6, 1.7 Hz, 1H), 4.16 (dd, *J* = 8.7, 2.4 Hz, 1H), 3.99 (d, *J* = 8.6 Hz, 1H), 3.92 (d, *J* = 17.8 Hz, 1H), 2.66 – 2.60 (m, 1H), 2.53 (t, *J* = 7.6 Hz, 2H), 2.50 – 2.42 (m, 1H), 2.38 – 2.29 (m, 1H), 2.17 – 2.10 (m, 1H), 1.98 – 1.56 (m, 14H), 1.53 – 1.42 (m, 3H), 1.36 (s, 3H), 1.32 (s, 9H), 1.28 (s, 3H), 0.98 – 0.90 (m, 6H), 0.86 (s, 3H).

¹³C NMR (101 MHz, Methanol-*d*₄) δ 176.4, 174.8, 174.5, 174.4, 166.4, 150.5, 148.0, 139.1, 131.6, 130.9, 129.4, 129.0, 119.6, 84.3, 81.2, 77.4, 60.8, 58.0, 53.6, 44.4, 44.1 (CHB (broad)), 41.4, 40.0, 39.2, 37.7, 36.8, 34.7, 30.2, 30.1, 29.6, 28.3, 27.8, 27.7, 26.7, 26.3, 26.0, 24.6, 15.7, 11.1.

HR-MS (ESI/TOF) calcd for C₄₃H₆₃BN₅O₈ [M+H]⁺ 788.4770, found 788.4771



tert-Butyl (3S,6S,12R)-6-((S)-sec-butyl)-1-(4-cyano-1H-indol-2-yl)-3-cyclopentyl-1,4,7,10-tetraoxo-12-((3aS,4S,6S,7aR)-3a,5,5-trimethylhexahydro-4,6-methano-

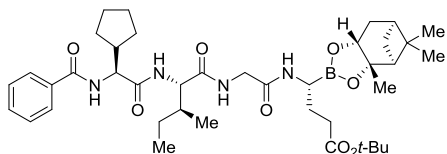
benzo[d][1,3,2]dioxaborol-2-yl)-2,5,8,11-tetraaza-pentadecan-15-oate (88c)

Prepared in analogy to **82**: **87c** (85 mg, 0.177 mmol) was mixed with **54f** (102 mg, 0.212 mmol) and DMAP (7 mg, 0.057 mmol) in anhydrous CHCl₃ (3 mL). The white suspension was cooled to -15 °C and then *N*-methylmorpholine (60 μL, 0.546 mmol) and T₃P reagent (21 μL, 0.351 mmol) was added. Yield: 93 mg (66%, amorphous solid).

¹H NMR (400 MHz, Methanol-*d*₄) δ 7.78 (dt, *J* = 8.3, 1.0 Hz, 1H), 7.52 (dd, *J* = 7.4, 1.0 Hz, 1H), 7.37 (d, *J* = 1.0 Hz, 1H), 7.35 (dd, *J* = 8.4, 7.3 Hz, 1H), 4.63 (d, *J* = 9.5 Hz, 1H), 4.39 (dd, *J* = 17.9, 1.8 Hz, 1H), 4.16 (dd, *J* = 8.6, 2.3 Hz, 1H), 3.95 (d, *J* = 8.7 Hz, 1H), 3.91 (d, *J* = 17.9 Hz, 1H), 2.76 – 2.66 (m, 1H), 2.57 – 2.49 (m, 2H), 2.39 – 2.30 (m, 2H), 2.18 – 2.09 (m, 1H), 2.05 – 1.93 (m, 2H), 1.91 – 1.76 (m, 5H), 1.75 – 1.63 (m, 5H), 1.61 – 1.53 (m, 2H), 1.51 – 1.44 (m, 11H), 1.36 (s, 3H), 1.29 – 1.18 (m, 4H), 0.94 (d, *J* = 6.8 Hz, 3H), 0.90 (t, *J* = 7.4 Hz, 3H), 0.87 (s, 3H).

¹³C NMR (101 MHz, Methanol-*d*₄) δ 176.7, 175.3, 174.6, 162.8, 137.8, 134.5, 129.6, 127.0, 124.7, 119.1, 118.6, 104.9, 102.7, 84.2, 82.0, 77.3, 61.1, 58.5, 53.6, 44.2 (CHB (broad)), 43.8, 41.4, 39.9, 39.2, 37.8, 36.7, 34.9, 30.7, 30.2, 29.6, 28.5, 28.4, 27.81, 27.77, 26.8, 26.4, 25.9, 24.6, 15.6, 11.2.

HR-MS (ESI/TOF) calcd for C₄₅H₆₅BN₅O₈ [M+H]⁺ 801.4722, found 801.4725



tert-Butyl (3S,6S,12R)-6-((S)-sec-butyl)-3-cyclopentyl-1,4,7,10-tetraoxo-1-phenyl-12-((3aS,4S,6S,7aR)-3a,5,5-trimethylhexahydro-4,6-methanobenzo[d][1,3,2]dioxaborol-2-yl)-

2,5,8,11-tetraazapentadecan-15-oate (88d)

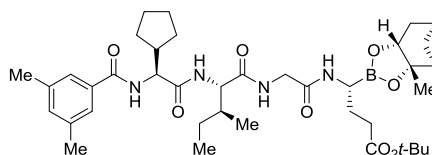
Prepared in analogy to **82**: **87d** (100 mg, 0.240 mmol) was mixed with **54f** (173 mg, 0.359 mmol) and DMAP (9 mg, 0.074 mmol) in anhydrous CHCl₃ (3 mL). The white suspension was cooled to -15 °C and then *N*-methylmorpholine (80 μL, 0.728 mmol) and T₃P reagent (290 μL, 0.484 mmol) was added. Yield: 63 mg (36%, amorphous solid).

¹H NMR (400 MHz, Methanol-*d*₄) δ 7.85 – 7.80 (m, 2H), 7.56 – 7.50 (m, 1H), 7.47 – 7.41 (m, 2H), 4.54 (d, *J* = 9.3 Hz, 1H), 4.36 (dd, *J* = 17.9, 1.8 Hz, 1H), 4.16 (dd, *J* = 8.7, 2.4 Hz, 1H), 3.94 (d, *J* = 8.6 Hz, 1H), 3.90 (d, *J* = 17.8 Hz, 1H), 2.64 – 2.54 (m, 1H), 2.53 – 2.47 (m, 1H), 2.45 – 2.30 (m, 3H), 2.16 – 2.09 (m, 1H), 1.99 – 1.90 (m, 2H), 1.89 – 1.53 (m, 12H), 1.51 – 1.39 (m, 11H), 1.36 (s, 3H), 1.28 (s, 3H), 1.26 – 1.20 (m, 1H), 0.97 – 0.92 (m, 6H), 0.88 (s, 3H).

¹³C NMR (101 MHz, Methanol-*d*₄) δ 176.8, 175.4, 175.0, 174.5, 170.4, 135.4, 132.8, 129.5, 128.6, 128.5, 84.1, 81.7, 77.3 61.0, 58.8, 53.6, 44.2 (CHB (broad)), 43.6, 41.4, 39.8,

39.2, 37.8, 36.7, 34.8, 30.5, 30.3, 29.6, 28.4, 28.4, 27.8, 26.7, 26.4, 26.0, 24.6, 24.6, 15.6, 11.2.

HR-MS (ESI/TOF) calcd for C₄₀H₆₂BN₄O₈ [M+H]⁺ 737.4661, found 737.4688



***tert*-Butyl (3*S*,6*S*,12*R*)-6-((*S*)-*sec*-butyl)-3-cyclopentyl-1-(3,5-dimethylphenyl)-1,4,7,10-tetraoxo-12-((3*aS*,4*S*,6*S*,7*aR*)-3*a*,5,5-trimethylhexahydro-4,6-**

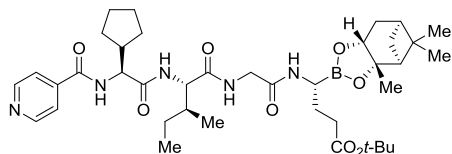
yl)-2,5,8,11-tetraazapentadecan-15-oate (88e)

Prepared in analogy to **82**: **87e** (100 mg, 0.224 mmol) was mixed with **54f** (162 mg, 0.336 mmol) and DMAP (9 mg, 0.074 mmol) in anhydrous CHCl₃ (5 mL). The white suspension was cooled to -15 °C and then *N*-methylmorpholine (80 μl, 0.728 mmol) and T₃P reagent (270 μL, 0.451 mmol) was added. Yield: 63 mg (37%, amorphous solid).

¹H NMR (400 MHz, Methanol-*d*₄) δ 7.44 (s, 2H), 7.18 (s, 1H), 4.51 (d, *J* = 9.5 Hz, 1H), 4.37 (dd, *J* = 17.9, 1.8 Hz, 1H), 4.16 (dd, *J* = 8.7, 2.4 Hz, 1H), 3.93 (d, *J* = 8.6 Hz, 1H), 3.89 (d, *J* = 17.9 Hz, 1H), 2.68 – 2.57 (m, 1H), 2.53 – 2.39 (m, 2H), 2.38 – 2.27 (m, 8H), 2.20 – 2.08 (m, 1H), 2.02 – 1.90 (m, 2H), 1.90 – 1.51 (m, 12H), 1.48 (d, *J* = 10.4 Hz, 1H), 1.45 – 1.39 (m, 10H), 1.36 (s, 3H), 1.28 (s, 3H), 1.26 – 1.21 (m, 1H), 0.99 – 0.91 (m, 6H), 0.87 (s, 3H).

¹³C NMR (101 MHz, Methanol-*d*₄) δ 176.8, 175.5, 174.9, 174.5, 170.6, 139.3, 135.3, 134.2, 126.2, 84.1, 81.8, 77.3, 61.1, 58.8, 53.6, 44.1 (CHB (broad)), 43.7, 41.4, 39.9, 39.2, 37.8, 36.7, 34.8, 30.6, 30.3, 29.6, 28.4, 28.4, 27.8, 27.8, 26.7, 26.4, 25.9, 24.6, 21.3, 15.6, 11.2.

HR-MS (ESI/TOF) calcd for C₄₂H₆₆BN₄O₈ [M+H]⁺ 765.4974, found 765.5001



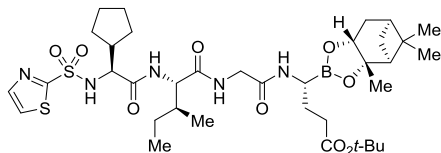
***tert*-Butyl (3*S*,6*S*,12*R*)-6-((*S*)-*sec*-butyl)-3-cyclopentyl-1,4,7,10-tetraoxo-1-(pyridin-4-yl)-12-((3*aS*,4*S*,6*S*,7*aR*)-3*a*,5,5-trimethylhexahydro-4,6-methanobenzo[d]-[1,3,2]dioxaborol-2-yl)-2,5,8,11-**

tetraazapentadecan-15-oate (88f)

Prepared in analogy to **82**: **87f** (111 mg, 0.265 mmol) was mixed with **54f** (173 mg, 0.359 mmol) and DMAP (10 mg, 0.082 mmol) in anhydrous CHCl₃ (3 mL). The white suspension was cooled to -15 °C and then *N*-methylmorpholine (100 μl, 0.910 mmol) and T₃P reagent (320 μL, 0.534 mmol) was added. Yield: 77 mg (39%, amorphous solid).

¹H NMR (400 MHz, Methanol-*d*₄) δ 8.70 – 8.65 (m, 2H), 7.80 – 7.76 (m, 2H), 4.55 (d, *J* = 9.3 Hz, 1H), 4.37 (dd, *J* = 17.9, 1.7 Hz, 1H), 4.16 (dd, *J* = 8.6, 2.4 Hz, 1H), 3.95 (d, *J* = 8.7 Hz, 1H), 3.90 (d, *J* = 17.9 Hz, 1H), 2.64 – 2.54 (m, 1H), 2.51 – 2.40 (m, 2H), 2.40 – 2.27 (m, 2H), 2.18 – 2.08 (m, 1H), 2.00 – 1.91 (m, 2H), 1.90 – 1.51 (m, 12H), 1.47 (d, *J* = 10.3 Hz, 1H), 1.45 – 1.40 (m, 10H), 1.36 (s, 3H), 1.28 (s, 3H), 1.27 – 1.21 (m, 1H), 0.98 – 0.92 (m, 6H), 0.88 (s, 3H).

^{13}C NMR (101 MHz, Methanol- d_4) δ 176.8, 175.1, 175.0, 174.4, 168.0, 150.9, 143.7, 123.2, 84.1, 81.9, 77.3, 61.0, 58.8, 53.6, 44.2 ($\underline{\text{CHB}}$ (broad)), 43.6, 41.4, 39.8, 39.2, 37.8, 36.7, 34.8, 30.5, 30.2, 29.6, 28.42, 28.35, 27.8, 26.7, 26.3, 25.9, 24.6, 15.6, 11.1.
 UPLC-MS (ESI) calcd for $\text{C}_{39}\text{H}_{61}\text{BN}_5\text{O}_8$ $[\text{M}+\text{H}]^+$ 738.75, found 739.15



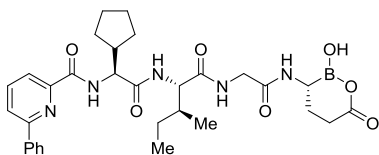
***tert*-Butyl (*R*)-4-(2-((2*S*,3*S*)-2-((*S*)-2-cyclopentyl-2-(thiazole-2-sulfonamido)-acetamido)-3-methylpentanamido)acetamido)-4-((3*aS*,4*S*,6*S*,7*aR*)-3*a*,5,5-trimethylhexahydro-4,6-methanobenzo[*d*]-[1,3,2]dioxaborol-2-yl) butanoate (88g)**

Prepared in analogy to **82**: **87g** (100 mg, 0.217 mmol) was mixed with **54f** (157 mg, 0.326 mmol) and DMAP (8 mg, 0.066 mmol) in anhydrous CHCl_3 (3 mL). The white suspension was cooled to -15°C and then *N*-methylmorpholine (80 μL , 0.728 mmol) and T_3P reagent (260 μL , 0.434 mmol) was added. Yield: 78 mg (46%, amorphous solid).

^1H NMR (400 MHz, Methanol- d_4) δ 7.94 (d, $J = 3.2$ Hz, 1H), 7.91 – 7.90 (m, 1H), 4.32 (dd, $J = 17.9$, 1.7 Hz, 1H), 4.15 (dd, $J = 8.6$, 2.4 Hz, 1H), 4.07 (d, $J = 7.6$ Hz, 1H), 3.84 (d, $J = 17.9$ Hz, 1H), 3.69 (d, $J = 8.6$ Hz, 1H), 2.51 – 2.41 (m, 3H), 2.38 – 2.30 (m, 1H), 2.24 – 2.09 (m, 2H), 1.96 – 1.85 (m, 3H), 1.81 – 1.70 (m, 2H), 1.68 – 1.57 (m, 6H), 1.56 – 1.42 (m, 13H), 1.35 (s, 3H), 1.28 (s, 3H), 1.26 – 1.16 (m, 2H), 0.95 (t, $J = 7.4$ Hz, 3H), 0.91 (d, $J = 6.8$ Hz, 3H), 0.87 (s, 3H).

^{13}C NMR (101 MHz, Methanol- d_4) δ 176.7, 175.1, 174.3, 174.3, 167.9, 145.1, 126.5, 84.1, 81.8, 77.3, 61.2, 61.0, 53.6, 44.2 (overlaps with $\underline{\text{CHB}}$ (broad)), 41.4, 39.7, 39.2, 37.8, 36.7, 34.7, 29.9, 29.6, 29.5, 28.4, 27.8, 27.7, 26.8, 26.3, 26.1, 24.6, 15.6, 11.2.

HR-MS (ESI/TOF) calcd for $\text{C}_{36}\text{H}_{59}\text{BN}_5\text{O}_9\text{S}_2$ $[\text{M}+\text{H}]^+$ 780.3847, found 780.3860



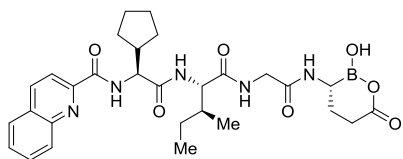
***N*-((*S*)-1-cyclopentyl-2-(((2*S*,3*S*)-1-(((2-(((*R*)-2-hydroxy-6-oxo-1,2-oxaborinan-3-yl)amino)-2-oxoethyl)amino)-3-methyl-1-oxopentan-2-yl)amino)-2-oxoethyl)-6-phenylpicolinamide (89a)**

Prepared in analogy to **84a**: a solution of **88a** (37 mg, 0.046 mmol) in MeCN/*n*-hexane (1:1, 1.8 mL) was treated with isobutylboronic acid (19 mg, 0.186 mmol) and 1 M HCl (115 μL). Yield: 26 mg (93 %, white solid).

^1H NMR (400 MHz, Methanol- d_4) δ 8.15 – 8.02 (m, 5H), 7.55 – 7.45 (m, 3H), 4.64 (d, $J = 7.7$ Hz, 1H), 4.38 – 4.28 (m, 1H), 4.18 – 4.06 (m, 2H), 2.89 (s, 1H), 2.50 – 2.41 (m, 1H), 2.27 – 2.19 (m, 2H), 1.92 – 1.75 (m, 5H), 1.73 – 1.56 (m, 5H), 1.53 – 1.40 (m, 2H), 1.29 – 1.17 (m, 1H), 0.96 (d, $J = 6.9$ Hz, 3H), 0.91 (t, $J = 7.5$ Hz, 3H).

^{13}C NMR (101 MHz, Methanol- d_4) δ 179.8, 176.6, 174.8, 174.5, 166.3, 157.7, 150.2, 140.0, 139.5, 130.7, 130.0, 128.0, 124.7, 121.6, 60.1, 57.7, 44.3, 42.7 ($\underline{\text{CHB}}$ (broad)), 39.3, 37.3, 30.3, 29.7, 29.1, 26.39, 26.37, 26.1, 25.5, 15.7, 11.2.

HR-MS (ESI/TOF) calcd for $\text{C}_{31}\text{H}_{41}\text{BN}_5\text{O}_7$ $[\text{M}+\text{H}]^+$ 606.3099, found 606.3125



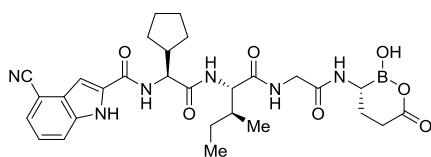
***N*-((*S*)-1-cyclopentyl-2-(((2*S*,3*S*)-1-((2-(((*R*)-2-hydroxy-6-oxo-1,2-oxaborinan-3-yl)amino)-2-oxoethyl)amino)-3-methyl-1-oxopentan-2-yl)amino)-2-oxoethyl)quinoline-2-carboxamide (89b)**

Prepared in analogy to **84a**: a solution of **88b** (95 mg, 0.121 mmol) in MeCN/*n*-hexane (1:1, 4.6 mL) was treated with isobutylboronic acid (49 mg, 0.482 mmol) and 1 M HCl (300 μ L). Yield: 57 mg (82%, white solid).

^1H NMR (400 MHz, Methanol- d_4) δ 8.48 (dd, $J = 8.6, 1.0$ Hz, 1H), 8.19 (d, $J = 8.5$ Hz, 1H), 8.15 (dd, $J = 8.5, 1.0$ Hz, 1H), 8.00 (dd, $J = 8.1, 1.7$ Hz, 1H), 7.84 (ddd, $J = 8.5, 6.9, 1.5$ Hz, 1H), 7.69 (ddd, $J = 8.1, 6.9, 1.2$ Hz, 1H), 4.61 (d, $J = 8.5$ Hz, 1H), 4.33 (d, $J = 17.5$ Hz, 1H), 4.19 – 4.10 (m, 2H), 2.91 (t, $J = 4.0$ Hz, 1H), 2.47 (h, $J = 8.6$ Hz, 1H), 2.34 – 2.20 (m, 2H), 1.92 – 1.58 (m, 10H), 1.54 – 1.41 (m, 2H), 1.28 – 1.17 (m, 1H), 0.95 (d, $J = 6.8$ Hz, 3H), 0.91 (t, $J = 7.4$ Hz, 3H).

^{13}C NMR (101 MHz, Methanol- d_4) δ 179.8, 176.7, 174.7, 174.5, 166.4, 150.4, 147.9, 139.2, 131.7, 130.9, 130.7, 129.5, 129.1, 119.5, 60.1, 58.2, 44.1, 42.7 ($\underline{\text{CHB}}$ (broad)), 39.3, 37.3, 30.3, 30.1, 29.2, 26.3, 26.0, 25.6, 15.7, 11.2.

HR-MS (ESI/TOF) calcd for $\text{C}_{29}\text{H}_{39}\text{BN}_5\text{O}_7$ $[\text{M}+\text{H}]^+$ 580.2943, found 580.2963



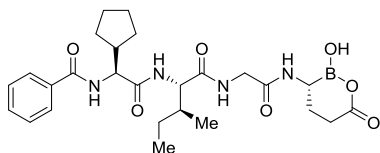
4-Cyano-*N*-((*S*)-1-cyclopentyl-2-(((2*S*,3*S*)-1-((2-(((*R*)-2-hydroxy-6-oxo-1,2-oxaborinan-3-yl)amino)-2-oxoethyl)amino)-3-methyl-1-oxopentan-2-yl)amino)-2-oxoethyl)-1*H*-indole-2-carboxamide (89c)

Prepared in analogy to **84a**: a solution of **88c** (78 mg, 0.097 mmol) in MeCN/*n*-hexane (1:1, 3.8 mL) was treated with isobutylboronic acid (40 mg, 0.390 mmol) and 1 M HCl (240 μ L). Yield: 51 mg (88%, white solid).

^1H NMR (400 MHz, Methanol- d_4) δ 7.77 (dt, $J = 8.3, 1.0$ Hz, 1H), 7.53 (dd, $J = 7.4, 1.0$ Hz, 1H), 7.41 (d, $J = 1.0$ Hz, 1H), 7.36 (dd, $J = 8.4, 7.3$ Hz, 1H), 4.53 – 4.49 (m, 1H), 4.32 (dd, $J = 17.5, 1.4$ Hz, 1H), 4.22 – 4.14 (m, 2H), 2.88 (t, $J = 4.0$ Hz, 1H), 2.43 (dq, $J = 16.8, 8.2$ Hz, 1H), 2.31 – 2.17 (m, 2H), 1.99 – 1.81 (m, 4H), 1.77 – 1.54 (m, 6H), 1.50 – 1.35 (m, 2H), 1.29 – 1.16 (m, 1H), 0.94 (d, $J = 6.8$ Hz, 3H), 0.88 (t, $J = 7.4$ Hz, 3H).

^{13}C NMR (101 MHz, Methanol- d_4) δ 179.7, 176.7, 175.0, 174.7, 162.9, 137.8, 134.4, 134.4, 129.6, 127.1, 124.8, 119.1, 118.6, 105.0, 102.8, 59.9, 59.5, 42.9 (overlaps with $\underline{\text{CHB}}$ (broad)), 39.3, 37.7, 30.9, 30.5, 29.2, 26.4, 26.2, 26.0, 25.6, 15.8, 11.3.

HR-MS (ESI/TOF) calcd for $\text{C}_{29}\text{H}_{38}\text{BN}_6\text{O}_7$ $[\text{M}+\text{H}]^+$ 593.2895, found 593.2910



***N*-((*S*)-1-cyclopentyl-2-(((2*S*,3*S*)-1-((2-(((*R*)-2-hydroxy-6-oxo-1,2-oxaborinan-3-yl)amino)-2-oxoethyl)amino)-3-methyl-1-oxopentan-2-yl)amino)-2-oxoethyl) benzamide (89d)**

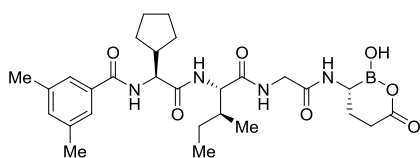
Prepared in analogy to **84a**: a solution of **88d**

(61 mg, 0.083 mmol) in MeCN/*n*-hexane (1:1, 4 mL) was treated with isobutylboronic acid (34 mg, 0.334 mmol) and 1 M HCl (210 μ L). Yield: 35 mg (80%, white solid).

^1H NMR (400 MHz, Methanol- d_4) δ 7.84 – 7.79 (m, 2H), 7.58 – 7.52 (m, 1H), 7.49 – 7.43 (m, 2H), 4.41 (d, J = 10.0 Hz, 1H), 4.29 (d, J = 17.5 Hz, 1H), 4.18 – 4.09 (m, 2H), 2.88 (t, J = 3.8 Hz, 1H), 2.39 (h, J = 8.5 Hz, 1H), 2.31 – 2.18 (m, 2H), 1.96 – 1.79 (m, 4H), 1.78 – 1.55 (m, 6H), 1.48 – 1.31 (m, 2H), 1.29 – 1.16 (m, 1H), 0.95 (d, J = 6.9 Hz, 3H), 0.91 (t, J = 7.5 Hz, 3H).

^{13}C NMR (101 MHz, Methanol- d_4) δ 179.8, 176.7, 175.0, 174.6, 170.5, 135.3, 132.9, 129.6, 128.5, 59.9, 59.8, 42.8 (overlaps with $\underline{\text{C}}\text{HB}$ (broad)), 39.3, 37.5, 30.8, 30.5, 29.2, 26.4, 26.2, 26.0, 25.6, 15.8, 11.3.

HR-MS (ESI/TOF) calcd for $\text{C}_{26}\text{H}_{38}\text{BN}_4\text{O}_7$ $[\text{M}+\text{H}]^+$ 529.2834, found 529.2851



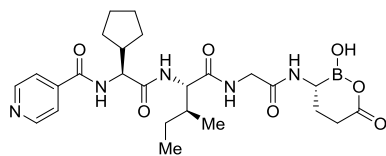
***N*-((*S*)-1-cyclopentyl-2-(((2*S*,3*S*)-1-((2-(((*R*)-2-hydroxy-6-oxo-1,2-oxaborinan-3-yl)amino)-2-oxoethyl)amino)-3-methyl-1-oxopentan-2-yl)amino)-2-oxoethyl)-3,5-dimethylbenzamide (89e)**

Prepared in analogy to **84a**: a solution of **88e** (62 mg, 0.081 mmol) in MeCN/*n*-hexane (1:1, 4 mL) was treated with isobutylboronic acid (33 mg, 0.324 mmol) and 1 M HCl (210 μ L). Yield: 34 mg (75%, white solid).

^1H NMR (300 MHz, Methanol- d_4) δ 7.43 (s, 2H), 7.19 (s, 1H), 4.39 (d, J = 10.1 Hz, 1H), 4.29 (d, J = 17.5 Hz, 1H), 4.17 – 4.08 (m, 2H), 2.88 (d, J = 4.0 Hz, 1H), 2.45 – 2.30 (m, 7H), 2.30 – 2.20 (m, 2H), 1.94 – 1.80 (m, 4H), 1.78 – 1.51 (m, 6H), 1.48 – 1.31 (m, 2H), 1.28 – 1.14 (m, 1H), 0.98 – 0.86 (m, 6H).

^{13}C NMR (101 MHz, Methanol- d_4) δ 179.8, 176.7, 175.1, 174.6, 170.9, 139.5, 135.3, 134.3, 126.2, 59.9, 59.7, 42.8 (overlaps with $\underline{\text{C}}\text{HB}$ (broad)), 39.3, 37.5, 30.8, 30.5, 29.2, 26.4, 26.2, 26.0, 25.6, 21.3, 15.8, 11.3.

HR-MS (ESI/TOF) calcd for $\text{C}_{28}\text{H}_{42}\text{BN}_4\text{O}_7$ $[\text{M}+\text{H}]^+$ 557.3147, found 557.3158



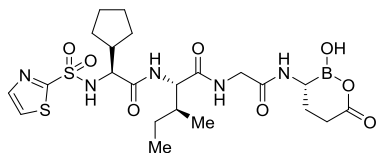
***N*-((*S*)-1-cyclopentyl-2-(((2*S*,3*S*)-1-((2-(((*R*)-2-hydroxy-6-oxo-1,2-oxaborinan-3-yl)amino)-2-oxoethyl)amino)-3-methyl-1-oxopentan-2-yl)amino)-2-oxoethyl) isonicotinamide (89f)**

Prepared in analogy to **84a**: a solution of **88f** (110 mg, 0.149 mmol) in MeCN/*n*-hexane (1:1, 5.8 mL) was treated with isobutylboronic acid (61 mg, 0.596 mmol) and 1 M HCl (370 μ L). Yield: 70 mg (89%, white solid).

^1H NMR (400 MHz, Methanol- d_4) δ 8.71 – 8.66 (m, 2H), 7.92 – 7.87 (m, 2H), 4.46 (d, J = 10.0 Hz, 1H), 4.14 (d, J = 7.9 Hz, 1H), 3.97 (d, J = 16.7 Hz, 1H), 3.76 (d, J = 16.7 Hz, 1H), 3.09 (dd, J = 6.3, 4.3 Hz, 1H), 2.42 – 2.30 (m, 2H), 2.26 – 2.15 (m, 1H), 1.92 – 1.81 (m, 2H), 1.80 – 1.53 (m, 8H), 1.49 – 1.40 (m, 1H), 1.39 – 1.30 (m, 1H), 1.28 – 1.16 (m, 1H), 0.96 (d, J = 6.8 Hz, 3H), 0.91 (t, J = 7.4 Hz, 3H).

^{13}C NMR (101 MHz, Methanol- d_4) δ 179.7, 173.8, 173.7, 171.5, 167.6, 150.9, 143.6, 123.3, 60.0, 59.6, 43.8, 43.3, 37.7 (overlaps with $\underline{\text{CHB}}$ (broad)), 31.0, 30.9, 30.5, 26.3, 26.3, 26.1, 25.8, 15.9, 11.4.

HR-MS (ESI/TOF) calcd for $\text{C}_{25}\text{H}_{37}\text{BN}_5\text{O}_7$ $[\text{M}+\text{H}]^+$ 530.2786, found 530.2809



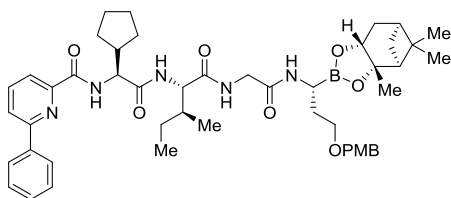
(2*S*,3*S*)-2-((*S*)-2-cyclopentyl-2-(thiazole-2-sulfonamido)acetamido)acetamido-*N*-(2-(((*R*)-2-hydroxy-6-oxo-1,2-oxaborinan-3-yl)amino)-2-oxoethyl)-3-methylpentanamide (89g)

Prepared in analogy to **84a**: a solution of **88g** (71 mg, 0.091 mmol) in MeCN/*n*-hexane (1:1, 3.6 mL) was treated with isobutylboronic acid (37 mg, 0.363 mmol) and 1 M HCl (230 μL). Yield: 43 mg (82%, white solid).

^1H NMR (400 MHz, Methanol- d_4) δ 7.96 (d, J = 3.1 Hz, 1H), 7.92 (d, J = 3.1 Hz, 1H), 4.29 (d, J = 17.4 Hz, 1H), 4.09 (d, J = 18.0 Hz, 1H), 3.99 (d, J = 8.5 Hz, 1H), 3.90 (d, J = 8.1 Hz, 1H), 2.85 (d, J = 3.6 Hz, 1H), 2.33 – 2.12 (m, 3H), 1.93 – 1.72 (m, 3H), 1.71 – 1.46 (m, 7H), 1.43 – 1.34 (m, 1H), 1.26 – 1.11 (m, 2H), 0.98 – 0.89 (m, 6H).

^{13}C NMR (101 MHz, MeOD) δ 179.8, 176.7, 174.5, 174.2, 168.0, 145.1, 126.5, 61.6, 60.2, 44.0, 42.7 ($\underline{\text{CHB}}$ (broad))), 39.2, 37.3, 29.93, 29.87, 29.2, 26.4, 26.3, 25.8, 25.5, 15.7, 11.4.

HR-MS (ESI/TOF) calcd for $\text{C}_{22}\text{H}_{35}\text{BN}_5\text{O}_8\text{S}_2$ $[\text{M}+\text{H}]^+$ 572.2020, found 572.2039



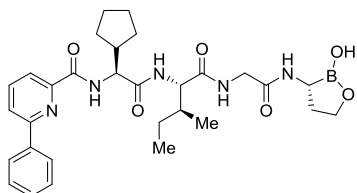
***N*-((5*R*,11*S*,14*S*)-11-((*S*)-*sec*-butyl)-14-cyclopentyl-1-(4-methoxyphenyl)-7,10,13-trioxo-5-((3*aS*,4*S*,6*S*,7*aR*)-3*a*,5,5-trimethylhexahydro-4,6-methanobenzo[*d*][1,3,2]dioxaborol-2-yl)-2-oxa-6,9,12-triazatetradecan-14-yl)-6-phenylpicolinamide (90)**

Prepared in analogy to **82**: **87a** (118 mg, 0.239 mmol) was mixed with **54f** (148 mg, 0.290 mmol) and DMAP (9 mg, 0.07 mmol) in anhydrous CHCl_3 (3 mL). The white suspension was cooled to $-15\text{ }^\circ\text{C}$ and then *N*-methylmorpholine (80 μL , 0.728 mmol) and T_3P reagent (290 μL , 0.484 mmol) was added. Yield: 96 mg (47%, amorphous solid).

^1H NMR (400 MHz, Methanol- d_4) δ 8.12 – 8.03 (m, 5H), 7.55 – 7.43 (m, 3H), 6.97 (d, J = 8.8 Hz, 2H), 6.69 (d, J = 8.7 Hz, 2H), 4.64 (d, J = 7.9 Hz, 1H), 4.31 (dd, J = 17.8, 1.7 Hz, 1H), 4.17 – 4.11 (m, 3H), 3.95 (d, J = 8.6 Hz, 1H), 3.93 – 3.87 (m, 1H), 3.71 (s, 3H), 3.51 (tt, J = 5.8, 2.7 Hz, 2H), 2.77 – 2.70 (m, 1H), 2.45 – 2.36 (m, 1H), 2.35 – 2.26 (m, 1H), 2.15 – 2.06 (m, 1H), 1.94 (t, J = 5.5 Hz, 1H), 1.88 – 1.49 (m, 12H), 1.47 – 1.39 (m, 3H), 1.34 (s, 3H), 1.27 (s, 4H), 0.98 – 0.90 (m, 6H), 0.86 (s, 3H).

^{13}C NMR (101 MHz, Methanol- d_4) δ 176.2, 174.7, 174.4, 166.1, 160.5, 157.7, 150.3, 140.0, 139.4, 131.7, 130.7, 130.2, 130.0, 128.1, 124.7, 121.6, 114.5, 84.3, 77.3, 73.3, 69.5, 60.9, 57.4, 55.6, 53.5, 44.7, 41.8, 41.4 ($\underline{\text{CHB}}$ (broad)), 40.0, 39.2, 37.6, 36.8, 32.5, 30.2, 29.7, 29.6, 27.8, 27.6, 26.7, 26.3, 26.0, 24.6, 15.7, 11.1.

UPLC-MS (ESI) calcd for $\text{C}_{48}\text{H}_{65}\text{BN}_5\text{O}_8$ $[\text{M}+\text{H}]^+$ 850.89, found 851.10



***N*-((*S*)-1-cyclopentyl-2-(((2*S*,3*S*)-1-((2-(((*R*)-2-hydroxy-1,2-oxaborolan-3-yl)amino)-2-oxoethyl)amino)-3-methyl-1-oxopentan-2-yl)amino)-2-oxoethyl)-6-phenyl-picolinamide (**91**)**

A solution of **90** (83 mg, 0.098 mmol) in MeOH/*n*-hexane (1:1, 3.8 mL) was treated with isobutylboronic acid (40 mg, 0.39 mmol, 4 equiv) and 1 M HCl (244 μ L). After stirring for 18 h at room temperature, the methanolic phase was washed with *n*-hexane (2 \times 5 mL) and the combined *n*-hexane layers were washed with MeOH (2 \times 5 mL). The combined methanol phase was evaporated in vacuo.

Full deprotection of PMB group was achieved by treating the crude mixture with TFA (200 μ L) in CHCl₃ (2 mL) for 20 min. Mixture was evaporated and purified by flash chromatography on reversed phase silica gel eluting with 10–100% MeCN in H₂O to provide **91** (44 mg, 77%) as a white amorphous compound.

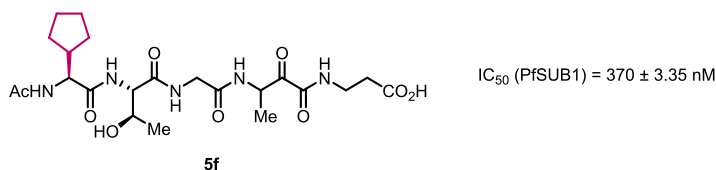
¹H NMR (400 MHz, Methanol-*d*₄) δ 8.15 – 8.02 (m, 5H), 7.55 – 7.44 (m, 3H), 4.63 (d, *J* = 7.9 Hz, 1H), 4.27 (d, *J* = 17.4 Hz, 1H), 4.13 – 4.00 (m, 2H), 3.86 – 3.76 (m, 1H), 3.55 – 3.45 (m, 1H), 2.90 – 2.80 (m, 1H), 2.47 (h, *J* = 8.3 Hz, 1H), 1.94 – 1.55 (m, 10H), 1.53 – 1.40 (m, 2H), 1.31 – 1.17 (m, 1H), 1.02 – 0.86 (m, 6H).

¹³C NMR (101 MHz, Methanol-*d*₄) δ 178.0, 174.7, 174.4, 166.4, 157.8, 150.3, 139.9, 139.5, 130.7, 130.0, 128.0, 124.6, 121.6, 64.7, 60.2, 57.8, 44.3, 43.5, 39.4, 37.3, 34.4, 30.3, 29.8, 26.4, 26.1, 15.7, 11.2.

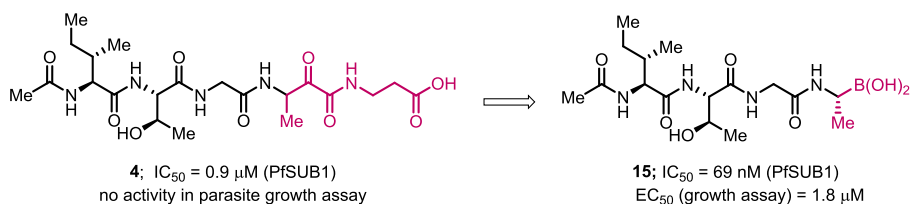
HR-MS (ESI/TOF) calcd for C₃₀H₄₁BN₅O₆ [M+H]⁺ 578.3150, found 578.3162

Conclusions

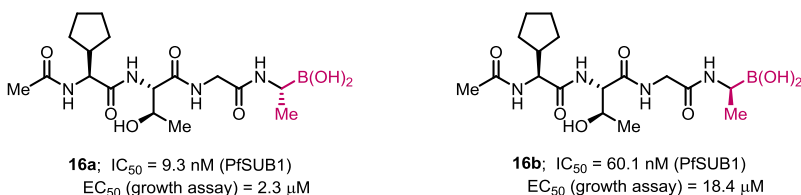
1. Rationally designed SUB1 inhibitors based on the peptidic sequence of natural substrates of SUB1 are more potent compared to inhibitors found by screening of compound libraries.
2. Peptidic α -ketoamide **5** bearing cyclopentyl substituent at P4 position shows the highest SUB1 inhibitory potency, confirming the hydrophobic nature of S4 pocket on the enzyme.



3. Replacement of ketoamide to boronic acid as a serine binding group in peptidic SUB1 inhibitors enabled inhibitory potency at nanomolar level. Selected peptidic boronic acids suppressed parasite replication in cell based assay.

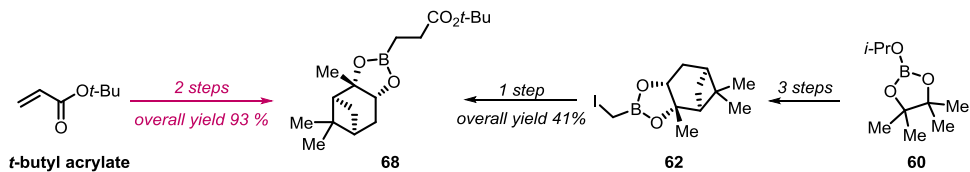


4. Substituents at P1 position of peptidic boronic acids **16** require the stereochemistry that resembles L-amino acid stereochemistry to obtain more potent inhibitors of PfsUB1.



5. Substitution of P3 amino acid side chain with more lipophilic residues in peptidic boronic acids provides the necessary hydrophobic interactions with the S3 pocket resulting in derivatives which possess improved PfsUB1 inhibitory and sub-micromolar potency in cell based parasite growth assay.
6. Compounds **84** with different *N*-acyl groups and *N*-sulfonyl group at P5 position (*N*-capping group) show low nanomolar inhibitory potency, implying that a wide variety of substituents could be installed at this position. On the contrary, compounds without carbonyl group at P5 position show decreased potency.

7. The introduction of glutamic acid side chain at P1 of peptidic boronic acids decreases the off-target effect against human proteasome.
8. Copper catalyzed β -borylation of *t*-butyl acrylate and subsequent transesterification was more effective route towards key intermediate **68** compared to the initial attempt to synthesise it from intermediate **62**.



9. The most efficient reagent for coupling of peptidic scaffold with α -amino boronic acid building block was propanephosphonic anhydride minimizing protodeboronated by-product formation in the coupling reaction.

References

- (1) World malaria report 2021. Geneva: World Health Organization; 2021. Licence: CC BY-NC-SA 3.0 IGO
- (2) Sirawaraporn, W. Dihydrofolate Reductase and Antifolate Resistance in Malaria. *Drug Resist. Updat.* **1998**, *1*, 397–406.
- (3) Nsanzabana, C. Resistance to Artemisinin Combination Therapies (ACTs): Do Not Forget the Partner Drug! *Trop. Med. Infect. Dis.* **2019**, *4*, 26.
- (4) Sajid, M.; Withers-Martinez, C.; Blackman, M. J. Maturation and Specificity of Plasmodium Falciparum Subtilisin-like Protease-1, a Malaria Merozoite Subtilisin-like Serine Protease. *J. Biol. Chem.* **2000**, *275*, 631–641.
- (5) Pino, P.; Caldelari, R.; Mukherjee, B.; Vahokoski, J.; Klages, N.; Maco, B.; Collins, C. R.; Blackman, M. J.; Kursula, I.; Heussler, V.; Brochet, M.; Soldati-Favre, D. A Multistage Antimalarial Targets the Plasmepsins IX and X Essential for Invasion and Egress. *Science* **2017**, *358*, 522–528.
- (6) Collins, C. R.; Hackett, F.; Strath, M.; Penzo, M.; Withers-Martinez, C.; Baker, D. A.; Blackman, M. J. Malaria Parasite CGMP-Dependent Protein Kinase Regulates Blood Stage Merozoite Secretory Organelle Discharge and Egress. *PLoS Pathog.* **2013**, *9*, e1003344.
- (7) Yeoh, S.; O'Donnell, R. A.; Koussis, K.; Dluzewski, A. R.; Ansell, K. H.; Osborne, S. A.; Hackett, F.; Withers-Martinez, C.; Mitchell, G. H.; Bannister, L. H.; Bryans, J. S.; Kettleborough, C. A.; Blackman, M. J. Subcellular Discharge of a Serine Protease Mediates Release of Invasive Malaria Parasites from Host Erythrocytes. *Cell* **2007**, *131*, 1072–1083.
- (8) Singh, J.; Petter, R. C.; Baillie, T. A.; Whitty, A. The Resurgence of Covalent Drugs. *Nat. Rev. Drug Discov.* **2011**, *10*, 307–317.
- (9) Bandyopadhyay, A.; Gao, J. Targeting Biomolecules with Reversible Covalent Chemistry. *Curr. Opin. Chem. Biol.* **2016**, *34*, 110–116.
- (10) Krajnc, A.; Lang, P. A.; Panduwawala, T. D.; Brem, J.; Schofield, C. J. Will Morphing Boron-Based Inhibitors Beat the β -Lactamases? *Curr. Opin. Chem. Biol.* **2019**, *50*, 101–110.
- (11) Tan, M. S. Y.; Blackman, M. J. Malaria Parasite Egress at a Glance. *J. Cell Sci.* **2021**, *134*, jcs257345.

- (12) Burns, A. L.; Dans, M. G.; Balbin, J. M.; de Koning-Ward, T. F.; Gilson, P. R.; Beeson, J. G.; Boyle, M. J.; Wilson, D. W. Targeting Malaria Parasite Invasion of Red Blood Cells as an Antimalarial Strategy. *FEMS Microbiol. Rev.* **2019**, *43*, 223–238.
- (13) Withers-Martinez, C.; Saldanha, J. W.; Ely, B.; Hackett, F.; O'Connor, T.; Blackman, M. J. Expression of Recombinant *Plasmodium Falciparum* Subtilisin-like Protease-1 in Insect Cells. *J. Biol. Chem.* **2002**, *277*, 29698–29709.
- (14) Withers-Martinez, C.; Strath, M.; Hackett, F.; Haire, L. F.; Howell, S. A.; Walker, P. A.; Christodoulou, E.; Dodson, G. G.; Blackman, M. J. The Malaria Parasite Egress Protease SUB1 Is a Calcium-Dependent Redox Switch Subtilisin. *Nat. Commun.* **2014**, *5*, 3726.
- (15) Ranol, T. A.; Timkey, T.; Peterson, E. P.; Rotonda, J.; Becker, J. W.; Chapman, K. T.; Thornberry, N. A. A Combinatorial Approach for Determining Protease Specificities: Application to Interleukin-1 p Converting Enzyme (ICE). *Chem. Biol.* **1997**, *4*, 149–55.
- (16) Siezen, R. J.; Leunissen, J. A. M. Subtilases: The Superfamily of Subtilisin-like Serine Proteases: Subtilases. *Protein Sci.* **1997**, *6*, 501–523.
- (17) Koussis, K.; Withers-Martinez, C.; Yeoh, S.; Child, M.; Hackett, F.; Knuepfer, E.; Juliano, L.; Woehlbier, U.; Bujard, H.; Blackman, M. J. A Multifunctional Serine Protease Primes the Malaria Parasite for Red Blood Cell Invasion. *EMBO J.* **2009**, *28*, 725–735.
- (18) Withers-Martinez, C.; Suarez, C.; Fulle, S.; Kher, S.; Penzo, M.; Ebejer, J.-P.; Koussis, K.; Hackett, F.; Jirgensons, A.; Finn, P.; Blackman, M. J. *Plasmodium* Subtilisin-like Protease 1 (SUB1): Insights into the Active-Site Structure, Specificity and Function of a Pan-Malaria Drug Target. *Int. J. Parasitol.* **2012**, *42*, 597–612.
- (19) Fulle, S.; Withers-Martinez, C.; Blackman, M. J.; Morris, G. M.; Finn, P. W. Molecular Determinants of Binding to the *Plasmodium* Subtilisin-like Protease 1. *J. Chem. Inf. Model.* **2013**, *53*, 573–583.
- (20) Robello, M.; Barresi, E.; Baglini, E.; Salerno, S.; Taliani, S.; Settimo, F. D. The Alpha Keto Amide Moiety as a Privileged Motif in Medicinal Chemistry: Current Insights and Emerging Opportunities. *J. Med. Chem.* **2021**, *64*, 3508–3545.
- (21) Kher, S. S.; Penzo, M.; Fulle, S.; Finn, P. W.; Blackman, M. J.; Jirgensons, A. Substrate Derived Peptidic α -Ketoamides as Inhibitors of the Malarial Protease PfSUB1. *Bioorg. Med. Chem. Lett.* **2014**, *24*, 4486–4489.

- (22) Lidumniece, E.; Withers-Martinez, C.; Hackett, F.; Collins, C. R.; Perrin, A. J.; Koussis, K.; Bisson, C.; Blackman, M. J.; Jirgensons, A. Peptidic Boronic Acids Are Potent Cell-Permeable Inhibitors of the Malaria Parasite Egress Serine Protease SUB1. *Proc. Natl. Acad. Sci.* **2021**, *118*, e2022696118.
- (23) Giganti, D.; Bouillon, A.; Tawk, L.; Robert, F.; Martinez, M.; Crublet, E.; Weber, P.; Girard-Blanc, C.; Petres, S.; Haouz, A.; Hernandez, J.-F.; Mercereau-Puijalon, O.; Alzari, P. M.; Barale, J.-C. A Novel Plasmodium-Specific Prodomain Fold Regulates the Malaria Drug Target SUB1 Subtilase. *Nat. Commun.* **2014**, *5*, 4833.
- (24) Gelb, M. H.; Svaren, J. P.; Abeles, R. H. Fluoro Ketone Inhibitors of Hydrolytic Enzymes. *Biochemistry* **1985**, *24*, 1813–1817.
- (25) Giovani, S.; Penzo, M.; Brogi, S.; Brindisi, M.; Gemma, S.; Novellino, E.; Savini, L.; Blackman, M. J.; Campiani, G.; Butini, S. Rational Design of the First Difluorostatone-Based PfSUB1 Inhibitors. *Bioorg. Med. Chem. Lett.* **2014**, *24*, 3582–3586.
- (26) Brogi, S.; Giovani, S.; Brindisi, M.; Gemma, S.; Novellino, E.; Campiani, G.; Blackman, M. J.; Butini, S. In Silico Study of Subtilisin-like Protease 1 (SUB1) from Different Plasmodium Species in Complex with Peptidyl-Difluorostatones and Characterization of Potent Pan-SUB1 Inhibitors. *J. Mol. Graph. Model.* **2016**, *64*, 121–130.
- (27) Giovani, S.; Penzo, M.; Butini, S.; Brindisi, M.; Gemma, S.; Novellino, E.; Campiani, G.; Blackman, M. J.; Brogi, S. Plasmodium Falciparum Subtilisin-like Protease 1: Discovery of Potent Difluorostatone-Based Inhibitors. *RSC Adv.* **2015**, *5*, 22431–22448.
- (28) Fu, H.; Fang, H.; Sun, J.; Wang, H.; Liu, A.; Sun, J.; Wu, Z. Boronic Acid-Based Enzyme Inhibitors: A Review of Recent Progress. *Curr. Med. Chem.* **2014**, *21*, 3271–3280.
- (29) Diaz, D. B.; Yudin, A. K. The Versatility of Boron in Biological Target Engagement. *Nat. Chem.* **2017**, *9*, 731–742.
- (30) Plescia, J.; Moitessier, N. Design and Discovery of Boronic Acid Drugs. *Eur. J. Med. Chem.* **2020**, *195*, 112270.
- (31) Bastianelli, G.; Bouillon, A.; Nguyen, C.; Crublet, E.; Pêtres, S.; Gorgette, O.; Le-Nguyen, D.; Barale, J.-C.; Nilges, M. Computational Reverse-Engineering of a Spider-Venom Derived Peptide Active Against Plasmodium Falciparum SUB1. *PLoS ONE* **2011**, *6*, e21812.

- (32) Blackman, M. J.; Corrie, J. E. T.; Croney, J. C.; Kelly, G.; Eccleston, J. F.; Jameson, D. M. Structural and Biochemical Characterization of a Fluorogenic Rhodamine-Labeled Malarial Protease Substrate. *Biochemistry* **2002**, *41*, 12244–12252.
- (33) Arastu-Kapur, S.; Ponder, E. L.; Fonović, U. P.; Yeoh, S.; Yuan, F.; Fonović, M.; Grainger, M.; Phillips, C. I.; Powers, J. C.; Bogyo, M. Identification of Proteases That Regulate Erythrocyte Rupture by the Malaria Parasite Plasmodium Falciparum. *Nat. Chem. Biol.* **2008**, *4*, 203–213.
- (34) Gemma, S.; Giovani, S.; Brindisi, M.; Tripaldi, P.; Brogi, S.; Savini, L.; Fiorini, I.; Novellino, E.; Butini, S.; Campiani, G.; Penzo, M.; Blackman, M. J. Quinolylhydrazones as Novel Inhibitors of Plasmodium Falciparum Serine Protease PfSUB1. *Bioorg. Med. Chem. Lett.* **2012**, *22*, 5317–5321.
- (35) Bouillon, A.; Giganti, D.; Benedet, C.; Gorgette, O.; Pêtres, S.; Crublet, E.; Girard-Blanc, C.; Witkowski, B.; Ménard, D.; Nilges, M.; Mercereau-Puijalon, O.; Stoven, V.; Barale, J.-C. In Silico Screening on the Three-Dimensional Model of the Plasmodium Vivax SUB1 Protease Leads to the Validation of a Novel Anti-Parasite Compound. *J. Biol. Chem.* **2013**, *288*, 18561–18573.
- (36) Kher, S. S.; Penzo, M.; Fulle, S.; Ebejer, J. P.; Finn, P. W.; Blackman, M. J.; Jirgensons, A. Quinoxaline-Based Inhibitors of Malarial Protease PfSUB1*. *Chem. Heterocycl. Compd.* **2015**, *50*, 1457–1463.
- (37) Moneriz, C.; Mestres, J.; Bautista, J. M.; Diez, A.; Puyet, A. Multi-Targeted Activity of Maslinic Acid as an Antimalarial Natural Compound: Maslinic Acid Targets on Plasmodium Falciparum. *FEBS J.* **2011**, *278*, 2951–2961.
- (38) Carginin, S. T.; Staudt, A. F.; Medeiros, P.; de Medeiros Sol Sol, D.; de Azevedo dos Santos, A. P.; Zanchi, F. B.; Gosmann, G.; Puyet, A.; Garcia Teles, C. B.; Gnoatto, S. B. Semisynthesis, Cytotoxicity, Antimalarial Evaluation and Structure-Activity Relationship of Two Series of Triterpene Derivatives. *Bioorg. Med. Chem. Lett.* **2018**, *28*, 265–272.
- (39) Carpino, L. A.; Ghassemi, S.; Ionescu, D.; Ismail, M.; Sadat-Aalae, D.; Truran, G. A.; Mansour, E. M. E.; Siwruk, G. A.; Eynon, J. S.; Morgan, B. Rapid, Continuous Solution-Phase Peptide Synthesis: Application to Peptides of Pharmaceutical Interest. *Org. Process Res. Dev.* **2003**, *7*, 28–37.
- (40) Höck, S.; Marti, R.; Riedl, R.; Simeunovic, M. Thermal Cleavage of the Fmoc Protection Group. *CHIMIA* **2010**, *64*, 200–202.

- (41) Matteson, D. S.; Sadhu, K. M.; Peterson, M. L. 99% Chirally Selective Syntheses via Pinanediol Boronic Esters: Insect Pheromones, Diols, and an Amino Alcohol. *J. Am. Chem. Soc.* **1986**, *108*, 810–819.
- (42) Dembitsky, V.; Quntar, A.; Srebnik, M. Recent Advances in the Medicinal Chemistry of α -Aminoboronic Acids, Amine-Carboxyboranes and Their Derivatives. *Mini-Rev. Med. Chem.* **2004**, *4*, 1001–1018.
- (43) Oerlemans, R.; Berkers, C. R.; Assaraf, Y. G.; Scheffer, G. L.; Peters, G. J.; Verbrugge, S. E.; Cloos, J.; Slootstra, J.; Meloen, R. H.; Shoemaker, R. H.; Dijkmans, B. A. C.; Scheper, R. J.; Ovaa, H.; Jansen, G. Proteasome Inhibition and Mechanism of Resistance to a Synthetic, Library-Based Hexapeptide. *Invest. New Drugs* **2018**, *36*, 797–809.
- (44) Castulik, J.; Zabadal, M. Process for Making Bortezomib and Intermediates for the Process. **2012**, WO2012/048745.
- (45) Mun, S.; Lee, J.-E.; Yun, J. Copper-Catalyzed β -Boration of α,β -Unsaturated Carbonyl Compounds: Rate Acceleration by Alcohol Additives. *Org. Lett.* **2006**, *8*, 4887–4889.
- (46) Corey, P. F.; Ward, F. E. Buffered Potassium Peroxymonosulfate-Acetone Epoxidation of α,β -Unsaturated Acids. *J. Org. Chem.* **1986**, *51*, 1925–1926.
- (47) Grill, J. M.; Ogle, J. W.; Miller, S. A. An Efficient and Practical System for the Catalytic Oxidation of Alcohols, Aldehydes, and α,β -Unsaturated Carboxylic Acids. *J. Org. Chem.* **2006**, *71*, 9291–9296.
- (48) Fringuelli, F.; Pizzo, F.; Vaccaro, L. AlCl_3 as an Efficient Lewis Acid Catalyst in Water. *Tetrahedron Lett.* **2001**, *42*, 1131–1133.
- (49) Elford, T. G.; Nave, S.; Sonawane, R. P.; Aggarwal, V. K. Total Synthesis of (+)-Erogorgiaene Using Lithiation–Borylation Methodology, and Stereoselective Synthesis of Each of Its Diastereoisomers. *J. Am. Chem. Soc.* **2011**, *133*, 16798–16801.
- (50) Gao, M.; Thorpe, S. B.; Santos, W. L. $\text{Sp}^2\text{-sp}^3$ Hybridized Mixed Diboron: Synthesis, Characterization, and Copper-Catalyzed β -Boration of α,β -Unsaturated Conjugated Compounds. *Org. Lett.* **2009**, *11*, 3478–3481.
- (51) Gozhina, O. V.; Svendsen, J. S.; Lejon, T. Synthesis and Antimicrobial Activity of α -Aminoboronic-Containing Peptidomimetics. *J. Pept. Sci.* **2014**, *20*, 20–24.

Appendix

Lidumniece, E., Withers-Martinez, C., Hackett, F., Collins, C. R., Perrin, A. J., Koussis, K., Bisson, C., Blackman, M. J., Jirgensons, A. Peptidic boronic acids are potent cell-permeable inhibitors of the malaria parasite egress serine protease SUB1. *Proc. Natl. Acad. Sci. U. S. A.*, **2021**, *118*, e2022696118

Copyright © 2021 the Author(s). Published by PNAS. This open access article is distributed under Creative Commons Attribution License 4.0 (CC BY).

The supporting information is available free of charge on the PNAS publication website at <https://doi.org/10.1073/pnas.2022696118>



Peptidic boronic acids are potent cell-permeable inhibitors of the malaria parasite egress serine protease SUB1

Elina Lidumniece^a, Chrislaine Withers-Martinez^b, Fiona Hackett^b, Christine R. Collins^b, Abigail J. Perrin^b, Konstantinos Koussis^b, Claudine Bisson^{c,d}, Michael J. Blackman^{b,e,1}, and Aigars Jirgensons^{a,1}

^aLatvian Institute of Organic Synthesis, Riga LV-1006, Latvia; ^bMalaria Biochemistry Laboratory, The Francis Crick Institute, London NW1 1AT, United Kingdom; ^cDepartment of Biological Sciences, Institute of Structural and Molecular Biology, Birkbeck College, University of London, London WC1E 7HX, United Kingdom; ^dCentre for Ultrastructural Imaging, Kings College London, London SE1 1UL, United Kingdom; and ^eFaculty of Infectious and Tropical Diseases, London School of Hygiene & Tropical Medicine, London WC1E 7HT, United Kingdom

Edited by Thomas E. Wellems, NIH, Gaithersburg, MD, and approved April 12, 2021 (received for review October 30, 2020)

Malaria is a devastating infectious disease, which causes over 400,000 deaths per annum and impacts the lives of nearly half the world's population. The causative agent, a protozoan parasite, replicates within red blood cells (RBCs), eventually destroying the cells in a lytic process called egress to release a new generation of parasites. These invade fresh RBCs to repeat the cycle. Egress is regulated by an essential parasite subtilisin-like serine protease called SUB1. Here, we describe the development and optimization of substrate-based peptidic boronic acids that inhibit *Plasmodium falciparum* SUB1 with low nanomolar potency. Structural optimization generated membrane-permeable, slow off-rate inhibitors that prevent *P. falciparum* egress through direct inhibition of SUB1 activity and block parasite replication in vitro at submicromolar concentrations. Our results validate SUB1 as a potential target for a new class of antimalarial drugs designed to prevent parasite replication and disease progression.

serine protease | boronic acid | egress | *Plasmodium falciparum* | malaria

Malaria, a disease caused by obligate intracellular parasites of the genus *Plasmodium*, is a global health problem threatening more than half the earth's population (1). Recent decades have seen a considerable reduction in the incidence of clinical malaria and malaria-related mortality, largely due to the availability of efficacious chemotherapies and control of the mosquito vector (2). However, efforts toward malaria eradication are impeded by the alarming spread of drug-resistant parasites, rendering existing drugs ineffective in many regions (3, 4). Of particular concern, resistance has now been reported to nearly all clinically used antimalarial drugs including artemisinins, the current front line drug class (5). There is therefore an urgent need to bolster the antimalarial drug arsenal with new chemotherapeutics, particularly those with as yet unexploited mechanisms of action.

Clinical malaria results from repeated rounds of replication of the parasite in circulating red blood cells (RBCs). Merozoites invade the cells and divide asexually within a membrane-bound parasitophorous vacuole (PV) to produce a mature multinucleated form called a schizont. This then undergoes segmentation to generate 16 or more daughter merozoites, which are eventually released through a lytic process called egress, in the process destroying the infected RBC. Shortly before egress, activation of a parasite cyclic GMP-dependent protein kinase called PKG induces the discharge of a subtilisin-like serine protease called SUB1 from specialized merozoite secretory organelles called exosomes (6, 7). Upon its release into the PV lumen, SUB1 rapidly cleaves and activates a number of PV-resident and merozoite surface proteins, leading within minutes to explosive rupture of the PV membrane (PVM) and RBC membrane to allow merozoite release (8–12). The free parasites immediately invade fresh RBCs to repeat the cycle.

All *Plasmodium* species, including the most important human malaria pathogens *Plasmodium falciparum*, *Plasmodium vivax*, and *Plasmodium knowlesi*, possess a single ortholog of SUB1 with

similar (though not identical) substrate specificity (13). Genetic experiments have shown that SUB1 is indispensable for parasite survival, with *SUB1* gene disruption leading in asexual blood stages and the preceding liver stages of infection to a complete block in merozoite egress (12, 14, 15). This, together with the lack of structural resemblance of SUB1 to human serine proteases (16, 17), has focused interest on SUB1 as an attractive pharmacological target for antimalarial drug discovery. However, the identification of potent drug-like SUB1 inhibitors has proven to be a difficult task. Attempts to identify ligands of SUB1 by screening of synthetic or natural product libraries, and through in silico screening, met with limited success (6, 18, 19), probably due to the relatively shallow and elongated cavity of the enzyme active site (16, 17). We have previously reported the rational design of peptidic ketoamide inhibitors of *P. falciparum* SUB1 (PISUB1) based on the substrate specificity of the enzyme (Fig. 1) (13, 20). Preliminary structure-activity relationships analysis of these inhibitors revealed a tetrapeptide mimic on the nonprime side and an oxycarbonyl ethyl group on the prime side as structural features required to attain submicromolar inhibitory potency. Given the capacity of boronic acids to form strong covalent but reversible bonds with the catalytic Ser residue of serine

Significance

Malaria remains a major global health threat. In the face of increasing resistance to available chemotherapeutics, new antimalarial drugs with new modes of action are urgently needed. The causative agent of malaria is a single-celled parasite that invades and replicates within red blood cells. Escape from the red cell, a process called egress, involves a proteolytic pathway triggered by an essential parasite subtilisin-like serine protease called SUB1. Here, we describe the development and rational optimization of a potent, membrane-permeable substrate-based boronic acid compounds that block egress and parasite proliferation by direct inhibition of SUB1 activity. The compounds could form the basis of a new type of antimalarial medicine that would both protect against infection and treat disease.

Author contributions: A.J. designed inhibitors; E.L., C.W.-M., F.H., C.R.C., A.J.P., K.K., and C.B. performed research; E.L., C.W.-M., F.H., C.R.C., A.J.P., and K.K. analyzed data; M.J.B. and A.J. wrote the paper; and C.B. generated the B11-EXP2-mNeonGreen parasite line.

The authors declare no competing interest.

This article is a PNAS Direct Submission.

This open access article is distributed under [Creative Commons Attribution License 4.0 \(CC BY\)](https://creativecommons.org/licenses/by/4.0/).

See [online](https://www.pnas.org/lookup/suppl/doi:10.1073/pnas.2022696118/-DCSupplemental) for related content such as Commentaries.

¹To whom correspondence may be addressed. Email: Mike.Blackman@crick.ac.uk or aigars@osi.lv.

This article contains supporting information online at <https://www.pnas.org/lookup/suppl/doi:10.1073/pnas.2022696118/-DCSupplemental>.

Published May 11, 2021.

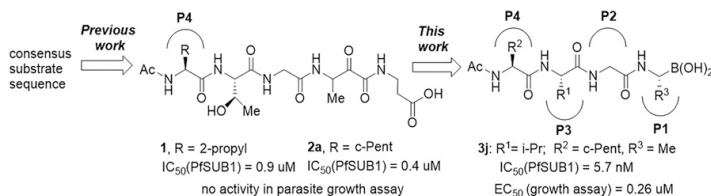


Fig. 1. Development of rationally designed peptidic PfSUB1 inhibitors.

proteases, here we have investigated peptidic boronic acids as PfSUB1 inhibitors. These efforts have generated nanomolar PfSUB1 inhibitors that can access PfSUB1 in the intraerythrocytic parasite and prevent parasite replication through direct inhibition of egress.

Results

Discovery of Potent Substrate-Based Peptidyl Boronic Acid Inhibitors of PfSUB1. We previously described the development of a fluorescence-based in vitro assay suitable for the evaluation of substrate-based PfSUB1 inhibitors, using recombinant PfSUB1 (rPfSUB1) and fluorogenic peptide substrates based on cleavage sites within endogenous protein substrates of PfSUB1 (13, 21). In our earlier work (13, 20), we used the assay to identify a substrate-based pentapeptidic α -ketoamide with a P4 Ile residue and P2 Gly residue as our most potent inhibitor **1** (IC_{50} ~900 nM; Fig. 1). Unfortunately, this and related α -ketoamides showed no anti-parasite activity in vitro. This was perhaps unsurprising due to the high molecular mass and polar nature of these compounds, including the presence of a carboxylic acid moiety that was designed to mimic endogenous PfSUB1 protein substrates by interacting with the basic S' surface of the PfSUB1 active-site cleft (16). Collectively, these features likely rendered the compounds poorly membrane penetrant.

To build on that work, we first explored a range of P4 substituents of the N-acetyl peptidyl α -ketoamide scaffold, maintaining the P1 Ala, P2 Gly, and P3 Thr sidechains unaltered. Replacement of the P4 Ile side chain with a cyclopentane improved potency, resulting in an peptidic α -ketoamide **2a** with an IC_{50} ~370 nM (*S1 Appendix, Table S1*). Reasoning that the exploration of alternative warheads with known activity against serine proteases might prove fruitful, we replaced the α -ketoamide functionality of this compound with a boronic acid warhead, in the process removing the prime side carboxylate. This resulted in compound **3a**, which gratifyingly demonstrated an ~sevenfold increase in potency over the best α -ketoamide (Table 1). Combining the features of the α -ketoamide and compound **3a** by adding back the P4 cyclopentane improved potency by a further ~13-fold, leading to the low nanomolar IC_{50} compound **3b** (Table 1).

To examine the importance of the stereochemistry of the aminoboronic acid substructure at the P1 position, the PfSUB1 inhibitory potency of boronic acid epimer **3c** was examined (Table 1). We found that **3c** was significantly less potent than **3b** (Table 1), indicating the requirement for a chiral center configuration matching that of the L-amino acid in native substrates of SUB1. We therefore maintained this stereochemistry in all subsequent boronic acid analogs.

Further work focused on enhancing the potency of the compound **3b** structural template. Removal of the methyl side chain at the P1 subsite (compound **3d**) reduced potency by eightfold. On the other hand, attempts to improve potency by exploring extended alkyl or phenyl substituents at the P1 subsite (compounds **3e**, **3f**, **3g**, and **3h**) met with only limited success, although compound **3e** bearing a hydroxyethyl substituent displayed ~twofold increased potency over compound **3b**. This appears to contradict earlier

substrate specificity studies, which indicated a preference for the S1 subpocket of PfSUB1 to accommodate polar sidechains (13). The observation may be explained by a preference of nucleophilic P1 side-chain residues to form cyclic boronic acids, preventing the polar hydroxyl group from engaging in interactions with the enzyme.

Conditional gene disruption experiments have shown that PfSUB1 is essential for asexual blood-stage parasite survival in vitro (12). To assess the capacity of the compounds to interfere with parasite replication, we used an in vitro growth assay, which exploits the DNA-binding fluorescent dye SYBR Green I to measure parasite proliferation in human RBCs (which do not possess a nucleus) (22). This showed that while all the compounds inhibited parasite replication, with EC_{50} values as low as 1.8 μ M, there was a poor correlation between growth inhibition and the PfSUB1 enzyme-inhibitory potency of the compounds (Table 1). In particular, the most potent inhibitor of PfSUB1 enzymatic activity, compound **3e**, was more than sixfold less growth inhibitory than compound **3b**. We reasoned that the polar nature of **3e** likely limits its membrane permeability. It was concluded that this set of compounds suffered from poor access to PfSUB1 within the intracellular parasite, probably due to low cellular permeability.

P3 Modification Results in Peptidic Boronic Acids with Submicromolar Parasite Growth Inhibitory Activity.

To seek insights into how the most potent PfSUB1-inhibitory compounds of this first boronic acid series might be accommodated into the PfSUB1 active-site groove, we took advantage of the X-ray crystal structure of PfSUB1 (16) to perform in silico molecular docking of compounds (**3b** and **3e**; Fig. 2). We examined the bound molecules in a docked pose in which the boron atom was involved in a tetrahedrally coordinated intermediate involving the catalytic His428 (N_{E2}H) and the oxyanion hole partner N520 (N₈) and engaged in a covalent bond with the O_γ of the catalytic Ser606 of PfSUB1. This showed conservation of the substrate-enzyme canonical H-bond pattern, with the inhibitor peptidic backbone interacting with PfSUB1 residues Gly467 (NH), Ser490 (NH), and Ser492 (NH). For both inhibitors, the P4 cyclopentane was nicely accommodated into the S4 pocket (shaded green for hydrophobicity and delimited by a thick solid line to indicate optimal steric filling in Fig. 2B). The inhibitor **3b** P1 Ala side chain did not fill the S1 pocket entirely (indicated by the absence of a solid line at the bottom of the S1 pocket) but occupied the hydrophobic part of the pocket. In the case of inhibitor **3e**, docked in the form of an acyclic boronic acid, the P1 hydroxyethyl extension filled the S1 pocket fully and was stabilized by hydrogen bonding with Ser490 O_γ and Ser492 O_γ at the bottom of the pocket. Despite this, little improvement in potency of inhibitor **3e** over inhibitor **3a** was observed, which as mentioned above we suspect is likely explained by compound **3e** adopting the preferential cyclic form of the boronic acid.

Consistent with the X-ray crystal structure of PfSUB1, which includes its propeptide bound into the active-site groove of the catalytic domain in a substrate-like manner, the P3 Thr side chain

Table 1. PfsUB1 enzyme inhibitory and parasite growth inhibitory potency of peptidic boronic acids

Entry	Compound	Structure	IC ₅₀ (nM) (rPfsUB1)*	EC ₅₀ (μM) (parasite growth) [†]
1	3a		69.4 ± 1.2	1.8 ± 0.6
2	3b		9.3 ± 0.5	2.3 ± 1.4
3	3c		60.1 ± 2.1	18.4 ± 1.8
4	3d		54.3 ± 1.1	1.9 ± 0.4
5	3e		4.6 ± 0.1	15.0 ± 3.6
6	3f		204.2 ± 7.5	N.D.
7	3g		18.7 ± 1.3	N.D.
8	3h		112.0 ± 2.3	N.D.
9	3i		7.8 ± 0.3	0.34 ± 0.08
10	3j		5.7 ± 0.1	0.26 ± 0.06

*IC₅₀ values were determined by quantifying inhibition of rPfsUB1-mediated proteolytic cleavage of a fluorogenic peptide substrate. Values are mean averages from at least three independent measurements ± SD.

[†]EC₅₀ values were obtained by quantifying inhibition of *P. falciparum* growth in vitro over a period of 96 h (two erythrocytic growth cycles) using the DNA-binding fluorescent dye SYBR Green I to measure parasite replication (22). Values are mean averages from at least three independent measurements ± SD. N.D., not determined.

of the docked compounds **3b** and **3e** was observed to extend into solvent, with no significant contacts with the molecular surface of the PfsUB1 catalytic domain. Interestingly, however, in both docking poses we noticed potential for modifying and/or extending the P3 side chain (openness depicted in gray in the two-dimensional diagram) in order to promote hydrophobic interactions with the side-chain carbon atoms of Lys465 and Leu466 that line the side of the S3 pocket. In silico replacement of the P3 Thr with Val supported this, revealing potential hydrophobic interactions between the Val P3 side chain and the side chains of Leu466 and Lys465 (Fig. 2B).

In accord with this, we prepared compounds **3i** and **3j** in which the P3 Thr of compound **3b** was replaced, respectively, with an Ala and Val side chain (Table 1). The new compounds showed slightly improved (**3i**; IC₅₀ ~7.8 nM) or nearly twofold improved (**3j**; IC₅₀ ~5.7 nM) potency relative to compound **3b** in the in vitro PfsUB1 enzyme assay. Significantly, compounds **3i** and **3j** displayed ~10-fold improved growth inhibitory potency in the SYBR Green I parasite growth assay, likely due to their increased lipophilicity, which was expected to confer better membrane permeability.

Inhibition of *P. falciparum* Egress by Selective Peptidic Boronic Acids that Access PfSUB1 in Intracellular Parasites. To determine their mode of action, the four most potent growth inhibitory compounds were next evaluated using very short-term cell-based assays focused on the narrow window within the asexual blood-stage lifecycle during which the parasite undergoes egress from host RBCs and invasion into fresh cells. For this, *P. falciparum* cultures containing synchronous, highly mature schizonts were supplemented with compounds **3b**, **3e**, **3i**, and **3j** at a range of dilutions, then allowed to undergo egress and invasion for just 4 h in the continued presence of the compounds, before assessing formation of newly invaded “ring” stage parasites by flow cytometry. This confirmed a dose-dependent inhibitory effect on the transition from schizont to ring stage, with the relatively lipophilic compounds **3i** and **3j** displaying similar EC₅₀ values that were significantly lower than those of **3b** and **3e** (Fig. 3A). Microscopic examination of the cultures revealed schizonts arrested by compounds **3i** and **3j**, confirming inhibition of schizont rupture. Importantly, the arrested schizonts were morphologically indistinguishable from those arrested by the reversible PKG inhibitor (4-[7-[(dimethylamino)methyl]-2-(4-fluorophenyl)imidazo[1,2- α]pyridine-3-yl]pyrimidin-2-amine (C2)), appearing as segmented forms trapped within an apparently intact PVM and RBC membrane (Fig. 3B). This egress-arrest phenotype is similar to that obtained by genetic disruption of PfSUB1 and was clearly different from that following arrest by the cysteine protease inhibitor E64 (Fig. 3B), which does not inhibit PfSUB1 directly but which blocks a cysteine protease-dependent step in egress following SUB1 discharge and PVM rupture (12).

Examination of the inhibitory activity of compound **3j** against the mammalian trypsin-family serine proteases trypsin, chymotrypsin, and elastase revealed a high degree of selectivity for PfSUB1 (>>100-fold; *SI Appendix*, Figs. S1–S3), encouraging us to focus subsequent work on this compound. To directly visualize the inhibitory effects of compound **3j** on parasite egress and to examine the reversibility of inhibition, we used live time-lapse video microscopy to observe the behavior of schizonts exposed to the compound for just 1 h immediately prior to egress. For this, we used a transgenic parasite line expressing a PVM protein (EXP2) fused with the green fluorescent protein mNeon Green, facilitating real-time visualization of PVM integrity as previously reported by Glushakova and colleagues (23). As shown in Fig. 4A and *Movie S1*, this clearly demonstrated significant inhibition of PVM rupture and egress in parasites treated with **3j**, with no signs of egress even 30 min following washout of the compound. Importantly, **3j**-treated parasites remained viable, as shown by their continued capacity to incorporate the vital mitochondrial dye MitoTracker Red CMXRos (24) (*SI Appendix*, Fig. S4), but showed no signs of the PVM rounding and other morphological changes that typically precede egress (23, 25), indicating a complete and selective block in the egress pathway. These egress-associated transitions were also absent from PfSUB1-null parasites (12), indicating that the effects of **3j** closely mimic genetic disruption of PfSUB1. Further extended incubation of the treated, washed schizonts with fresh RBCs resulted in only very limited appearance of new ring stage parasites (Fig. 4B). This confirmed that even short-term treatment with compound **3j** could dramatically impede parasite escape from the host RBC and that the egress inhibition over these timescales was effectively irreversible.

These results suggested that compound **3j** can access and inhibit PfSUB1 in an intracellular location (i.e., within the intraerythrocytic parasite, or in the PV, or both). To seek unambiguous confirmation that PfSUB1 is the intracellular target of compound **3j**, we examined the effects of the compound on the PfSUB1-mediated proteolytic processing of the established endogenous PfSUB1 substrate SERA5, an abundant parasite PV protein that only becomes accessible to cleavage upon discharge of PfSUB1 into the PV in the minutes leading up to egress and is then released in a processed form into culture supernatants (6, 11, 12). As shown in Fig. 4C,

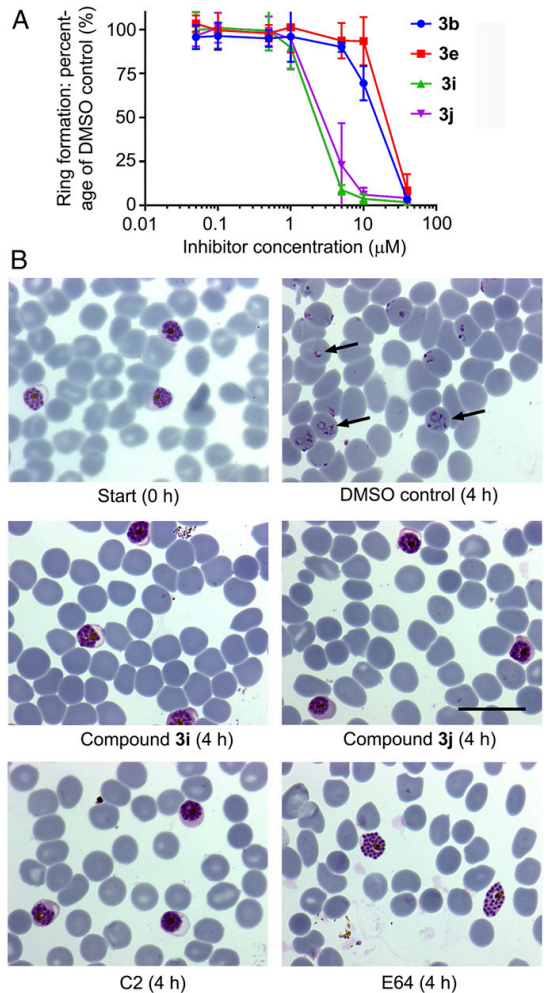


Fig. 3. Peptidic boronic acid PfSUB1 inhibitors prevent *P. falciparum* egress. (A) Dose-response curves showing ring formation following incubation of highly mature 3D7 schizonts with RBCs for 4 h in the presence of the indicated compounds. Values are means of three independent experiments. Calculated EC₅₀ values were as follows: compound **3b**, 12.7 ± 0.8 μM; **3e**, 15.7 ± 2.5 μM; **3i**, 2.0 ± 0.1 μM; and **3j**, 2.5 ± 0.3 μM. Error bars, SD. (B) Light micrographs of Giemsa-stained thin films prepared from selected cultures similar to those described in A, sampled prior to start or following the 4 h incubation step. Extensive ring formation is evident in the control culture (examples indicated by arrows). In contrast, cultures containing compounds **3i** or **3j** (10 μM) show arrest of unruptured schizonts with no ring formation. Note that the phenotype of the **3i**- or **3j**-arrested schizonts is similar to that of C2-treated parasites but distinct from those arrested by the cysteine protease inhibitor E64, where PVM rupture occurs allowing release of the enclosed merozoites into the RBC cytosol. (Scale bar, 20 μm.)

treatment with compound **3j** reproducibly prevented proteolytic processing and release of SERA5 into culture supernatants in a dose-dependent manner, even following compound washout. Crucially, at higher concentrations of the drug where egress and release of processed SERA5 was completely blocked, no intracellular

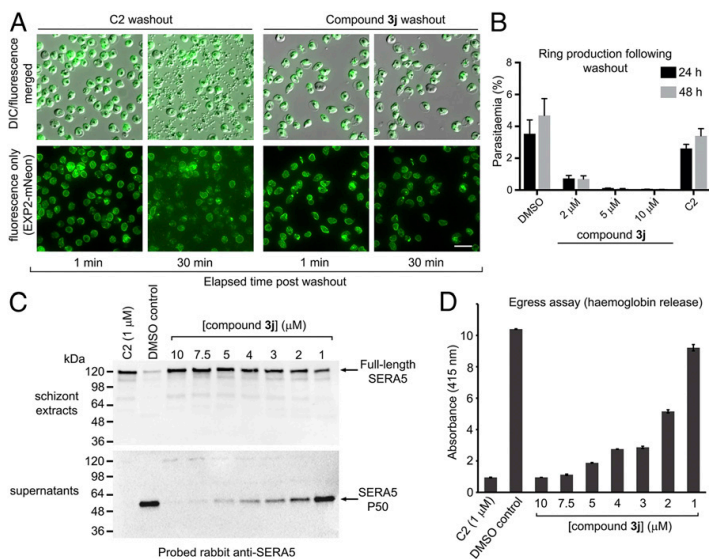


Fig. 4. Washout experiments show that peptidic boronic acid **3j** is a membrane-permeable inhibitor of PfSUB1 and *P. falciparum* egress. (A) Stills from time-lapse video microscopic monitoring of purified schizonts following washout of the indicated treatments. The parasites express an mNeonGreen fusion of the PVM protein EXP2. Washout of drug from schizonts arrested with the reversible PKG inhibitor C2 (1 μM) resulted in normal egress, initiating at ~6.5 min following washout. In contrast, no egress occurred over the course of 30 min following washout of parasites treated with saturating amounts (10 μM) of compound **3j**, and there was no discernible change in shape or integrity of the PVM (although slight time-dependent photobleaching of the fluorescence signal is evident). Identical results were obtained in four independent experiments. (Scale bar, 20 μm.) Also reference [Movies S1](#) and [S2](#). (B) Ring formation following incubation with fresh RBCs of schizonts pretreated with vehicle only (DMSO), C2 (1 μM), or compound **3j**. Drugs were washed away before addition of RBCs. Ring production was assessed at 24 h. Parasitaemia was also assessed at 48 h to ensure that the rings detectable at 24 h were viable. No rings were produced by the 10 μM **3j** pretreated schizonts, whereas schizonts pretreated with the reversible PKG inhibitor C2 produced rings efficiently. Results shown are from three independent experiments in different batches of blood. Error bars, ± SD. (C) Western blot analysis of mature schizonts and culture supernatants thereof following pretreatment for 4 h with compound **3j** at the indicated concentrations, then washout before analysis of egress. The parasite PV protein SERA5, which is proteolytically converted to the P50 fragment through the action of PfSUB1, appeared in the supernatants of control schizonts (which underwent egress) but remained intracellular in its intact, full-length form at higher concentrations of **3j**. As expected, SERA5 processing was also blocked by C2 (positive control). (D) Quantitation of hemoglobin release into culture supernatants (an indicator of the extent of egress) in the assay analyzed in C. Error bars, SD. Data shown are typical of four independent experiments.

processing of SERA5 was evident in the intact egress-arrested schizonts. Quantitation of egress in these same washout assays by measuring release of residual hemoglobin from the rupturing schizonts showed an EC_{50} of ~2 μM (Fig. 4D), similar to the EC_{50} value for new ring generation previously determined by flow cytometry (Fig. 3A). It was concluded that compound **3j** prevents egress and parasite proliferation through direct inhibition of intracellular PfSUB1.

An Optimized Membrane-Penetrant Peptidic Boronic Acid Displays Time-Dependent, Slowly Reversible Binding Kinetics to PfSUB1.

Boronic acids form reversible covalent bonds with serine and threonine proteases (26). Inhibition is generally time dependent, and the covalent nature of the binding can result in relatively long target occupancy times despite the reversibility of the bond. That this might be the case with compound **3j** binding to PfSUB1 was initially suggested by our washout experiments (Fig. 4), which showed that egress inhibition by compound **3j** following washout was much longer lasting than the rapidly reversible egress inhibition mediated by C2. To analyze the kinetic characteristics of the interaction between **3j** and rPfSUB1, we used progress curve analysis to continuously monitor rPfSUB1-mediated cleavage of a fluorogenic substrate in the presence of a range of concentrations of **3j**. As shown in [SI Appendix, Fig. S5](#), under conditions where substrate cleavage in the absence of inhibitor (control reaction) displayed a

linear relationship with time, indicating negligible substrate depletion, progress curves in the presence of compound **3j** became progressively nonlinear, characteristic of slow-binding (time-dependent) inhibition. Under such conditions, fit of the progress curves by nonlinear regression to Eq. 1 (see [Materials and Methods](#)) allows determination of k_{obs} , the pseudo first-order rate constant for onset of inhibition. The k_{obs} is effectively a composite of the on and off rates, so least linear squares regression of the calculated k_{obs} values against inhibitor concentration allows determination of values of the pseudo first-order dissociation rate constant k_{off} and the second-order association rate constant k_{on} for the inhibitor-rPfSUB1 interaction, based respectively on values from the y-intercept and slope. The y-intercept value corresponds to a k_{off} of $3.7 \times 10^{-4} s^{-1}$, which equates to a $t_{1/2}^{off}$ (bound half-life) of ~31 min. The calculated k_{on} value was $3.6 \times 10^5 M^{-1} \cdot s^{-1}$, allowing calculation of an apparent equilibrium inhibition constant K_1^{kin} (k_{off}/k_{on}) of 1.0 nM. It was concluded that compound **3j** is a potent, slowly reversible inhibitor of PfSUB1, completely consistent with the washout data.

Discussion

Prior to parasite egress from the confines of its host RBC, SUB1 is stored in membrane-bound merozoite secretory organelles called exonemes before its discharge into the PV lumen minutes before egress to encounter its endogenous substrates. As a result, in order to gain access to the intracellular enzyme prior to

substrate cleavage, exogenously applied inhibitory compounds likely need to cross at least two and as many as four distinct biological membranes: the RBC membrane, the PVM, the parasite plasma membrane, and the exoneme membrane (Fig. 5). This poses particular challenges for the design of substrate-based inhibitors. In the case of covalent modifying compounds, such as those described here, access to the exoneme-resident enzyme could potentially allow inactivation of the stored SUB1 long before its PKG-regulated discharge into the PV. In this work, we did not determine the intracellular site of PfSUB1 inhibition, so we cannot state whether inhibition took place within the PV, or the exonemes, or both. Regardless, by gradual optimization of the structure and lipophilicity of our compounds we have now successfully developed potent PfSUB1-inhibitory compounds that can functionally inactivate PfSUB1 within intact, parasite-infected RBCs and block egress.

Our conclusion that the intracellular inhibition of PfSUB1 mediated by compound **3j** is directly and causally responsible for the observed block in egress is most clearly supported by the phenotype of the arrested schizonts, which was indistinguishable from that resulting from conditional genetic disruption of the *PfSUB1* (12) or *PKG* gene (27), or following treatment with the PKG inhibitor C2, with no signs of the morphological changes that typically precede egress such as PVM rounding or PV rupture. We cannot rule out the possibility of effects on other parasite enzymes at the concentrations used to obtain complete egress inhibition, even in the short-term assays designed to focus on the short window of the parasite life cycle over which egress occurs. However, we consider off-target effects unlikely given that no other parasite serine protease has been implicated in egress; the only two other subtilisin-like enzymes expressed in the parasite, SUB2 and SUB3, are respectively dispensable for egress (28) or nonessential in blood stages (29). The ~10-fold higher potency of **3j** in the long-term SYBR Green-based parasite growth assay (EC_{50} 0.26 μ M; Table 1) may be a result of the fact that this assay captures the combined effects of egress inhibition over the course of two erythrocytic cycles in the continuous presence of the drug, although again off-target effects cannot be formally ruled out. We anticipate that further

optimization of the PfSUB1-inhibitory potency and membrane permeability of **3j** is highly feasible. Work is already underway to determine the atomic structure of the **3j**-PfSUB1 complex to facilitate structure-based inhibitor improvement.

Peptidic boronic acids have long-established therapeutic potential, as best exemplified by the widespread clinical use for multiple myeloma of the proteasome inhibitors bortezomib (Velcade) and ixazomib, the latter of which is orally bioavailable in its citric acid form, Ninlaro. The clinical success of these compounds is in part due to the long drug target residence times that can be obtained with slowly reversible covalent inhibitors. Target binding by boronic acid protease inhibitors is generally time dependent, perhaps further explaining the differences in potency we observed between the long-term and short-term cellular assays with compounds **3i** and **3j**. However, our wash-out experiments with compound **3j** suggest that, once bound to PfSUB1 in the exonemes and/or PV, it takes at least 30 min for the level of target engagement to fall below a threshold that allows successful egress. Examination of the capacity of schizonts treated with saturating levels of **3j** to productively egress and form new rings following compound washout showed that the egress block under these conditions was effectively irreversible. An alternative explanation for this apparently irreversible inhibition of egress by **3j** is that the inhibitor is not easily washed out due to its accumulation in the parasite (or infected RBC) at high concentrations. We cannot formally rule out this possibility. However, our *ex vivo* kinetic analysis of the inhibition of rPfSUB1 by compound **3j** fully supports a slow off rate, with an estimated bound half-life ($t_{1/2}^{off}$) of ~30 min, very similar to that of the interaction between bortezomib and the $\beta 5$ chymotrypsin-like subunit of the human proteasome (30–32). Even if cellular accumulation does contribute to the prolonged egress inhibition exerted by **3j**, this is only likely to favor efficacy; indeed, intracellular accumulation is an important component of the mode of action of the important antimalarial 4-aminoquinoline chloroquine (33). While peptide-based drug development can present challenges for *in vivo* applications due to metabolic instability, covalent compounds can be effective even with relatively short plasma half-lives, since target residence time can be longer than plasma half-life. Peptidyl boronic acids can anyway have excellent pharmacodynamic properties; for example, the terminal half-life of ixazomib is ~9.5 d (a fact that allows weekly dosing of patients for treatment of multiple myeloma; ref. 34), which is nearly five times the duration of the *P. falciparum* asexual blood-stage lifecycle.

SUB1 has an unusual substrate specificity, which differs subtly between different *Plasmodium* species, suggesting that the enzyme and its multiple cognate parasite substrates have coevolved to ensure optimal cleavage efficiency (13). As a result, inhibitors of PfSUB1 are unlikely to show similar potency against SUB1 orthologs from rodent malaria parasite species such as *Plasmodium berghei*, making these parasite species unsuitable as model systems for assessing the *in vivo* efficacy of our compounds. Importantly, SUB1 also lacks structural resemblance to any known human serine protease (16), reducing the likelihood of substrate-based SUB1 inhibitors displaying toxicity due to off-target activity against host enzymes. In support of this, we found here that **3j** is only poorly potent against the mammalian serine proteases examined. Toxicity can be especially problematic where long-term or life-long treatment regimens are required due to chronic infection (e.g., with HIV). However, malaria is an acute disease, and long-term therapeutic regimens are rare; indeed, current standard treatments for uncomplicated falciparum malaria are just 3 d long. Since SUB1 plays an essential role in the development and release of exoerythrocytic (liver-stage) merozoites that initiate blood-stage infection (14, 15), medicines based on SUB1 inhibitors have prophylactic as well as therapeutic potential. Optimized SUB1 inhibitors could

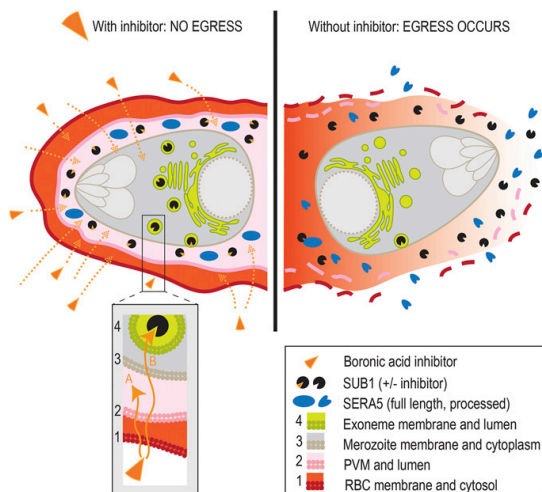


Fig. 5. Schematic indicating the requirement for inhibitors of SUB1 to cross at least two and up to four membranes to access and inactivate the enzyme in intraerythrocytic parasites. Inhibition likely occurs either in the PV (route A), or the exonemes (route B), or both.

also potentially be combined with inhibitors of other essential enzymes in the egress pathway, including PKG (35–37) and the SUB1 aspartic protease maturase plasmepsin X (38–41). Such combinations could yield additive or synergistic enhancement of potency and decrease opportunities to select for drug resistance.

In conclusion, we have produced substrate-based peptidic boronic acids that block asexual blood-stage *P. falciparum* proliferation through direct, effectively irreversible inhibition of intracellular PfSUB1. Further investigation of the pharmacokinetic properties and structure-based improvement of these compounds has the potential to generate compounds suitable for preclinical trials in animal models of malaria.

Materials and Methods

***P. falciparum* Maintenance and Manipulation.** Asexual blood stages of *P. falciparum* (clones 3D7 and B11) (42) were routinely maintained at 37 °C in human erythrocytes at 1 to 4% hematocrit in RPMI 1640 containing AlbuMax II (Thermo Scientific) supplemented with 2 mM L-glutamine in a low oxygen atmosphere using standard procedures (43). Human blood was obtained from anonymized donors through the UK National Blood and Transplant service and was used within 2 wk of receipt. No ethical approval is required for its use. For synchronization, mature schizont-stage parasites were isolated on cushions of 70% (volume/volume) Percoll (GE Healthcare) adjusted to isotonicity as described (43). Routine microscopic examination of parasite growth was performed by fixing air-dried thin blood films with 100% methanol before staining with 10% Giemsa stain (VWR International) in 6.7 mM phosphate buffer, pH 7.1.

Generation of the B11-EXP2-mNeonGreen line was achieved by fusing mNeonGreen to the endogenous C terminus of EXP2 using Cas9-mediated gene editing, following the methods of ref. 23. A pair of guide RNAs were designed targeting a region toward the 3' end of the EXP2 locus (oligo 1: ATTGATATT-ATGTACAGTACTGA, oligo 2: AAACCTCAGACTGTACATAATAT) (Sigma). This oligonucleotide pair was annealed with T4 PNK ligase (New England Biolabs) and ligated with T4 ligase (New England Biolabs) into the U6 cassette of the Cas9 vector (pDC2-Cas9_U6-hDHFR) previously digested with Bsb1-HF (New England Biolabs). The plasmid was propagated under ampicillin selection in *Escherichia coli* and sequenced to check for correct incorporation of the guide (Genewiz). The resulting plasmid was cotransfected into B11 schizonts along with the repair plasmid pPM2GT-EXP2-mNG (a kind gift of Josh Beck, Iowa State University, Ames, IA), linearized with AflIII (New England Biolabs). Drug selection for integration was carried out with 2.5 nM WR99210 (Sigma-Aldrich) from 24 h posttransfection, and clonal lines of the resulting B11-EXP2-mNeonGreen line were obtained by limiting dilution cloning and treatment with 1 μM Ancotic (5-fluorocytosine) before use.

Parasite Growth, Egress, and Invasion Assays. The impact of the peptidic boronic acids on replication of asexual blood-stage *P. falciparum* (done 3D7) was assessed using a SYBR Green I assay, essentially as described by Smilkstein et al. (22). Briefly, test compounds (dissolved in dimethyl sulfoxide [DMSO] at concentrations ranging from 4 mM to 5 μM) were added in triplicate to wells of flat bottomed, 96-well microtiter plates (1 μL per well). Wells were then supplemented with 100 μL per well of a *P. falciparum* parasite culture at 0.1% parasitaemia, 1% hematocrit. Each assay plate also included DMSO-only control wells (1% vol/vol), as well as additional control wells containing uninfected RBCs only. Plates were incubated in sealed, humidified gassed chambers at 37 °C for 96 h to allow the parasites to undergo two entire cycles of erythrocytic growth. Wells were then supplemented with 100 μL 1:5,000 dilution of stock SYBR Green I (Life Technologies, catalog no. S7563) diluted in 20 mM Tris-HCl pH 7.5, 5 mM EDTA, 0.008% (weight/vol) saponin, 0.08% (vol/vol) Triton x100. Plates were agitated to mix, incubated for a further 1 h in the dark at room temperature, then 150 μL samples from each well transferred to a fresh white microwell plate and fluorescence quantified using a SpectraMax M5e plate reader and SoftMax Pro-6.3 software (Ex 485 nm/Em 530 nm). IC₅₀ values were determined from dose-response curves obtained after subtracting background fluorescence values (obtained from the RBC-only wells) from all experimental readings.

Short-term egress, invasion, and washout assays were performed essentially as described previously (27, 28, 42). Briefly, highly synchronous mature Percoll-enriched schizonts with or without added fresh RBCs (~5% parasitaemia final) were incubated with compounds under test or vehicle only (DMSO, 1% vol/vol). For washout assays, schizonts were treated with C2 or various concentrations of inhibitor 3j for 1 to 4 h, then washed extensively (at least four times) prior to addition to fresh RBCs where required. After incubation at

37 °C for just 1 to 4 h (or overnight for invasion assays) to allow schizont rupture, cells were pelleted. Clarified culture supernatants were assessed for extent of hemoglobin release (a measure of schizont rupture) by absorption spectroscopy at 415 nm as described previously (28) or analyzed by Western blot using antibodies against SERA5 (7, 11). To quantify generation of new rings, samples of the cultures were fixed with 4% paraformaldehyde/0.02% glutaraldehyde and stained with SYBR Green I (Life Technologies) and then analyzed by flow cytometry on a BD FACVerse using BD FACSuite software. Data were analyzed using FlowJo software. All cultures were also routinely analyzed by microscopic examination of Giemsa-stained thin films to visually assess parasite morphology.

Time-Lapse and Live Fluorescence Microscopy. Viewing chambers for live parasite microscopic examination were constructed as previously described (7). All images were recorded on a Nikon Eclipse Ni light microscope fitted with a Hamamatsu C11440 digital camera and Nikon N Plan Apo λ 63x/1.45NA oil immersion objective. For time-lapse video microscopy, differential interference contrast (DIC) images were taken at 10 s intervals over 30 min while fluorescence (mNeon Green) images were taken every 2 min to prevent bleaching. Time-lapse videos were analyzed and annotated using Fiji (44). For viability staining using the vital mitochondrial dye MitoTracker Red CMXRos (ThermoFisher Scientific; stored as a 10 μM stock in DMSO), the dye was added (20 nM final concentration) to a suspension of schizonts pretreated for 1 h with either DMSO (control, 1% vol/vol) or compound 3j (10 μM). The schizonts were incubated with the dye for 15 min at 37 °C, then washed twice, transferred to a viewing chamber, and observed immediately by dual DIC/fluorescence microscopy.

Protease Inhibition Assays: IC₅₀ Calculations and Progress Curve Kinetics. Proteolytic activity of rPfSUB1 was quantified at room temperature by monitoring cleavage of the peptidic fluorogenic substrate SERA4st1F-6R12 (Ac-CKITAQDDEESC-OH possessing tetramethylrhodamine labeling of both cysteine residues) (13). Fluorescence of this peptide is quenched by rhodamine dimerization in the intact substrate but increases upon cleavage at the internal Q-D bond. Chymotrypsin-treated rPfSUB1 (expressed and purified as described previously (16)) was stored at –80 °C as a 228 U/mL stock in 20 mM Tris-HCl pH 8.2, 150 mM NaCl, 10% glycerol, and diluted for use (1:500 or 1:600) in reaction buffer (20 mM Tris-HCl pH 8.2, 150 mM NaCl, 12 mM CaCl₂, 25 mM CHAPS). Peptidic boronic acid inhibitors were dissolved in 100% DMSO at 10 or 20 mM, then further diluted in DMSO to generate stock solutions ranging from 500 to 0.01 μM and then used diluted 1:100 in the enzyme reactions. All reactions were performed in wells of white 96-well microwell plates (Nunc); 50 μL diluted rPfSUB1 was preincubated for 5 min with 1 μL each of the serially diluted boronic acid inhibitors, followed by addition of 50 μL substrate solution (0.1 μM final). Subsequent fluorescence increase was continuously monitored using a SpectraMax M5e plate reader and SoftMax Pro-6.3 software, with readings taken every 5 min for 60 min using excitation and emission values of 552 and 580 nm, respectively. Initial rates were calculated over the first 25 min of the assay, during which period progress curves were linear, and IC₅₀ values were calculated with GraphPad Prism 8.0 using the nonlinear regression, [inhibitor] versus response, variable slope (four parameters). All experiments were performed in duplicate.

Details of the methodology used to evaluate the effects of compound 3j on the proteolytic activity of the mammalian serine proteases trypsin, chymotrypsin, and elastase are provided in [SI Appendix](#).

Progress Curve Kinetic Analysis of Compound 3j. Progress curves of SERA4st1F-6R12 cleavage by rPfSUB1 were acquired at seven concentrations of inhibitor compound 3j over a period of 35 min, during which fluorescence increases in the absence of inhibitor were linear. The obtained progress curves (four independent replicates) were fit using GraphPad Prism 8.0 software to the following time-dependent inhibition equation:

$$[P] = V_s \times t + ((V_i - V_s)/k_{obs}) \times (1 - \exp(-k_{obs} \times t)). \quad [1]$$

In the equation, V_i is the initial velocity, V_s is the final steady-state velocity, and k_{obs} reflects the observed pseudo first-order rate of inactivation. The obtained k_{obs} values were plotted against compound concentration using a linear least squares fit. All statistical analysis was carried out using GraphPad Prism 8.

Covalent Docking. Flexible covalent docking of peptidyl boronic acid compounds into the active site of PfSUB1 (Protein Data Bank: 4LVN) was performed using the Internal Coordinate Mechanics software (ICM-Pro) package version

3.9-1c/MacOSX (Molsoft LLC). The inhibitors were drawn using the ICM chemistry molecular editor and compiled into an sdf docking table. After adding hydrogen atoms to the structure, the C-terminal region of the SUB1 propeptide (P4 to P1 positions that occupy the SUB1 active site) was used to define boundaries within the enzyme active site for the docking procedure and then removed from the active site along with all water molecules prior to docking. The catalytic histidine (His428, N_ε) was protonated as part of the catalytic process, resulting from covalent binding of the boron atom ligand to the active Ser (Ser606 O_γ). The boronic acid covalent mechanism was selected from the ICM program reactions list. Potential energy maps of the SUB1 receptor pocket and docking preferences were set up using the program default parameters. Energy terms were based on the all-atom vacuum force field ECEPP/3, and conformational sampling was based on the biased probability Monte Carlo procedure (45). Four independent docking runs were performed per compound, with a length of simulation (thoroughness) varied from three to four and the selection of two docking poses. Ligands were ranked according to their ICM energetics (ICM score, unitless), which weighs the internal force-field energy of the ligand combined with other ligand-receptor energy parameters.

Statistical Analysis. All statistical analysis was carried out using GraphPad Prism 8.0.

Data Availability. All study data are included in the article and/or supporting information.

ACKNOWLEDGMENTS. We gratefully acknowledge Josh Beck (Iowa State University) and Joshua Zimmerberg (NIH) for the kind gift of construct pyPM2GT-EXP2-mNeonGreen and are indebted to Justin Molloy (The Francis Crick Institute) for invaluable discussions and advice on the kinetic analysis. This research was funded in part by the Wellcome Trust (Grant 106239/Z/14/A to M.J.B.). This work was supported by funding to M.J.B. from the Francis Crick Institute (<https://www.crick.ac.uk/>), which receives its core funding from Cancer Research United Kingdom (FC001043; <https://www.cancerresearchuk.org>), the UK Medical Research Council (FC001043; <https://mrc.ukri.org/>), and the Wellcome Trust (FC001043; <https://wellcome.org/>). The work was also supported by funding to A.J. from the European Regional Development Fund (Agreement No. 1.1.1.1/16/A/290) and by Wellcome ISSF2 funding to the London School of Hygiene & Tropical Medicine. The funders had no role in study design, data collection and analysis, decision to publish, or preparation of the manuscript.

- WHO, World malar. Rep. 2018 World Health Organ. Geneva 2016. <https://www.who.int/malaria/publications/world-malaria-report-2018/report/en>. Accessed 29 October 2020.
- T. N. Wells, R. Hoof van Huijsduijnen, W. C. Van Voorhis, Malaria medicines: A glass half full? *Nat. Rev. Drug Discov.* **14**, 424–442 (2015).
- T. N. Wells, P. L. Alonso, W. E. Gutteridge, New medicines to improve control and contribute to the eradication of malaria. *Nat. Rev. Drug Discov.* **8**, 879–891 (2009).
- J. E. Hyde, Drug-resistant malaria—An insight. *FEBS J.* **274**, 4688–4698 (2007).
- A. M. Dondorp *et al.*, Artemisinin resistance in *Plasmodium falciparum* malaria. *N. Engl. J. Med.* **361**, 455–467 (2009).
- S. Yeoh *et al.*, Subcellular discharge of a serine protease mediates release of invasive malaria parasites from host erythrocytes. *Cell* **131**, 1072–1083 (2007).
- C. R. Collins *et al.*, Malaria parasite cGMP-dependent protein kinase regulates blood stage merozoite secretory organelle discharge and egress. *PLoS Pathog.* **9**, e1003344 (2013).
- K. Koussis *et al.*, A multifunctional serine protease primes the malaria parasite for red blood cell invasion. *EMBO J.* **28**, 725–735 (2009).
- N. C. Silmon de Monerri *et al.*, Global identification of multiple substrates for *Plasmodium falciparum* SUB1, an essential malarial processing protease. *Infect. Immun.* **79**, 1086–1097 (2011).
- S. Das *et al.*, Processing of *Plasmodium falciparum* merozoite surface protein MSP1 activates a spectrin-binding function enabling parasite egress from RBCs. *Cell Host Microbe* **18**, 433–444 (2015).
- C. R. Collins, F. Hackett, J. Atid, M. S. Y. Tan, M. J. Blackman, The *Plasmodium falciparum* pseudoprotease SERAS regulates the kinetics and efficiency of malaria parasite egress from host erythrocytes. *PLoS Pathog.* **13**, e1006453 (2017).
- J. A. Thomas *et al.*, A protease cascade regulates release of the human malaria parasite *Plasmodium falciparum* from host red blood cells. *Nat. Microbiol.* **3**, 447–455 (2018).
- C. Withers-Martinez *et al.*, *Plasmodium* subtilisin-like protease 1 (SUB1): Insights into the active-site structure, specificity and function of a pan-malaria drug target. *Int. J. Parasitol.* **42**, 597–612 (2012).
- C. Suarez, K. Volkman, A. R. Gomes, O. Billker, M. J. Blackman, The malarial serine protease SUB1 plays an essential role in parasite liver stage development. *PLoS Pathog.* **9**, e1003811 (2013).
- L. Tawk *et al.*, A key role for *Plasmodium* subtilisin-like SUB1 protease in egress of malaria parasites from host hepatocytes. *J. Biol. Chem.* **288**, 33336–33346 (2013).
- C. Withers-Martinez *et al.*, The malaria parasite egress protease SUB1 is a calcium-dependent redox switch subtilisin. *Nat. Commun.* **5**, 3726 (2014).
- D. Giganti *et al.*, A novel *Plasmodium*-specific prodomain fold regulates the malaria drug target SUB1 subtilase. *Nat. Commun.* **5**, 4833 (2014).
- A. Bouillon *et al.*, In Silico screening on the three-dimensional model of the *Plasmodium vivax* SUB1 protease leads to the validation of a novel anti-parasite compound. *J. Biol. Chem.* **288**, 18561–18573 (2013).
- S. Arastu-Kapur *et al.*, Identification of proteases that regulate erythrocyte rupture by the malaria parasite *Plasmodium falciparum*. *Nat. Chem. Biol.* **4**, 203–213 (2008).
- S. S. Kher *et al.*, Substrate derived peptidic α -ketoamides as inhibitors of the malarial protease PfSUB1. *Bioorg. Med. Chem. Lett.* **24**, 4486–4489 (2014).
- M. J. Blackman *et al.*, Structural and biochemical characterization of a fluorogenic rhodamine-labeled malarial protease substrate. *Biochemistry* **41**, 12244–12252 (2002).
- M. Smilkstein, N. Sriwilaijaroen, J. X. Kelly, P. Wilairat, M. Riscoe, Simple and inexpensive fluorescence-based technique for high-throughput antimalarial drug screening. *Antimicrob. Agents Chemother.* **48**, 1803–1806 (2004).
- S. Glushakova *et al.*, Rounding precedes rupture and breakdown of vacuolar membranes minutes before malaria parasite egress from erythrocytes. *Cell. Microbiol.* **20**, e12868 (2018).
- P. S. Jogdand *et al.*, Flow cytometric readout based on Mitotracker Red CMXRos staining of live asexual blood stage malarial parasites reliably assesses antibody dependent cellular inhibition. *Malar. J.* **11**, 235 (2012).
- S. Glushakova *et al.*, New stages in the program of malaria parasite egress imaged in normal and sickle erythrocytes. *Curr. Biol.* **20**, 1117–1121 (2010).
- R. Smoum, A. Rubinstein, V. M. Dembitsky, M. Srebnik, Boron containing compounds as protease inhibitors. *Chem. Rev.* **112**, 4156–4220 (2012).
- K. Koussis, C. Withers-Martinez, D. A. Baker, M. J. Blackman, Simultaneous multiple allelic replacement in the malaria parasite enables dissection of PKG function. *Life Sci. Alliance* **3**, e201900626 (2020).
- C. R. Collins *et al.*, The malaria parasite sheddase SUB2 governs host red blood cell membrane sealing at invasion. *eLife* **9**, e61121 (2020).
- M. Zhang *et al.*, Uncovering the essential genes of the human malaria parasite *Plasmodium falciparum* by saturation mutagenesis. *Science* **360**, eaap7847 (2018).
- B. B. Hasinoff, Progress curve analysis of the kinetics of slow-binding anticancer drug inhibitors of the 20S proteasome. *Arch. Biochem. Biophys.* **639**, 52–58 (2018).
- M. J. Williamson *et al.*, Comparison of biochemical and biological effects of ML858 (salinosporamide A) and bortezomib. *Mol. Cancer Ther.* **5**, 3052–3061 (2006).
- E. Kupperman *et al.*, Evaluation of the proteasome inhibitor MLN9708 in preclinical models of human cancer. *Cancer Res.* **70**, 1970–1980 (2010). Corrected in: *Cancer Res.* **70**, 3853 (2010).
- A. Ecker, A. M. Lehane, J. Clain, D. A. Fidock, PfCRT and its role in antimalarial drug resistance. *Trends Parasitol.* **28**, 504–514 (2012).
- N. Gupta *et al.*, Clinical pharmacology of ixazomib: The first oral proteasome inhibitor. *Clin. Pharmacokinet.* **58**, 431–449 (2019).
- A. N. Matralis *et al.*, Development of chemical entities endowed with potent fast-killing properties against *Plasmodium falciparum* malaria parasites. *J. Med. Chem.* **62**, 9217–9235 (2019).
- D. A. Baker *et al.*, A potent series targeting the malarial cGMP-dependent protein kinase clears infection and blocks transmission. *Nat. Commun.* **8**, 430 (2017).
- M. Vanarschot *et al.*, Inhibition of resistance-refractory P. Falciparum kinase PKG delivers prophylactic, blood stage, and transmission-blocking antiplasmodial activity. *Cell Chem. Biol.* **27**, 806–816.e8 (2020).
- P. Pino *et al.*, A multistage antimalarial targets the plasmepsins IX and X essential for invasion and egress. *Science* **358**, 522–528 (2017).
- A. S. Nasamu *et al.*, Plasmepsins IX and X are essential and druggable mediators of malaria parasite egress and invasion. *Science* **358**, 518–522 (2017).
- R. Zogota *et al.*, Peptidomimetic plasmepsin inhibitors with potent anti-malarial activity and selectivity against cathepsin D. *Eur. J. Med. Chem.* **163**, 344–352 (2019).
- P. Favuzza *et al.*, Dual plasmepsin-targeting antimalarial agents disrupt multiple stages of the malaria parasite life cycle. *Cell Host Microbe* **27**, 642–658.e12 (2020).
- A. J. Perrin *et al.*, The actinomyosin motor drives malaria parasite red blood cell invasion but not egress. *MBio* **9**, e00905–e00918 (2018).
- M. J. Blackman, Purification of *Plasmodium falciparum* merozoites for analysis of the processing of merozoite surface protein-1. *Methods Cell Biol.* **45**, 213–220 (1994).
- J. Schindelin *et al.*, Fiji: An open-source platform for biological-image analysis. *Nat. Methods* **9**, 676–682 (2012).
- R. Abagyan, M. Totrov, Biased probability Monte Carlo conformational searches and electrostatic calculations for peptides and proteins. *J. Mol. Biol.* **235**, 983–1002 (1994).

Lidumniec *et al.*

Peptidic boronic acids are potent cell-permeable inhibitors of the malaria parasite egress serine protease SUB1

PNAS | 9 of 9

<https://doi.org/10.1073/pnas.2022696118>

Lidumniece, E., Withers-Martinez, C., Hackett, F., Blackman, M., Jirgensons, A. Subtilisin-like Serine Protease 1 (SUB1) as an Emerging Antimalarial Drug Target: Current Achievements in Inhibitor Discovery. *J. Med. Chem.* **2022**, *65*, 12535–1254.

Reprinted with the permission from ACS

Copyright © 2022 American Chemical Society

Subtilisin-like Serine Protease 1 (SUB1) as an Emerging Antimalarial Drug Target: Current Achievements in Inhibitor Discovery

Miniperspective

Elina Lidumniece, Christlaine Withers-Martinez, Fiona Hackett, Michael J. Blackman, and Aigars Jirgensons*

Cite This: *J. Med. Chem.* 2022, 65, 12535–12545

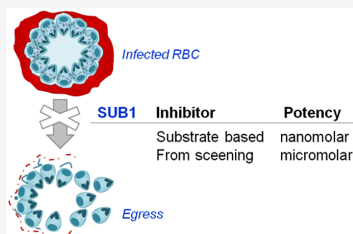
Read Online

ACCESS |

Metrics & More

Article Recommendations

ABSTRACT: Widespread resistance to many antimalarial therapies currently in use stresses the need for the discovery of new classes of drugs with new modes of action. The subtilisin-like serine protease SUB1 controls egress of malaria parasites (merozoites) from the parasite-infected red blood cell. As such, SUB1 is considered a prospective target for drugs designed to interrupt the asexual blood stage life cycle of the malaria parasite. Inhibitors of SUB1 have potential as wide-spectrum antimalarial drugs, as a single orthologue of SUB1 is found in the genomes of all known *Plasmodium* species. This mini-perspective provides a short overview of the function and structure of SUB1 and summarizes all of the published SUB1 inhibitors. The inhibitors are classified by the methods of their discovery, including both rational design and screening.



INTRODUCTION

Enzymes of microbial pathogens are well-established drug targets, from the bacterial transpeptidase targets of beta-lactam antibiotics to the protease and reverse transcriptase targets of several antiviral drugs. Pathogenic protozoa such as the *Plasmodium* species that cause malaria are no exception, and two of the historically most successful antimalarial drugs (pyrimethamine and proguanil) target the parasite dihydrofolate reductase.¹ However, resistance to these antifolate drugs is now widespread, and reports of the emergence of parasite resistance to other front-line antimalarial therapeutics, including artemisinin-based combinations (ACTs), are of great concern.² There is a widely accepted need to strengthen the antimalarial drug pipeline by the identification of new classes of antimalarial drugs with new modes of action.

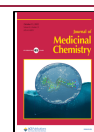
All the clinical manifestations of malaria are caused by cycles of parasite proliferation within red blood cells (Figure 1). Specialized developmental forms called merozoites invade the red cell and rapidly transform within a parasitophorous vacuole (PV) into feeding forms called trophozoites. Over a period of around 48 h in the case of the most virulent *Plasmodium* species, *P. falciparum*, the intracellular parasite enlarges, undergoes nuclear division, and finally segments to form 16 or more daughter merozoites. These are released from the host cell in a lytic process called egress to allow the merozoites to invade fresh red cells and repeat the cycle. Work over the past three decades has revealed that egress is regulated by a parasite enzyme pathway, with a central role for a calcium-dependent

serine protease called SUB1. A single orthologue of SUB1 is found in the genomes of all known *Plasmodium* species, and gene disruption studies have shown that SUB1 is essential for parasite survival. SUB1 is synthesized as an enzymatically inactive zymogen, which undergoes at least two proteolytic processing events.³ First, autocatalytic cleavage forms p54 (a 54 kDa form), then a second processing step produces the mature p47 (47 kDa form) from p54. The second processing event is mediated by plasmepsin X, a parasite aspartic protease.⁴

SUB1 is initially stored in a set of merozoite secretory organelles called exonemes and then discharged into the PV lumen just prior to egress in order to encounter and precisely cleave its substrates, leading ultimately to rupture of the PV and red blood cell (RBC) membranes (Figure 1). A cGMP-dependent parasite protein kinase G (PKG) is required for discharge of SUB1 from exonemes.⁵ Multiple substrates of SUB1 have been identified, including merozoite surface proteins and a set of soluble PV proteins called the serine-rich antigen (SERA) family.⁶ In genetically SUB1-null parasites, rupture of neither the PV nor RBC membrane

Received: July 7, 2022

Published: September 22, 2022



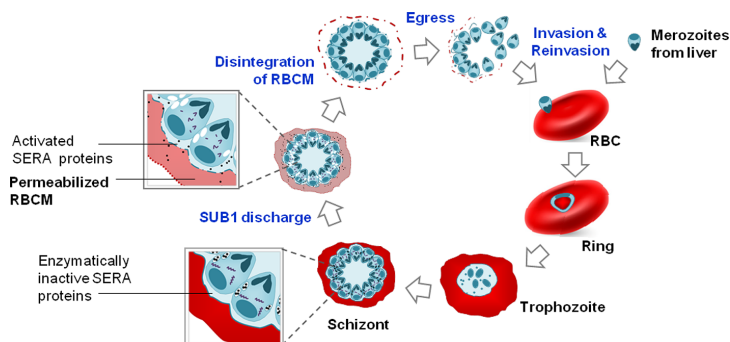


Figure 1. Asexual blood stage life cycle of *P. falciparum* and the role of SUB1 in egress.

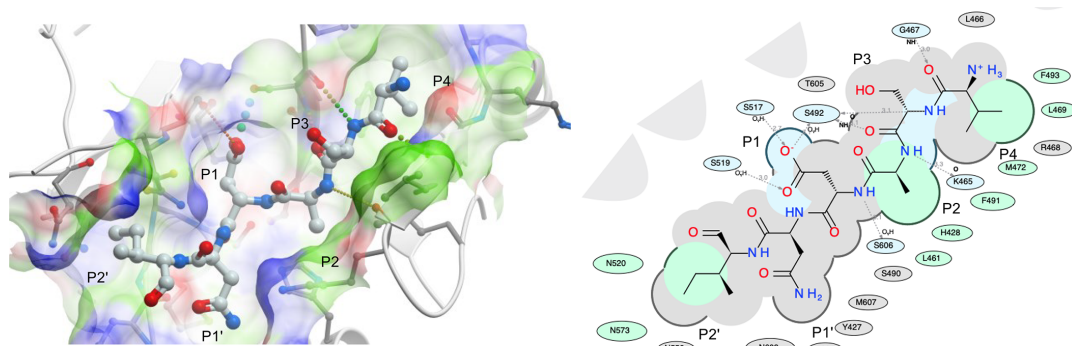


Figure 2. SUB1 P4–P2' endogenous substrate peptide (SUB1 prodomain) within the SUB1 active site (PDB 4VLO). Figure generated in ICM-Pro (Molsoft).

occurs, leading eventually to death of the trapped parasites, so small-molecule inhibitors of SUB1 are anticipated to similarly block egress and prevent parasite replication. As such, SUB1 inhibitors hold promise to attain the antimalarial target product profile 1 (TTP-1) and target candidate profile 1 (TCP-1)⁷ of the Medicines for Malaria Venture (MMV), a product development partnership focused on antimalarial drug development. The first tool compounds have now become available to study the suitability of SUB1 for drug development.

Several review articles have been published summarizing the function of SUB1 in the life cycle of a parasite.^{8,9} To complement these, we here have prepared a comprehensive mini-review covering inhibitor discovery efforts for SUB1 inhibitors.

■ STRUCTURE AND A SUBSTRATE SPECIFICITY OF SUB1

X-ray crystal structures of SUB1 have shown that it is closely related to several bacterial subtilisins¹⁰ and have provided detailed insights into the architecture of the SUB1 active site cleft, which interacts with protein and peptide substrates. This was aided by the fact that both structures comprise a complex between the SUB1 catalytic domain and its inhibitory prodomain, the C-terminal segment of which lies in the active site groove in a substrate-like manner.¹¹

A detailed understanding of protease specificity is useful to design potent, selective inhibitors. Toward this, substrate scanning methods were performed to identify protease preferences for certain amino acids.¹² In initial work to evaluate specific substrates of PfSUB1, peptides were synthesized based on the known autocatalytic cleavage site²¹⁵LVSAD↓NID1²²³ (Figure 2).³ The specificity of subtilases mainly relies on interactions between P4–P1 residue side chains with enzyme S4–S1 binding sites.¹³ Therefore, a range of modifications of the original motif at the P1, P2, or P4 positions was made and tested for efficiency of cleavage by recombinant *P. falciparum* SUB1 (rPfSUB1).

The results indicated that the enzyme prefers polar or small amino acid residues at the P1 position and is unable to cleave the peptide bond if leucine is at this position. Replacing the P4 valine with either lysine or alanine resulted in a remarkable decrease in cleavage efficiency, revealing that the P4 position has a significant role in substrate recognition by PfSUB1 and is consistent with the hydrophobic nature of the S4 pocket.^{10,14} Substrate scanning of the P2 position clearly showed that only alanine or glycine could be accommodated at this position, with a slight preference for glycine.¹⁴ A comparison of merozoite surface protein (MSP) processing sites with the internal PfSUB1 processing site, the known SERA5 processing sites, and the predicted processing sites in SERA4 and SERA6

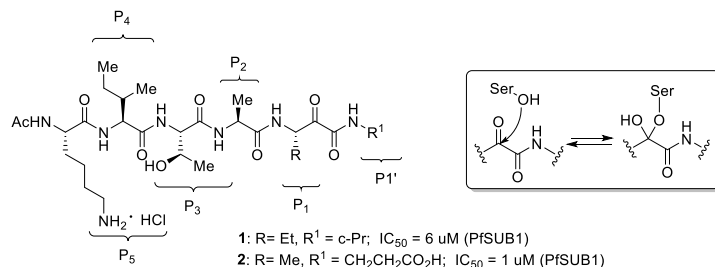


Figure 3. PoC substrate-derived SUB1 inhibitor with a ketoamide functionality as a serine trap.

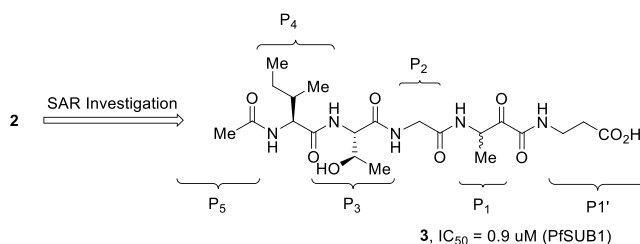


Figure 4. Optimized ketoamide containing inhibitor 3 and SAR of P5–P1' substitution (see text).

identified a consensus PfsSUB1 recognition motif of Ile/Leu/Val/Thr-Xaa-Gly/Ala-Paa(not Leu)Xaa (where Xaa is any amino acid residue and Paa tends to be a polar residue) and an intriguing preference for acidic residues and/or serine and threonine on the prime side of the scissile bond.^{6,14} A structural model of the enzyme and the identification that the most efficiently cleaved peptide corresponded to the SERA4 cleavage site 1 (KITAQJDDDEES)¹⁴ showed that the P1–P4 segment is held relatively tightly in the enzyme active site groove. Molecular modeling demonstrated that the enzyme S4 pocket is characterized by a lining of hydrophobic residues well-suited to the aliphatic residues preferred at the P4 position. The PfsSUB1 S3 pocket is not well-defined, while the substrate P3 residue side chain extends out toward the solvent, explaining the relative lack of specificity at this position. The most obvious characteristic of the S2 pocket is that it is small due to the side chain of lysine 465 (for most of the S8A subtilisins this residue is glycine), explaining the strict limitation for accommodating only small residues at the P2 position. The S1 pocket of PfsSUB1 is characterized by a cluster of five polar serine residues. Molecular modeling showed that the S' surface has a highly basic character, supporting the evidence from cleavage site alignments that prime side interactions are important for substrate binding. Experimental investigation of a modified SERA4 site1 substrate confirmed the preference for acidic or hydroxyl-containing prime side substrate residues.¹⁵

Molecular dynamics (MD) simulations together with free energy calculations were used to further understand which residues are essential for binding and what are the key interactions. These results¹⁶ suggested that strong canonical hydrogen bonds are formed between peptide residues P4–P2' and the PfsSUB1 binding site cleft, but the P3'–P5' residues undergo pronounced conformational changes and bind only occasionally for a short period of time to different regions of the PfsSUB1 structure. It was concluded that peptide residues

P4 and P2–P1' have the largest impact on the effective free energy with the most favorable interactions formed by residues P4 and P1. The results further suggested that the P5 residue might not be needed to achieve strong binding.¹⁶

■ RATIONALLY DESIGNED SUB1 INHIBITORS

Since peptide α -ketoamides are known to act as covalent inhibitors of serine proteases,¹⁷ potential inhibitor 1 (Figure 3) was synthesized based on the sequence of the best known natural substrate SERA4 site1 (KITAQJDDDEES).¹⁵ Ketoamide 1 contained the KITA segment of the peptide sequence, an ethyl group in the P1 position, and a cyclopropyl group placed toward the P' side. Dose–Response experiments confirmed this proof-of-concept inhibitor, determining a half-maximal inhibitory concentration (IC₅₀) for inhibition of rPfsSUB1 of $\sim 6 \mu\text{M}$. Compound 1 was also able to inhibit SUB1 of the other important *Plasmodium* species *P. vivax* (PvSUB1) and *P. knowlesi* (PkSUB1) with similar IC₅₀ values of ~ 12 and $\sim 6 \mu\text{M}$, respectively. Based on further modeling and experimental data, a modified compound called KS-466 was synthesized, which possessed a carboxylic group on the prime side of the α -ketoamide functionality, designed to mimic the prime side preference for acid groups. Dose–Response experiments showed improved IC₅₀ values against PfsSUB1 and PkSUB1 of $\sim 1 \mu\text{M}$, and an IC₅₀ against PvSUB1 of $\sim 2 \mu\text{M}$.

A systematic structure–activity relationship (SAR) investigation of peptidic α -ketoamides based on the structure of 2 (Figure 4) was performed to explore crucial enzyme–inhibitor interactions.¹⁸ When the P5 lysine residue was omitted (based on the outcome of the MD simulation studies), this resulted in twofold lower inhibitory activity compared to compound 2; however, the structure was considerably simpler so subsequent analogues for SAR were synthesized without this lysine residue. Analysis of the prime side residue (P1') revealed that the best linker resembles an aspartic acid residue. Longer or shorter chains or an amide analogue resulted in decreased activity.

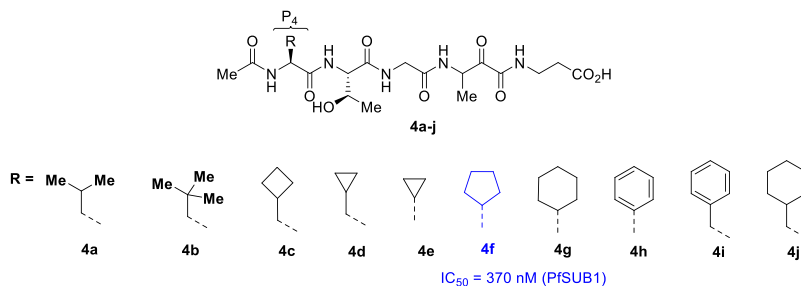


Figure 5. Peptidic ketoamide series 4 with a modified P4 position.

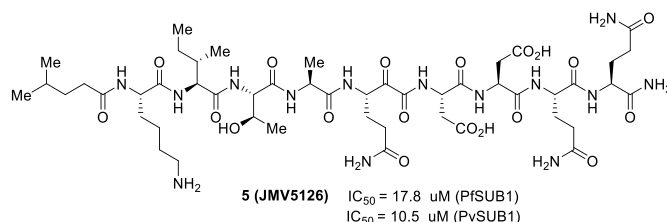


Figure 6. Ketoamide containing inhibitor JMV5126 with substituents extended to the prime part of the SUB1 active site.

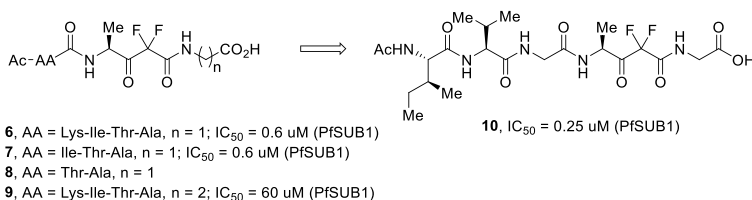


Figure 7. SUB1 inhibitors containing a difluorostatone moiety.

Previous data suggested that only small amino acids can be accommodated at the P2 position, so the original methyl substituent was replaced with dimethyl and cyclopropyl substituents; again, both compounds showed decreased activity. As a result, only glycine at the P2 position showed increased activity with respect to the starting compound. The relevance of the substituent at the P4 position was investigated by substitution with alanine. This produced a dramatic loss of inhibitory activity, in agreement with previous results showing that the hydrophobic S4 pocket accommodates an isoleucine residue very well and that this is important for binding. Substitution of this residue with a less hydrophobic methyl group resulted in loss of crucial van der Waals interactions. Replacement of the threonine at the P3 position with alanine led to decreased inhibitory potency, which was interpreted as likely resulting from an increased solvation penalty as the side chain of P3 points away from the binding site toward the solvent. Exploration of the P1 position revealed that a glutamine side chain (preferred in the original substrate sequence KITAQJ DDEES) was not compatible with the ketoamide functional group. A series of different P1 substituents was investigated, showing that only small substituents can be placed at this position.

Based on the importance of the P4 position for binding and recognition, a peptidic ketoamide series 4 was synthesized by

the incorporation of a range of unnatural amino acids to explore this side chain (Figure 5).¹⁹ Investigations of potency relative to the parent isoleucine analogue 3 revealed an improved inhibitor 4 containing a hydrophobic P4 cyclopentyl substituent ($IC_{50} \approx 370$ nM). Unfortunately, none of the ketoamide inhibitors 4a–4j showed measurable activity against the parasite *in vitro* at concentrations up to 100 μ M, probably due to poor membrane-permeability properties and their charged nature.

The SERA4 site1 cleavage sequence was used as the basis for another ketoamide-based inhibitor,²⁰ the nonapeptide isocaproyl-KITAQ(CO)DDEE-NH₂ 5 (called JMV5126) (Figure 6). Reported IC_{50} values for this compound were 17.8 ± 2.9 μ M against PfsUB1 and 10.5 ± 1.6 μ M against PvsUB1.

A difluorostatone moiety (a substructure of statine-derived 3,3-difluoro-6,6-dimethyl-2-heptanoic acid²¹) was another serine trap that was exploited for rationally designed inhibitors of PfsUB1. These compounds were also based on the PfsUB1 substrate SERA4 site 1 (Figure 2). A carboxylic acid with one or two carbon linkers (compounds 6–9) was added to mimic the P1' element of the substrate (Figure 7).²² Molecular dynamics simulations were confirmed by potency assays, which indicated that the best length of the linker is one carbon, as in compound 6. Molecular docking results showed that compound 6 can form several important hydrogen bonds

with key residues in the SUB1 binding cleft as well as strong interactions between the terminal carboxylic group and amino acid residues in the *S'* pocket, while inhibitor **9** did not show this pattern of interactions. Removal of the terminal lysine generated compound **7** with the same IC_{50} value as the parent compound ($IC_{50} = 0.6 \mu M$). This was in line with modeling experiments indicating that the P5 side chain is not involved in important binding interactions with the enzyme. However, further truncation of the P4 amino acid (isoleucine) resulted in almost no inhibition of recombinant enzyme suggesting that it is necessary to have at least a tripeptide at the nonprime side of difluorostatones for binding to the enzyme. Both inhibitors **6** and **7** were tested against other *Plasmodium* species SUB1 enzymes and found to possess low micromolar activity against PkSUB1 ($IC_{50} = 1.12 \mu M$ for **6** and $IC_{50} = 0.68 \mu M$ for **7**) and PvSUB1 ($IC_{50} = 2.5 \mu M$ and $IC_{50} = 2.2 \mu M$, respectively).²³

SAR investigation of P2–P4 substituents of the difluorostatone-based inhibitor **7** involved modification of the original structure by replacing amino acids in the parent inhibitor with different natural and non-natural amino acid analogues.²⁴ Overall, from these SAR studies it was concluded that the P4 and P3 side chains form hydrophobic interactions with SUB1, since isoleucine was preferred in the P4 position and valine as well as benzyl-protected threonine at P3 helped to improve the inhibitory potency. The most potent inhibitor **10** from these series of compounds, with an $IC_{50} = 0.25 \mu M$, possessed valine in P3 together with glycine in the P2 position (Figure 7).

An attempt to reduce the peptidic nature of the inhibitors was made by introducing different end-capping groups at the P3/P4 position. Decent inhibitory activity against PfSUB1 ($IC_{50} = 1 \mu M$) was achieved for compound **11** (Figure 8) from all of the synthesized analogues with a reduced peptidic nature.

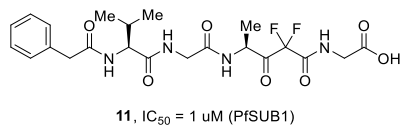


Figure 8. Difluorostatone based SUB1 inhibitor with reduced peptidic nature.

Examination of the structurally related serine traps trifluoromethylketone and carboxydifluoromethylketone (Figure 9) was performed. However, compounds **12** and **13** were not able to inhibit SUB1 at concentrations as high as $50 \mu M$.

Boronic acids are well-established warheads in inhibitors of serine proteases^{25–27} and have been clinically validated as drug-compatible substructures in marketed drugs such as bortezomib, ixazomib, vaborbactam, and tavaborole.²⁸ Replacement of the α -ketoamide functionality in compound **3** with boronic acid resulted in inhibitor **14** with substantially increased PfSUB1 inhibitory potency ($IC_{50} = 69 \text{ nM}$, Figure 10).¹⁹ A 10-fold lower IC_{50} value was achieved when both the

cyclopentyl group at P4 and the boronic acid serine trap moiety were combined, resulting in compound **15** with low nanomolar potency ($IC_{50} = 9.3 \text{ nM}$). Expanding the study to analyze the stereochemistry of the boronic acid moiety indicated that the chiral center has to resemble L-amino acid stereochemistry. SAR investigations of substituents at the P1 position of the boronic acid compounds revealed a compound bearing a hydroxyethyl substituent **16** that displayed increased SUB1-inhibitory potency ($IC_{50} = 4.6 \text{ nM}$). Unfortunately, compound **16** did not show high antiparasite potency in vitro compared to the parental compound **15** (half-maximal effective concentration (EC_{50}) = 15.0 vs $2.3 \mu M$).

Interestingly, significantly improved potency in the parasite growth assay was achieved for boronic acid-based peptidic inhibitors **17** and **18**, which possessed a modified P3 position, that is, replacement of threonine with alanine and valine, respectively (Figure 11). This was explained by the increased lipophilicity of these compounds, which likely resulted in better membrane permeability. Compound **18** is the best inhibitor of PfSUB1 known to date, with low nanomolar enzymatic inhibitory activity and sub-micromolar potency in parasite growth assays ($IC_{50} = 5.7 \text{ nM}$ and $EC_{50} = 0.26 \mu M$). Importantly the compounds showed considerable potency in inhibiting merozoite egress from infected RBCs.¹⁹

INHIBITORS IDENTIFIED BY A SCREENING OF COMPOUND LIBRARIES

An interesting SUB1 inhibitor of protein origin was identified by screening the antimalarial activity of the components of venom of the spider *Psalmopoeus cambridgei*. A protein called psalmopeotoxin I (PcFK1) was reported to inhibit the growth of *P. falciparum* parasites with an EC_{50} of $116 \mu M$.²⁹ The sequence of PcFK1 was compared to the PfSUB1 autocatalytic cleavage sequence as well as to cleavage site sequences within SERA family members and merozoite surface proteins. Two regions of PcFK1 were found to share structural similarities (called sites 1 and 2). Through computational analysis, the authors concluded that site 2 most likely interacts with the enzyme to mediate inhibitory activity. In rPfSUB1 and rPvSUB1 enzymatic assays, PcFK1 displayed inhibition constants (K_i) of 29.3 and $36.3 \mu M$, respectively, supporting the hypothesis that SUB1 is a target of the spider venom protein.

To discover small-molecule inhibitors of PfSUB1, a fluorescence-based assay³⁰ was used to screen more than 170 000 low molecular weight compounds from a range of sources.⁶ This identified a natural product **19** (called MRT12113, Figure 12), which inhibited PfSUB1 with an $IC_{50} = 0.3 \mu M$. Further characterization revealed that **19** is a highly selective inhibitor of PfSUB1, showing no inhibition of several other tested proteases at concentrations up to $50 \mu M$. More detailed experiments showed that **19** prevented egress of *P. falciparum* merozoites in vitro and prevented RBC invasion

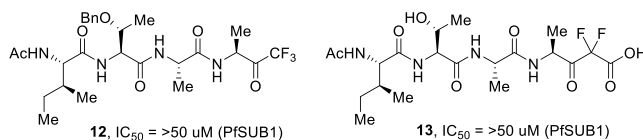


Figure 9. Trifluoromethylketone- and carboxydifluoromethylketone-containing inhibitors.

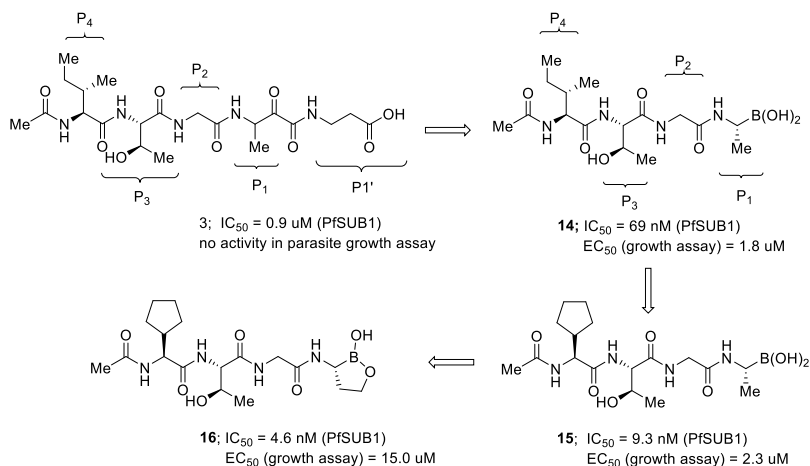


Figure 10. Development of boronic acid-containing peptidic SUB1 inhibitors.

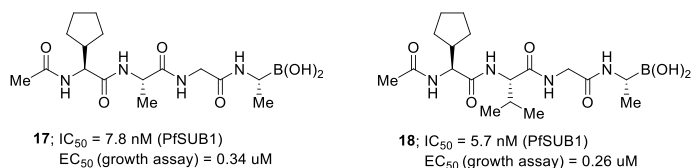


Figure 11. Inhibitors of PfSUB1 with activity in cell-based parasite growth and egress assays.

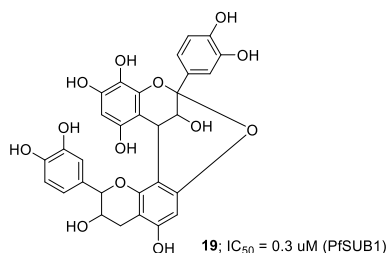


Figure 12. Natural product MRT12113 identified by screening.

(ED_{50} against schizont rupture around 108 μM and invasion 25 μM). Crucially, the compound was found to prevent maturation of SERA family proteins but also processing of merozoite surface proteins, shedding the first insights into the endogenous substrates of SUB1.

In a separate study, a screen of a library containing around 1200 irreversible small-molecule protease inhibitors identified a number of specific serine and cysteine protease inhibitors.³¹ All these compounds were characterized for their purity, stability, and effects on different stages of the *P. falciparum* blood stage parasite life cycle. The final set of hit compounds was tested for their general toxicity. From these, chloroisocoumarin 20 (Figure 13) was selected as the best inhibitor of PfSUB1 with an IC_{50} of 18 μM and an EC_{50} of 22 μM . The authors searched for analogues of this compound to establish a structure-activity relationship; however, none of the six follow-up compounds 21–26 showed improved activity compared to the parent inhibitor 20.

A screening of a library comprising ~450 peptidic and nonpeptidic compounds was performed. This resulted in identification of the quinolyldiazone 27 (Figure 14) as an inhibitor of PfSUB1 with an $IC_{50} = 20 \mu\text{M}$.³² Analogues of the hit compound were prepared to investigate SAR and improve potency. First, substituents at the arylidene moiety were explored. The results indicated that hydrogen-bond acceptor/donor groups do not improve inhibitory potency. From the analogues bearing electron-withdrawing groups at the arylidene, only compound 28 bearing a cyano group showed potency, although slightly reduced with respect to the original compound 27. Second, substituents at the quinoline moiety were explored. The results suggested that the fused dioxolane ring can be replaced with a 6-methoxy group, though inhibitory potency was somewhat decreased (29, $IC_{50} = 20\text{--}30 \mu\text{M}$) compared to 27. Other modifications, such as replacement of the quinoline with pyridine, benzimidazole, or tetrahydroacridine, generated less potent PfSUB1 inhibitors. Substitution of the hydrazone linker with other linkers also did not improve the inhibitory potency. The authors hypothesized that quinolyldiazones could be covalent inhibitors through attack of the active site serine by the relatively electrophilic bezylidene carbon. However, the enzyme recovered its activity after removal of the inhibitor 27 implying either a competitive or covalent reversible inhibition mechanism.

In silico screening against a PvSUB1 model and assaying of the inhibitory potency for the most promising compounds resulted in a set of five compounds (Figure 15) displaying inhibitory potency at low micromolar concentrations, which provides a good starting point for further development.³³ Compounds 30–32 showed improved activity against PvSUB1

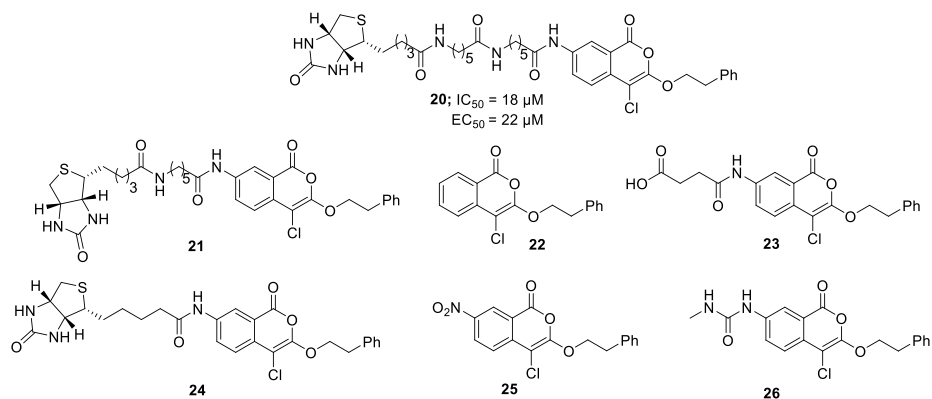


Figure 13. Chloroisocoumarin-containing SUB1 inhibitor **20** and its analogues.

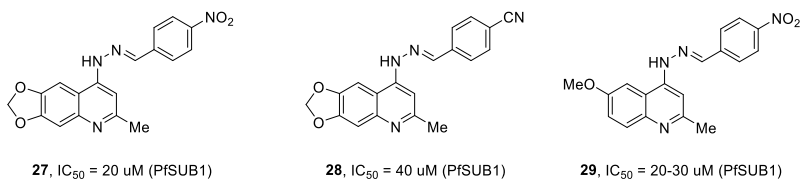


Figure 14. Quinolyhydrazone-containing inhibitors.

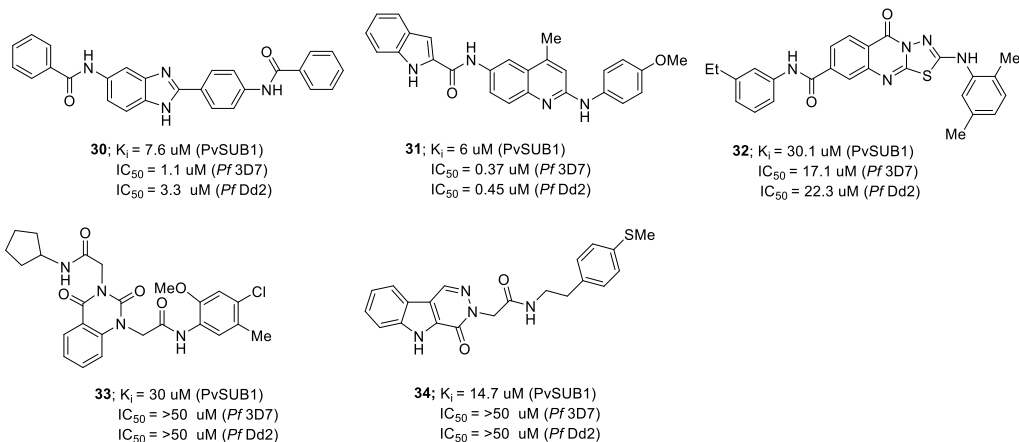


Figure 15. SUB1 inhibitors identified by virtual screening.

and also against both the *P. falciparum* chloroquine-sensitive 3D7 and chloroquine-resistant Dd2 clones. Dose-dependent reduction of processing of the endogenous PfSUB1 substrate SERA5 demonstrated that the most promising compound **31** is able to inhibit endogenous PfSUB1. Compounds **33** and **34** showed activity against recombinant PvSUB1; however, they did not inhibit *P. falciparum* growth in vitro (EC₅₀ > 50 μM). According to the docking pose of compound **31** into a model of PvSUB1 the inhibitor almost completely occupies the PvSUB1 catalytic groove. The indole carboxamide part of the inhibitor forms two hydrogen bonds in the S4 subpocket while

the aniline moiety resides in the S1 subpocket, forming three hydrogen bonds.

To search for nonpeptidic inhibitors of PfSUB1, the Malaria Box (a collection of 400 compounds with confirmed antimalarial activity) was screened³⁴ using the PFSUB1 enzyme assay.¹⁵ The screen identified a quinoxaline derivate **35** as a hit compound with an IC₅₀ of 10 μM (Figure 16). A range of analogues was prepared by varying R substituents; however, none of them gave improved activity. In fact, only the disubstituted (3-Cl-4-Br) quinoxaline analogue **36** possessed similar activity with respect to the hit compound **35**. The substitution pattern in the quinoxaline moiety was briefly

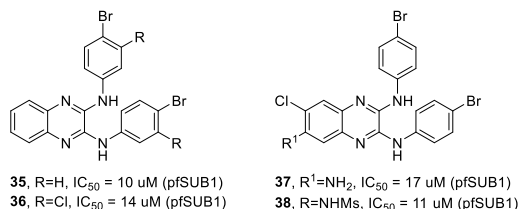


Figure 16. Malaria Box quinoxaline derivatives as PfSUB1 inhibitors.

explored. The results indicated that one of the hydrogen atoms at the quinoxaline can be replaced with chloride and the another with an amino- or mesylamino group to obtain inhibitors 37 and 38 with the potency very similar to that of the parent inhibitor 35.

Maslinic acid 39 (MA), a natural pentacyclic triterpene with known potential to inhibit intraerythrocytic stages of *P. falciparum*, was tested on four different representative proteases of the classes known to be expressed in the *Plasmodium* parasite life cycle.³⁵ *Bacillus licheniformis* subtilisin A was used as model serine protease and was found to be inhibited by MA with an IC_{50} of $59 \mu\text{M}$ (Figure 17). Given the similarity of PfSUB1 to subtilisin A, the effects of MA on maturation of merozoite surface proteins in parasite cultures (mediated by PfSUB1) were examined. Although inhibition of MSP1 processing by MA was observed, the compound had no effect on parasite replication. In contrast, the previously reported highly specific PfSUB1 inhibitor⁶ showed no apparent effect on parasite preschizont stages but, rather, very specific inhibition of schizont rupture and reduced invasion of the released merozoites. Cultures treated with MA displayed an increased fraction of ring, trophozoite, or schizont stages, leading the authors to suggest that MA might have additional targets in the intraerythrocytic stages, possibly through inhibition of parasite metalloproteases.

Two other natural pentacyclic triterpenes—ursolic acid and betulinic acid—and their analogues were presented as potential SUB1 inhibitory compounds (Figure 17), although these have not been tested in an SUB1 enzymatic assay.³⁶ From the analogues investigated for ability to inhibit parasite growth in vitro the most active compound was betulinic acid condensed with butanoic acid at C-3 (compound 40), which demonstrated an IC_{50} value of $3.4 \mu\text{M}$ against the *P. falciparum* W2 clone. Docking of compound 40 into the active site of the PfSUB1 model revealed a binding energy -7.02 kcal/mol . The most important contribution for this binding stems from interactions between the carboxylic acid and ester groups of

compound 40 with the target protein. Possible inhibition of PfSUB1 by compound 40 in vitro was analyzed using *Bacillus licheniformis* subtilisin A as a model protein, but this revealed only relatively low inhibitory potency ($IC_{50} = 93 \mu\text{M}$). The antimalarial activity of the compound may result from targeting other parasite proteins, or alternatively compound 40 could exhibit higher potency against PfSUB1 than against subtilisin A.

SUMMARY

The past decade has seen considerable progress in SUB1 inhibitor discovery. The most potent inhibitors have been identified by rational design based on detailed investigation of the preferred substrate amino acid sequence. Reversible covalent serine traps such as α -ketoamides, difluorostanones, trifluoromethyl ketone, and boronic acids have been used as the basis of peptidic inhibitors. Of the substrate-based reversible covalent inhibitors, peptidic boronic acids have shown the most potent inhibition of PfSUB1, with IC_{50} values in the low nanomolar range. Some of the peptidic boronic acids were able to inhibit merozoite egress from infected RBCs and importantly were also able to inhibit parasite proliferation at sub-micromolar concentrations. These achievements validate SUB1 as an antimalarial target for which the development of small-molecule inhibitors is tractable. Moreover they provide the first tool compounds suitable to investigate the ability of *Plasmodium* strains to develop resistance to SUB1 inhibitors. Nevertheless, the peptidic nature of substrate-based inhibitors and a covalent binding mechanism can pose challenges in achieving desirable drug-like properties. Consequently, depeptidisation studies together with profiling of physicochemical and ADMET properties are expected future directions for the development of reversible covalent inhibitors suitable as candidate antimalarial drugs.

Screening of small compound libraries has been less successful in providing potent SUB1 inhibitors. So far, both covalent and noncovalent inhibitors with micromolar potency have been identified, which have not been further developed to more potent analogues. This may be explained by the relatively shallow and elongated pocket of the SUB1 catalytic site. It might be expected that availability of more precise protein models based on the X-ray crystal structures of inhibitors bound to SUB1 could provide further valuable insights for structure-based drug discovery to facilitate hit-to-lead development from compound screens.

Other drug discovery methods, such as fragment-based lead discovery and the application of DNA encoded libraries (DELs), hold potential as yet unexplored alternatives to

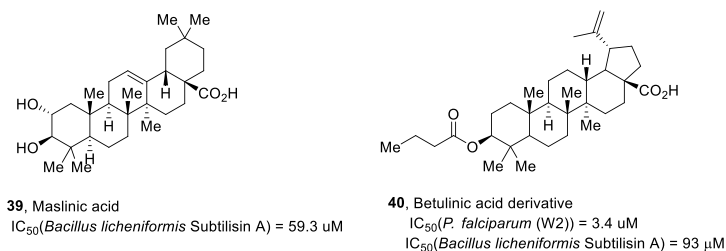


Figure 17. Pentacyclic triterpenes as putative SUB1 inhibitors.

expand the chemotypes amenable for development of SUB1 inhibitors.

AUTHOR INFORMATION

Corresponding Author

Aigars Jirgensons – *Latvian Institute of Organic Synthesis, Riga LV-1006, Latvia*; orcid.org/0000-0002-8937-8792;
Email: aigars@osi.lv

Authors

Elina Lidumniece – *Latvian Institute of Organic Synthesis, Riga LV-1006, Latvia*

Christlaine Withers-Martinez – *Malaria Biochemistry Laboratory, The Francis Crick Institute, London NW1 1AT, United Kingdom*

Fiona Hackett – *Malaria Biochemistry Laboratory, The Francis Crick Institute, London NW1 1AT, United Kingdom*

Michael J. Blackman – *Malaria Biochemistry Laboratory, The Francis Crick Institute, London NW1 1AT, United Kingdom; Faculty of Infectious and Tropical Diseases, London School of Hygiene & Tropical Medicine, London WC1E 7HT, United Kingdom*; orcid.org/0000-0002-7442-3810

Complete contact information is available at:
<https://pubs.acs.org/10.1021/acs.jmedchem.2c01093>

Notes

The authors declare no competing financial interest.

Biographies

Elina Lidumniece obtained her MSc degree in Chemistry working on synthetic methodology related to ruthenium catalyzed C–H activation at the University of Latvia in 2015. Currently, she is a PhD student at Riga Technical University and works at the Latvian Institute of Organic Synthesis under the guidance of Prof. Aigars Jirgensons on the synthesis and design of new PfSUB1 inhibitors. As a part of her PhD studies Elina had a short-term secondment to the group of Assoc. Prof. Henrik Franzyk at the Department of Drug Design and Pharmacology at the University of Copenhagen in 2022 to receive training in the design and synthesis of antibacterial peptidomimetics.

Christlaine Withers-Martinez obtained an MSc degree in 1988, a predoctoral degree in 1989, and a PhD degree in 1992 in biological crystallography at the University of Paris XI and Marseilles, France. In 1993 she performed postdoctoral studies at Unilever research in Vlaardingen (Holland) under the supervision of Prof. Theo Verrips. In 1994, she was appointed at the Centre National de la Recherche Scientifique (CNRS) as a “chargé de recherche” (CR2) to work in the “Architecture et Fonction des Macromolécules Biologiques” (AFMB) laboratory directed by Christian Cambillau in Marseilles. She joined the UK Medical Research Council’s National Institute for Medical Research (NIMR) in 1997 to work with Mike Blackman in the Division of Parasitology and is now working at the Francis Crick Institute in the Blackman group. Her work focuses on the structure–function characterization of essential malaria proteins and in the rational design of small-molecule drugs for therapeutic applications in the malaria field.

Fiona Hackett. After completing a degree and MSc from Bangor University in 1980, followed by 2 years in Tanzania, Fiona worked at NIMR from 1983, first of all on the immunological response of mice to schistosomiasis and then on malaria with Louis Schofield for a brief period before joining Mike Blackman’s lab in 1995, with whom she has been working ever since. For several years her work involved studies on red blood cell invasion by *Plasmodium falciparum* and the

proteases involved, but more recently the focus of the work has moved to egress and collaborative projects, which are developing a targeted approach to rational antimalarial drug design.

Michael J. Blackman obtained an MSc degree by research in 1985 working in Prof. Alan Morris’ group at the University of Warwick on the antiviral mode of action of interferon gamma. Later that same year Mike took up a post as a research officer in the Medical Research Council’s unit in The Gambia, West Africa, where he initiated his interest in the biology of the malaria parasite. He returned to the UK in 1988 to study for a PhD in Tony Holder’s lab at NIMR (now part of the Francis Crick Institute). Following this he stayed at NIMR, taking up a career track appointment and then being awarded tenure in 2000. Currently Mike Blackman is a Principal Group Leader at the Francis Crick Institute. He also holds a position as Professor of Molecular Parasitology at the London School of Hygiene & Tropical Medicine. His research interests include egress and host cell invasion by the malaria parasite and other apicomplexan parasites, with a particular focus on the proteolytic and kinase-mediated pathways that control these steps in the parasite lifecycle.

Aigars Jirgensons obtained his MSc. degree in 1997 and PhD degree in 2000 from the Latvian University working under the supervision of Dr. V. Kauss at the Latvian Institute of Organic Synthesis (LIOS), Riga. In 2002, he performed postdoctoral studies in the group of Prof. Roberto Pellicciari, University of Perugia, Italy, with a fellowship awarded by Merz Pharmaceuticals. In 2003, Aigars returned to LIOS to take up a role as a project leader on drug discovery projects in collaboration with Merz Pharmaceuticals. In 2006, Aigars established his own independent research group. Currently, he is scientific director and head of the group at LIOS and Professor at Riga Technical University. His research is focused on the discovery of antimalarial and antibacterial agents as well as the development of novel synthetic methodology.

ACKNOWLEDGMENTS

E.L. and A.J. thank the Latvian Council of Science for financial support (Grant No. lzp-2020/1-0327). This work was also supported by funding to M.J.B. from the Francis Crick Institute (<https://www.crick.ac.uk/>), which receives its core funding from Cancer Research UK (FC001043; <https://www.cancerresearchuk.org>), the UK Medical Research Council (FC001043; <https://www.mrc.ac.uk/>), and the Wellcome Trust (FC001043; <https://wellcome.ac.uk/>).

ABBREVIATIONS

ACTs, artemisinin-based combinations; DELs, DNA encoded libraries; MA, maslinic acid; MSP, merozoite surface protein; *P.*, *Plasmodium*; Paa, polar amino acid; PcFK1, Psalmopeptoxin I; PKG, parasite protein kinase; PV, parasitophorous vacuole; kDa, kilodalton; RBC, red blood cell; rPfSUB1, recombinant *Plasmodium falciparum* subtilisin-like serine protease; rPkSUB1, recombinant *Plasmodium knowlesi* subtilisin-like serine protease; rPvSUB1, recombinant *Plasmodium vivax* subtilisin-like serine protease; SERA, serine-rich antigen; SUB1, subtilisin-like serine protease; TCP, target candidate profile; TTP, target product profile; Xaa, any amino acid

REFERENCES

- (1) Sirawaraporn, W. Dihydrofolate Reductase and Antifolate Resistance in Malaria. *Drug Resist. Updat.* **1998**, *1*, 397–406.
- (2) Nsanabana, C. Resistance to Artemisinin Combination Therapies (ACTs): Do Not Forget the Partner Drug! *Trop. Med. Infect. Dis.* **2019**, *4*, 26.

- (3) Sajid, M.; Withers-Martinez, C.; Blackman, M. J. Maturation and Specificity of *Plasmodium Falciparum* Subtilisin-like Protease-1, a Malaria Merozoite Subtilisin-like Serine Protease. *J. Biol. Chem.* **2000**, *275*, 631–641.
- (4) Pino, P.; Caldelari, R.; Mukherjee, B.; Vahokoski, J.; Klages, N.; Maco, B.; Collins, C. R.; Blackman, M. J.; Kursula, L.; Heussler, V.; Brochet, M.; Soldati-Favre, D. A Multistage Antimalarial Targets the Plasmepps IX and X Essential for Invasion and Egress. *Science* **2017**, *358*, 522–528.
- (5) Collins, C. R.; Hackett, F.; Strath, M.; Penzo, M.; Withers-Martinez, C.; Baker, D. A.; Blackman, M. J. Malaria Parasite CGMP-Dependent Protein Kinase Regulates Blood Stage Merozoite Secretory Organelle Discharge and Egress. *PLoS Pathog.* **2013**, *9*, e1003344.
- (6) Yeoh, S.; O'Donnell, R. A.; Koussis, K.; Dlugowski, A. R.; Ansell, K. H.; Osborne, S. A.; Hackett, F.; Withers-Martinez, C.; Mitchell, G. H.; Bannister, L. H.; Bryans, J. S.; Kettleborough, C. A.; Blackman, M. J. Subcellular Discharge of a Serine Protease Mediates Release of Invasive Malaria Parasites from Host Erythrocytes. *Cell* **2007**, *131*, 1072–1083.
- (7) Burrows, J. N.; Duparc, S.; Gutteridge, W. E.; van Huijsduijnen, R. H.; Kaszubska, W.; Macintyre, F.; Mazzuri, S.; Möhrle, J. J.; Wells, T. N. C. New developments in anti-malarial target candidate and product profiles. *Malar. J.* **2017**, *16*, 26.
- (8) Tan, M. S. Y.; Blackman, M. J. Malaria Parasite Egress at a Glance. *J. Cell Sci.* **2021**, *134*, jcs257345.
- (9) Burns, A. L.; Dans, M. G.; Balbin, J. M.; de Koning-Ward, T. F.; Gilson, P. R.; Beeson, J. G.; Boyle, M. J.; Wilson, D. W. Targeting Malaria Parasite Invasion of Red Blood Cells as an Antimalarial Strategy. *FEMS Microbiol. Rev.* **2019**, *43* (3), 223–238.
- (10) Withers-Martinez, C.; Saldanha, J. W.; Ely, B.; Hackett, F.; O'Connor, T.; Blackman, M. J. Expression of Recombinant *Plasmodium Falciparum* Subtilisin-like Protease-1 in Insect Cells. *J. Biol. Chem.* **2002**, *277* (33), 29698–29709.
- (11) Withers-Martinez, C.; Strath, M.; Hackett, F.; Haire, L. F.; Howell, S. A.; Walker, P. A.; Christodoulou, E.; Dodson, G. G.; Blackman, M. J. The Malaria Parasite Egress Protease SUB1 Is a Calcium-Dependent Redox Switch Subtilisin. *Nat. Commun.* **2014**, *5*, 3726.
- (12) Rano, T. A.; Timkey, T.; Peterson, E. P.; Rotonda, J.; Nicholson, D. W.; Becker, J. W.; Chapman, K. T.; Thornberry, N. A. A Combinatorial Approach for Determining Protease Specificities: Application to Interleukin-1 p Converting Enzyme (ICE). *Chem. Biol.* **1997**, *4*, 149–55.
- (13) Siezen, R. J.; Leunissen, J. A. M. Subtilases: The Superfamily of Subtilisin-like Serine Proteases: Subtilases. *Protein Sci.* **1997**, *6*, 501–523.
- (14) Koussis, K.; Withers-Martinez, C.; Yeoh, S.; Child, M.; Hackett, F.; Knuepfer, E.; Juliano, L.; Woelblier, U.; Bujard, H.; Blackman, M. J. A Multifunctional Serine Protease Primes the Malaria Parasite for Red Blood Cell Invasion. *EMBO J.* **2009**, *28*, 725–735.
- (15) Withers-Martinez, C.; Suarez, C.; Fulle, S.; Kher, S.; Penzo, M.; Ebejer, J.-P.; Koussis, K.; Hackett, F.; Jirgensons, A.; Finn, P.; Blackman, M. J. *Plasmodium Subtilisin-like Protease 1 (SUB1)*: Insights into the Active-Site Structure, Specificity and Function of a Pan-Malaria Drug Target. *Int. J. Parasitol.* **2012**, *42*, 597–612.
- (16) Fulle, S.; Withers-Martinez, C.; Blackman, M. J.; Morris, G. M.; Finn, P. W. Molecular Determinants of Binding to the *Plasmodium Subtilisin-like Protease 1*. *J. Chem. Inf. Model.* **2013**, *53*, 573–583.
- (17) Robello, M.; Barresi, E.; Baglini, E.; Salerno, S.; Taliani, S.; Settimo, F. D. The Alpha Keto Amide Moiety as a Privileged Motif in Medicinal Chemistry: Current Insights and Emerging Opportunities. *J. Med. Chem.* **2021**, *64*, 3508–3545.
- (18) Kher, S. S.; Penzo, M.; Fulle, S.; Finn, P. W.; Blackman, M. J.; Jirgensons, A. Substrate Derived Peptidic α -Ketoamides as Inhibitors of the Malarial Protease PfSUB1. *Bioorg. Med. Chem. Lett.* **2014**, *24*, 4486–4489.
- (19) Lidumniece, E.; Withers-Martinez, C.; Hackett, F.; Collins, C. R.; Perrin, A. J.; Koussis, K.; Bisson, C.; Blackman, M. J.; Jirgensons, A. Peptidic Boronic Acids Are Potent Cell-Permeable Inhibitors of the Malaria Parasite Egress Serine Protease SUB1. *Proc. Natl. Acad. Sci. U. S. A.* **2021**, *118* (20), No. e2022696118.
- (20) Giganti, D.; Bouillon, A.; Tawk, L.; Robert, F.; Martinez, M.; Crublet, E.; Weber, P.; Girard-Blanc, C.; Petres, S.; Haouz, A.; Hernandez, J.-F.; Mercereau-Puijalon, O.; Alzari, P. M.; Barale, J.-C. A Novel *Plasmodium*-Specific Prodomain Fold Regulates the Malaria Drug Target SUB1 Subtilase. *Nat. Commun.* **2014**, *5*, 4833.
- (21) Gelb, M. H.; Svaren, J. P.; Abeles, R. H. Fluoro Ketone Inhibitors of Hydrolytic Enzymes. *Biochemistry* **1985**, *24*, 1813–1817.
- (22) Giovani, S.; Penzo, M.; Brogi, S.; Brindisi, M.; Gemma, S.; Novellino, E.; Savini, L.; Blackman, M. J.; Campiani, G.; Butini, S. Rational Design of the First Difluorostatone-Based PfSUB1 Inhibitors. *Bioorg. Med. Chem. Lett.* **2014**, *24*, 3582–3586.
- (23) Brogi, S.; Giovani, S.; Brindisi, M.; Gemma, S.; Novellino, E.; Campiani, G.; Blackman, M. J.; Butini, S. In Silico Study of Subtilisin-like Protease 1 (SUB1) from Different *Plasmodium* Species in Complex with Peptidyl-Difluorostatones and Characterization of Potent Pan-SUB1 Inhibitors. *J. Mol. Graph. Model.* **2016**, *64*, 121–130.
- (24) Giovani, S.; Penzo, M.; Butini, S.; Brindisi, M.; Gemma, S.; Novellino, E.; Campiani, G.; Blackman, M. J.; Brogi, S. *Plasmodium Falciparum* Subtilisin-like Protease 1: Discovery of Potent Difluorostatone-Based Inhibitors. *RSC Adv.* **2015**, *5*, 22431–22448.
- (25) Fu, H.; Fang, H.; Sun, J.; Wang, H.; Liu, A.; Sun, J.; Wu, Z. Boronic Acid-Based Enzyme Inhibitors: A Review of Recent Progress. *Curr. Med. Chem.* **2014**, *21*, 3271–3280.
- (26) Diaz, D. B.; Yudin, A. K. The Versatility of Boron in Biological Target Engagement. *Nat. Chem.* **2017**, *9*, 731–742.
- (27) Krajnc, A.; Lang, P. A.; Panduwawala, T. D.; Brem, J.; Schofield, C. J. Will Morphing Boron-Based Inhibitors Beat the β -Lactamases? *Curr. Opin. Chem. Biol.* **2019**, *50*, 101–110.
- (28) Plescia, J.; Moitessier, N. Design and Discovery of Boronic Acid Drugs. *Eur. J. Med. Chem.* **2020**, *195*, 112270.
- (29) Bastianelli, G.; Bouillon, A.; Nguyen, C.; Crublet, E.; Pêtres, S.; Gorgette, O.; Le-Nguyen, D.; Barale, J.-C.; Nilges, M. Computational Reverse-Engineering of a Spider-Venom Derived Peptide Active Against *Plasmodium Falciparum* SUB1. *PLoS One* **2011**, *6*, e21812.
- (30) Blackman, M. J.; Corrie, J. E. T.; Croney, J. C.; Kelly, G.; Eccleston, J. F.; Jameson, D. M. Structural and Biochemical Characterization of a Fluorogenic Rhodamine-Labeled Malarial Protease Substrate. *Biochemistry* **2002**, *41*, 12244–12252.
- (31) Arastu-Kapur, S.; Ponder, E. L.; Fonović, U. P.; Yeoh, S.; Yuan, F.; Fonović, M.; Grainger, M.; Phillips, C. I.; Powers, J. C.; Bogoy, M. Identification of Proteases That Regulate Erythrocyte Rupture by the Malaria Parasite *Plasmodium Falciparum*. *Nat. Chem. Biol.* **2008**, *4*, 203–213.
- (32) Gemma, S.; Giovani, S.; Brindisi, M.; Tripaldi, P.; Brogi, S.; Savini, L.; Fiorini, I.; Novellino, E.; Butini, S.; Campiani, G.; Penzo, M.; Blackman, M. J. Quinolylhydrazones as Novel Inhibitors of *Plasmodium Falciparum* Serine Protease PfSUB1. *Bioorg. Med. Chem. Lett.* **2012**, *22*, 5317–5321.
- (33) Bouillon, A.; Giganti, D.; Benedet, C.; Gorgette, O.; Pêtres, S.; Crublet, E.; Girard-Blanc, C.; Witkowski, B.; Ménard, D.; Nilges, M.; Mercereau-Puijalon, O.; Stoven, V.; Barale, J.-C. In Silico Screening on the Three-Dimensional Model of the *Plasmodium Vivax* SUB1 Protease Leads to the Validation of a Novel Anti-Parasite Compound. *J. Biol. Chem.* **2013**, *288*, 18561–18573.
- (34) Kher, S. S.; Penzo, M.; Fulle, S.; Ebejer, J. P.; Finn, P. W.; Blackman, M. J.; Jirgensons, A. Quinoxaline-Based Inhibitors of Malarial Protease PfSUB1. *Chem. Heterocycl. Compd.* **2015**, *50*, 1457–1463.
- (35) Moneriz, C.; Mestres, J.; Bautista, J. M.; Diez, A.; Puyet, A. Multi-Targeted Activity of Maslinic Acid as an Antimalarial Natural Compound: Maslinic Acid Targets on *Plasmodium Falciparum*. *FEBS J.* **2011**, *278*, 2951–2961.
- (36) Cargnin, S. T.; Staudt, A. F.; Medeiros, P.; de Medeiros Sol, D.; de Azevedo dos Santos, A. P.; Zanchi, F. B.; Gosmann, G.; Puyet, A.; Garcia Teles, C. B.; Gnoatto, S. B. Semisynthesis, Cytotoxicity,

Antimalarial Evaluation and Structure-Activity Relationship of Two Series of Triterpene Derivatives. *Bioorg. Med. Chem. Lett.* **2018**, *28*, 265–272.

Recommended by ACS

Discovery of Novel Quinoline-Based Proteasome Inhibitors for Human African Trypanosomiasis (HAT)

Dennis C. Koester, Srinivasa P. S. Rao, *et al.*

AUGUST 22, 2022
JOURNAL OF MEDICINAL CHEMISTRY

READ 

Identification of Inhibitors of the *Schistosoma mansoni* VKR2 Kinase Domain

Indran Mathavan, Konstantinos Beis, *et al.*

OCTOBER 05, 2022
ACS MEDICINAL CHEMISTRY LETTERS

READ 

Design, Synthesis, and Optimization of Macrocyclic Peptides as Species-Selective Antimalaria Proteasome Inhibitors

Hao Zhang, Gang Lin, *et al.*

JUNE 21, 2022
JOURNAL OF MEDICINAL CHEMISTRY

READ 

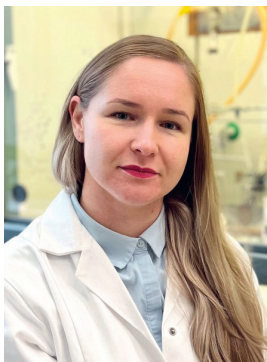
Effects of Structurally Different HDAC Inhibitors against *Trypanosoma cruzi*, *Leishmania*, and *Schistosoma mansoni*

Elisabetta Di Bello, Antonello Mai, *et al.*

JUNE 22, 2022
ACS INFECTIOUS DISEASES

READ 

Get More Suggestions >



Elīna Līdumniece dzimusi 1990. gadā Smiltēnē, augusi Rankā. Latvijas Universitātē ieguvusi dabaszinātņu bakalaura grādu ķīmijā (2013) par tēmu "4,5,6,7-Tetrahidro-1*H*-indazola atvasinājumu sintēze azīdu-alkīnu ciklopievienošanas reakcijās" un dabaszinātņu maģistra grādu ķīmijā (2015), aizstāvot darbu "*N*-Acilsulfonamīdi kā virzošās grupas rutēnija katalizētās anelēšanas reakcijās" (izstrādāts *Dr. chem. A. Jirgensona* vadībā).

Paralēli studijām strādā Latvijas Organiskās sintēzes institūtā Organiskās sintēzes metodoloģijas grupā. Galvenais pētījumu virziens – jaunu SUB1 inhibitoru izveide, kam nākotnē būtu potenciāls kļūt par jaunām pretmalārijas zālēm. Līdzšinējie zinātniskā darba rezultāti publicēti trīs starptautiski citējamajos žurnālos, impaktfaktors līdz pat 12,779 (*Proc. Natl. Acad. Sci. U. S. A.*), kā arī prezentēti vairākās starptautiskās konferencēs.

Elīna Līdumniece was born in 1990 in Smiltene and grew up in Ranka. In 2013, she earned a Bachelor's degree of Natural Sciences in Chemistry from University of Latvia with Bachelor Thesis "Synthesis of 4,5,6,7-tetrahydro-1-*H*-indazole derivatives in azide-alkyne cycloaddition reactions". In 2015, she received a Master's degree of Natural Sciences in Chemistry from LU with Master Thesis "*N*-Acyl sulfonamides as directing groups in ruthenium catalyzed annulation reactions" (supervisor *Dr. chem. A. Jirgensons*).

Elīna Līdumniece is currently a research assistant with Latvian Institute of Organic Synthesis (Organic Synthesis Methodology Group). Her research interests are focused on the development of new inhibitors of SUB1 that could potentially lead to new anti-malarial compounds. She is a co-author of 3 scientific publications submitted to international journals (*IF* up to 12,779 for *Proc. Natl. Acad. Sci. U. S. A.*) and has presented her work at several international conferences.